1-1-2013

# New Bimetallic Iridium Cluster Carbonyl Complexes

Mingwei Chen
*University of South Carolina*

# NEW BIMETALLIC IRIDIUM CLUSTER CARBONYL COMPLEXES

by

Mingwei Chen

Bachelor of Science
University of Science and Technology of China, 2008

---

Submitted in Partial Fulfillment of the Requirements

For the Degree of Doctor of Philosophy in

Chemistry and Biochemistry

College of Arts and Science

University of South Carolina

2013

Accepted by:

Richard D. Adams, Major Professor

Francis A. Gadala-Maria, Committee Member

Linda S. Shimizu, Committee Member

Daniel L. Reger, Chairperson, Examining Committee

Lacy Ford, Vice Provost and Dean of Graduate Studies

## ACKNOWLEDGEMENTS

There are a number of people without whom this thesis might not have been written, and to whom I am greatly indebted.

I would first like to thank my research advisor, Dr. Richard D. Adams, for his guidance, patience and support. His passion for chemistry and his expertise in the field of organometallic chemistry improved my research skills, inspired me to think and prepared me for future challenges.

I would like to thank the members of my research committee: Dr. Daniel L. Reger, Dr. Francis A. Gadala-Maria and Dr. Linda Shimizu, for their time, energy and contributions throughout my graduate life. I would also like to thank Dr. Xinzheng Yang for doing the DFT molecular orbital calculations; to Dr. Mark Smith for his invaluable help with X-ray crystallography; to Dr. Perry J. Pellechia and Dr. Helga J. Cohen for their helpful assistance and training in NMR measurements; to Dr. Mike Walla and Dr. William Cotham for conducting all my mass spectrometry measurements.

I would like to thank my former and current lab mates: Dr. Eszter Trufan, Dr. Minglai Fu and Dr. William C. Pearl for the guidance and advice at the start of my research; to Qiang Zhang and Yuwei Kan for being great companions and for all the things of great value in research as well as in life I learnt from you; to newcomers: Fang Fang, Yuen Onn Wong, Gaya Elpitiya and Joseph Kiprotich for the great time we have spent together; good luck with your research.

Thank you to my parents and grandparents for your unconditional support and endless love. No matter what important decisions I made, you were always behind me, supporting me and encouraging me to pursue my dreams.

Thank you, Rongrong Huang, my wife for your endless patience and support. Distance and separation in the past years did not fade our love, not even a little, nor will time! In addition, on December 1st of this past year I got the best gift I have ever received, a baby girl, Celine X. Chen. It is to all I love that this dissertation and the work contained herein is dedicated.

## ABSTRACT

Platinum group metal derived bimetallic clusters have been used as precursors to nanoscale catalysts which have been proven to be more effective than their monometallic counterparts. Iridium is a platinum group metal and its applications in catalysis continue to grow. To take advantage of the synergies between mixed-metals, we modified iridium clusters with other metal ligands like tin, germanium, and group IB (gold, silver, copper etc.) and obtained a fairly large number of new iridium derived bimetallic clusters which could be precursors to catalysts with properties superior to those of the catalysts available nowadays.

The reaction of $Ir_4(CO)_{12}$ with $Ph_3SnOH$ in the presence of $[Bu_4N]OH$ gave two products: $[Bu_4N]][Ir_4(CO)_{11}(SnPh_3)]$ (**2.1**; 45% yield) and $[Bu_4N][Ir_4(\mu\text{-}H)(CO)_{10}(SnPh_3)_2]$ (**2.2**; 5.5% yield). Compound **2.2** can be obtained from **2.1** in better yield by treatment with an excess of $Ph_3SnOH$ in the presence of $[Bu_4N]OH$ at 25℃ over 15h. The reaction of $Ir_4(CO)_{11}(PPh_3)$ with $Ph_3SnOH$ in the presence of $[Bu_4N]OH$ gave the complex $Ir_4(\mu\text{-}H)(CO)_{10}(SnPh_3)(PPh_3)$ (**2.3**, 44% yield). It is proposed that these reactions occur by the addition of the anion $[OSnPh_3]^-$ generated in situ to a CO ligand of the $Ir_4(CO)_{12}$ to form a stanyl-substituted metallocarboxylate ligand that subsequently loses $CO_2$ and transfers the $SnPh_3$ group to a metal atom. Similar reactions of $Os_3(CO)_{12}$ with the compounds $Ph_3MOH$, M = Sn, Ge under basic conditions yielded the first examples of metal carbonyl cluster complexes containing bridging stannyl- and germyl- substituted

metallocarboxylate ligands in the complexes $Os_3(CO)_{10}(\mu\text{-}O{=}COMPh_3)(\mu\text{-}OH)$, M = Sn, Ge, **2.4**, **2.5** which further validated the above proposal.

The reaction of $Ir_4(CO)_{11}(PPh_3)$ with $GePh_3H$ and $Me_3NO$ at room temperature has yielded a new complex $Ir_4(CO)_{10}(PPh_3)(GePh_3)(\mu\text{-}H)$, **3.1** in 54% yield by decarbonylation and oxidative addition of the GeH bond of the $GePh_3H$ to the cluster. Compound **3.1** was converted to the $GePh_2$-bridged complex $Ir_4(CO)_{10}(PPh_3)(\mu\text{-}GePh_2)$, **3.2** in 95% yield when heated to 40℃, by the cleavage of a phenyl ring from the $GePh_3$ ligand and the elimination of a molecule of benzene. The reaction of **3.2** with $GePh_3H$ at 65℃ yielded the new tetrahedral $Ir_4$ complex $Ir_4(CO)_7(PPh_3)(GePh_2)(GePh_3)(\mu_3\text{-}\eta^2\text{-}GePhC_6H_4)(\mu\text{-}H)_2$, **3.3**. Compound **3.3** was converted to the complex $Ir_4(CO)_7(PPh_3)(GePh_2)_2(\mu_3\text{-}\eta^2\text{-}GePhC_6H_4)(\mu\text{-}H)$, **3.5** by cleavage of a phenyl ring from the $GePh_3$ ligand and the elimination of a molecule of benzene. The structure of **3.3** and **3.5** both consist of a tetrahedral $Ir_4$ cluster with a rare ortho-metallated bridging $\mu_3\text{-}\eta^2\text{-}GePh(C_6H_4)$ ligand. The reaction of **3.2** with $GePh_2H_2$ at 40℃ yielded the tetrairidium complex $Ir_4(CO)_6(PPh_3)(GePh_2)_3(GePh_2H)(\mu\text{-}H)_3$, **3.6**.

A new air-stable σ-phenyl tetrairidium carbonyl salt $[Et_4N][Ir_4(CO)_{11}Ph]$, **4.1**, has been obtained by transmetalation reactions between $[Et_4N][Ir_4(CO)_{11}Br]$ and $SnPh_3OH$ in 45% yield or $SnPh_4$ in 36% yield. Compound **4.1** reacts with $PPh_3$ to yield the complex $[Et_4N][Ir_4(CO)_{10}(\mu\text{-}\eta^2\text{-}PPh_2C_6H_4)]$, **4.2** which contains an ortho-metalated bridging $\mu\text{-}\eta^2\text{-}PPh_2C_6H_4$ ligand. Compound **4.1** reacts with $Ir(CO)(PPh_3)_2Cl$ by halide displacement to yield two new uncharged pentairidium complexes $Ir_5(CO)_{12}(Ph)(PPh_3)$, **4.3**, and $Ir_5(CO)_{11}(PPh_3)(\mu\text{-}\eta^2\text{-}PPh_2C_6H_4)$, **4.4**. Compound **4.3** and **4.4** both contain trigonal-

bipyramidal clusters of iridium atoms. Compound **4.4** was also obtained from **4.3** by reaction with $PPh_3$.

The reaction of compound **4.1** with [Ir(COD)Cl] (COD=1,5-cyclooctadiene) yielded the two known tetrairidium compounds $Ir_4(CO)_{10}(COD)$ and $Ir_4(CO)_7(COD)(\mu_4\text{-}C_8H_{10})$, **4.5** and the three new higher nuclearity complexes $Ir_5(CO)_{11}(Ph)(COD)$, **4.6**, $Ir5(CO)_9(Ph)(COD)_2$, **4.7** and $Ir_9(CO)_{15}(Ph)(\mu_3\text{-}C_8H_{10})(COD)$, **4.8**, containing σ-coordinated phenyl ligands. Compound **4.6** and **4.7** contain trigonal-bypyramidal $Ir_5$ clusters. Compound **4.8** was shown to be formed by the condensation of **4.5** and **4.6** with nine iridium atoms in the form of a tricapped octahedron. Compound **4.7** reacts with COD to yield the compound $Ir_5(CO)_7(COD)_2(\mu_4\text{-}\eta^2\text{:}\eta^1\text{-}C_8H_{11})$ **4.9** in a cluster-opening process that cleaves two hydrogen atoms form one of the COD C-C double bonds, eliminates the σ-phenyl ligand, and transfers one of the hydrogen atoms the other C-C double bond to form a metalated $\mu_4\text{-}\eta^2\text{:}\eta^1\text{-}C_8H_{11}$ cyclooctyne ligand.

The reaction of compound **4.1** with $[Au(PPh_3)][NO_3]$ yields a new iridium-gold complex $Ir_4(CO)_{11}(Ph)(\mu\text{-}AuPPh_3)$, **5.1**. Two new iridium-gold complexes $Ir_4(CO)_{10}(AuPPh_3)_2$, **5.2**, and $Ir_4(CO)_{11}(AuPPh_3)_2$, **5.3**, were obtained from the reaction of $[HIr_4(CO)_{11}]^-$ with $[Au(PPh_3)][NO_3]$. The octahedral $Ir_4Au_2$ cluster of **5.2** is reversibly converted into the $Au(PPh_3)$-capped $Ir_4Au$ trigonal bipyramidal cluster of **5.3** by adding CO. Compound **5.2** adds $PPh_3$ to form the compound $Ir_4(CO)_{10}(PPh_3)(AuPPh_3)_2$, **5.4**, which is structurally similar to **5.3**. Compound **5.4** loses CO and benzene when heated to form the compound $Ir_4(CO)_9(\mu_3\text{-}PPhC_6H_4)(AuPPh_3)_2$, **5.5**, which contains a triply bridging $PPhC_6H_4$ ligand.

The compounds $Ir_4(CO)_{11}(R)(\sigma\text{-}AuPPh_3)$, (**5.1**, R = $C_6H_5$, **5.6**, R = $CH_3$, and **5.7**, R = 2-$C_{16}H_{10}$) were obtained from the reactions of $[NEt_4][Ir_4(CO)_{11}Br]$ with $(R)Au(PPh_3)$, R = $C_6H_5$, $CH_3$, and 1-$C_{16}H_{10}$ at 25 $^oC$ by the loss of $Br^-$ and the oxidative addition of the Au-C bond of the $(R)Au(PPh_3)$ to the $Ir_4$ cluster. The reaction of $(CH_3)Au(PPh_3)$ with $[PPN][HIr_4(CO)_{11}]$ yielded compound **5.6** and the higher nuclearity compound $Ir_4(CO)_9(CH_3)_2(AuPPh_3)_4$, **5.8**. The reaction of $PhAu(PPh_3)$ with $[PPN][HIr_4(CO)_{11}]$ yielded compound **5.1** and the higher nuclearity compounds $Ir_4(CO)_9(PPh_3)(Ph)(AuPPh_3)_3$, **5.9** and $Ir_4(CO)_9(Ph)_2(AuPPh_3)_4$, **5.10**. Compounds **5.8** and **5.10** were obtained in better yields from the reactions of $Ir_4(CO)_{11}(AuPPh_3)_2$, **5.3** with $(CH_3)Au(PPh_3)$ and $PhAu(PPh_3)$, respectively. Compound **5.9** was obtained independently in a high yield by the reaction of $Ir_4(CO)_{10}(PPh_3)(AuPPh_3)_2$, **5.4** with $PhAu(PPh_3)$. The reaction of **5.7** with $(CH_3)Au(PPh_3)$ was found to yield the digold compound $Ir_4(CO)_9(\mu\text{-}\eta^3\text{-}O{=}CC_{16}H_8)(\mu\text{-}AuPPh_3)(\mu_3\text{-}AuPPh_3)$, **5.11** in 25% yield.

Reactions of the tetrairidium anion $[Ir_4(CO)_{11}(Ph)]$, **4.1** with $[Cu(NCMe)_4][BF_4]$ and $Ag[NO_3]$ have yielded the new iridium-copper and iridium-silver complexes $Ir_4(CO)_{11}(\mu\text{-}\eta^1\text{-}Ph)[\mu_3\text{-}Cu(NCMe)]$, **6.2** and the $[Et_4N][\{Ir_4(CO)_{11}Ph\}_2(\mu_4\text{-}Ag)]$, **6.3**, respectively. Compound **6.3** reacts with a second equivalent of $Ag[NO_3]$ to yield the uncharged complex $[Ir_4(CO)_{11}]_2(\mu_4\text{-}Ag)(\mu\text{-}Ag)(\mu_3\text{-}Ph)(\mu\text{-}Ph)$, **6.4** that contains two $Ir_4(CO)_{11}$ clusters linked by a quadruply-bridging silver atom and one triply bridging Ph ligand. When dissolved in NCMe, compound **6.4** is split in two and adds one equivalent of NCMe to the Ag atom in each half to form the compound $Ir_4(CO)_{11}(\eta^1\text{-}Ph)[\mu_3\text{-}Ag(NCMe)]$, **6.5** (73% yield). Unlike **6.2**, the phenyl ligand in **6.5** is terminally coordinated. When **6.4** was treated with $PPh_3$, the complex $Ir_4(CO)_{11}(\mu\text{-}\eta^1\text{-}Ph)[\mu_3\text{-}$

$Ag(PPh_3)]$, **6.6** was obtained in 87% yield. The cluster of **6.6** is structurally similar to that of **6.5** except that the phenyl ligand has adopted a semi-bridging coordination to the silver atom similar to that found for the phenyl ligand and the copper atom in **6.2**.

# TABLE OF CONTENTS

# LIST OF FIGURES

# LIST OF SCHEMES

# LIST OF TABLES

# LIST OF EQUATIONS

# CHAPTER ONE

## Introduction

Vladimir Haesel who worked for Universal Oil Products (also known as UOP), developed a catalytic reforming process using a catalyst containing platinum in the 1940s. Catalytic petroleum-reforming has aroused great attention and has become one of the most important processes in the world.[1] The objective of the process is to increase the octane number of gasoline by converting saturated hydrocarbons (alkanes and cycloalkanes) in petroleum naphtha fractions to aromatic hydrocarbons as selectively as possible through a series of catalytic reforming reactions such as dehydrogenation, dehydroisomerization, dehydrocyclization, isomerization and fragmentation. Vladimir. Haesel greatly increased the octane number of gasolines by using catalyst of platinum supported on alumina for hydrocarbon reforming.[2] Since then as a result of tremendous industrial needs, great efforts have been devoted to develop more and more efficient catalysts to improve product selectivity, enhance catalyst lifetimes and reduce production costs.

The use of platinum catalysts as the active agent was a huge success in the upgrading of low octane petroleum naphtha to high-quality products. The technology quickly became the principal method of producing high octane gasoline and great attentions have been drawn to the other platinum group metals such as palladium and iridium which have also been found to exhibit excellent performance in petroleum-

reforming. Meanwhile, the introduction of a second metal has been shown increase selectivity effects in catalysis by tuning of electronic structures of the metals. It was discovered by Sinfelt and coworkers that the activity of the Group VIII metal for hydrogenolysis reactions of hydrocarbons was decreased markedly by a presence of the Group IB metal.[3] For instance, the presence of copper strongly suppresses the catalytic activity of ruthenium for the hydrogenolysis of ethane to methane by three orders of magnitude in ruthenium-copper system. It was shown that the inhibition of hydrogenolysis produced to improved selectivity for alkane isomerization reactions and convesion to aromatic hydrocarbons.

Moreover, studies by Sinfelt and coworkers on mixed metals catalysts Pt-Ir and Pt-Re dispersed on alumina showed that bimetallic catalysts were superior to the pure Pt catalysts. [4] It was shown that catalysts consisting of bimetallic clusters of platinum and iridium supported on $Al_2O_3$ were more active than the platinum-on-alumina reforming catalysts and exhibited much longer lifetimes. This discovery was important for the production of unleaded gasolines and, hence, the Pt-Ir and Pt-Re systems have largely replaced the older platinum-alumina catalysts in reforming units. Since this discovery, there has been significant interest in the development of bimetallic catalysts due to the superior catalytic properties bimetallic nanocatalysts exhibit over monometallic catalysts. The enhancement of the catalytic properties such as enhanced lifetimes, increased activity, improved stability and selectivity are proposed to be a result of a cooperative interactions often referred to as "synergistic effects" between the different metals.[5] One remarkable example is the addition of tin to platinum which significantly boosts the catalytic activity of the catalysts in dehydrogenation and petroleum-reforming reactions. Studies by Burch

and Garla showed that tin serves as great modifier leading to enhanced activity and selectivity by 1) modifying the acidity of the support which results in higher selectivity and 2) modifying the properties of platinum metals by reducing poisoning effects.[5d-5f]

Accompanied with the great interest in the development of bimetallic catalysts, scientists sought to develop a fundamental understanding of the superiority of bimetallic catalysts to their monometallic counterparts. One first challenging question is:" How will the two metals interact? Is there direct bonding between them?" In another words, people need to characterize the catalysts. Many techniques have been developed for the identification of the catalysts including, for example, $H_2$ and CO chemisorption, high-resolution electron microscopy, extended X-ray absorption fine structure (EXAFS), Mössbauer effect spectroscopy, $^{129}$Xe NMR spectroscopy, scanning tunneling microscopy(STM), and atomic force microscopy(AFM). [6] In particular, EXAFS spectroscopy, although it still developing rapidly, has become a valuable tool for obtaining structural information of supported catalysts most precisely when they are very small and nearly uniform. EXAFS investigations by Sinfelt performed on Pt-Ir alloy on $SiO_2$ support reveal the interatomic Pt-Ir distance is 2.751Å, which is close to the known interatomic distances for platinum-platinum and iridium-iridium in pure metals, 2.775 Å and 2.714 Å, respectively. It was concluded that there are significant direct platinum-iridium interactions in the bimetallic catalyst.[7]

Metal cluster complexes have aroused great interest as catalyst precursors, [8] following the proposal by Mutterties in 1975 that these complexes would exhibit novel properties. Muetterties proposed that metal clusters are analogues to metal surfaces where catalytic transformations of small molecules take place at the multicenter sites. In this

manner, the metal clusters can have reactivities different from those of mononuclear complexes, because they have neighboring metal centers that would be expected to facilitate reactions like those catalyzed on metal surfaces but which are not available to mononuclear complexes. One obvious advantage of metal clusters is that they already contain intimately bonded metal atoms which enable the cooperative interactions between metal atoms during the catalytic process. Another advantage related to using metal clusters as precursors to heterogeneous catalysts is the ability to monitor the reactions by various solution and solid state techniques like IR, NMR, mass spectrometry and X-ray diffraction analyses. In a typical process, supported metal cluster catalysts are made by impregnation of a porous support (e.g. $Al_2O_3$ and $SiO_2$) with an aqueous solution of metal clusters (e.g. $Ir_4(CO)_{12}$), after slow removal of solvent followed by heating in air (or under vacuum) and reduction in hydrogen. Studies by Gates have confirmed that the metal framework remains intact and the clusters are well dispersed after deposition on support and $H_2$ reduction and activation by high temperature.[9] This new approach, to some extent, provided a very good solution to uniformity of the metals particles throughout the catalyst. Thus, using metal clusters as catalyst precursors provides an apparent advantage for high dispersion in uniform size on supports in addition to facilitating predetermined stoichiometrically precise metal compositions.

Research interests in iridium for catalysis stem from the famous Vaska complex $IrCl(CO)(PPh_3)_2$ which shows the ability of iridium to engage in oxidative addition reactions, a fundamental reaction step in homogeneous catalysis. The work of Lauri Vaska showed that a variety of molecules A-B were able to add to $IrCl(CO)(PPh_3)_2$ to yield $Ir(A)(B)Cl(CO)(PPh_3)_2$, an oxidative addition product. [10] Yet, applications for

iridium in catalysis have developed slowly compared to those of other metals from the platinum group metals such as Pd, Pt, Ru, Rh which gained advantages over Ir and Os in the early work in homogeneous catalysis. [11] Today applications of iridium in catalysis continue to grow. There is great interest in the use of iridium for many applications in homogeneous and heterogeneous catalysis ever since the first demonstration of dehydrogenation of alkanes by a soluble iridium complex reported by Crabtree in 1979.[12] This discovery constitutes a C-H activation which spurred great interest to iridium applied in catalysis considering the importance of olefin intermediates in the commodity and petrochemical industries and the great versatility of olefins as reagents in organic synthesis.

Crabtree and his co-workers reported the cationic complex $[IrH_2(PPh_3)_2(acetone)_2][BF_4]$ to dehydrogenate cyclopentane or cyclooctane (COA) in the presence of TBE (3,3-dimethyl-1-butene or t-butylethene) which served as a hydrogen acceptor, to produce the corresponding cyclopentadiene or cyclooctadiene complexes (scheme 1.1).[12] Catalytic dehydrogenations of alkanes was a giant leap forward in Ir-catalyzed chemistry and has been drawn great attention to this element. Subsequently, a new family of pincer-ligated iridium complex investigated by Jensen, Kaska and Goldman[13] has shown excellent catalytic activity for dehydrogenation of cycloalkanes and long-term stability at high temperatures. Compared to Crabtree's system which suffered from limited turnover number ($\leq 70$), this new princer-ligated iridium complex was able to achieve close to 1,000 turnovers in the dehydrogenation of cyclodecane without an acceptor and selectively dehydrogenates the terminal position of n-alkanes to give α-olefins. [14] Dehydrogenation of alkanes has been proved to be the driving force

for many interesting examples of the activation of C-H bonds including alkane metathesis, borylation of arenes and silylation of arenes etc. [15]

Like other transition metals, iridium plays an important role in organic transformations through hydrogenation. By careful selection and design of the ligands, Ir-catalyzed hydrogenation is one of the most efficient methods for reduction of C=C, C=O, and C=N double bonds. For instance, iridium complexes containing bidentate diphosphines have been mainly used as catalysts in the asymmetric hydrogenation of imines for the preparation of chiral amines.[16] Iridium complexes with chiral N,P and C,N ligands show advantages over rhodium- and ruthenium-diphosphine complexes applied in traditional asymmetric hydrogenation with high enantioselectivity and unconstrained to substrates.[17] Another fantastic application of iridium complexes is to catalyze the hydrogen transfer reaction for the reduction of a range of substrates, typically an alcohol or formic acid, which has been termed " borrowing hydrogen". [18] In this chemistry, an iridium catalyst activates normally unreactive alcohols by removal ("borrow") of hydrogen to give an aldehyde or ketone intermediate. The more reactive aldehyde is then condensed with an amine and the return of hydrogen from the catalyst provides a method for the formation of amines or C-C bonds. (scheme 1.2)

Studies have shown that mixed-metal cluster complexes can serve as precursors to valuable bi- and multimetallic supported heterogeneous catalysts[19] with important applications ranging from 1) petroleum refining to 2) Fischer-Tropsch synthesis of hydrocarbon fuels and to 3) vehicle exhaust clean up. Although most catalytic applications are of a homogeneous type as discussed above, it has been shown that iridium clusters can serve as precursors to heterogeneous nanoscale catalysts that exhibit

good activity for the hydrogenation of aromatics and olefins.[6(a),20] When metals were loaded on supports, the catalytic performance of supported catalysts was influenced by the size and structure of the metal particles, the ligands bonded to the metal, and the identity of supports.

Studies by Gates and coworkers of supported iridium clusters reveals many interesting and unique behaviors of iridium in catalytic activities. 1)$Ir_4$ and $Ir_6$ cluster frames remained intact during catalysis. [6(a)] EXAFS spectroscopy showed that the first shell Ir-Ir coordination numbers characterizing both the fresh and used MgO-supported $Ir_4(CO)_{12}$ or $[HIr_4(CO)_{11}]^-$ are 3, the value for a tetrahedron, as in $Ir_4(CO)_{12}$ or $[HIr_4(CO)_{11}]^-$. EXAFS data show that decarbonylated $Ir_6$ clusters maintain the octahedral arrangement as the precursor hexairidium carbonyls had and, indicated a coordination number of approximately 4. Later studies revealed that the metal frame undergoes slight rearrangements (to swell and flex away from the support) to accommodate reactive intermediates. [20(d)]

2) Supported iridium clusters show size-dependent catalytic activities.[21] It was found that the rate of ethene hydrogenation on supported $Ir_4$ clusters is typically several times greater than that of $Ir_6$ clusters. It can be inferred that $Ir_6$ was more nearly saturated with hydrocarbon adsorbates that hindered the adsorption of hydrogen. It was also found that the catalytic activity increased several fold as mononuclear iridium was converted into clusters. A reasonable explanation is that by conversion of the mononuclear iridium complexes into small clusters provided neighboring iridium sites where both the coordination and activation of both ethene and hydrogen could take place.

3) Supports can behave as ligands and influence the catalytic activities.[21(c)] For iridium clusters supported on solids with widely different properties, e.g. highly dehydroxylated MgO, a strong electron-donor ligand, or highly dealuminated HY zeolite (DAY zeolite), an electron-withdrawing ligand, the performance for ethene hydrogenation of isostructural iridium species differed significantly. The activity of the iridium complexes on the zeolite was more than four times that of the isostructural iridium clusters on MgO, and it was even twenty times that of the monoiridium complexes on this support. Studies by IR and EXAFS spectroscopy showed that the iridium species were bonded to the MgO through two Ir-O bonds and bonded to the zeolites through Ir-Al bonds. It was inferred that the electron-withdrawing properties of the zeolite support enabled the iridium atoms to bond to both substrates ($C_2H_4$) and $H_2$ to facilitate the catalysis.

4) Sinter-Resistant supported iridium clusters form on certain supports. [22] It was found that triggered by the activation of $H_2$ and the formation of iridium hydride, accompanied by the breaking of iridium-support bonds led to the formation of $Ir_4$ clusters from zeolite supported $Ir(C_2H_4)_2$ complexes. Further investigations showed that treatments of iridium complexes on various supports under harsh reductive conditions (e.g., 837 K in $H_2$) led to the formation of only uniform iridium clusters limited to a diameter of ~ 1nm. Such iridium nanocluster catalysts resist sintering because the clusters of a critical size do not coalesce. They are "smart" catalysts with the properties that hinder the process of sintering, a process that generally causes deactivation of supported metal catalysts. Noteworthy, it was suggested that bimetallic clusters incorporating

iridium might also offer the advantages of resistance to sintering. This suggestion was validated by some recent experimental evidence [23] which may further stimulate great research interest in bimetallic catalysts containing iridium with similar advantages.

As discussed above, iridium exhibits interesting catalytic properties and shows possibilities to offer such interesting properties to bimetallic clusters incorporating iridium. To develop a better understanding of the synergies between iridium and other metals, much effort has been devoted to design new mixed metal cluster complexes containing iridium. [24] However, due to its low reactivity it is difficult in introduce other metals into tetrairidium dodecacarbonyl, a typical iridium reagent. Herein, we developed a new method for introducing main group metals into tetrairidium dodecacarbonyl include iridium-tin and iridium-germanium bimetallic compounds. We also obtained a σ-phenyl coordinated complex, $[Ir_4(CO)_{11}Ph]^-$, from which a fairly large number of iridium-gold, iridium-silver and iridium-copper have been obtained.

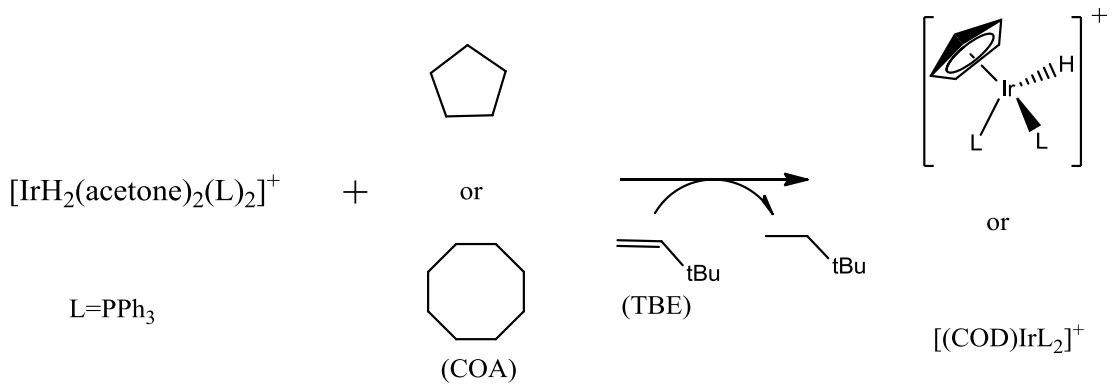


Scheme 1.1 Schematic diagram of dehydrogenation of cyclopentane or cyclooctane (COA) catalyzed by $[IrH_2(PPh_3)_2(acetone)_2][BF_4]$ in the presence of TBE.

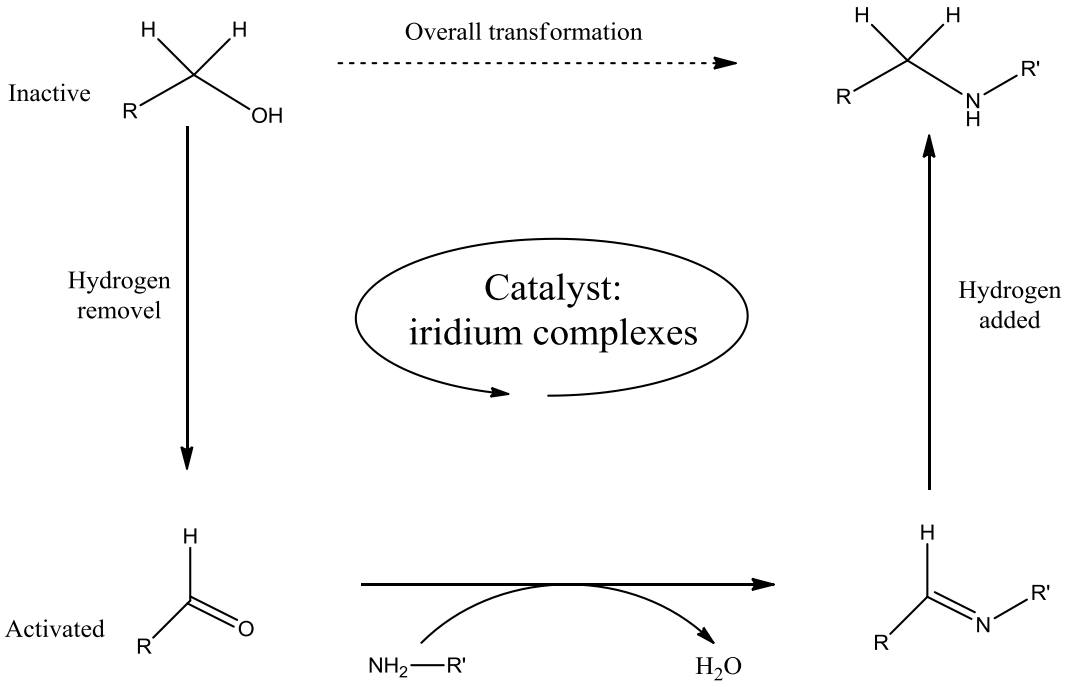


Scheme 1.2 Schematic diagram for hydrogen transfer catalysis.

## References


1. "*A Biographical Memoir of Vladimir Haesnsel*" written by Stanley Gembiki, published by the National Academy of Sciences in 2006.

2. Haensel, V. "*Chemistry of Petroleum Hydrocarbons*", eds Brooks, B.T.; Boord, C.E.;Kurtz, S.S. and Schmerling, L., New York, Reinhold 1955, 6, 189.

3. (a) Sinfelt, J.H.; Carter, J.L.; and Yates, D.J.C. *J. Catal.* 1972，24, 283-296. (b) Sinfelt, J.H.; Lam, Y.L.; Cusumano, J.A.; and Barnett, A. E. *J. Catal.* 1976, 42, 227-237. (c) Sinfelt, J.H. *J. Catal*. 1973, 29, 308-315.

4. (a) Sinfelt, J.H. *Bimetallic Catalysts: Discoveries, Concepts, and Applications*; Wiley, New York, 1983. (b) Sinfelt, J.H. and Via, G.H. *J.Catal.* 1979, 56, 1-11. (c) Sinfelt, J.H. *Chem. Eng. News.* 1972, 50, 18-19.

5. (a) Dombek, B.D. *Organometallics*, 1985, 4, 1707-1712. (b) Rice, R.W.; Lu, K. *J.Catal.* 1982, 77, 104-117. (c) Castiglioni, M.; Giordano, R.; Sappa, E. *J. Organomet.* Chem. 1987, 319, 167-181. (d) Burch, R. *J. Catal.* 1981, 71, 348-359. (e) Srinivasan, R.; Davis, B.H. *Platinum Met. Rev.* 1992, 36, 151. (f) Park, Y. K.; Ribeiro, F.H.; Somorjai, G.A. *J. Catal.* 1998, 178, 66-75.

6. (a) Gates, B.C. *Chem. Rev.* 1995, 95, 511-522. (b) Sayers, D.E.; Lytle, F.W.; and Stern, E. *Phys. Rev. Lett.* 1971, 27, 1204-1207.

7. Sinfelt, J.H.; Via, G.H. ; and Lytle, F.W. *J. Chem. Phys.* 1982, 76, 2779-2789.

8. (a) Muetterties, E. L. *Bull. Soc. Chim. Belg.* 1975, 84, 959-986. (b) Muetterties, E.L.; Rhodin, T.N.; Band, E.; Brucker, C.F.; Retzer, W.R. *Chem. Rev.* 1979, 79, 91-136. (c) Muetterties, E. L. *Bull. Soc. Chim. Belg.* 1976, 85, 451-470.

9. (a) Xu. Z.; Xiao, F.S.; Purnell, S.K.; Alexeev, Q.; Kawi, S.; Deutsch, S.E.; and Gates, B.C. *Nature*, 1994, 372, 346-348. (b) Gates, B.C. *Chem. Rev.* 1995, 95, 511-522. (c) Fung, A.S.; McDevitt, M.R.; Tooley, P.A.; Kelley, M.J.; Koningsberger, D.C.; Gates, B.C. *J.Catal.* 1993, 140, 190-208.

10. Vaska L. *Accounts. Chem. Res.* 1968, 1, 335-344.

11. Crabtree, R.H. *Top. Organomet. Chem.* 2011, 34, 1-10.

12. Crabtree, R.H.; Mihelcic, J.M.; Quirk, J.M. *J. Am. Chem. Soc.* 1979, 101, 7738-7740.

13. (a) Gupta, M.; Hagen, C.; Kaska, W. C.; Cramer, R. E.; Jensen C. M. *J. Am. Chem. Soc.* 1997, 119, 840-841. (b) Xu, W.; Rosini, G. P.; Gupta M.; Jensen C.M.; Kaska, W.C.; Krogh-Jespersen, K.; Goldman, A.S. *Chem. Commun.* 1997, 2273-3374.

14. (a) Liu, F.; Goldman, A.S. *Chem. Commun.* 1999, 655-656. (b) Liu, F.; Pak, E.B.; Singh, B.; Jensen, C.M.; Goldman, A.S. *J. Am. Chem. Soc.* 1999, 125, 7770-7771.

15. Choi, J.; Goldman, A. S. *Top. Organomet. Chem.* 2011, 34, 139-168.

16. (a) Sablong, R.; Osborn, J.A. *Tetrahedron: Asymmetry* 1996, 7, 3059. (b). Margalef-Catala, R.; Claver, C.; Salagre, P.; Fernandez, E. *Tetrahedron: Asymmetry* 2000, 11, 1469.

17. Woodmansee, D. H.; Pfaltz, A. *Top. Organomet. Chem.* 2011, 34, 31-76.

18. Watson, A.J.A.; Williams, J.M.J. *Science* 2010, 329, 635-636.

19. (a) Thomas, J.M.; Johnson, B.F.G.; Raja, R.; Sankar, G.; Midgley, P.A. *Acc. Chem. Res*. 2003, 36, 20-30. (b) Braunstein, P.; Rose, J. in *Catalysis by Di- and Polynuclear Metal Cluster Complexes*; Adams, R.D., Cotton, F.A.; Eds.; Wiley-VCH: New York, 1998; Chapter 13.

20. (a) Bayram, E.; Zahmakiran, M.; Ozkar, S.; Finke, R.G. *Langmuir* 2010, 26, 12455-12464. (b) Uzun, A.; Dixon, D.A.; Gates, B.C. *ChemCatChem* 2011, 3, 95-107. (c) Fonseca, G.S.; Umpierre, A.P.; Fichtner, P.F.P.; Teixeira, S.R.; Dupont, J. *Chem. Eur. J.* 2003, 9, 3263-3269. (d) Argo, A.M.; Odzak, J.F.; Goellner, J.F.; Lai, F.S.; Xiao, F.S.; Gates, B.C. *J.Phys.Chem. B* 2006, 110, 1775-1786.

21. (a) Xu, Z.; Xiao, F.S.; Purnell, S.K.; Alexeev, O.; Kawi, S.; Deutsch, S.E.; Gates, B.C. *Nature*, 1994, 372, 346-348. (b) Argo, A.M.; Odzak, J. F.; Gates, B.C. *J. Am. Chem. Soc.* 2003, 125, 7107-7115. (c) Lu, J.; Serna, P.; Aydin, C.; Browning, N.D.; Gates, B.C. *J. Am. Chem. Soc.* 2011, 133, 16186-16195.

22. (a) Lu, J.; Aydin, C.; Browning, N.D.; Gates, B.C. *J. Am. Chem. Soc.* 2012, 134, 5022-5025. (b) Lu, J.; Aydin, C.; Browning, N.D.; Wang, L.; Gates, B.C. *Catal. Lett.* 2012, 142, 1445-1451. (c) Aydin, C.; Lu. J.; Browning, N.D.; Gates, B.C. *Angew. Chem. Int. Ed.* 2012, 51, 5929-5934.

23. Piccolo, L.; Nassreddine, S.; Aouine, M.; Geantet, C. *J. Catal.* 2012, 292, 173-180.

24. (a) Arena, C. G.; Drommi, D.; Faraone, F.; Lanfranchi, M.; Nicolo, F.; Tiripicchio, A. *Organometallics*, 1996, 15, 3180-3175. (b) Braga, D.; Grepioni, F.; Livotto, F. S.; Vargas, M.D. *J. Organomet. Chem.* 1990, 391, C28-C32. (c) Fumagalli, A.; Della Pergola, R.; Bonacina, F.; Garlaschelli, L.; Moret, M.; Sironi, A. *J. Am. Chem. Soc.* 1989, 111, 165-173. (d) Araujo, M.H.; Avent, A.G.; Hitchcock, P.B.; Nixon, J.F.; Vargas, M.D. *Organometallics*, 1998, 17, 5460-5466. (e) Della Pergola, R.; Ceriotti, A.; Garlaschelli, L.; Demartin, F.; Manassero, M.; Masciocchi, N.; Sansoni, M. *Inorg. Chem.* 1993, 32, 3277-3281. (f) Della Pergola, R.; Garlaschelli, L.; Demartin, F.; Manassero, M.; Masciocchi, N.; Sansoni, M.; Fumagalli, A. *Dalton, Trans.* 1989, 1109-1116. (g) Benvenutti, M.H.; Hitchcock, P.B.; Nixon, J.F.; Vargas, M.D. *Chem. Commun.* 1996, 441-443. (h) Fumagalli, A.; Koetzle, T.F.; Takusagawa, F. *J. Organomet. Chem.* 1981, 213, 365-377. (i) Adams, R.D.; Captain, B.; Smith, J. L. *Inorg. Chem.* 2005, 44, 1413-1420. (j) Adams, R.D.; Captain, B.; Hall, M.B.; Smith, J. L.; Webster, C.E. *J. Am. Chem. Soc.* 2005, 127, 1007-1014.

# CHAPTER TWO

# A New Method for Introducing Tin Ligands to Tetrairidium Dodecacarbonyl

## Introduction

Tin has been shown to be a valuable modifier for both homogeneous[1] and heterogeneous[2-4] transition metal catalysts. It has been shown that introduction of tin will improve the selectivity of certain types of catalytic hydrogenation reactions.[5-9] Iridium is known to exhibit interesting catalytic properties,[10] however, due to its low reactivity, it is difficult in introduce tin ligands in tetrairidium dodecacarbonyl. We have recently shown that the triiridum complex $Ir_3(CO)_6(\mu\text{-}SnPh_2)_3(SnPh_3)_3$ is formed in a low yield from the reaction of $Ir_4(CO)_{12}$ with $SnPh_3$ at 125 $^oC$, eq. 2.1, but this reaction leads to degradation of the tetrairidium cluster.[11]

In an effort to find a more convenient route to tetrairidium-tin carbonyl complexes, we have examined the reactions of $Ir_4(CO)_{12}$ and $Ir_4(CO)_{11}(PPh_3)$ with $Ph_3SnOH$ under basic conditions. The reaction gave two products: $[Bu_4N][Ir_4(CO)_{11}(SnPh_3)]$, **2.1** (45% yield) and $[Bu_4N][Ir_4(CO)_{10}(SnPh_3)_2(\mu\text{-}H)]$, **2.2** (5.5% yield). Both products were characterized crystallographically. Compound **2.2** was also obtained from **2.1** by reaction with an additional quantity of $Ph_3SnOH$ in the presence of $[Bu_4N]OH$. The reaction of $Ir_4(CO)_{11}(PPh_3)$ with $Ph_3SnOH$ in the presence of $[Bu_4N]OH$ yielded the complex

$Ir_4(CO)_{10}(SnPh_3)(PPh_3)(\mu\text{-}H)$, **2.3** in 44% yield. Compound **2.3** was characterized crystallographically. It is proposed that the reactions occur by the addition of the anion $[OSnPh_3]^-$ to a CO ligand on $Ir_4(CO)_{12}$ to form a stannylmetallocarbonylate ligand that subsequently loses $CO_2$ with transfer of the $SnPh_3$ group to a metal atom.

It's noteworthy that the above assumption was verified by further investigation of similar reactions of $Os_3(CO)_{12}$ with the compounds $Ph_3MOH$, M = Sn, Ge in the presence of $[Bu_4N][OH]$ from which we have obtained the first examples of metal carbonyl cluster complexes containing bridging stannyl- and germyl-substituted metallocarboxylate ligands in the complexes $Os_3(CO)_{10}(\mu\text{-}O{=}COMPh_3)(\mu\text{-}OH)$, M = Sn, Ge, **2.4**, **2.5**, scheme 2.1. [12]

**Experimental Details**

**General Data**. Reagent grade solvents were dried by the standard procedures and were freshly distilled prior to use. Infrared spectra were recorded on a Thermo Nicolet Avatar 360 FT-IR spectrophotometer. $^1$H NMR spectra were recorded on a Varian Mercury 300 spectrometer operating at 300.1 MHz. Mass spectrometric (MS) measurements performed by a direct-exposure probe using electron impact ionization (EI) and electronspray ionization (ESI) were made on a VG 70S instrument. $SnPh_3OH$ and $Ir_4(CO)_{12}$ were obtained from STREM and were used without further purification. $Ir_4(CO)_{11}(PPh_3)$ was prepared according to the published procedure.[13] Product separations were performed by TLC in air on Analtech 0.25, 0.5 and 1.0 mm silica gel 60 Å $F_{254}$ glass plates.

**Reaction of $Ir_4(CO)_{12}$ with $SnPh_3OH$ in the presence of $Bu_4NOH$.**

A 70 mg (0.190 mmol) portion of $SnPh_3OH$ was added to 50 mg (0.045 mmol) of $Ir_4(CO)_{12}$ in 20 mL of methanol and 0.12 mL 2M $[Bu_4N]OH$. The reaction was heated to reflux for 30 min. The solvent was then removed *in vacuo*, and the product was then isolated by TLC using a 1:3 hexane/methylene chloride solvent mixture to yield 34.2 mg (45%) of $[Bu_4N][Ir_4(CO)_{11}(SnPh_3)]$, **2.1** and 5.0 mg (5.5%) of $[Bu_4N][HIr_4(CO)_{10}(SnPh_3)_2]$, **2.2**. Spectral data for **2.1**: IR $\nu_{CO}$ ($cm^{-1}$ in $CH_2Cl_2$): 2066(m), 2028(vs), 1990(s), 1823(m), 1804(m). $^1H$ NMR ($CDCl_3$, in ppm) $\delta$ = 7.17-7.53 (m, 15H, Ph), 0.90-0.93 (t, 12H, $CH_3$), 1.185-1.481(m, 8H, $CH_2$), 2.75-2.80 (t, 8H, $CH_2$). Mass Spec. ES(negative)/MS for **2.1:** *m*/*z*=1427 ($[Ir_4(CO)_{11}(SnPh_3)]^-$ anion). Spectral data for **2.2**: IR $\nu_{CO}$ ($cm^{-1}$ in $CH_2Cl_2$): 2064(m), 2035(vs), 2019(vs), 1991(m). $^1H$ NMR ($CDCl_3$, in ppm) $\delta$ = 7.21-7.49 (m, 30H, Ph), 0.96-0.99 (t, 12H, $CH_3$), 1.19-1.64(m, 8H, $CH_2$), 2.94-2.98 (t, 8H, $CH_2$), -19.69 (s, 1H, μ-H, $^2J_{Sn-H}$ = 9.51Hz). Mass Spec. ES(negative)/MS for **2.2** *m*/*z*=1749 ($[HIr_4(CO)_{10}(SnPh_3)_2]^-$ - H).

**Conversion of 2.1 to 2.2** A 22 mg (0.060 mmol) portion of $SnPh_3OH$ was added to 18.5 mg (0.011 mmol) of compound **2.1** in 20 mL methanol under nitrogen. 50 μL 2M $Bu_4NOH$ was added to the above mixture and stirred at r.t. for 15 h. The solvent was removed *in vacuo*, and the products were then isolated by TLC by using a 1:2 hexane/methylene chloride solvent mixture to yield 3.2 mg (18%) of compound **2.2** and 3.3 mg of unreacted compound **2.1**.

**Reaction of $Ir_4(CO)_{11}(PPh_3)$ with $SnPh_3OH$ in the presence of $[Bu_4N]OH$.**

A 42.0 mg (0.114 mmol) portion of $SnPh_3OH$ was added to 15.0 mg (0.011 mmol) of $Ir_4(CO)_{11}(PPh_3)$ in 25 mL of methanol and 50 μL 2M $[Bu_4N]OH$. The reaction was

stirred at rt for 16 h. The solvent was removed *in vacuo*, and the product was then isolated by TLC using a 3:1 hexane/methylene chloride solvent mixture. 6.6 mg (44% yield) of $HIr_4(CO)_{10}(SnPh_3)(PPh_3)$, **2.3**, 1.83 mg (13% yield) of $Ir_4(CO)_{10}(PPh_3)_2$[1], and 3.0 mg unreacted $Ir_4(CO)_{11}(PPh_3)$ (20%) was obtained. Spectral data for **2.3**: IR $\nu_{CO}$ ($cm^{-1}$ in $CH_2Cl_2$): 2085(s), 2056(vs), 2048(s), 2033(s), 2012(m), 1990(w). $^1H$ NMR ($CDCl_3$, in ppm) $\delta$ = 7.17-7.50 (m, 30H, Ph), -18.37 (s, 1H, μ-H). $^{31}P\{^1H\}$ NMR ($CDCl_3$) $\delta$ = -15.18 ppm (s, 1P) Mass Spec. ES(positive)/MS for **2.3:** *m*/*z*=1701 (M+K).

**Crystallographic Analyses:** Red single crystals of $[Et_4N][Ir_4(CO)_{11}(SnPh_3)]$, **2.1-Et** suitable for x-ray diffraction analyses were obtained by slow evaporation of solvent (hexane/methylene chloride) at -25 ℃ from a solution containing a mixture of compound **2.1** and $[Et_4N]Br$. Yellow crystals of **2.2** and orange crystals of **2.3** suitable for x-ray diffraction analyses were obtained by slow evaporation of solvent at -25 ℃ from solutions of the pure compound in hexane/methylene chloride solvent mixtures. The data crystals were glued onto the end of thin glass fibers. X-ray intensity data were measured by using a Bruker SMART APEX CCD-based diffractometer using Mo Kα radiation (λ = 0.71073 Å). The raw data frames were integrated with the SAINT+ program by using a narrow-frame integration algorithm[14]. Correction for Lorentz and polarization effects were also applied with SAINT+. An empirical absorption correction based on the multiple measurement of equivalent reflections was applied in each analysis by using the program SADABS. All structures were solved by a combination of direct methods and difference Fourier syntheses, and refined by full-matrix least-squares on $F^2$, using the SHELXTL software package[15]. All non-hydrogen atoms were refined with anisotropic displacement parameters. The hydrogen atoms on carbon atoms were placed in

geometrically idealized positions and included as standard riding atoms during the least-squares refinements. Crystal data, data collection parameters, and results of the analyses are listed in Table 2.1. Compounds **2.1** and **2.3** both crystallized in the triclinic crystal system. The space group *P-1* was assumed and confirmed by the successful solution and refinement of both structures. There are two symmetry independent molecules in the asymmetric unit in the structure of **2.3**. The Sn and P atoms for the $PPh_3$ and the $SnPh_3$ ligands in both independent molecules of **2.3** were disordered between these two ligand sites. The disorder was refined and converged to Sn1/P2 = 0.51/0.49, P1/Sn2 = 0.49/0.51 for molecule 1 and Sn3/P4 = 0.71/0.29, P3/Sn4 = 0.29/0.71 for molecule 2. The hydride ligands in both of the independent molecules of **2.3** were located by difference Fourier analysis and refined without restraints. Compound **2.2** crystallized in the monoclinic crystal system. The space group $P2_1/c$ was identified uniquely on the basis of the systematic absences in the intensity data. The hydrido ligand in **2.2** was located and refined in the analysis with the restraint Ir – H = 1.80 Å.

**Results and Discussion**

Two products $[Bu_4N][Ir_4(CO)_{11}(SnPh_3)]$, **2.1** (45% yield) and $[Bu_4N][Ir_4(CO)_{10}(SnPh_3)_2(\mu\text{-}H)]$, **2.2** (5.5% yield) were obtained from the reaction of $Ir_4(CO)_{12}$ with $Ph_3SnOH$ in the presence of $[Bu_4N]OH$ in methanol solvent at reflux for 30 min, see Scheme 2.2.

Compound **2.2** can be obtained from **2.1** in 18% yield by treatment with $Ph_3SnOH$ in methanol solvent in the presence of $[Bu_4N]OH$ at 25 $^oC$ over 15 h. The structures of the complex anions of **2.1** and **2.2** were established by a combination IR, $^1H$ NMR,

negative ion mass spectra and single-crystal X-ray diffraction analyses of their $[Et_4N]^+$ and $[Bu_4N]^+$ salts, respectively. An ORTEP diagram of the structure of the anion of **2.1** is shown in Figure 2.1. The anion consists of a tetrahedral cluster of four iridium atoms with one $SnPh_3$ ligand and eleven carbonyl ligands. Three of the carbonyl ligands are edge-bridging ligands about the Ir(1) – Ir(3) triangular group of metal atoms. All the others are linear terminal carbonyl ligands. The Ir – Ir bond distances range from 2.7061(4) Å - 2.7610(3) Å. These values are slightly longer than the Ir – Ir distances of 2.692 Å found in $Ir_4(CO)_{12}$ which has a disordered structure in the solid state.[16] The $SnPh_3$ ligand lies approximately trans to the Ir1 – Ir4 bond, Ir4 – Ir1– Sn1 = 164.246(15)$^o$. The Ir1 – Sn1 distance, 2.6358(4) Å, is significantly shorter than the Ir – Sn distances to the $SnPh_3$ ligands found in the crowded triiridium cluster complex $Ir_3(CO)_6(SnPh_3)_3(\mu\text{-}SnPh_2)_3$, 2.6736(9) Å - 2.6981(11) Å,[11] but it is similar to the Ir – Sn distance 2.6216(5) Å found in the less-crowded mono-iridium complex $Ir(COD)(CO)_2SnPh_3$.[17]

An ORTEP diagram of the structure of the anion of **2.2** is shown in Figure 2.2. The anion consists of a tetrahedral cluster of four iridium atoms with two $SnPh_3$ ligands, one on each of the two neighboring iridium atoms, Ir(1) and Ir(2). Each tin-substituted iridium atom contains two linear terminal carbonyl ligands; the other two iridium atoms have three carbonyl ligands. There is a bridging hydrido ligand across the Ir(1) – Ir(2) bond, $\delta$ = -19.69 ($^2J_{Sn\text{-}H}$ = 9.51Hz) in the H NMR spectrum. As expected[18], the hydride-bridged Ir – Ir distance, 2.8610(6) Å, is significantly longer than the unbridged Ir – Ir distances which range from 2.7072(7) Å - 2.7227(7) Å. The Ir – Sn bond distances, Ir1 - Sn1 = 2.6450(9) Å and Ir2 - Sn2 = 2.6627(10) Å, are similar to that found in **2.1**. Each of the metal atoms in **2.1** and **2.2** has 18 electron configurations.

For comparison, we have also investigated the reaction of the $PPh_3$ derivative of $Ir_4(CO)_{11}(PPh_3)$[13] with $Ph_3SnOH$. The new tin complex $Ir_4(CO)_{10}(SnPh_3)(PPh_3)(\mu\text{-}H)$, **2.3** was isolated by TLC in 44% yield after stirring a solution of $Ph_3SnOH$ with $Ir_4(CO)_{11}(PPh_3)$ with $[Bu_4N]OH$ for 16 h at 25 $^oC$. An ORTEP diagram of the molecular structure of **2.3** is shown in Figure 2.3. In the solid state, there are two independent molecules of **2.3** in the asymmetric crystal unit. Both molecules are structurally similar and contain one $PPh_3$ ligand and one $SnPh_3$ ligand. The $PPh_3$ and $SnPh_3$ ligands are disordered in both molecules; thus, the Ir – Sn/P distances measured here are not of high accuracy, but the structural analysis does confirm the gross structure of molecule. The tetrahedral arrangement of iridium atoms is not disordered so the Ir – Ir distances are reliable. The Ir – Ir bond between the $PPh_3$ and $SnPh_3$ ligands contains a bridging hydrido ligand and this Ir – Ir distance, molecule 1: Ir1 – Ir2 = 2.8851(5) Å, molecule 2: Ir5 – Ir6 = 2.8730(5) Å, is significantly longer than the other Ir – Ir distances which range from 2.7012(5) Å - 2.7159(5) Å.[18] The hydride ligand exhibits the usual upfield shift, $\delta$ = -18.37. The phosphine ligand exhibits at typical $^{31}P$ resonance shift, $\delta$ = -15.18 ppm.

Although **2.3** is an uncharged, neutral molecule, we have been not yet unable to isolate any uncharged forms of the two anions of **2.1** and **2.2** by acidification with protic acids. This may be due simply to the relative differences in basicity of the corresponding anions. Because of the presence of the $PPh_3$ ligand, an anionic cluster derived from **2.3** should be considerably more basic than that of **2.1** and thus may be more stable in a protonated form. These studies are still in progress.

It is worthwhile to consider mechanisms for the formation of the anions **2.1** and **2.2** and the neutral molecule **2.3**. A number of years ago, Garlaschelli et al. showed that

alkoxides add to the carbonyl ligands of $Ir_4(CO)_{12}$ to form metallocarboxylate ligands.[19] In the basic media used herein, a similar process involving $[OSnPh_3]^-$ could lead to a similar triphenylstannylmetallocarboxylate, such as **A**, see Scheme 2.3. Stannylmetallocarboxylate complexes have been observed previously although they have been obtained by different procedures.[20-21] In these complexes, the tin atom is typically bonded to both oxygen atoms, but these ligand groups are known to undergo decarboxylation that lead to metal – tin bonds.[20] A similar loss of $CO_2$ from **A** and a transfer of the $SnPh_3$ group to an iridium atom would lead to the anion **2.1**. A similar process occurring with $Ir_4(CO)_{11}(PPh_3)$ combined with a proton addition step would yield **2.3**. A second application of this mechanism to **2.1** could lead to **2.2**. We believe that reactions of $[OSnR_3]^-$ anions with metal carbonyl complexes could be general and lead to a variety of new tin-containing transition metal carbonyl complexes that may be useful as precursors to new tin-containing homogeneous and heterogeneous catalysts.

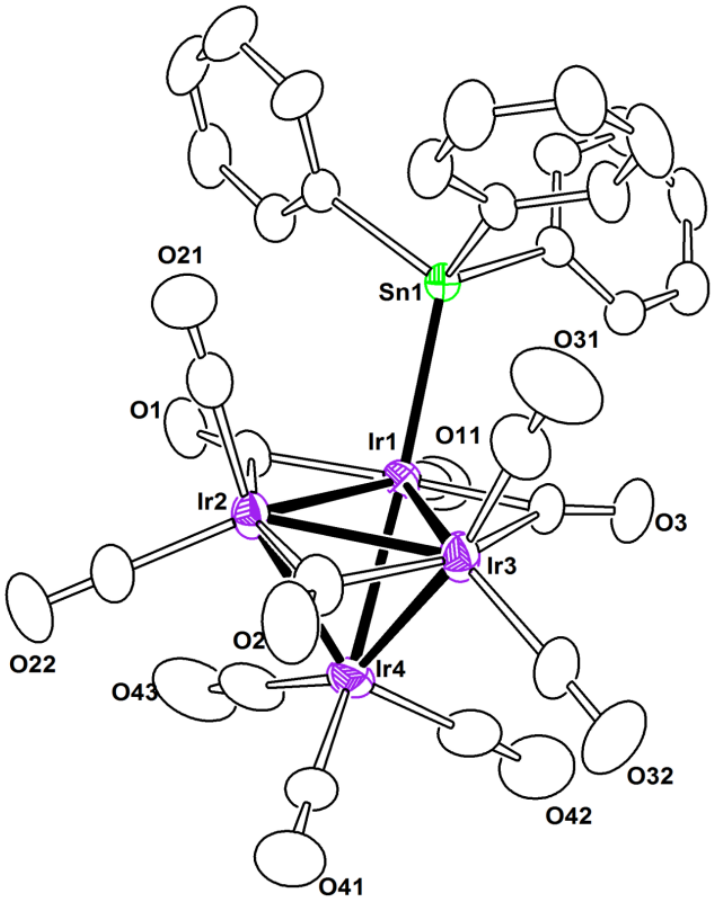


**Figure 2.1.** An ORTEP diagram of the molecular structure of the anion $[Ir_4(CO)_{11}(SnPh_3)]^-$ of **2.1-Et** showing 30% probability thermal ellipsoids.

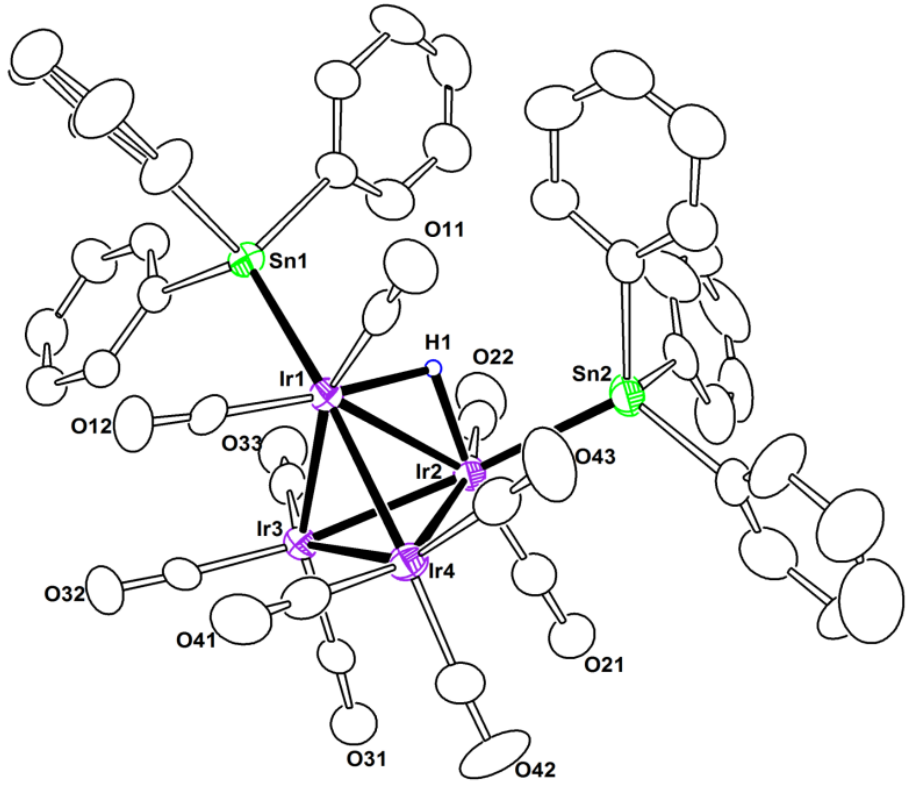


**Figure 2.2.** An ORTEP diagram of the molecular structure of $[HIr_4(CO)_{10}(SnPh_3)_2]^-$, **2.2**, showing 30% probability thermal ellipsoids.

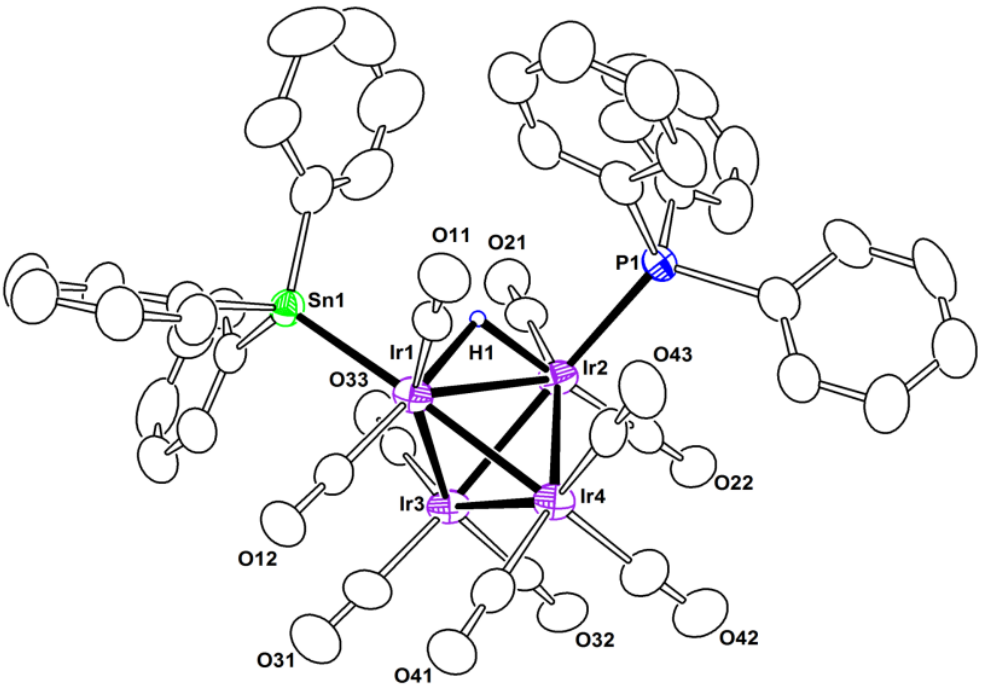


**Figure 2.3.** An ORTEP diagram of the molecular structure of $HIr_4(CO)_{10}(SnPh_3)(PPh_3)$, **2.3**, showing 30% probability thermal ellipsoids (the disorder between Sn and P is not shown).

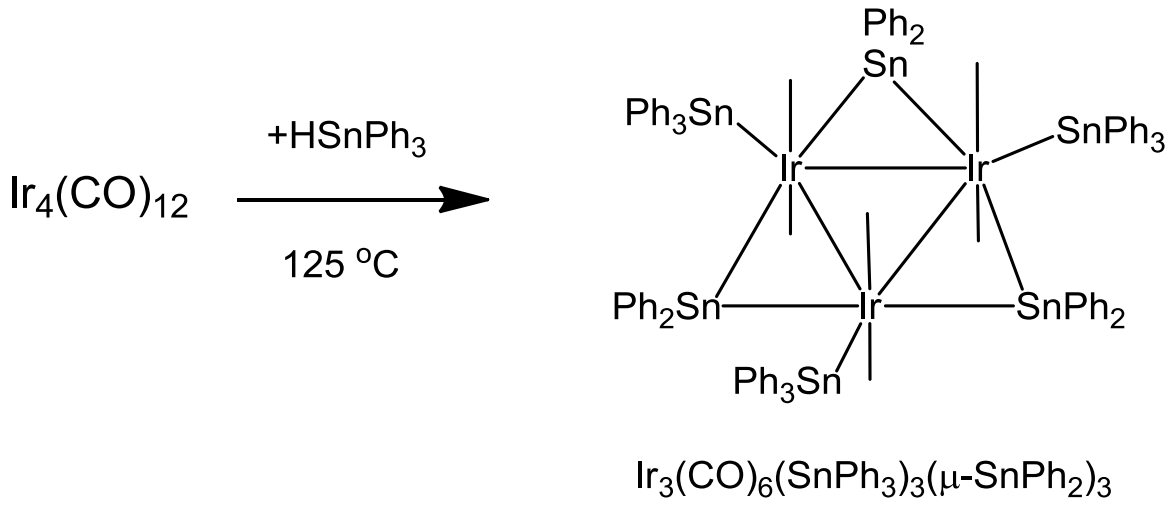


Equation 2.1 Reaction of $Ir_4(CO)_{12}$ with $HSnPh_3$ at 125℃.

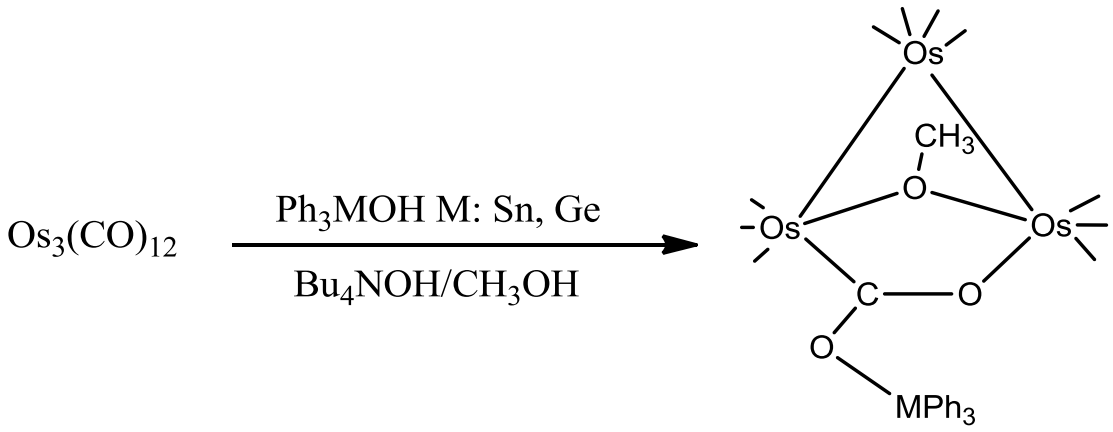


M= Sn, **2.4**; Ge, **2.5**

Scheme 2.1 Schematic diagram of the reaction of $Os_3(CO)_{12}$ with $Ph_3SnOH$ and $Ph_3GeOH$ under basic conditions.

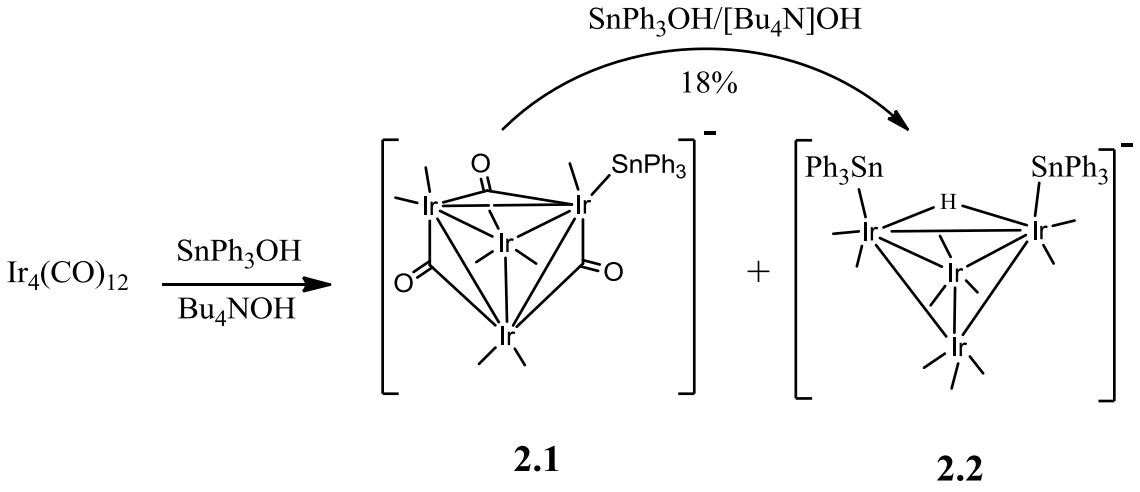


Scheme 2.2 Schematic diagram of reaction of $Ir_4(CO)_{12}$ with $SnPh_3OH$ in the presence of $[Bu_4N]OH$.

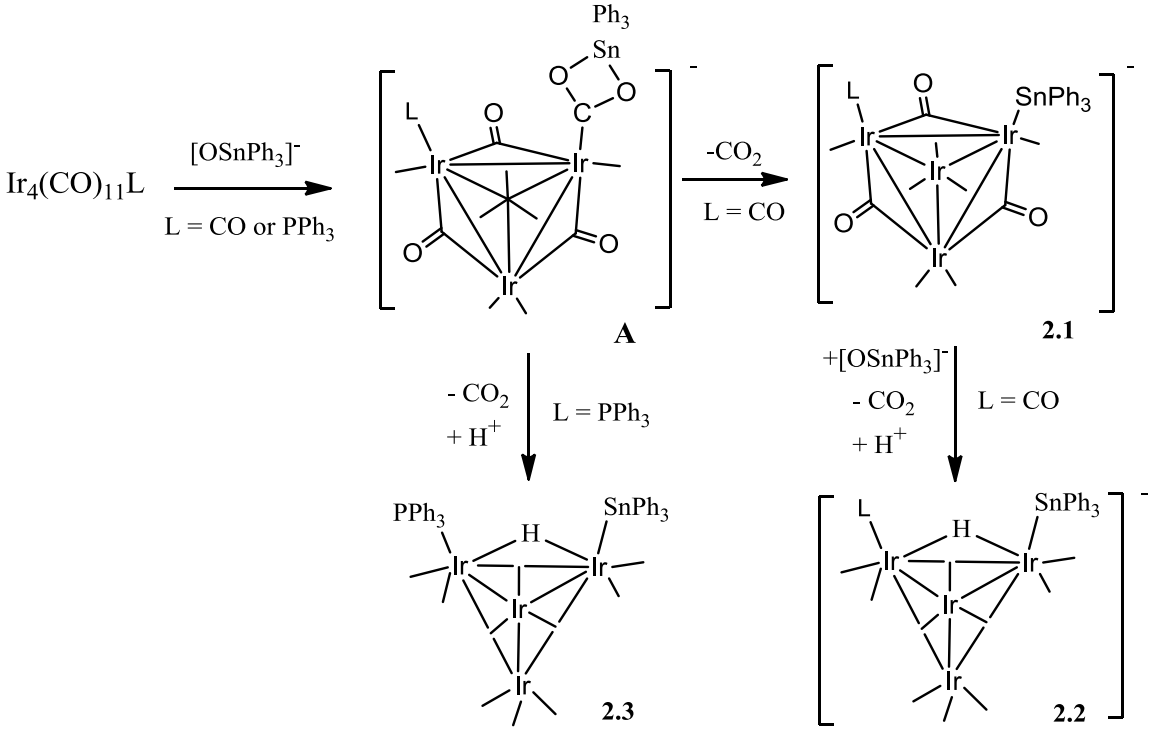


Scheme 2.3 Proposed mechanism for the formation of the anions **2.1** and **2.2** and the neutral molecule **2.3**.

**Table 2.1. Crystallographic Data for Compounds 2.1, 2.2 and 2.3.**

| Compound | **1** | **2** | **3** |
|---|---|---|---|
| Empirical formula | $Ir_4Sn_1C_{37}H_{35}O_{11}N_1$ | $Ir_4Sn_2C_{62}H_{67}O_{10}N_1$ | $Ir_4P_1Sn_1C_{46}H_{31}O_{10}$ |
| Formula weight | 1557.25 | 1992.48 | 1662.28 |
| Crystal system | Triclinic | Monoclinic | Triclinic |
| Lattice parameters | | | |
| a (Å) | 11.4876(5) | 17.4174(5) | 14.9667(5) |
| b (Å) | 13.0624(6) | 18.1114(5) | 15.1697(5) |
| c (Å) | 14.9583(7) | 21.1090(6) | 22.6389(8) |
| $\alpha$ (deg) | 84.5810(10) | 90 | 87.5100(10) |
| $\beta$ (deg) | 87.8580(10) | 104.0800(10) | 80.4450(10) |
| $\gamma$ (deg) | 77.7450(10) | 90 | 68.5890(10) |
| V ($Å^3$) | 2183.28(17) | 6458.9(3) | 4718.0(3) |
| Space group | P-1 | $P2_1/c$ | P-1 |
| Z value | 2 | 4 | 4 |
| $\rho_{calc}$ (g / $cm^3$) | 3.279 | 2.049 | 2.339 |
| $\mu$ (Mo K$\alpha$) ($mm^{-1}$) | 19.128 | 9.024 | 11.852 |
| Temperature (K) | 294(2) | 294(2) | 294(2) |
| $2\Theta_{max}$ (°) | 56.60 | 50.06 | 50.06 |
| No. Obs. ( $I > 2\sigma(I)$) | 7714 | 11413 | 16642 |
| No. Parameters | 491 | 719 | 1127 |
| Goodness of fit (GOF) | 1.045 | 1.047 | 1.006 |
| Max. shift in cycle | 0.001 | 0.001 | 0.001 |
| Residuals*: R1; wR2 | 0.0298; 0.0763 | 0.0505; 0.1128 | 0.0364; 0.0803 |
| Absorption Correction, | Multi-scan | Multi-scan | Multi-scan |
| Max/min | 1.000 / 0.362854 | 1.000 / 0.251373 | 1.000 / 0.654 |
| Largest peak in Final | 1.672 | 1.310 | 1.553 |

[a] $R = \Sigma_{hkl}(||F_{obs}|-|F_{calc}||)/\Sigma_{hkl}|F_{obs}|$; $R_w = [\Sigma_{hkl}w(|F_{obs}|-|F_{calc}|)^2/\Sigma_{hkl}wF^2_{obs}]^{1/2}$; $w = 1/\sigma^2(F_{obs})$; GOF = $[\Sigma_{hkl}w(|F_{obs}|-|F_{calc}|)^2/(n_{data} - n_{vari})]^{1/2}$.

Table 2.2 Selected intramolecular angles and bond distances for compound **2.1**.[a]

| **Distances** | | | **Angles** | | | |
|---|---|---|---|---|---|---|
| Atom | Atom | Distance (Å) | Atom | Atom | Atom | Angle(deg) |
| Ir1 | Ir2 | 2.7610(3) | Sn1 | Ir1 | Ir2 | 107.660(13) |
| Ir1 | Ir3 | 2.7616(4) | Sn1 | Ir1 | Ir4 | 164.246(15) |
| Ir1 | Ir4 | 2.7435(4) | | | | |
| Ir1 | Sn1 | 2.6358(4) | | | | |

[a] Estimated Standard deviations in the least significant figure are given in parentheses.

Table 2.3 Selected intramolecular angles and bond distances for compound **2.2**.[a]

| **Distances** | | | **Angles** | | | |
|---|---|---|---|---|---|---|
| Atom | Atom | Distance (Å) | Atom | Atom | Atom | Angle(deg) |
| Ir1 | Ir2 | 2.8609(6) | Sn1 | Ir1 | Ir4 | 165.74(3) |
| Ir1 | Ir3 | 2.7115(6) | Sn2 | Ir2 | Ir3 | 163.86(3) |
| Ir1 | H1 | 1.801(15) | | | | |
| Ir1 | Sn1 | 2.6446(8) | | | | |
| Ir2 | H1 | 1.796(15) | | | | |
| Ir2 | Sn2 | 2.6626(10) | | | | |

[a] Estimated Standard deviations in the least significant figure are given in parentheses.

Table 2.4 Selected intramolecular angles and bond distances for compound **2.3** (molecule 1).[a]

| **Distances** | | | **Angles** | | | |
|---|---|---|---|---|---|---|
| Atom | Atom | Distance (Å) | Atom | Atom | Atom | Angle(deg) |
| Ir1 | Ir2 | 2.8851(5) | Sn1(P2) | Ir1 | Ir4 | 166.54(4) |
| Ir1 | Ir3 | 2.7100(5) | P1(Sn2) | Ir2 | Ir3 | 167.24(3) |
| Ir1 | H1 | 1.76(5) | | | | |
| Ir1 | Sn1(P2) | 2.5212(10) | | | | |
| Ir2 | H1 | 1.79(6) | | | | |
| Ir2 | P1(Sn2) | 2.5126(10) | | | | |

[a] Estimated Standard deviations in the least significant figure are given in parentheses.

## References


1. Holt, M.S.; Wilson, W.L.; Nelson, J.H. *Chem. Rev.* **1989**, *89*, 11-49.

2. Burch, R.; Garla, L.C. *J. Catal.* **1981**, *71*, 360-372.

3. Park, Y.-K.; Ribeiro, F. H.; Somorjai, G. A., *J. Catal.* **1998**, *178*, 66-75.

4. Jerdev, D. I.; Olivas, A.; Koel, B. E., *J. Catal.* **2002**, *205*, 278-288.

5. Adams, R. D.; Trufan, E., *Phil. Trans Royal. Soc.* **2010**, *368*, 1473-1493.

6. Thomas, J. M.; Adams, R. D.; Boswell, E. M.; Captain, B.; Grönbeck, H.; Raja, R., *Faraday Disc.* **2008**, *138*, 301-315.

7. Hungria, A. B.; Raja, R.; Adams, R. D.; Captain, B.; Thomas, J. M.; Midgley, P. A.; Golvenko, V., Johnson, B. F. G., *Angew. Chem. int. Ed.*, **2006**, *45*, 4782-4785.

8. Adams, R. D.; Boswell, E. M.; Captain, B.; Hungria, A. B.; Midgley, P. A.; Raja, R.; Thomas, J. M., *Angew. Chem.. int. Ed.*, **2007**, *46*, 8182-8185.

9. Adams, R. D.; Blom, D. A.; Captain, B.; Raja, R.; Thomas, J. M.; Trufan, E., *Langmuir*, **2008**, *24*, 9223-9226.

10. (a) Gates, B. C. *Chem. Rev.* **1995**, *95*, 511-522. (b) Argo, A. M.; Odzak, J. F.; Goellner, J. F.; Lai, F. S.; Xiao, F.-S.; Gates, B. C. *J. Phys. Chem. B* **2006**, *110*, 1775-1786. (c) Argo, A. M.; Odzak, J. F.; Gates, B. C. *J. Am. Chem. Soc.* **2003**, *125*, 7107-7115. (d) Xu, Z.; Xiao, F.-S.; Purnell, S. K.; Alexeev, O.; Kawi, S.; Deutsch, S.; Gates, B. C. *Nature* **1994**, *372*, 346-348. (e) Li, F.; Gates, B. C. *J. Phys. Chem. C* **2007**, *111* 262-267. (f) Moura, F. C. C.; dos Santos, E. N.; Lago, R. M.; Vargas, M. D.; Araujo, M. H. *J. Molec. Catal. A: Chem.* **2005**, *226*, 243 – 251.

11. Adams, R. D.; Captain, B.; Smith, Jr., J. L. *Inorg. Chem.* **2005**, *44*, 1413 – 1420.

12. Adams, R.D.; Chen, M.; Trufan, E. *J. Organomet. Chem.* **2011**, 2894-2898.

13. Ros, R.; Scrivanti, A. *J. Chem. Soc. Dalton Trans.* **1986**, 11 2411-2421.

14. SAINT+, version 6.2a, Bruker Analytical X-ray Systems, Inc., Madison, WI, 2001.

15. G. M. Sheldrick, SHELXTL, version 6.1, Bruker Analytical X-ray Systems, Inc., Madison, WI, 1997

16. Churchill, M. R.; Hutchinson, J. P. *Inorg. Chem.* **1987**, *17*, 3528 – 3535.

17. Adams, R. D.; Trufan, E. *Organometallics* **2010**, *29*, 4346-4353.

18. Bau, R.; Drabnis, M. H. *Inorg. Chim. Acta* **1997**, *259*, 27-50. (b) Teller, R. G.; Bau, R., *Struc. Bonding* **1981**, 41, 1-82..

19. Garlaschelli, L.; Martinengo, S.; Chini, P.; Canziani, F.; Bau, R. *J. Organomet. Chem.* **1981**, *213*, 379-388.

20. Senn, D. R.; Gladysz, J. A.; Emerson, K.; Larsen, R. D. *Inorg. Chem.* **1987**, *17*, 2737-2739.

21. Hirano, M.; Akita, M.; Tani, K.; Kumagai, K.; Kasuga, N.; Fukuoka, A.; Komiya, S. *Organometallics* **1997**, *16*, 4206-4213.

# CHAPTER THREE

## Synthesis and Structures of New Tetrairidium Carbonyl Clusters Containing Phenylgermyl Ligands

### Introduction

Iridium is notable for catalyzed C-H activations especially since the first dehydrogenation of alkanes by a soluble iridium complex reported by Crabtree in 1979.[1] Applications of iridium in catalysis continue to grow, ranging from hydrogenation of hydrocarbons,[2] selective ring opening of naphthenes[3] to dehydrogenation of many organic substrates.[4] Although most of the catalytic applications are of a homogeneous type, iridium carbonyl cluster complexes have been shown to serve as precursors to heterogeneous nanoscale catalysts that exhibit good activity for the hydrogenation of aromatics and olefins.[5]

Recently, iridium shows some unique and interesting catalytic properties studied by Gates.[6] For instance, it's found that the catalytic activity of tetrairidium in ethylene hydrogenation is typically several times greater than that of hexairidium and mononuclear iridium. A reasonable explanation is that tetrairidium is of moderate size and will provide neighboring iridium sites where both coordination and activation of both ethylene and hydrogen can take place. In comparasion, hexairidium was more nearly saturated with hydrocarbon adorbates that hindered the adsorption of hydrogen. Mononulcear iridium lacks of neighboring iridium sites to facilitate the reactions. It's also found that treatments of mononuclear iridium complexes on various supports under harsh reductive conditions

(e.g. 837 K in $H_2$) lead to the formation of uniform tetrairidium cluster limited to a diagmeter of ~1 nm. Such supported iridium nanoclusters were termed "smart catalysts" because they show resistance to sintering behavior in contrast to many other noble metals.[7] Noteworthy, it's suggested that it might also offer such advantages of resistance to sintering to those bimetallic clusters incorporating iridium.

Germanium has been shown to be an valuable modifier of important heterogeneous catalysts.[8] The addition of germanium to iridium catalysts has been shown to improve the selectivity for aromatization reactions and hydrogenation of certain unsaturated hydrocarbons.[9] There have been only a few reports of iridium carbonyl cluster complexes containing organogermanium ligands to date. Examples of tetrahedral iridium complexes containing germanium are very rare.[10] Most of them were made either through condensation of mononuclear iridium or by the reactions of tetrairidium dodecacarbonyl complex with organogermanes, see Scheme 3.1. It is difficult to maintain the tetrahedral arrangement of the iridium atoms in these reaction.[10b] Most of the products are bi- or triiridium cluster complexes and only one of them, $Ir_4(CO)_7(GePh_3)(\mu\text{-}GePh_2)[\mu_3\text{-}\eta^2\text{-}GePh(C_6H_4)](\mu\text{-}H)_2$ made in low yield,[10b] contains tetrahedral iridium.

We have now investigated the reaction of $Ir_4(CO)_{11}(PPh_3)$ with $GePh_3H$. A series of new tetrahedral tetrairidium carbonyl cluster complexes, including $Ir_4(CO)_{10}(PPh_3)(GePh_3)(\mu\text{-}H)$, **3.1**, $Ir_4(CO)_{10}(PPh_3)(\mu\text{-}GePh_2)$, **3.2**, $Ir_4(CO)_7(PPh_3)(GePh_2)(GePh_3)(\mu_3\text{-}\eta^2\text{-}GePhC_6H_4)(\mu\text{-}H)_2$, **3.3** and $Ir_4(CO)_7(PPh_3)(GePh_2)_2(\mu_3\text{-}\eta^2\text{-}GePhC_6H_4)(\mu\text{-}H)$, **3.5** have been obtained and have been structurally characterized. We have also found that compound **3.2** reacts with $GePh_2H_2$ to yield the new compound $Ir_4(CO)_6(PPh_3)(GePh_2)_3(GePh_2H)(\mu\text{-}H)_3$, **3.6** which is also a

tetrahedral iridium carbonyl cluster complex containing up to four phenylgermanium ligands.

## Experimental Section

**General Data**. Reagent grade solvents were dried by the standard procedures and were freshly distilled prior to use. Infrared spectra were recorded on a Thermo Nicolet Avatar 360 FT-IR spectrophotometer. Room temperature $^{1}H$ NMR and $^{31}P\{^{1}H\}$ NMR were recorded on a Bruker Avance/DRX 400 NMR spectrometer operating at 300.1 and 162.0 MHz, respectively. Mass spectrometric (MS) measurements performed by a direct-exposure probe using electron impact ionization (EI) and electronspray ionization(ESI) were made on a VG 70S instrument. $GePh_3H$ and $GePh_2H_2$ were obtained from Gelest and were used without further purification. $Ir_4(CO)_{11}(PPh_3)$ was prepared according to the published procedure[11]. Product separations were performed by TLC in air on Analtech 0.25, 0.5 and 1.0 mm silica gel 60 Å $F_{254}$ glass plates.

### Synthesis of $Ir_4(CO)_{10}(PPh_3)(GePh_3)(\mu\text{-}H)$, 3.1.

A 20 mg (0.066 mmol) portion of $GePh_3H$ was added to 32 mg (0.024 mmol) of $Ir_4(CO)_{11}PPh_3$ in 20 mL of $CH_2Cl_2$. Then 2.4 mg (0.032 mmol) of $Me_3NO$ was added to above solution, and the mixture was stirred for 30 min at room temperature until the yellow solution turned red. The solvent was then removed *in vacuo*, and the product was then isolated by TLC using a 3:1 hexane/methylene chloride solvent mixture to yield 15.0 mg (54%) of $Ir_4(CO)_{10}(PPh_3)(GePh_3)(\mu\text{-}H)$, **3.1** and 9.1 mg $Ir_4(CO)_{11}PPh_3$ (recovered). Spectral data for **3.1**: IR $\nu_{CO}$ ($cm^{-1}$ in $CH_2Cl_2$): 2085(s), 2056(vs), 2047(s), 2033(s), 2012(m), 1991(w). $^{1}H$ NMR ($CDCl_3$, in ppm) $\delta$ = 7.11-7.47 (m, 30H, Ph), -17.88(s, 1H,

μ-H). $^{31}P\{^{1}H\}$ NMR ($CDCl_3$) δ = -15.99 ppm (s, $1PPh_3$) Mass Spec. ES(positive)/MS for **3.1:** *m*/*z*=1616 ($M^+$), 1655 (M+K).

**Synthesis of $Ir_4(CO)_{10}(PPh_3)(\mu\text{-}GePh_2)$, 3.2.**

A 12 mg (0.007 mmol) portion of $Ir_4(\mu\text{-}H)(CO)_{10}(PPh_3)(GePh_3)$, **3.1** was dissolved in 10 mL $CH_2Cl_2$. The solution was heated to reflux for 1.5 hours. The solvent was then removed *in vacuo*, and the product was then isolated by TLC using a 3:1 hexane/methylene chloride solvent mixture to yield 10.8 mg (95%) of $Ir_4(CO)_{10}(PPh_3)(\mu\text{-}GePh_2)$, **3.2.** Spectral data for **3.2**: IR $\nu_{CO}$ ($cm^{-1}$ in $CH_2Cl_2$): 2076(s), 2038(vs), 2018(s), 2001(m), 1861(w), 1811(m). $^{1}H$ NMR ($CDCl_3$, in ppm) δ = 7.18-7.45 (m, 25H, Ph). $^{31}P\{^{1}H\}$ NMR ($CDCl_3$) δ = -14.34 ppm (s, $1PPh_3$) Mass Spec. ES(negative)/MS for **3.2:** *m*/*z*=1619 ($M+Br^-$), 1583 ($M+HC_2O^-$).

**Conversion of 3.1 to 3.2 in NMR tube.**

A 14 mg (0.009 mmol) portion of $Ir_4(CO)_{10}(PPh_3)(GePh_3)(\mu\text{-}H)$, **3.1** was dissolved in $CDCl_3$ in an NMR tube. The NMR tube was placed in 40 ℃ oil-bath for 2 hours. $^{1}H$ NMR experiment was performed before and after heating which showed the disappearance of bridged hydride (s, -17.88 ppm) and the appearance of benzene (s, 7.36 ppm) which indicate the formation of compound **3.2** through the cleavage of one molecular of benzene.

**Reaction of 3.2 with $GePh_3H$**

A 11 mg (0.036 mmol) portion of $GePh_3H$ was added to 11 mg (0.007 mmol) of $Ir_4(CO)_{10}(PPh_3)(\mu\text{-}GePh_2)$, **3.2** in 20 mL of hexane. The mixture was heated to reflux for

1 hour until the yellow solution turned red. The solvent was then removed *in vacuo*, and the product was then isolated by TLC using a 3:1 hexane/methylene chloride solvent mixture to yield 6.4 mg (45%) of orange $Ir_4(CO)_7(PPh_3)(GePh_2)(GePh_3)(\mu_3\text{-}\eta^2\text{-}GePhC_6H_4)(\mu\text{-}H)_2$, **3.3** and 1.4 mg (yield 10%) of yellow $Ir_4(CO)_7(GePh_2)_2(GePh_3)(\mu_3\text{-}\eta^2\text{-}GePhC_6H_4)(\mu\text{-}H)_2$[10(b)], **3.4**. Spectral data for **3.3**: IR $\nu_{CO}$ ($cm^{-1}$ in $CH_2Cl_2$): 2077(m), 2038(vs), 2015(s), 1977(w), 1844(m). $^1H$ NMR ($CDCl_3$, in ppm) $\delta$ = 6.80-7.58 (m, 49H, Ph), -16.87(d, 1H, $\mu$-H $J_{P\text{-}H}$= 9.0Hz), -21.56(d, 1H, $\mu$-H $J_{P\text{-}H}$= 8.4Hz). $^{31}P\{^1H\}$ NMR ($CDCl_3$) $\delta$ = 35.76 ppm (s, $1PPh_3$) Mass Spec. ES(positive)/MS for **3.3:** *m*/*z*=2025 (M+K). ES(negative)/MS for **3.3:** *m*/*z*=2031 ($M+HC_2O^-$).

**Synthesis of $Ir_4(CO)_7(PPh_3)(GePh_2)_2(\mu_3\text{-}\eta^2\text{-}GePhC_6H_4)(\mu\text{-}H)$, 3.5.**

A 6.4 mg (0.003 mmol) portion of $Ir_4(CO)_7(PPh_3)(GePh_2)(GePh_3)(\mu_3\text{-}\eta^2\text{-}GePhC_6H_4)(\mu\text{-}H)_2$, **3.3** was dissolved in benzene and heated to reflux for 1 h. The solvent was then removed *in vacuo*, and the product was then isolated by TLC using a 3:1 hexane/methylene chloride solvent mixture to yield 3.6 mg (59%) of orange $Ir_4(CO)_7(PPh_3)(GePh_2)_2(\mu_3\text{-}\eta^2\text{-}GePhC_6H_4)(\mu\text{-}H)$, **3.5**. Spectral data for **3.5**: IR $\nu_{CO}$ ($cm^{-1}$ in $CH_2Cl_2$): 2057(m), 2029(vs), 2016(s), 2003(m), 1986(m). $^1H$ NMR ($CDCl_3$, in ppm) $\delta$ = 6.62-7.58 (m, 44H, Ph), -17.99(d, 1H, $\mu$-H, $J_{P\text{-}H}$=7.50Hz). $^{31}P\{^1H\}$ NMR ($CDCl_3$) $\delta$ = 28.80 ppm (s, $1PPh_3$) Mass Spec. ES(negative)/MS for **3.5:** *m*/*z*=1909 (M+H).

**Conversion of 3.3 to 3.5 in NMR tube.**

A 7.0 mg (0.004 mmol) portion of $Ir_4(CO)_7(PPh_3)(GePh_2)(GePh_3)(\mu_3\text{-}\eta^2\text{-}GePhC_6H_4)(\mu\text{-}H)_2$, **3.3** was dissolved in $CDCl_3$ in NMR tube. The NMR tube was place in 50 ℃ oil-bath

for 36 hours. $^{1}H$ NMR experiment was performed before and after heating and showed the change from two hydride peaks (-16.87 ppm and -21.56 ppm) to single hydride peak (-17.99 ppm) as well as the appearance of benzene (s, 7.36 ppm), which indicate the formation of compound **3.5** through the cleavage of one molecular of benzene..

**Reaction of 3.2 with $GePh_2H_2$.**

A 20 μL (0.107 mmol) portion of $GePh_2H_2$ was added to 13 mg (0.008 mmol) of $Ir_4(CO)_{10}(PPh_3)(GePh_2)$, **3.2** in 10 mL of benzene. The mixture was heated to reflux for 1 hour until the yellow solution turned red. The solvent was then removed *in vacuo*, and the product was then isolated by TLC using a 3:1 hexane/methylene chloride solvent mixture to yield 4.7 mg (26%) of red $Ir_4(CO)_6(PPh_3)(GePh_2)_3(GePh_2H)(\mu\text{-}H)_3$, **3.6.** Spectral data for **3.6**: IR $\nu_{CO}$ ($cm^{-1}$ in $CH_2Cl_2$): 2062(s), 2035(vs), 2020(vs), 1992(m), 1976(w). $^{1}H$ NMR ($CDCl_3$, in ppm) δ = 6.80-7.58 (m, 49H, Ph), 7.05 (d, 1H, $GePh_2H$, $J_{H-H}$=5.5 Hz), -19.13 (d, 1H, μ-H, $J_{P-H}$=17.8 Hz), -19.70 (m, 1H, μ-H, $J_{P-H}$=3.0 Hz, $J_{H-H}$=5.9 Hz), -19.91 (d, 1H, μ-H, $J_{P-H}$=5.4 Hz). $^{31}P\{^{1}H\}$ NMR ($CDCl_3$) δ = 14.11 ppm (s, $1PPh_3$) Mass Spec. ES(positive)/MS for **3.6:** *m*/*z*=2011 (M+H).

**Crystallographic Analyses:** Orange single crystals of **3.1, 3.2** and red single crystal of **3.6** suitable for x-ray diffraction analyses were obtained by slow evaporation of solvent from a hexane/methylene chloride solvent mixture at -25 ℃. Single crystals of **3.3** (orange) and **3.5** (orange) suitable for x-ray diffraction analyses were obtained by slow evaporation of solvent from a benzene/octane solvent mixture at room temperature. Each data crystal was glued onto the end of a thin glass fiber. X-ray intensity data were measured by using a Bruker SMART APEX CCD-based diffractometer using Mo Kα

radiation (λ = 0.71073 Å). The raw data frames were integrated with the SAINT+ program by using a narrow-frame integration algorithm[12]. Correction for Lorentz and polarization effects were also applied with SAINT+. An empirical absorption correction based on the multiple measurement of equivalent reflections was applied in each analysis by using the program SADABS. All structures were solved by a combination of direct methods and difference Fourier syntheses, and refined by full-matrix least-squares on $F^2$, using the SHELXTL software package[13]. All non-hydrogen atoms were refined with anisotropic displacement parameters. Hydrogen atoms were placed in geometrically idealized positions and included as standard riding atoms during the least-squares refinements. Crystal data, data collection parameters, and results of the analyses are listed in Tables 3.1-3.2. Compound **3.1** crystallized in the triclinic crystal system. The space group *P-1* was identified uniquely on the basis of the systematic absences in the intensity data. There are two symmetry independent molecules in the asymmetric unit in the structure of **3.1**. The Ge and P atoms for the $PPh_3$ and the $GePh_3$ ligands in both independent molecules of **3.1** were disordered between these two ligand sites. The disorder was refined and converged to Ge1A/P1B = 0.61/0.39, Ge1B/P1A = 0.39/0.61 for molecule 1 and Ge2A/P2B = 0.59/0.41, Ge2B/P2A = 0.41/0.59 for molecule 2. The hydride ligand in **3.1** was located and refined in the analysis without restraints. Compound **3.2** crystallized in the monoclinic crystal system. The space group *P2(1)/n* was assumed and confirmed by the successful solution and refinement of both structures. Compound **3.2** cocrystallized with half molecule of hexane in the asymmetric crystal unit. Compound **3.3** crystallized in the monoclinic crystal system. The space group *P2(1)/n* was identified uniquely on the basis of the systematic absences in the intensity data. One

half molecule of octane cocrystallized with one molecule of compound **3.3** in the asymmetric unit. The Ge1 and P1 atoms for the $PPh_3$ and the $GePh_3$ ligands in the independent molecule of **3.3** were disordered between these two ligand sites. The disorder was refined and converged to Ge1A/P1B = 0.86/0.14, Ge1B/P1A = 0.14/0.86. The hydride ligand in **3.3** was located and refined in the analysis without restraints. Compounds **3.5** crystallized in the Orthorhombic crystal system. The space group *C*mc$2_1$ was assumed and confirmed by the successful solution and refinement of the structure. There is half symmetry independent molecule in the asymmetric unit in the structure of **3.5**. The hydride ligand in **3.5** was located and refined in the analysis without restraints. Compound **3.6** crystallized in the monoclinic crystal system. The space group *P*$2_1$/c was identified uniquely on the basis of the systematic absences in the intensity data. One half molecule of hexane and two molecules of methylene chloride cocrystallized with one molecule of compound **3.6** in the asymmetric unit.

**Results and Discussion**

The new tetrairidium cluster complex $Ir_4(CO)_{10}(PPh_3)(GePh_3)(\mu\text{-}H)$, **3.1** was obtained in 54% yield from the reaction of $Ir_4(CO)_{11}PPh_3$ with $GePh_3H$ and $Me_3NO$ in a solution of methylene chloride solvent at room temperature. Compound **3.1** was characterized by a combination of IR and $H^1$ NMR spectroscopy, $P^{31}$ NMR spectroscopy, mass spectrometry, and a single-crystal X-ray diffraction analysis. An ORTEP diagram of the molecular structure of **3.1** is shown in Figure 3.1. In the solid state, there are two independent molecules of **3.1** in the asymmetric crystal unit. Both molecules are structurally similar and contain one $PPh_3$ ligand and one $GePh_3$ ligand. Like its Sn analogue, $Ir_4(\mu\text{-}H)(CO)_{10}(PPh_3)(SnPh_3)$, **2.3**, as we previous reported[14] (equation 3.1), the

$PPh_3$ and $GePh_3$ ligands are disordered in both molecules. Thus, the Ir-Ge/P distances measured here are not of high accuracy, but the structural analysis does confirm the structure of the molecule. The tetrahedral arrangement of iridium atoms is not disorded, therefore, the Ir-Ir distances are reliable. As expected,[15] the hydride-bridged Ir-Ir discance, 2.8805(5) Å, is significantly longer than those unbridged Ir-Ir distances, which range from 2.7092(6) to 2.7232(6) Å. The hydride ligand exhibits the usual upfield shift：δ -17.88. The phosphine ligand exhibits a typical $^{31}P$ resonance shift: δ -15.99 ppm.

When reflux in methylene chloride for 1.5 hours, compound **3.1** will transform to a $GePh_2$-bridged compound **3.2** accompanied with a cleavage of one molecule of benzene confirmed by NMR experiments. An ORTEP diagram of the molecular structure of **3.2** is shown in Figure 3.2. Compound **3.2** consists of a tetrahedral cluster of $Ir_4$ with one terminal $PPh_3$ and one bridged $GePh_2$. The $GePh_2$ and two CO are edge-bridging ligands about the Ir1-Ir2-Ir3 triangular group of metal atoms. Thus, the Ir-Ir bond distances within the bridged triangle range from 2.7551(4) to 2.7849(4)Å, are significantly longer than those unbridged Ir-Ir discane range from 2.7142(4) to 2.7269(4)Å. The $PPh_3$ ligand lies approximately trans to the Ir2-Ir4 bond: P1– Ir2 – Ir4 = 171.02(4) and exhibits a usual $^{31}P$ resonance shift：δ-14.34 ppm. The Ir-Ge distances [2.4866(6), 2.4775(6)Å] are significantly shorter than those found in crowded triiridium complex $Ir_3(CO)_6(GePh_3)_3(\mu\text{-}GePh_2)_3$ [2.5182(7) - 2.5653(7)Å][10(b)], but it's similar to the Ir-Ge distances found in the less crowded biiridium complex $H_2Ir_2(CO)_4(GePh_3)_2(\mu\text{-}GePh_2)_2$ [2.4739(7) - 2.4975(7)Å].[10(c)]

The reaction of compound **3.2** with excess of $GePh_3H$ at 65 ℃ yield two complexes $Ir_4(CO)_7(PPh_3)(GePh_2)(GePh_3)(\mu_3\text{-}\eta^2\text{-}GePhC_6H_4)(\mu\text{-}H)_2$, **3.3** and $Ir_4(CO)_7(GePh_2)_2(GePh_3)(\mu_3\text{-}\eta^2\text{-}GePhC_6H_4)(\mu\text{-}H)_2$, **3.4** in 45 and 10% yields, respectively. Compound **3.3** will transformed to a new tetrairidium cluster complex $Ir_4(CO)_7(PPh_3)(GePh_2)_2(\mu_3\text{-}\eta^2\text{-}GePhC_6H_4)(\mu\text{-}H)$, **3.5** in 59% yield, scheme 3.2. ORTEP diagrams of the molecular structures of **3.3** and **3.5** are shown in Figure 3.3 and 3.4. Compound **3.3**, **3.4** and **3.5** all contain one rare $\mu_3\text{-}\eta^2\text{-}GePh(C_6H_4)$ ligand by ortho-metallation of a phenyl ring bridging a $Ir_3$ triangle. Compound **3.3** consists of an $Ir_4$ tetrahedron with one ortho-metallated bridging $\mu_3\text{-}\eta^2\text{-}GePh(C_6H_4)$ group, one bridging $GePh_2$ ligand, one terminal $GePh_3$ ligand, and one $PPh_3$ ligand. The $PPh_3$ and $GePh_3$ ligands exhibit ~14% disordered in the solid state. The $^1H$ NMR spectrum of **3.3** show two resonances at -16.87 and -21.56 ppm, indicating the presence of two inequivalent hydrido ligands. Both hydride were located and refined crystallographically and were found to bridge the Ir1-Ir2 and Ir1-Ir3 bonds. As expected, the hydrido bridging bonds [Ir1-Ir2, 2.8532(7) Å; Ir1-Ir3, 2.9902(7) Å] are significantly longer than that of Ir1-Ir4 [2.7047(7) Å], which does not contain a bridging hydrido ligand. Compound **3.4** was reported before[10(b)] from the reaction of $Ir_4(CO)_{12}$ with $GePh_3H$ at 97℃. As in this reaction, it's assumed that compound **3.4** might come from the overreaction of compound **3.3** with $GePh_3H$ by replacing the $PPh_3$ ligand with a $HGePh_3$ followed by a cleavage of benzene forming a $GePh_2$-bridged ligand. The transformation of **3.3** to **3.5** accompanied with the cleavage of one molecule of benzene was indicated by NMR experiments. The disappearance of two hydrido resonance (-16.87 and -21.56 ppm) and the appearance of one new hydrido resonance (-17.99 ppm) and one singlet of free benzene resonance at

7.36 ppm indicate the complete of the transformation after compound **3.3** was heated in 50 ℃ for 36 hours in $CDCl_3$.

We also investigated the reaction of compound **3.2** with $GePh_2H_2$ and another new tetrairidium cluster complex $Ir_4(CO)_6(PPh_3)(GePh_2)_3(GePh_2H)(\mu\text{-}H)_3$, **3.6** was isolated by TLC in 26% yield. An ORTEP diagram of the molecular structure of **3.6** is shown in Figure 3.5. Compound **3.6** consists of a tetrahedron $Ir_4$ with three bridged $GePh_2$ ligands, one terminal $GePh_2H$ ligand, one $PPh_3$ ligand and three hydrido ligands. A 2D $^{1}H$-$^{31}P$ HSQC experiment was conducted and revealed the correlation map between the $PPh_3$ ligand (chmical shift at 14.11 ppm) and three hydrido ligands (δ: -19.13, -19.70, 19.91 ppm), which are consistent with the structure in solid state. The experiment also indicated an impurity complex with a hydrido ligand which we were unable to separate it. Three of the $GePh_2$ ligands are edge-bridging ligands about the Ir2-Ir3-Ir4 triangular group. The $GePh_2H$ ligand terminally lies on one of the iridium atoms in the Ir3 triangle. The $PPh_3$ lies on the apex iridium atom approximately trans to the Ir1-Ir4 bond: P1-Ir1-Ir4 = 170.47(5)Å. Two hydrides were located and refined crystallographically and were found to bridge the significantly long Ir-Ir bonds: Ir1-Ir2 [2.9747(6)Å] and Ir1-Ir3 [2.8973(6)Å]. The third hydride was fixed to bridge the relatively long Ir2-Ir4 [2.8190(6)Å] bond with DFIX restraint in the refinement. The cluster of **3.6** contains a total of 60 valence electrons: i.e., all 4 iridium atoms have 18-electron configurations.

**Summary and Conclusions**

New tetrahedral iridium cluster complexes containing phenylgermanium ligands have been obtained from reactions of $Ir_4(CO)_{11}(PPh_3)$ with $GePh_3H$ under relative mild

conditions. A summary of the reactions described in this report is shown in Scheme 3. Compound **3.1** and **3.3** undergo a transformation to **3.2** and **3.5** respectively through the cleavage of one molecule of benzene proved by NMR experiments. Compound **3.3**, **3.4** and **3.5** all contain one rare $\mu_3$-$\eta^2$-GePh($C_6H_4$) ligand by ortho-metallation of a phenyl ring bridging a $Ir_3$ triangle.

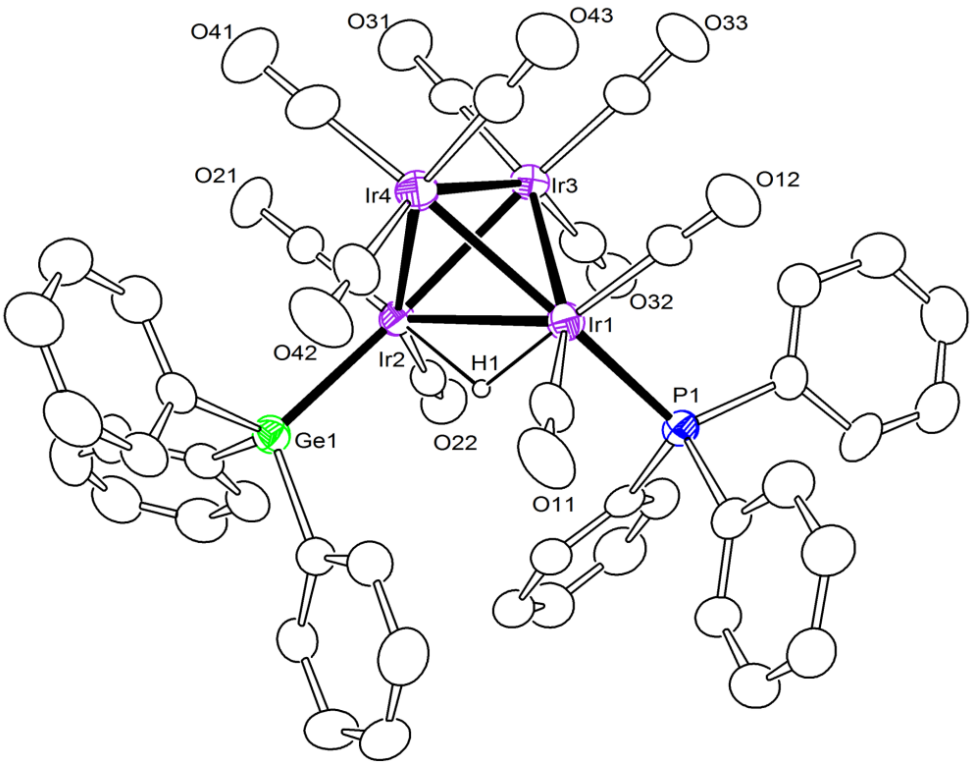


**Figure 3.1.** An ORTEP diagram of the molecular structure of $Ir_4(CO)_{10}(PPh_3)(GePh_3)(\mu\text{-}H)$, **3.1** showing 30% thermal ellipsoid probability.

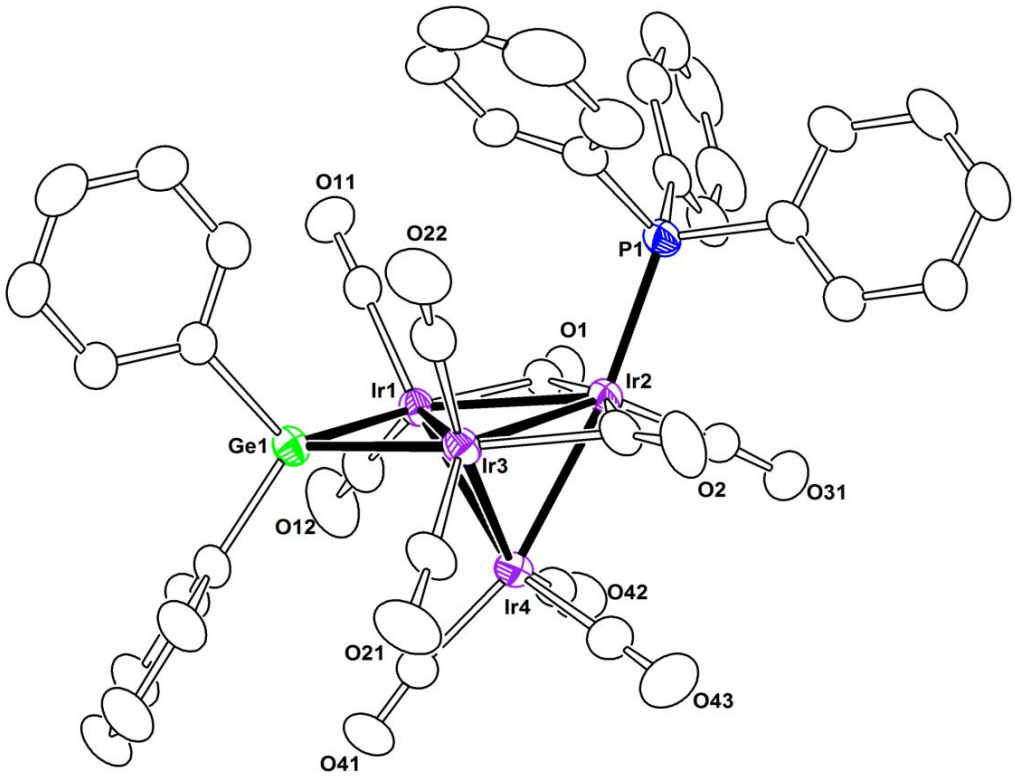


**Figure 3.2.** An ORTEP diagram of the molecular structure of $Ir_4(CO)_{10}(PPh_3)(\mu\text{-}GePh_2)$, **3.2**, showing 30% thermal ellipsoid probability.

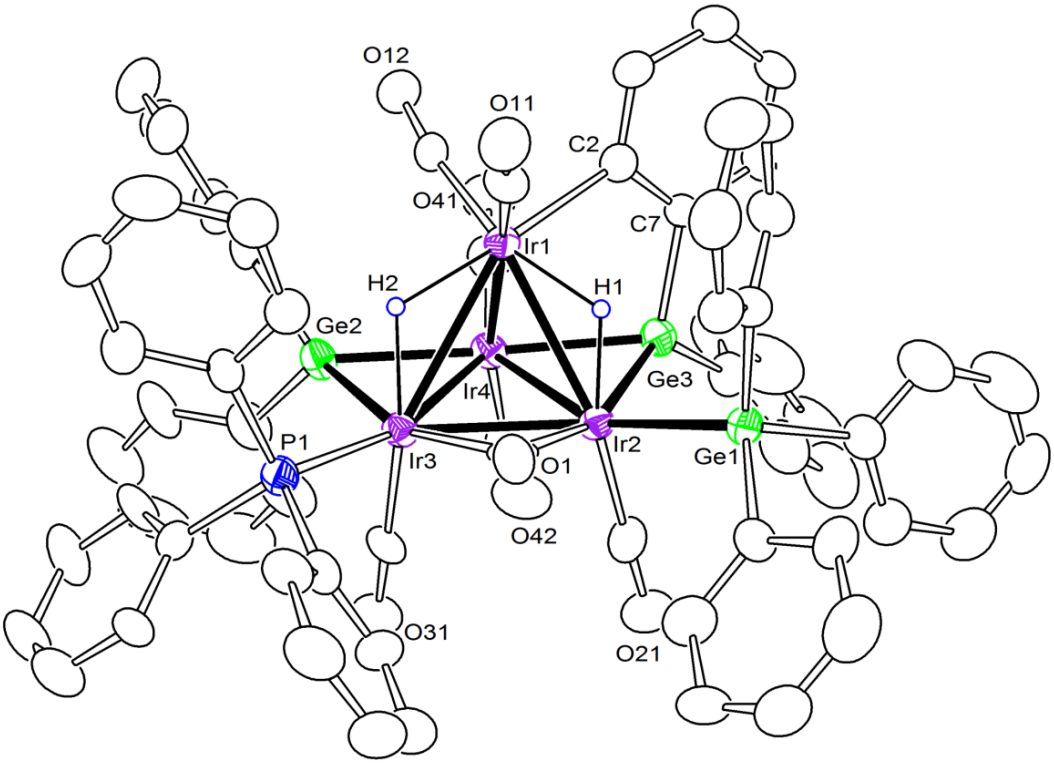


**Figure 3.3.** An ORTEP diagram of the molecular structure of $Ir_4(CO)_7(PPh_3)(GePh_2)(GePh_3)(\mu_3\text{-}\eta^2\text{-}GePhC_6H_4)(\mu\text{-}H)_2$, **3.3**, showing 30% thermal ellipsoid probability.

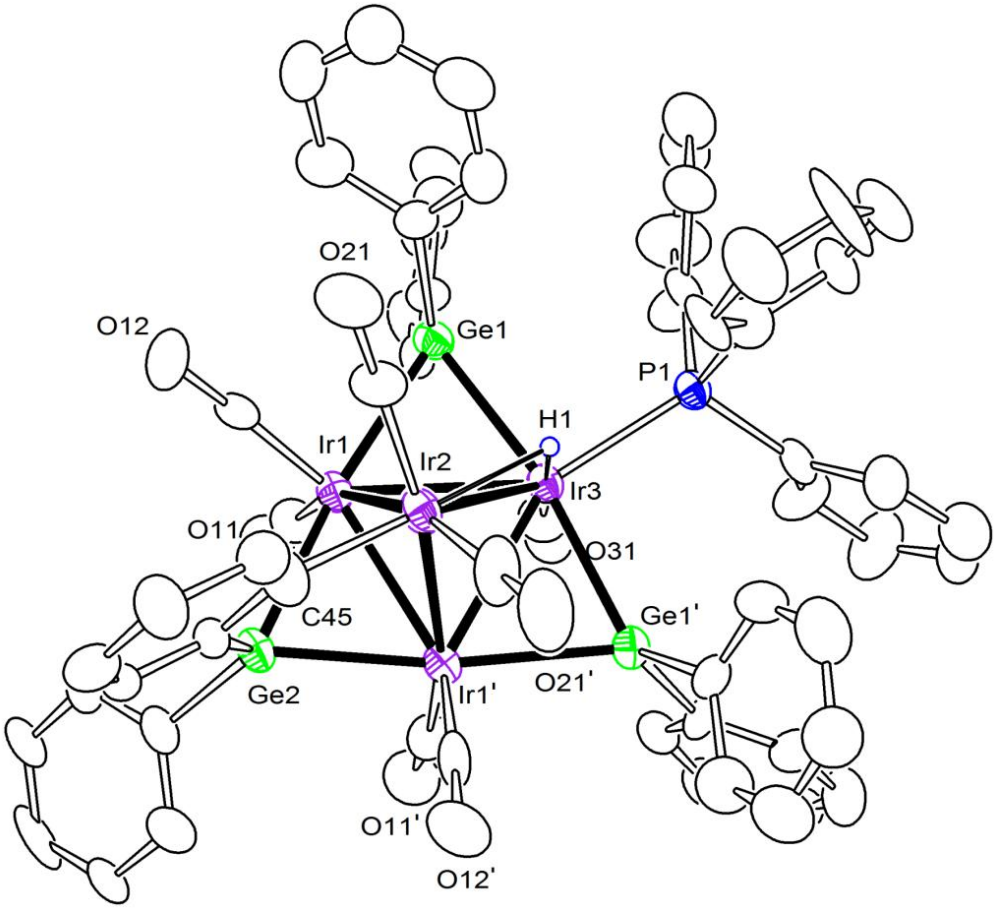


**Figure 3.4.** An ORTEP diagram of the molecular structure of $Ir_4(CO)_7(PPh_3)(GePh_2)_2(\mu_3\text{-}\eta^2\text{-}GePhC_6H_4)(\mu\text{-}H)$, **3.5**, showing 30% thermal ellipsoid probability.

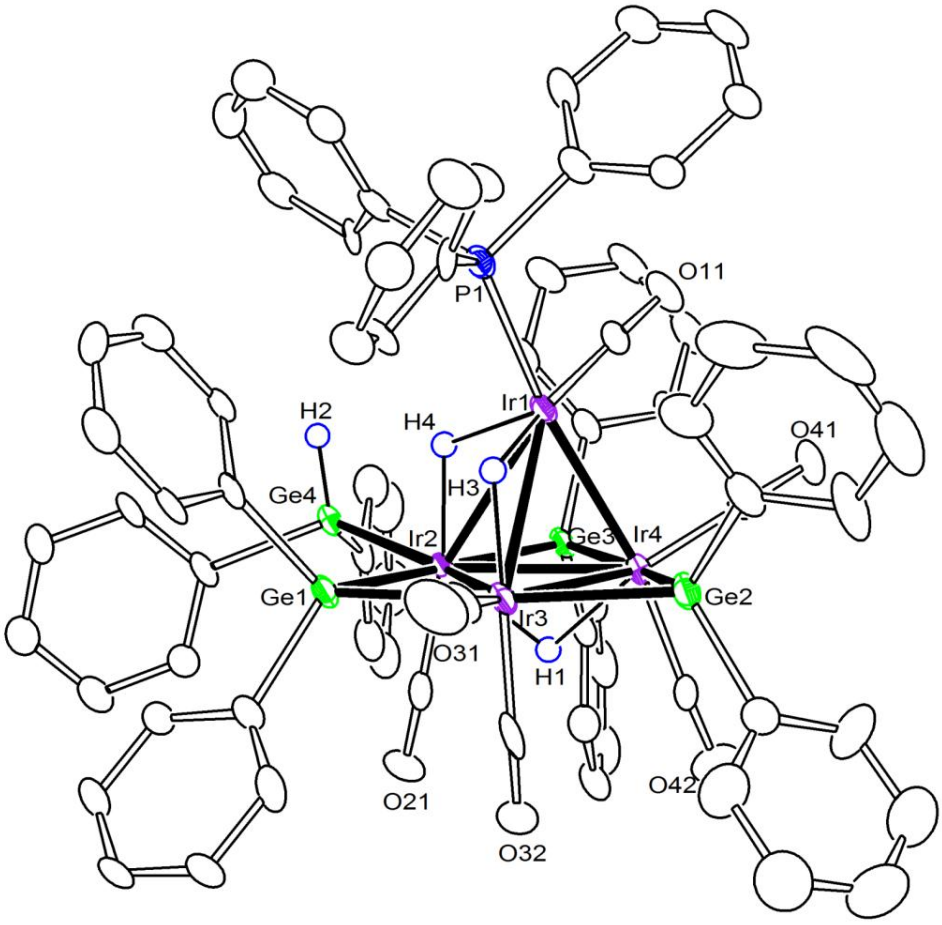


**Figure 3.5.** An ORTEP diagram of the molecular structure of $Ir_4(CO)_6(PPh_3)(GePh_2)_3(GePh_2H)(\mu\text{-}H)_3$, **3.6**, showing 60% thermal ellipsoid probability (disorder not shown).

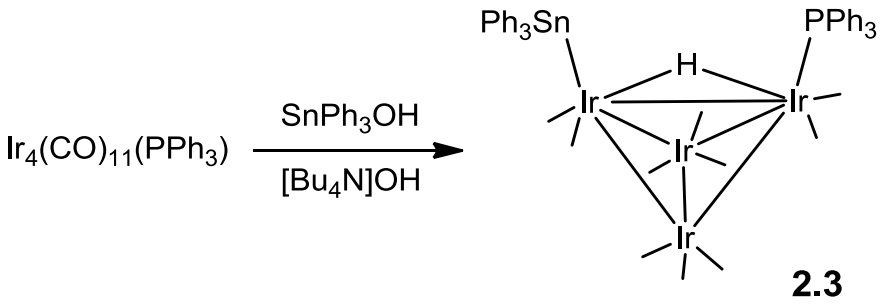


Equation 3.1 Reaction of $Ir_4(CO)_{11}(PPh_3)$ with $SnPh_3OH$ under basic condition.

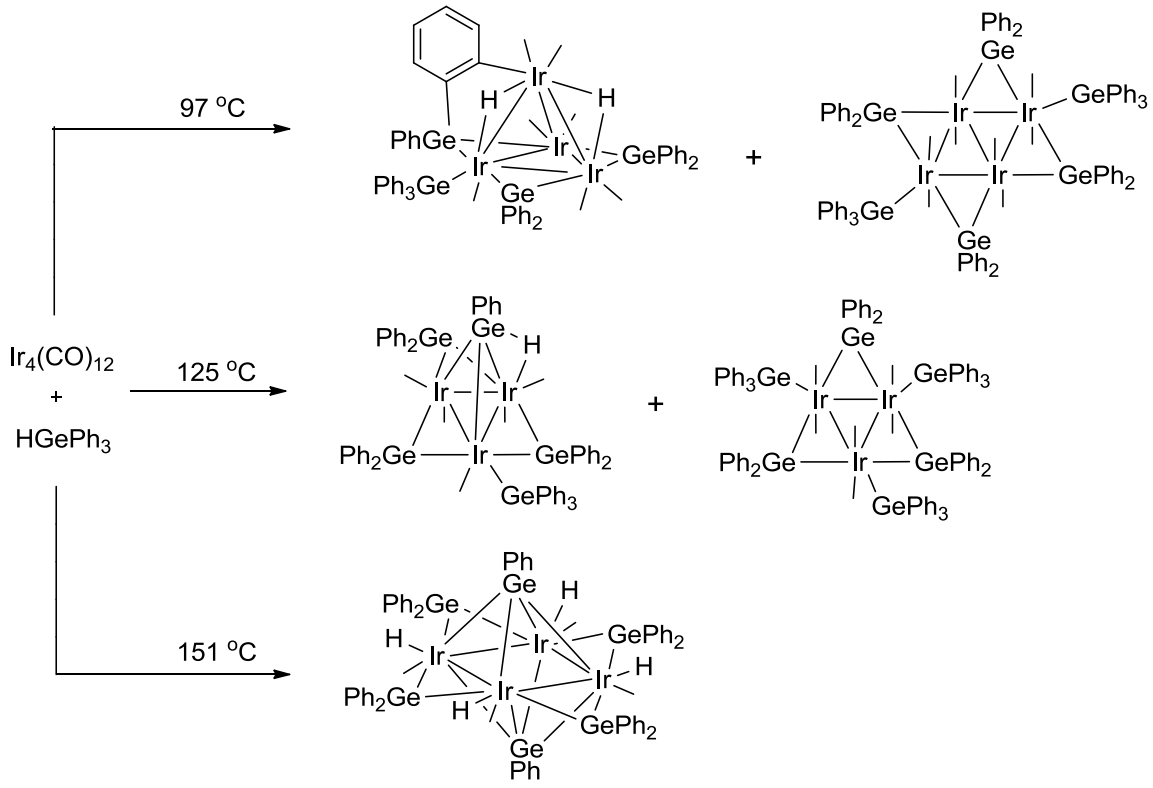


Scheme 3.1 Schematic diagram of reaction of $Ir_4(CO)_{12}$ with $HGePh_3$.

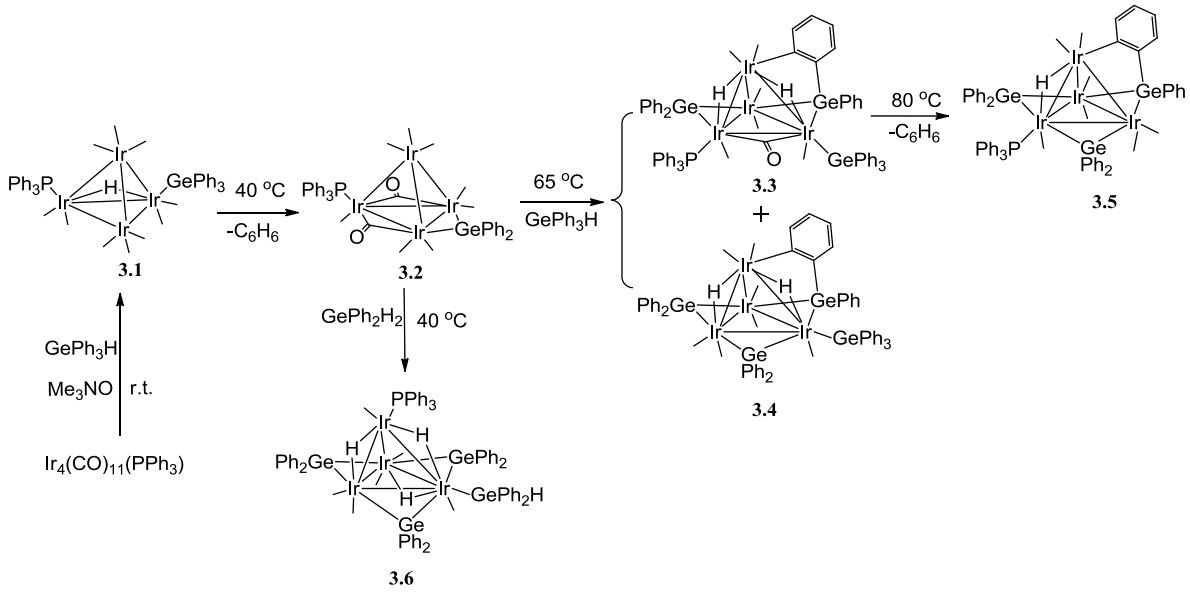


Scheme 3.2 Schematic diagram of reaction of $Ir_4(CO)_{11}(PPh_3)$ with $HGePh_3$

**Table 3.1. Crystallographic Data for Compounds 3.1-3.6.**

| Compound | **3.1** | **3.2** | **3.3** |
|---|---|---|---|
| Empirical formula | $Ir_4\ GeC_{46}H_{31}O_{10}P$ | $Ir_4GeC_{40}H_{25}O_{10}P$ $^1/_2\ C_6H_{14}$ | $Ir_4Ge_3C_{67}H_{51}O_7P$ $^1/_2C_8H_{18}$ |
| Formula weight | 1616.07 | 1581.05 | 2042.73 |
| Crystal system | Triclinic | Monoclinic | Monoclinic |
| Lattice parameters | | | |
| a (Å) | 14.9044(14) | 13.2634(15) | 17.9146(14) |
| b (Å) | 15.1217(14) | 17.039(2) | 20.3928(15) |
| c (Å) | 22.490(2) | 19.925(2) | 19.7053(15) |
| α (deg) | 87.719(2) | 90.00 | 90.00 |
| β (deg) | 80.559(2) | 101.312(2) | 115.345(1) |
| γ (deg) | 68.903(2) | 90.00 | 90.00 |
| V ($Å^3$) | 4663.9(8) | 4415.5(9) | 6506.0(9) |
| Space group | *P*-1 | $P2_1/n$ | $P2_1/n$ |
| Z value | 4 | 4 | 4 |
| $\rho_{calc}$ (g / $cm^3$) | 2.302 | 2.378 | 2.085 |
| μ (Mo Kα) ($mm^{-1}$) | 12.098 | 12.776 | 9.593 |
| Temperature (K) | 293(2) | 294(2) | 294(2) |
| $2\Theta_{max}$ ( ° ) | 45.98 | 56.52 | 38.72 |
| No. Obs. ( I > 2σ(I)) | 16470 | 7797 | 11476 |
| No. Parameters | 1119 | 506 | 765 |
| Goodness of fit (GOF) | 1.025 | 1.038 | 1.023 |
| Max. shift in cycle | 0.001 | 0.000 | 0.001 |
| Residuals*: R1; wR2 | 0.0356 ; 0.0901 | 0.0237 ; 0.0572 | 0.0504 ; 0.0880 |
| Absorption Correction, | Multi-scan | Multi-scan | Multi-scan |
| Max/min | 1.000 / 0.5213 | 1.000 / 0.0743 | 1.000 / 0.4807 |
| Largest peak in Final Diff. Map ($e^-$ / $Å^3$) | 2.41 | 1.22 | 1.09 |

[a] $R = \Sigma_{hkl}(||F_{obs}|-|F_{calc}||)/\Sigma_{hkl}|F_{obs}|$; $R_w = [\Sigma_{hkl}w(|F_{obs}|-|F_{calc}|)^2/\Sigma_{hkl}wF^2_{obs}]^{1/2}$; $w = 1/\sigma^2(F_{obs})$; $GOF = [\Sigma_{hkl}w(|F_{obs}|-|F_{calc}|)^2/(n_{data} - n_{vari})]^{1/2}$.

**Table 3.1(continue). Crystallographic Data for Compounds 3.1-3.6.**

| Compound | **3.5** | **3.6** |
|---|---|---|
| Empirical formula | $Ir_4\ Ge_3C_{61}H_{45}O_7P$ | $Ir_4Ge_4C_{72}H_{59}O_6P$ $2CH_2Cl_2 \cdot 1/_2\ C_6H_{14}$ |
| Formula weight | 1907.51 | 2323.26 |
| Crystal system | Orthorhombic | Monoclinic |
| Lattice parameters | | |
| a (Å) | 18.484(2) | 13.200(3) |
| b (Å) | 15.4870(17) | 19.276(4) |
| c (Å) | 19.790(2) | 30.457(6) |
| $\alpha$ (deg) | 90.00 | 90.00 |
| $\beta$ (deg) | 90.00 | 90.823(4) |
| $\gamma$ (deg) | 90.00 | 90.00 |
| V ($Å^3$) | 5665.2(11) | 7749(3) |
| Space group | $Cmc2_1$ | $P2_1/c$ |
| Z value | 4 | 4 |
| $\rho_{calc}$ ($g / cm^3$) | 2.236 | 1.991 |
| $\mu$ (Mo K$\alpha$) ($mm^{-1}$) | 11.008 | 8.578 |
| Temperature (K) | 294(2) | 100(2) |
| $2\Theta_{max}$ ( ° ) | 32.12 | 55.32 |
| No. Obs. ( $I > 2\sigma(I)$) | 5170 | 13669 |
| No. Parameters | 376 | 878 |
| Goodness of fit (GOF) | 0.981 | 1.093 |
| Max. shift in cycle | 0.000 | 0.000 |
| Residuals:[a] R; $R_w$ | 0.0549; 0.0775 | 0.0407; 0.1000 |
| Absorption Correction, | Multi-scan | Multi-scan |
| Max/min | 1.000 / 0.7106 | 1.000 / 0.5882 |
| Largest peak in Final Diff. Map ($e^- / Å^3$) | 0.94 | 1.08 |

[a] $R = \Sigma_{hkl}(\ |\ |F_{obs}| - |F_{calc}|\ |)/\Sigma_{hkl}|F_{obs}|$; $R_w = [\Sigma_{hkl}w(|F_{obs}| - |F_{calc}|)^2/\Sigma_{hkl}wF^2_{obs}]^{1/2}$; $w = 1/\sigma^2(F_{obs})$; GOF = $[\Sigma_{hkl}w(|F_{obs}| - |F_{calc}|)^2/(n_{data} - n_{vari})]^{1/2}$.

Table 3.2 Selected intramolecular angles and bond distances for compound **3.1**.(molecule 1)[a]

| **Distances** | | | **Angles** | | | |
|---|---|---|---|---|---|---|
| Atom | Atom | Distance (Å) | Atom | Atom | Atom | Angle(deg) |
| Ir1 | Ir2 | 2.8805(5) | Ge1A(P1B) | Ir2 | Ir3 | 167.68(3) |
| Ir1 | Ir3 | 2.7134(5) | P1A(Ge1B) | Ir1 | Ir4 | 164.89(4) |
| Ir1 | Ir4 | 2.7232(6) | | | | |
| Ir2 | Ir3 | 2.7175(5) | | | | |
| Ir2 | Ir4 | 2.7113(5) | | | | |
| Ir3 | Ir4 | 2.7092(6) | | | | |
| Ir1 | H1 | 1.6659 | | | | |
| Ir2 | H1 | 1.7983 | | | | |

[a] Estimated Standard deviations in the least significant figure are given in parentheses.

Table 3.3 Selected intramolecular angles and bond distances for compound **3.2.**[a]

| **Distances** | | | **Angles** | | | |
|---|---|---|---|---|---|---|
| Atom | Atom | Distance (Å) | Atom | Atom | Atom | Angle(deg) |
| Ir1 | Ir2 | 2.7704(3) | Ge1 | Ir1 | Ir4 | 88.887(15) |
| Ir1 | Ir3 | 2.7849(4) | P1 | Ir2 | Ir4 | 171.02(4) |
| Ir1 | Ir4 | 2.7269(4) | | | | |
| Ir2 | Ir3 | 2.7551(4) | | | | |
| Ir2 | Ir4 | 2.7178(3) | | | | |
| Ir3 | Ir4 | 2.7142(4) | | | | |
| Ir1 | Ge1 | 2.4775(6) | | | | |
| Ir3 | Ge1 | 2.4866(6) | | | | |
| Ir2 | P1 | 2.3379(14) | | | | |

[a] Estimated Standard deviations in the least significant figure are given in parentheses.

Table 3.4 Selected intramolecular angles and bond distances for compound **3.3.**[a]

| **Distances** | | | **Angles** | | | |
|---|---|---|---|---|---|---|
| Atom | Atom | Distance (Å) | Atom | Atom | Atom | Angle(deg) |
| Ir1 | Ir2 | 2.8532(7) | Ge1 | Ir2 | Ir4 | 152.82(4) |
| Ir1 | Ir3 | 2.9902(7) | Ge3 | Ir2 | Ir4 | 56.52(3) |
| Ir1 | Ir4 | 2.7047(7) | P1 | Ir3 | Ir4 | 163.42(7) |
| Ir2 | Ir3 | 2.7564(7) | | | | |
| Ir2 | Ir4 | 2.8096(7) | | | | |
| Ir1 | C2 | 2.137(12) | | | | |
| Ir1 | H1 | 1.86(8) | | | | |
| Ir2 | H1 | 1.62(8) | | | | |
| Ir1 | H2 | 1.99(13) | | | | |
| Ir3 | H2 | 2.06(12) | | | | |
| Ir2 | Ge1 | 2.4761(14) | | | | |
| Ir2 | Ge3 | 2.4364(13) | | | | |
| Ir4 | Ge3 | 2.5054(14) | | | | |
| Ir3 | Ge2 | 2.4675(13) | | | | |
| Ir4 | Ge2 | 2.5171(14) | | | | |
| Ir3 | P1 | 2.354(3) | | | | |

[a] Estimated Standard deviations in the least significant figure are given in parentheses.

Table 3.5 Selected intramolecular angles and bond distances for compound **3.5.**[a]

| **Distances** | | | **Angles** | | | |
|---|---|---|---|---|---|---|
| Atom | Atom | Distance (Å) | Atom | Atom | Atom | Angle(deg) |
| Ir1 | Ir2 | 2.7100(13) | Ge1 | Ir1 | Ir3 | 116.19(5) |
| Ir1 | Ir3 | 2.8101(11) | C45 | Ir2 | Ir1 | 96.4(6) |
| Ir2 | C45 | 2.13(3) | P1 | Ir3 | Ir1 | 149.92(4) |
| Ir2 | Ir3 | 2.9591(15) | | | | |
| Ir2 | H1 | 2.01(14) | | | | |
| Ir3 | H1 | 1.70(16) | | | | |
| Ir1 | Ge1 | 2.4930(18) | | | | |
| Ir3 | Ge1 | 2.5018(18) | | | | |
| Ir1 | Ge2 | 2.463(2) | | | | |
| Ir3 | P1 | 2.337(6) | | | | |

[a] Estimated Standard deviations in the least significant figure are given in parentheses.

Table 3.6 Selected intramolecular angles and bond distances for compound **3.6.**[a]

| **Distances** | | | **Angles** | | | |
|---|---|---|---|---|---|---|
| Atom | Atom | Distance (Å) | Atom | Atom | Atom | Angle(deg) |
| Ir1 | Ir2 | 2.9747(6) | P1 | Ir1 | Ir4 | 170.47(5) |
| Ir1 | Ir3 | 2.8973(6) | Ce4 | Ir2 | Ir3 | 152.71(3) |
| Ir1 | Ir4 | 2.7058(7) | | | | |
| Ir2 | Ir4 | 2.8190(6) | | | | |
| Ir3 | Ir4 | 2.7719(6) | | | | |
| Ir2 | Ir3 | 2.7811(6) | | | | |
| Ir1 | P1 | 2.330(2) | | | | |
| Ir1 | H4 | 1.86(7) | | | | |
| Ir2 | H4 | 1.76(7) | | | | |
| Ir2 | Ge1 | 2.4422(10) | | | | |
| Ir3 | Ge2 | 2.4783(10) | | | | |
| Ir3 | P1 | 2.330(2) | | | | |
| Ir4 | Ge3 | 2.5688(10) | | | | |
| Ir2 | Ge4 | 2.4729(10) | | | | |
| Ge4 | H2 | 1.25(9) | | | | |

[a] Estimated Standard deviations in the least significant figure are given in parentheses.

## References


1. Crabtree, R.H.; Mihelcic, J.M.; Quirk, J.M. *J. Am. Chem. Soc.* **1979**, 101, 7738-7740.

2. (a) Sablong, R.; Osborn, J.A. *Tetrahedron: Asymmetry* **1996**, 7, 3059. (b) Margalef-Catala, R.; Claver, C.; Salagre, P.; Fernandez, E. *Tetrahedron: Asymmetry* **2000**, 11, 1469. (c) Woodmansee, D. H.; Pfaltz, A. *Top. Organomet. Chem.* **2011**, 34, 31-76.

3. McVicker, G.B.; Daage, M.; Touvelle, M.S.; Hudson, C.W.; Klein, D.P.; Baird, W.C.; Cook, B.R.; Chen, J.G.; Hantzer, S.; Vaughan, D.E.W.; Ellis, E.S.; Feeley, O.C. *J. Catal.* **2002**, 210, 137-148.

4. Choi, J.; Goldman, A. S. *Top. Organomet. Chem.* 2011, 34, 139-168..

5. (a) Jones, J.H.; *Platinum Met. Rev.* **2000**, 44, 94-105. (b) Gates, B.C. *Chem.Rev.* **1995**, 95, 511-522. (c) Sinfelt, J.H. *Bimetallic Catalysts: Discoveries, Concepts, and Applications*; John Wiley & Sons: New York, **1983**.

6. (a) Argo, A.M.; Odzak, J. F.; Gates, B.C. *J. Am. Chem. Soc.* **2003**, 125, 7107-7115. (b) Lu, J.; Serna, P.; Aydin, C.; Browning, N.D.; Gates, B.C. *J. Am. Chem. Soc.* **2011**, 133, 16186-16195.

7. (a) Lu, J.; Aydin, C.; Browning, N.D.; Gates, B.C. *J. Am. Chem. Soc.* **2012**, 134, 5022-5025. (b) Lu, J.; Aydin, C.; Browning, N.D.; Wang, L.; Gates, B.C. *Catal. Lett.* **2012**, 142, 1445-1451. (c) Aydin, C.; Lu. J.; Browning, N.D.; Gates, B.C. *Angew. Chem. Int. Ed.* **2012**, 51, 5929-5934.

8. (a) Didillon, B.; Candy, J.P.; Lepepetier, F.; Ferretti, O.A.; Basset, J.M. *Studies Surf. Sci. Catal.* **1993**, 78, 147-154. (b) Lafaye, G.; Mihut, C.; Especel, C.; Marecot, P.; Amiridis, M.D. *Langmuir*, **2004**, 20, 10612-10616.

9. (a) Macleod, N.; Fryer, J.R.; Stirling , D.; Webb, G. *Catal. Today* **1998**, 46, 37-54. (b) Lafaye, G.; Micheaud-Especel,, G.; Montassier, C.; Marecot, P. *Appl. Catal. A: Gen.* **2002**, 230, 19-30. (c) Lafaye, G.; Micheaud-Especel, C.; Montassier, C.; Marecot, P. *Appl.Catal. A: Gen.* **2004**, 257, 107-117.

10. (a) Hawkins, S.M.; Hitchcock, P.B.; Lappert, M.F.; Rai, A.K.; *Chem.Commun.* **1986**, 1689-1690. (b) Adams, R.D.; Captain, B.; Smith, J.L., Jr. *Inorg.Chem.* **2005**, 44, 1413-1420. (c) Adams, R.D.; Trufan, E. *Organometallics* **2010**, 29, 4346-4353. (d) Adams, R.D.; Fang, F.; Zhang, Q.; Hall, M.B.; Trufan, E. *Organometallics* **2012**, 31, 2621-2630.

11. Ros, R. and Scrivanti, A. *J. Chem. Soc., Dalton Trans.* **1986**, 11 2411-2421.

12. SAINT+, version 6.2a, Bruker Analytical X-ray Systems, Inc., Madison, WI, **2001**.

13. G. M. Sheldrick, SHELXTL, version 6.1, Bruker Analytical X-ray Systems, Inc., Madison, WI, **1997**.

14. Adams, R. D.; Chen, M.; Trufan, E.; Zhang, Q. *Organometallics* **2011**, 30, 661-664.

15. (a) Bau, R.; Drabnis, M.H. *Inorg.Chim. Acta* **1997**, 259, 27-50. (b) Teller, R.G.; Bau, R. *Struct. Bonding* **1981**, 41, 1-82.

# CHAPTER FOUR

# New Family of Pentairidium Carbonyl Complexes: Condensation of New σ-Phenyl Bonded Tetrairidium Complex, $[Ir_4(CO)_{11}Ph]^-$, with Mononuclear Iridium Species.

## Introduction

The synthesis of higher nuclearity metal carbonyl cluster compounds by "redox" condensation processes has been successfully used for many years.[1] Following Chini's successful synthesis of a range of large metal carbonyl cluster complexes of rhodium,[1a] della Pergola and his colleagues in Milan prepared some interesting higher nuclearity cluster complexes of iridium by using similar methodology, e.g. Eqs. 4.1-4.2, CO ligands are not shown in the structures.[2,3]

We have recently obtained some new tetrairidium carbonyl complexes containing $SnPh_3$ ligands from the reactions of $Ir_4(CO)_{12}$ and $Ir_4(CO)_{11}(PPh_3)$ with $SnPh_3OH$ in the presence of $[OH]^-$, Eq 4.3.[4] We have also investigated the reaction of the anion $[Ir_4(CO)_{11}Br]^-$ with $SnPh_3OH$ and $SnPh_4$. Interestingly, the iridium containing product from these reactions $[Et_4N][Ir_4(CO)_{11}Ph]$, **4.1** does not contain a tin ligand, but instead contains a terminally coordinated σ-phenyl ligand. $SnPh_4$ has been shown to be useful as a source of phenyl for palladium-catalyzed Stille coupling reactions.[5] Tilley has reported

that hafnium complexes containing the $SnPh_3$ ligand can eliminate a $SnPh_2$ group to form complexes containing a σ-phenyl group, e.g. eq. 4.4.[6]

The new air-stable σ-phenyl tetrairidium carbonyl salt $[Et_4N][Ir_4(CO)_{11}Ph]$, **4.1** with significant yield (~45%) could be the ideal complex for further reactions. We have investigated the reactions of $[Et_4N][Ir_4(CO)_{11}Ph]$, **4.1** with several mononuclear iridium species such as $Ir(CO)(PPh_3)_2Cl$ and $[Ir(COD)Cl]_2$ and have obtained a new family of uncharged pentairidium complex and some other high nuclear complexes .[7]

.We found that compound **4.1** reacts with $Ir(CO)(PPh_3)_2Cl$ by halide displacement to yield the two new uncharged pentairidium complexes $Ir_5(CO)_{12}(Ph)(PPh_3)$, **4.3** and $Ir_5(CO)_{11}(PPh_3)(PPh_2C_6H_4)$, **4.4**. Compound **4.1** reacts with $PPh_3$ to yield the complex $[Et_4N][Ir_4(CO)_{11}(PPh_2C_6H_4)]$, **4.2** which contains an ortho-metallated bridging $PPh_2C_6H_4$ ligand across an edge of a tetrahedral cluster of four iridium atoms. We have also investigated the reaction of compound **4.1** with $[Ir(COD)Cl]_2$, and have obtained three new higher nuclearity COD iridium complexes containing σ–phenyl ligands: $Ir_5(CO)_{11}(Ph)(COD)$, **4.6** $Ir_5(CO)_9(Ph)(COD)_2$, **4.7** and $Ir_9(CO)_{15}(Ph)(\mu_3\text{-}C_8H_{10})(COD)$, **4.8**.

**Experimental Section**

**General Data**. Reagent grade solvents were dried by the standard procedures and were freshly under nitrogen distilled prior to use. Infrared spectra were recorded on a Thermo Nicolet Avatar 360 FT-IR spectrophotometer. $^1H$ NMR spectra were recorded on a Varian Mercury 300 spectrometer operating at 300.1 MHz. Mass spectrometric (MS) measurements performed by a direct-exposure probe using electron impact ionization (EI)

and electrospray ionization (ESI) were made on a VG 70S instrument. $SnPh_3OH$, $Ir(CO)(PPh_3)_2Cl$ and $[Ir(COD)Cl]_2$, COD = 1,5-cyclooctadiene were obtained from STREM and were used without further purification. $SnPh_4$ was purchased from Gelest. $[Et_4N][Ir_4(CO)_{11}Br]$ was prepared according to the published procedure.[8] Product separations were performed by TLC in air on Analtech 0.25 and 0.5 mm silica gel 60 Å $F_{254}$ glass plates.

**Synthesis of $[Et_4N][Ir_4(CO)_{11}Ph]$, 4.1.**

a) A 25.0 mg (0.068 mmol) portion of $SnPh_3OH$ was added to 30.0 mg (0.023 mmol) of $[Et_4N][Ir_4(CO)_{11}Br]$ in 25 mL of methanol. The reaction was stirred at room temperature for 12 h. The solvent was then removed *in vacuo*, and the product was isolated by TLC by eluting with methylene chloride solvent to yield light yellow $[Et_4N][Ir_4(CO)_{11}Ph]$, **4.1**, 13.5 mg (45% yield). Spectral data for **4.1**: IR $\nu_{CO}$ ($cm^{-1}$ in $CH_2Cl_2$): 2067(m), 2028(vs), 1991(s), 1821(m), 1801(m). $^1H$ NMR ($CDCl_3$, in ppm) $\delta$ = 6.65 - 6.69 (m, 5H, σ-Ph), 0.95-0.98 (t, 12H, $CH_3$), 1.182-1.452(m, 8H, $CH_2$). Mass Spec. ES (negative ion) for **4.1:** *m*/*z* = 1155 (MH). The isotope distribution pattern was consistent with the presence of four iridium atoms.

b) A 30.0 mg (0.076 mmol) portion of $SnPh_4$ was added to 25.0 mg (0.019 mmol) of $[Et_4N][Ir_4(CO)_{11}Br]$ in 25 mL of methanol. The reaction mixture was stirred at room temperature for 16 h. The solvent was then removed *in vacuo*. A $^{119}Sn$ NMR spectrum of the entire reaction mixture in $CD_2Cl_2$ solvent showed only two resonances $\delta$ = - 60.48 ($SnPh_3Br$)[9] and -129.79 (unreacted $SnPh_4$, confirmed by recording a spectrum of a sample

of the $SnPh_4$ from the reagent bottle). The product **4.1** was isolated by TLC by eluting with 6:1 methylene chloride/hexane solvent mixture to yield 10.9 mg (yield 36.4%).

**Reaction of 4.1 with $PPh_3$ at 80 ℃.**

A 2.0 mg (0.0076 mmol) portion of $PPh_3$ was added to 7.5 mg (0.0058 mmol) of **4.1** dissolved in 20 mL of benzene. The reaction solution was then heated to reflux for 1 h. After cooling, the solvent was removed *in vacuo*, and the product was isolated by TLC by eluting with a 3:1 hexane/methylene chloride solvent mixture to yield 5.0 mg of $[Et_4N][Ir_4(CO)_{10}(PPh_2C_6H_4)]$, **4.2** (60% yield). Spectral data for **4.2**: IR $\nu_{CO}$ ($cm^{-1}$ in $CH_2Cl_2$): 2044(s), 2012(vs), 1978(vs), 1800(m), 1761(m). $^1H$ NMR ($CDCl_3$, in ppm) $\delta$ = 7.19 - 7.32 (m, 14H, Ph), 0.91 - 0.97 (t, 12H, $CH_3$), 1.15 - 1.48 (m, 8H, $CH_2$). Mass Spec. ES (negative ion) for **4.2:** *m*/*z* = 1311 (MH). The isotope distribution pattern was consistent with the presence of four iridium atoms.

**Reaction of 4.2 with $HBF_4$ under CO.**

A 0.06 mL of $HBF_4$ (51% in diethylether) was added to 14.0 mg (0.0097 mmol) of $[Et_4N][Ir_4(CO)_{11}(PPh_2C_6H_4)]$, **4.2** dissolved in 20 mL of methanol. The reaction was stirred under an atmosphere of CO for 1 h. The solvent was removed *in vacuo*, and the product was then isolated by TLC by eluting with a 3:1 hexane/methylene chloride solvent mixture to yield 11.4 mg of the known compound $Ir_4(CO)_{11}(PPh_3)$[10] (81%) and 1.0 mg of $Ir_4(CO)_{12}$.

**Reaction of $[Et_4N][Ir_4(CO)_{11}Ph]$, 4.1 with $Ir(CO)(PPh_3)_2Cl$.**

A 9.20 mg (0.0118 mmol) portion of $Ir(CO)(PPh_3)_2Cl$ was added to 14.4 mg (0.0112 mmol) of $[Et_4N][Ir_4(CO)_{11}Ph]$ that was dissolved in 25 mL of benzene. The reaction solution was heated to reflux for 2 h. The solvent was then removed *in vacuo*, and the product was isolated by TLC by eluting with a 3:1 hexane/methylene chloride solvent mixture. This yielded in order of elution: 1.56 mg of brown $Ir_5(CO)_{12}Ph(PPh_3)$, **4.3** (11% yield), 3.50 mg of brown $Ir_5(CO)_{11}(PPh_3)(PPh_2C_6H_4)$, **4.4** (22% yield), 6.02 mg of yellow **4.2** (37% yield) and 1.21 mg of $Ir_4(CO)_{11}(PPh_3)$[10] (8% yield). The yield of **4.4** was increased to 40% at the expense of **4.3** (only a trace) and **4.2 (**17%) when the reflux period was increased to 5 h. Spectral data for **4.3**: IR $\nu_{CO}$ ($cm^{-1}$ in $CH_2Cl_2$): 2080(w), 2053(vs), 2045(vs), 2018(s), 1841(m), 1813(m). $^1H$ NMR ($CDCl_3$, in ppm) $\delta$ = 7.19-7.41 (m, 15H, Ph), 6.67-6.72 (m, 5H, σ-Ph). Mass Spec. ES (negative ion) for **4.3:** *m*/*z*=1635 (MH). The isotope distribution pattern was consistent with the presence of five iridium atoms. Spectral data for **4.4**: IR $\nu_{CO}$ ($cm^{-1}$ in $CH_2Cl_2$): 2061(s), 2038(vs), 2022(s), 2007(s), 1990(m), 1850(m), 1816(m), 1787(m). $^1H$ NMR ($CDCl_3$, in ppm) $\delta$ = 7.19-7.42 (m, 29H, Ph). Mass Spec. ES (positive ion) for **4.4:** *m*/*z*=1794 ($M^+$), 1831($M+K^+$). The isotope distribution pattern was consistent with the presence of five iridium atoms.

**Synthesis of 4.4 by the reaction of 4.2 with $Ir(CO)(PPh_3)_2Cl$.**

A 7.3 mg (0.0094 mmol) portion of $Ir(CO)(PPh_3)_2Cl$ was added to 13 mg (0.0090 mmol) of **4.4** dissolved in 25 mL of benzene. The reaction was heated to reflux for 5 h. The solvent was removed *in vacuo*, and the product was then isolated by TLC by eluting with a 3/1 hexane/methylene chloride solvent mixture. Yield: 1.78 mg of **4.4** (11%).

**Synthesis of 4.4 by the reaction of 4.3 with $PPh_3$.**

A 1.2 mg (0.0046 mmol) portion of $PPh_3$ was added to 5.6 mg (0.0042 mmol) of **4.3** dissolved in 20 mL of benzene. The reaction was heated to reflux for 1.5 h. The solvent was then removed *in vacuo*, and the product was isolated by TLC by eluting with a 3/1 hexane/methylene chloride solvent mixture. Yield: 2.66 mg of **4.4** (43% yield).

**Reaction of $[Et_4N][Ir_4(CO)_{11}Ph]$, 4.1 with $[Ir(COD)Cl]_2$ in benzene at reflux.**

A 8.0 mg (0.012 mmol) portion of $[Ir(COD)Cl]_2$ was added to 14.0 mg (0.011 mmol) of $[Et_4N][Ir_4(CO)_{11}Ph]$ that had been dissolved in 25 mL of benzene. The reaction solution was heated to reflux (80 $^oC$ ) for 2 h. The solvent was then removed *in vacuo*, and the products were isolated by TLC by eluting with a 3:1 hexane/methylene chloride solvent mixture. This yielded in order of elution: 0.30 mg of yellow $Ir_4(CO)_{10}(COD)$,[11] (2.4% yield), 1.45 mg of yellow $Ir_4(CO)_7(COD)(\mu_4\text{-}C_8H_{10})$,[11] **4.5** (11.3% yield), 1.24 mg of orange $Ir_5(CO)_{11}(Ph)(COD)$, **4.6** (9.8% yield), 0.84 mg of brown $Ir_9(CO)_{15}(Ph)(\mu_3\text{-}C_8H_{10})(COD)$, **4.8** (7.1% yield), 1.16 mg of orange $Ir_5(CO)_9(Ph)(COD)_2$, **4.7** (8.8% yield) and other minor products. Spectral data for **4.5**: IR $\nu_{CO}$ ($cm^{-1}$ in $CH_2Cl_2$): 2055(vs), 2027(vs), 1994(s), 1980(s), 1844(m). $^1H$ NMR ($CDCl_3$, in ppm) $\delta$ = 5.37-5.54 (m, 6H, CH), 2.21-2.47(m, 16H, $CH_2$). Mass Spec. ES (negative ion) for **4.5**: *m*/*z*=1259 $(M+Br)^-$, 1231 $(M+Br\text{-}CO)^-$. The isotope distribution pattern is consistent with the presence of four iridium atoms. Spectral data for **4.6**: IR $\nu_{CO}$ ($cm^{-1}$ in $CH_2Cl_2$): 2080(w), 2055(vs), 2044(vs), 2027(s), 2006(m), 1844(m), 1804(m). $^1H$ NMR ($CDCl_3$, in ppm) $\delta$ = 6.71-6.84 (m, 5H, $\sigma$-Ph) 5.23-5.57 (m, 4H, CH), 1.97-2.53(m, 8H, $CH_2$). Mass Spec. ES (negative ion) for **4.6:** *m*/*z*=1451 $(M\text{-}H\text{-}H_2)^-$. The isotope distribution pattern is consistent with the presence of five iridium atoms. Spectral data for **4.7**: IR $\nu_{CO}$ ($cm^{-1}$ in $CH_2Cl_2$): 2068(m),

2035(vs), 2016(s), 1997(m), 1844(w), 1825(w), 1785(w). $^1$H NMR ($CDCl_3$, in ppm) δ = 6.84-6.93(m, 5H, Ph), 5.21-5.37 (m, 8H, COD), 1.95 – 2.11 (m, 16H, $CH_2$). Mass Spec. ES (negative ion) for **4.7:** *m*/*z* = 1503 $(M\text{-}H\text{-}H_2)^-$. The isotope distribution pattern is consistent with the presence of five iridium atoms. Spectral data for **4.8**: IR $\nu_{CO}$ ($cm^{-1}$ in $CH_2Cl_2$): 2074(m), 2043(s), 2031(vs), 2025(vs), 1995(w), 1968(w), 1813(w). $^1$H NMR ($CDCl_3$, in ppm) δ = 6.84-6.91 (m, 5H, Ph), 5.23-5.51 (m, 6H, CH), 2.25 – 2.37 (m, 16H, $CH_2$). Mass Spec. ES (positive ion) for **4.8:** *m*/*z* = 2442 $(M^+)$, 2481$(M+K)^+$. The isotope distribution pattern is consistent with the presence of nine iridium atoms.

**Synthesis of $Ir_5(CO)_7(\mu_4\text{-}\eta^2\text{:}\eta^1\text{-}C_8H_{11})(COD)_2$, 4.9.**

A 6.7 mg (0.004 mmol) portion of compound **4.7** and 7 μL of 1,5-COD dissolved in 10 mL heptane were heated to reflux for 2h. 3.34 mg (51% yield) of **4.9** was isolated from this reaction mixture by TLC by eluting with a 3:1 hexane/methylene chloride solvent mixture. Spectral data for **4.9**: IR $\nu_{CO}$ ($cm^{-1}$ in $CH_2Cl_2$): 2030(m), 1997(vs), 1942(m), 1844(m). $^1$H NMR ($CDCl_3$, in ppm) δ = 5.23-5.40 (m, 9H, CH-cod), 1.55-1.93(m, 26H, $CH_2$-cod). Mass Spec. ES (positive ion) for **4.9:** *m*/*z* = 1480 $(M)^+$, 1481 $(M+H)^+$. The isotope distribution pattern is consistent with the presence of five iridium atoms.

**Improved Yield of 4.7**.

A 4.4 mg (0.007 mmol) portion of $[Ir(COD)Cl]_2$ was added to 9.0 mg (0.007 mmol) of **4.7** that was dissolved in 15 mL of benzene. 7 μL of 1,5-COD was added to the above mixture and the reaction solution was heated to reflux for 2 h. The solvent was then removed *in vacuo*, and the product was isolated by TLC by eluting with a 3:1 hexane/methylene chloride solvent mixture. This yielded in order of elution: 0.30 mg of

yellow $Ir_4(CO)_{10}(C_8H_{12})$, (3.7% yield), 0.94 mg of compound **4.5** (11.4% yield), 0.44 mg of compound **4.6** (5.4% yield), 0.41 mg of red $Ir_5(CO)_7(\mu_4\text{-}\eta^2\text{:}\eta^1\text{-}C_8H_{11})(COD)_2$, **4.9** (4.0% yield), 2.52 mg of orange compound **4.7** (30% yield).

**Improved Yield of 4.8 from the Reaction of 4.5 with 4.6 at 98℃.**

A 8.1 mg (0.007 mmol) portion of compound **4.5** and 6.2 mg (0.004 mmol) of compound **4.6** were dissolved in 15 mL of heptane. The reaction solution was heated to reflux for 1 h. The solvent was then removed *in vacuo*, and the product was isolated by TLC by eluting with a 3:1 hexane/methylene chloride solvent mixture to yield 1.71 mg of $Ir_9(CO)_{15}(Ph)(\mu_3\text{-}C_8H_{10})(COD)$, **4.8** (16% yield).

**Synthesis of $Ir_4(CO)_{10}(COD)$ and $Ir_4(CO)_8(COD)_2$ from $[Et_4N][Ir_4(CO)_{11}(Ph)]$, 4.1.**

A 10.1 mg (0.008 mmol) portion of $[Et_4N][Ir_4(CO)_{11}(Ph)]$, **4.1** was dissolved in 10 mL benzene stirred with 14 μL COD at room temperature. 7.0 μL of $HBF_4$ was added to the above mixture and stirred for 30 min. The solvent was then removed in vacuo, and the products were isolated by TLC by eluting with a 3:1 hexane/methylene chloride solvent mixture to yield 5.3 mg $Ir_4(CO)_{10}(COD)$[11] (58% yield) and 2.0 mg $Ir_4(CO)_8(COD)_2$[11], (21% yield).

**Crystallographic Analyses:** Single crystals of **4.1** (yellow)**, 4.2** (yellow), **4.3** (brown), **4.5** (black), **4.6** (black), and **4.7** (black) suitable for x-ray diffraction analyses were obtained by slow evaporation of solvent from hexane/methylene chloride solvent mixtures at -25 ℃. Single crystals of **4.4** (brown) and **4.8** (black) were grown from a benzene/methylene chloride solvent mixture by slow evaporation of solvent at room temperature. Black single crystals of **4.9** suitable for x-ray diffraction analysis were

obtained by slow evaporation of solvent from a benzene/octane solvent mixture at room temperature. Each data crystal was glued onto the end of a thin glass fiber. X-ray intensity data were measured by using a Bruker SMART APEX CCD-area detection diffractometer by using Mo Kα radiation (λ = 0.71073 Å). The raw data frames were integrated with the SAINT+ program by using a narrow-frame integration algorithm.[12] Corrections for Lorentz and polarization effects were also applied with SAINT+. An empirical absorption correction based on the multiple measurement of equivalent reflections was applied in each analysis by using the program SADABS. All structures were solved by a combination of direct methods and difference Fourier syntheses, and refined by full-matrix least-squares on $F^2$, using the SHELXTL software package.[13] All non-hydrogen atoms were refined with anisotropic displacement parameters. Hydrogen atoms were placed in geometrically idealized positions and included as standard riding atoms during the least-squares refinements. Crystal data, data collection parameters, and results of the analyses are listed in Table 4.1. Compounds **4.1, 4.2, 4.3, 4.4, 4.5, 4.6, 4.7, 4.8,** and **4.9** all crystallized in the monoclinic crystal system. The space group $P2_1/n$ was indicated by the systematic absences in the intensity data for compounds **4.1, 4.4, 4.5, 4.6,** and **4.8** and were confirmed by the successful solutions and refinements of those structures. There is one symmetry independent molecule in the asymmetric unit. There is one molecule of methylene chloride and a half molecule of benzene from the crystallization solvent cocrystallized with **4.4** in the asymmetric crystal unit. The solvent molecules were satisfactorily refined with isotropic thermal parameters. For compound **4.8** one and a half molecules of benzene from the crystallization solvent were cocrystallized with the complex in the asymmetric crystal unit. The solvent molecules

were refined with isotropic thermal parameters.The systematic absences in the intensity data for compound **4.2** were consistent with the space groups *C*c and *C*2/c. The centrosymmetric space group *C*2/c was selected and confirmed by the successful solution and refinement of the structure. There is one symmetry independent molecule of **4.2** in the asymmetric crystal unit**.** The crystal of **4.2** also contains a half molecule of hexane from the crystallization solvent that was cocrystallized with the complex. The space group $P2_1/c$ was identified uniquely on the basis of the systematic absences in the intensity data for compound **4.3, 4.7** and **4.9**. There is one symmetry independent molecule in the asymmetric crystal unit of each compound. For compound **4.9** after location of all non-hydrogen atoms, a very large (ca. 8 e-/$Å^3$) residual electron density peak remained, approximately at the midpoint of the C64-C65 bond. This peak was interpreted to arise from an fractionally occupied iridium atom of a disordered $Ir(COD)(CO)_2$ group. Refining this peak as a fractionally occupied iridium atom yielded an occupancy value near 10%. At the same time, refining the occupancy of iridium atom Ir2 yielded an occupancy value of ca. 90% (FVAR = 0.896240), accompanied by a sharp decrease in R-values and a flattening of the difference map, with the major peak now being 1.97 e-/$Å^3$, located near Ir5. The sum of the occupancies of Ir2 and Ir2B was very close to unity upon free refinement, which strongly supports the $Ir(COD)(CO)_2$ disorder model. For the final refinement cycles, the total occupancy of the disordered Ir atoms (Ir2 and Ir2B) was constrained to unity. The cod and carbonyl groups bonded to the minor disorder component (Ir2B) could not be modeled since they are populated in the crystal only to the extent of ca. 10%.

**Results and Discussion**

The new air-stable tetrairidium anion $[Ir_4(CO)_{11}(\sigma\text{-Ph}]^-$, **4.1** was isolated as the $[Et_4N]^+$ salt in 45% yield from the reaction of $[Et_4N][Ir_4(CO)_{11}Br]$ with $SnPh_3OH$. $[Et_4N]$**4.1** was characterized by a combination of IR, $^1H$ NMR, mass spec and single crystal X-ray diffraction analyses. An ORTEP diagram of the tetrairidium anion **4.1** is shown in Figure 4.1. The structure of the anion **1** is similar to that of the complex anion $[Ir_4(CO)_{11}Br]^-$ from which it was made.[14] The anion **4.1** consists of a tetrahedral $Ir_4$ cluster with eleven carbonyl ligands distributed as shown in the figure. There are three bridging carbonyl ligands. All of CO the others are terminally coordinated. The Ir – Ir bond distances are similar to those found in the anion $[Ir_4(CO)_{11}Br]^-$.[14] The anion **4.1** contains one σ-phenyl ligand that is terminally coordinated to iridium atom Ir(1). The Ir – C bond distance to the phenyl ligand Ir(1) – C(44) = 2.125(13) Å, is slightly longer than the Ir – C distances to the σ-phenyl ligands in the previously reported $Ir_3$, $Ir_4$ and $Ir_8$ complexes: $Ir_3(CO)_9(Ph)(\mu_3\text{-PPh})(\mu\text{-dppm})$, 2.084(16) Å,[15] $Ir_4(CO)_8(\mu\text{-Ph})[\mu_4\text{-}\eta^3\text{-PhPC(H)CPh}](\mu\text{-PPh}_2)$, 2.09(1) Å[16] and $Ir_8(CO)_{16}(\sigma\text{-Ph})(\mu\text{-PPh}_2)(\mu_4\text{-PPh})$, 2.06(4) Å.[17]

Compound **4.1** was also obtained in 36.4% yield from the reaction of $SnPh_4$ with $[Et_4N][Ir_4(CO)_{11}Br]$ in methanol solvent over a 16 h period. An analysis of a reaction mixture by $^{119}Sn$ NMR spectroscopy revealed a resonance at δ = - 60.48 which is consistent with the formation of the tin compound $SnPh_3Br$.[9] This observation confirms that the formation of **4.1** by the reaction with $SnPh_4$ occurs by Br for Ph transmetalation, eq. (4.5). Transmetalation reactions between aryltin compounds and metal halide complexes of platinum[18] and palladium[19] have been known for some years. Recently, aryltin compounds have been used to transfer aryl groups to gold (I) halides.[20] Tin compounds also form the basis for the important transmetalation step in the well-known

Stille coupling reactions.[5] Although $SnPh_3OH$ reacts with $Ir_4(CO)_{12}$ in the presence of base to yield $Ir_4Sn$ complexes eq. (4.3), we think the reaction with the bromo complex $[Ir_4(CO)_{11}Br]^-$ reported to yield **4.1** here in the absence of base proceeds instead by a transmetalation process.

When compound **4.1** was allowed to react with $PPh_3$ in benzene solvent at reflux for 1 h, the new compound $[Et_4N][Ir_4(CO)_{10}(PPh_2C_6H_4)]$, **4.2** was obtained and isolated in 60% yield. Compound **4.2**, a salt, was characterized by a combination of IR, $^1H$ NMR, mass spec and single crystal X-ray diffraction analyses. An ORTEP diagram of the tetrairidium anion of **4.2** is shown in Figure 4.2. The anion of **4.2** consists of a tetrahedral $Ir_4$ cluster with ten carbonyl ligands. Three of the CO ligands are bridging ligands about the Ir(1) – Ir(2) – Ir(3) triangle. The other CO ligands are terminally coordinated. The most interesting ligand is an edge-bridging $PPh_2C_6H_4$ group derived from the $PPh_3$ reagent that became ortho-metallated to one of the Ir atoms. The aryl group is σ-bonded to Ir(3). The Ir – C bond, Ir3 – C56 = 2.096(12) Å is similar in length to that of the σ-bonded phenyl group in anion **4.1**. The shortest Ir – Ir bond in the cluster is the one bridged by the $PPh_2C_6H_4$ ligand, Ir1 – Ir3 = 2.6633(6) Å. The longest Ir – Ir bond is the one trans to the σ-bonded aryl group, Ir3 - Ir4 = 2.7728(7) Å. This may be due to a strong trans-structural effect of the σ-bonded aryl group.[21] The fate of the phenyl group that was eliminated from **4.1** in the reaction and that of the hydrogen atom that was cleaved from the ortho-position of the metallated phenyl ring in **4.2** has not been established. It is presumed that they have been combined to form benzene.

Interestingly, when anion **4.2** was treated with $HBF_4$ under an atmosphere of CO for 1 h, the anion was neutralized by the addition of $H^+$. The $H^+$ was added to the carbon

atom of the metallated phenyl ring. A CO ligand was added to the complex and the known compound $Ir_4(CO)_{11}(PPh_3)$[10] was obtained in 81% yield together with a trace of $Ir_4(CO)_{12}$.

Compounds **4.2** (37% yield) and $Ir_4(CO)_{11}(PPh_3)$ (8% yield) together with two new pentairidium compounds, $Ir_5(CO)_{12}Ph(PPh_3)$, **4.3** (11% yield) and $Ir_5(CO)_{11}(PPh_3)(PPh_2C_6H_4)$, **4.4** (22% yield) were obtained from the reaction of **4.1** with $Ir(CO)(PPh_3)_2Cl$ in a benzene at reflux. The yield of **4** was increased to 40% at the expense of the formation of **4.3** by increasing the reaction time to 5h, probably because **4.3** reacts with $PPh_3$ to yield **4.4**, see below. Compounds **4.3** and **4.4** were both characterized by single crystal X-ray diffraction analysis. An ORTEP diagram of the molecular structure of **4.3** is shown in Figure 4.3. The compound contains a trigonal pyramidal cluster of five iridium atoms. The apical iridium atom Ir(1) contains a $PPh_3$ ligand and apical iridum atom Ir(5) contains a terminally coordinated σ-phenyl ligand. The Ir – Ir bond distances span a considerable range, 2.6848(4) Å – 2.8269(8) Å. The two longest Ir – Ir bonds lie trans to the phosphine and σ-phenyl ligands, Ir(1) – Ir(3) = 2.8269(8) Å and Ir(4) – Ir(5) = 2.7912(8) Å, respectively. The Ir – C bond to the σ-phenyl ligand is similar in length to that found in **1**, Ir5 – C4 = 2.116(16) Å. Compound **4.3** has four bridging carbonyl ligand with two bridging to each of the apical Ir atoms of the cluster.

An ORTEP diagram of the molecular structure of **4.4** is shown in Figure 4.4. This compound also consists of a trigonal pyramidal cluster of five iridium atoms. As in **4.3**, the apical iridium atom Ir(1) also contains a $PPh_3$ ligand. There is a bridging $PPh_2C_6H_4$ ligand similar to that found in **4.2** with the phosphorus atom coordinated to Ir(5) and the

metallated phenyl ring coordinated to the equatorial Ir atom, Ir(2), Ir2 – C70 = 2.14(2) Å. The $PPh_2C_6H_4$-bridged bond Ir(2) – Ir(5) is the shortest in the molecule, 2.6891(8) Å, and the Ir(1) – Ir(3) bond that lies trans to the $PPh_3$ ligand is the longest in the molecule, 2.8269(8) Å, as found in **4.3**. Anion **4.2** was found to react with $Ir(CO)(PPh_3)_2Cl$ to give compound **4.4** in 11% yield, and **4.3** was transformed into **4.4** in 43% yield in a CO ligand substitution reaction with $PPh_3$.

A summary of the reactions described in this report is shown in Scheme 4.1. The new air-stable anionic tetrairidium complex **4.1** containing a terminally coordinated ligand was obtained via a phenyl for Br exchange (transmetalation) reaction between $[Ir_4(CO)_{11}Br]^-$ and the tin reagents $SnPh_3OH$ and $SnPh_4$. Anion **4.1** reacts with $PPh_3$ to yield the tetrairidium anion **4.2** by the addition of one $PPh_3$ ligand, loss of one CO ligand and an ortho-metallation of one of the phenyl rings of the $PPh_3$ ligand. The original phenyl ligand in **4.1** and the hydrogen atom that was cleaved from the metallated phenyl ring were eliminated from the complex in this reaction, presumably they were combined to form benzene. When **4.2** was treated with $H^+$ in the presence of CO, the ortho-metallation was reversed presumably via protonation at one of the metal atoms followed by C-H reductive elimination of the metallated phenyl ring and the addition of CO to that site. Treatment of **4.1** with $Ir(CO)(PPh_3)_2Cl$ also yielded some **4.2**, possibly by a simple competing reaction of **4.1** with some $PPh_3$ released from the $Ir(CO)(PPh_3)_2Cl$. In addition the two new pentairidium complexes **4.3** and **4.4** were obtained from this reaction. Complex **4.3** was formed by an addition of one equivalent of $Ir(CO)(PPh_3)_2Cl$ to **4.1** accompanied by the loss of one $PPh_3$ ligand and $Cl^-$. Compound **4.4** was formed by an addition of one equivalent of $Ir(CO)(PPh_3)_2Cl$ to **4.1** accompanied by the loss of one CO

ligand and $Cl^-$. Interestingly, compound **4.1** was also obtained by the reaction of **4.2** with one equivalent of $Ir(CO)(PPh_3)_2Cl$ that was accompanied by the loss of one $PPh_3$ ligand and $Cl^-$ and also by reaction of **4.3** with $PPh_3$ that was accompanied by the elimination of the σ-phenyl ligand and the hydrogen atom from the metallated phenyl ring.

The reaction of the $[Et_4N][Ir_4(CO)_{11}Ph]$, **4.1** with $[Ir(COD)Cl]_2$ has yielded the two tetrairidium compounds $Ir_4(CO)_{10}(COD)$,[11] (2.4% yield), $Ir_4(CO)_7(COD)(\mu_4\text{-}C_8H_{10})$,[11] **4.5** (11.3% yield), and the three new higher nuclearity complexes $Ir_5(CO)_{11}(Ph)(COD)$, **4.6** (9.8% yield), $Ir_5(CO)_9(Ph)(COD)_2$, **4.7** (8.8% yield) and $Ir_9(CO)_{15}(Ph)(\mu_3\text{-}C_8H_{10})(COD)$, **4.8** (7.1% yield) that contain σ-phenyl ligands, scheme 4.2. $Ir_4(CO)_{10}(COD)$ was obtained previously from the reaction of $Ir_4(CO)_{12}$ with COD in refluxing thf in the presence of $Me_3NO$.[11] We have found that $Ir_4(CO)_{10}(COD)$ can be obtained in good yield (58%) along with some $Ir_4(CO)_8(COD)_2$[11] (23% yield) from the reaction of $[Et_4N][Ir_4(CO)_{11}Ph]$, **4.1** with COD in the presence of $HBF_4$. We suspect that some free COD (derived from the $[Ir(COD)Cl]_2$) and adventitious $H^+$ in our reaction of $[Et_4N][Ir_4(CO)_{11}Ph]$, **4.1** with $[Ir(COD)Cl]_2$ led to the formation of the small quantities of $Ir_4(CO)_{10}(COD)$ in this reaction. Compound **4.5** was obtained previously from the reaction of $Ir_4(CO)_{12}$ with COD by heating in chlorobenzene to reflux and by heating $Ir_4(CO)_8(COD)_2$ in cyclohexane to reflux.[11]

Compound **4.5** has not yet been characterized crystallographically and thus, a single-crystal X-ray diffraction analysis of the molecular structure of **4.5** was performed as a part of this work. An ORTEP diagram of the molecular structure compound **4.5** as found in the solid state is shown in Figure 4.5. The structure consists of a butterfly-tetrahedral cluster of four iridium atoms with seven carbonyl ligands. Two of the seven

CO ligands are bridging ligands across oppositely positioned hinge-wingtip Ir – Ir edges of the cluster. There is a bidentate COD ligand coordinated to the wingtip metal atom Ir(4) and a $C_8H_{10}$, cycloocta-1-ene-5-yne ligand that bridges all four metal atoms. The yne functional group lies in the fold of the butterfly cluster and exhibits the typically long C – C bond length, C(33) – C(34) = 1.443(8) Å. Although they are not common, cycloocta-1-ene-5-yne ligands have been formed previously in high temperature reactions of metal cluster complexes with COD including the synthesis of a similar tetranuclear $Ir_4$ derivative of **4.5**, $Ir_4(CO)_5(COD)_2(\mu_4\text{-}C_8H_{10})$.[11]

An ORTEP diagram of the molecular of **4.6** is shown in Figure 4.6. Compound **4.6** contains five iridium atoms in the form of a trigonal bipyramid. There is a COD ligand on the apical atom Ir(5) and a σ-phenyl ligand that is terminally coordinated to the other apical atom iridium atom Ir(1). The Ir – C bond distance to the σ-phenyl ligand, Ir1 - C43 = 2.082(10) Å, is slightly shorter than the Ir – C distance to the σ-phenyl ligand in $[Et_4N][Ir_4(CO)_{11}(Ph)]$, **4.1** 2.125(13) Å, but is similar to those in the complexes: $Ir_5(CO)_{12}(Ph)(PPh_3)$, **4.3**, 2.096(12) Å, $Ir_3(CO)_9(Ph)(\mu_3\text{-}PPh)(\mu\text{-dppm})$, 2.084(16) Å,[22] $Ir_4(CO)_8(\sigma\text{-}Ph)[\mu_4\text{-}\eta^3\text{-}PhPC(H)CPh](\mu\text{-}PPh_2)$, 2.09(1) Å[23] and $Ir_8(CO)_{16}(\sigma\text{-}Ph)(\mu\text{-}PPh_2)(\mu_4\text{-}PPh)$, 2.06(4) Å.[24] Compound **4.3** contains a trigonal bipyramidal $Ir_5$ cluster similar to **4.6** and also has a σ-phenyl ligand on one of the apical Ir atoms of the trigonal bipyramid. The principal difference between **4.6** and **4.3** is the presence of a COD ligand on the other apical iridium atom in **4.6** in the place of the $PPh_3$ ligand and one CO ligand in **4.3**. The Ir – Ir bond distances in **4.6** are very similar to those in **4.3**. The cluster of **4.6** contains a total of 72 valence electrons, i. e. all five iridium atoms have 18 electron configurations.

Compound **4.7** can be viewed as a COD derivative of **4.6** and it was obtained in a better yield (30%) when COD is added to the reaction of $[Et_4N][Ir_4(CO)_{11}Ph]$, **4.1** with $[Ir(COD)Cl]_2$. An ORTEP diagram of the molecular structure of **4.7** is shown in Figure 4.7. Like **4.6** and **4.3**, the metal cluster of **4.7** also has the shape of a trigonal bipyramid, but its σ -phenyl ligand is coordinated to one of the equatorial Ir atoms instead of one of the apical Ir atoms. The Ir – C bond Ir2 - C43 = 2.120(9) is longer than that in **4.6** and **4.3**, probably due to the increased sterics of the equatorial metal site. There are two COD ligands in **4.7** and both are coordinated to the apical Ir atoms, one COD to each Ir. The Ir – Ir bond distances in **4.7** are very similar to those in **4.6** and **4.3**. The cluster of **4.7** contains a total of 72 valence electrons, thus, all five iridium atoms have an 18 electron configurations. Interestingly, the parent ions observed in negative ion electrospray mass spectra of **4.6** and **4.7** show the loss of two hydrogen atoms. Loss of $H_2$ has been observed previously in the mass spectra of iridium carbonyl cluster complexes containing COD ligands.[11] The $H_2$ elimination may be related to the conversion of the COD olefinic functions into "yne" functions as shown below in the conversion of **4.7** to **4.9**.

Compound **4.8** is perhaps the most interesting product from this study, and it turns out that it is really derived from a secondary condensation reaction between compounds **4.5** and **4.6** (16% yield) that is accompanied by the loss of three CO ligands and one COD ligand. Compound **4.8** was characterized crystallographically and an ORTEP diagram of its molecular structure is shown in Figure 4.8. Compound **4.8** contains nine iridium atoms. The cluster is best described as a tricapped octahedron. Although there are many examples multicapped octahedra among the families of higher nuclearity metal carbonyl cluster complexes,[25] they are very rare in the iridium group. In fact, this is the first

structural characterization of a pure iridium multicapped $Ir_6$ octahedron, although there are examples of heteronuclear capped $Ir_6$ octahedra, e.g. $[Ir_6Ru_3(CO)_{23}]^{2-}$ and $[Ir_6(CO)_{23}(HgCl)_2]^{2-}$,[26,27] and the osmium anion $[HOs_9(CO)_{24}]^-$ was found to contain a tricapped octahedral $Os_9$ cluster at its core.[28] The capping atom Ir(8) in **4.8** contains a σ-phenyl ligand carried in from **4.6** and the triangular group Ir(3), Ir(6) and Ir(9) contain a cycloocta-1-ene-5-yne ligand carried in from **4.5**. Unlike that in **4.5**, the cycloocta-1-ene-5-yne ligand in **4.8** is only a triply-bridging ligand, and as a result the C – C bond of the yne function has decreased in length, C(92) – C(93)= 1.33(7) Å. Capping atom Ir(7) contains a COD ligand, but there is no way to determine if that ligand was derived from the COD ligand in **4.5** or **4.6**. The Ir – C bond distance to the σ-phenyl ligand is Ir(8) – C(83)= 2.17(5) Å. Compound **4.8** contains a total of 122 cluster valence electrons which is in accord with the predictions of the condensed polyhedra principles of the Polyhedral Skeletal Electron Pair theory.[29]

When compound **4.7** was allowed to react with COD at 98 $^oC$ for 2 h, the new compound **4.9** was obtained in 51% yield. The structure of **4.9** was established by a single-crystal X-ray diffraction analysis and an ORTEP diagram of its molecular structure is shown in Figure 4.9. Compound **4.9** contains five iridium atoms and the structure of the metal cluster can be described as a Ir-capped, Ir(1), butterfly tetrahedron, Ir(2) – Ir(5). Atoms Ir(1) and Ir(5) contain COD ligands and there is a quadruply-bridging $\eta^2:\eta^1$-$C_8H_{11}$ (1-irida-cycloocta-4-yne) ligand coordinated to the butterfly portion of the cluster with the C – C triple bond lying in the fold of the butterfly. The C – C triple bond was formed by the abstraction of the two hydrogen atoms from one of the C – C double bonds of a COD ligand. One of these hydrogen atoms was apparently transferred to one of the

carbon atoms of the other C – C double bond of that COD ligand. The remaining carbon atom of that double bond is σ-bonded to the cluster at atom Ir(2), Ir(2) – C(60) = 2.173(13) Å. The second of the abstracted hydrogen atoms was probably combined with the phenyl ligand and eliminated as benzene. The C – C triple bond distance is long, C(64) – C(65) = 1.48(3) Å, due to its coordination to the four metal atoms. Compound **4.9** contains a total of 72 cluster valence electrons and is thus formally unsaturated by the amount of two electrons.[29] Curiously, the Ir(1) – Ir(2) distance, 2.8947(7) Å, is much longer than all of the other Ir – Ir bonds in this molecule. If this bond was ignored, then atom Ir(1) would formally have a 16 electron configuration and the "unsaturation" would be located formally on Ir(1). A similarly long Ir – Ir bond was found to the $Ir(CO)_2$ capping group in the anion $[Ir_{12}(CO)_{24}]^{2-}$.[30]

**Summary and Conclusions**

Phenyl-substituted tin compounds are active for the synthesis of anionic stable σ-phenyl iridium carbonyl cluster complexes by transmetalation reactions. The anion **4.1** has sufficient nucleophilicity to react with the several mononuclear iridium species such as $Ir(CO)(PPh_3)_2Cl$ and $[Ir(COD)Cl]_2$ through condensation to yield a new family of uncharged pentairidium complexes.

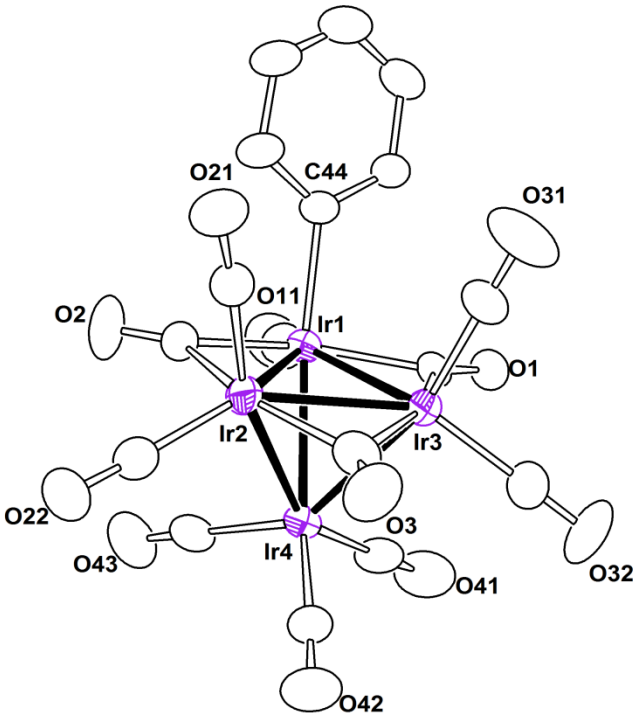


**Figure 4.1.** An ORTEP diagram of the molecular structure of the complex anion $[Ir_4(CO)_{11}Ph]^-$ of **4.1** showing 30% thermal ellipsoid probability.

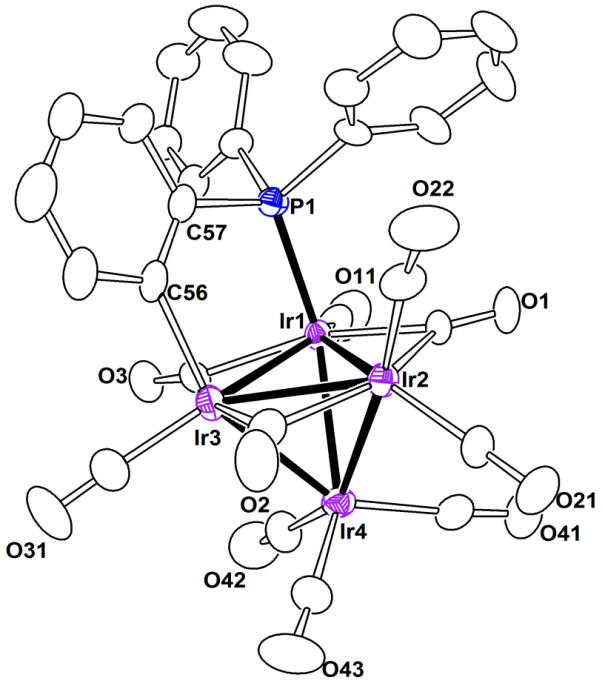


**Figure 4.2.** An ORTEP diagram of the molecular structure of the complex anion $[Ir_4(CO)_{10}(PPh_2C_6H_4)]^-$ of **4.2** showing 30% thermal ellipsoid probability.

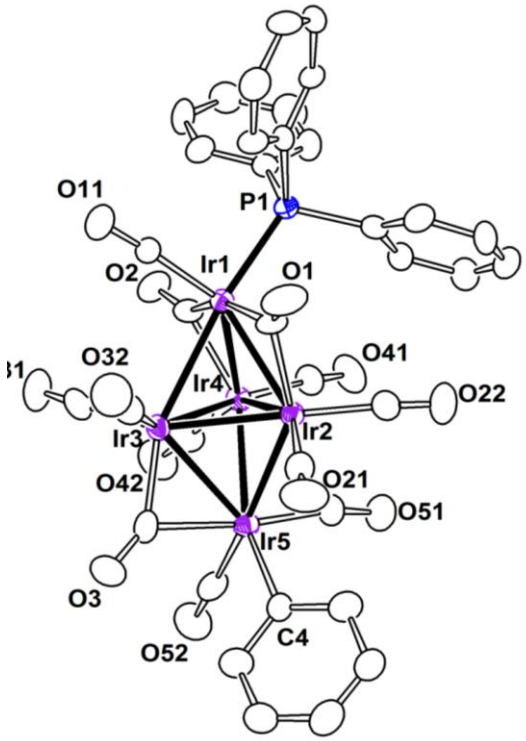


**Figure 4.3.** An ORTEP diagram of the molecular structure of $Ir_5(CO)_{12}Ph(PPh_3)$, **4.3**, showing 30% thermal ellipsoid probability.

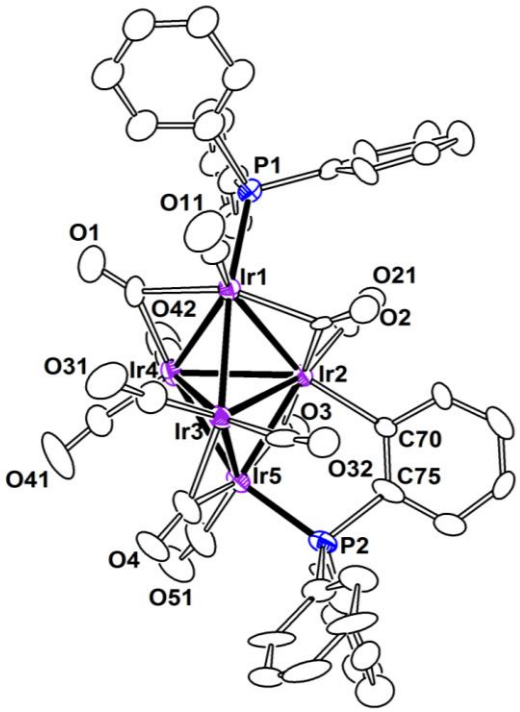


**Figure 4.4.** An ORTEP diagram of the molecular structure of $Ir_5(CO)_{11}(PPh_3)(PPh_2C_6H_4)$, **4.4** showing 30% thermal ellipsoid probability.

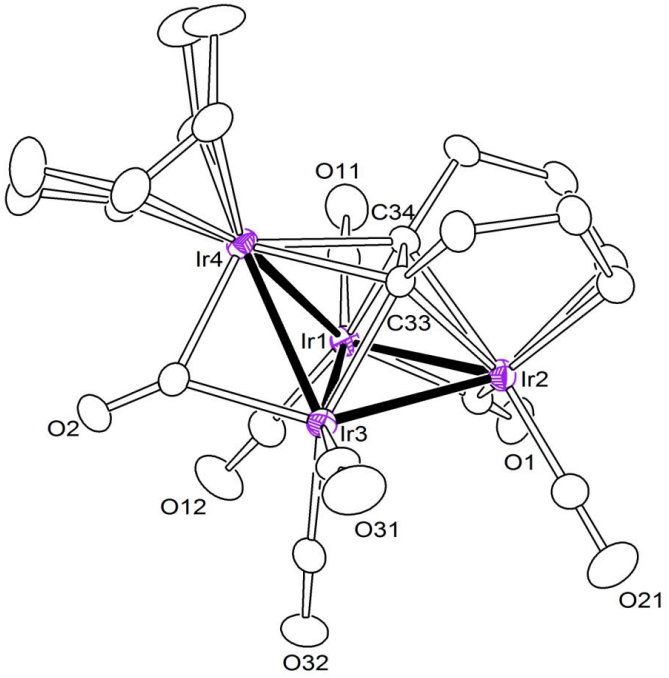


**Figure 4.5.** An ORTEP diagram of the molecular structure of $Ir_4(CO)_7(COD)(\mu_4\text{-}C_8H_{10})$, **4.5** showing 30% thermal ellipsoid probability.

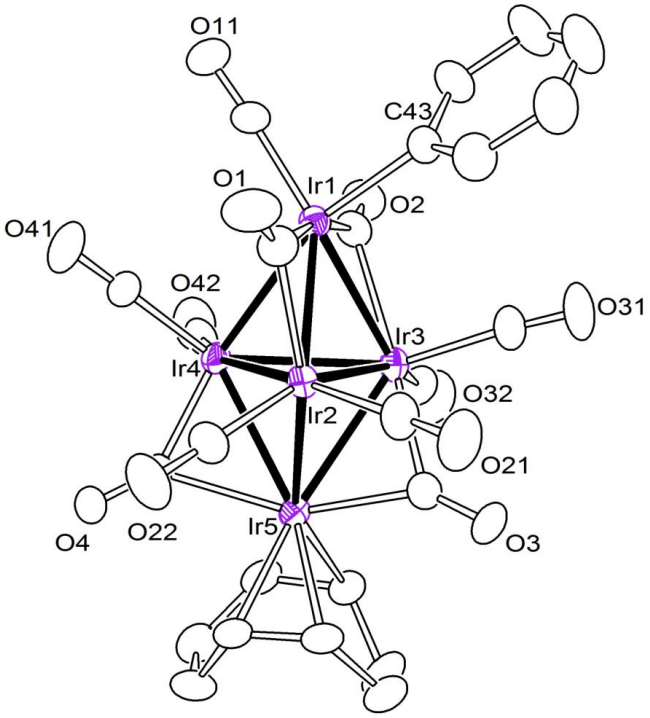


**Figure 4.6.** An ORTEP diagram of the molecular structure of $Ir_5(CO)_{11}(Ph)(COD)$, **4.6** showing 30% thermal ellipsoid probability.

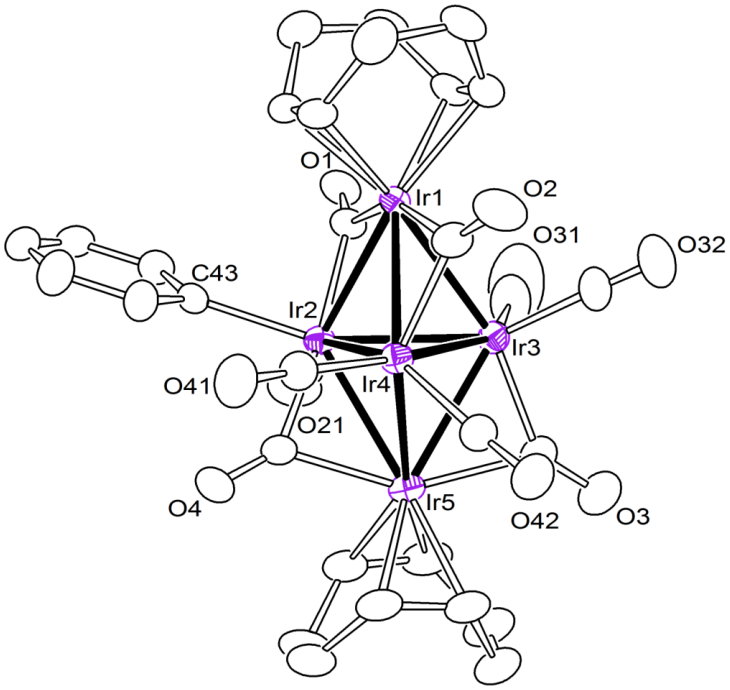


**Figure 4.7.** An ORTEP diagram of the molecular structure of $Ir_5(CO)_9(Ph)(COD)_2$, **4.7** showing 30% thermal ellipsoid probability.

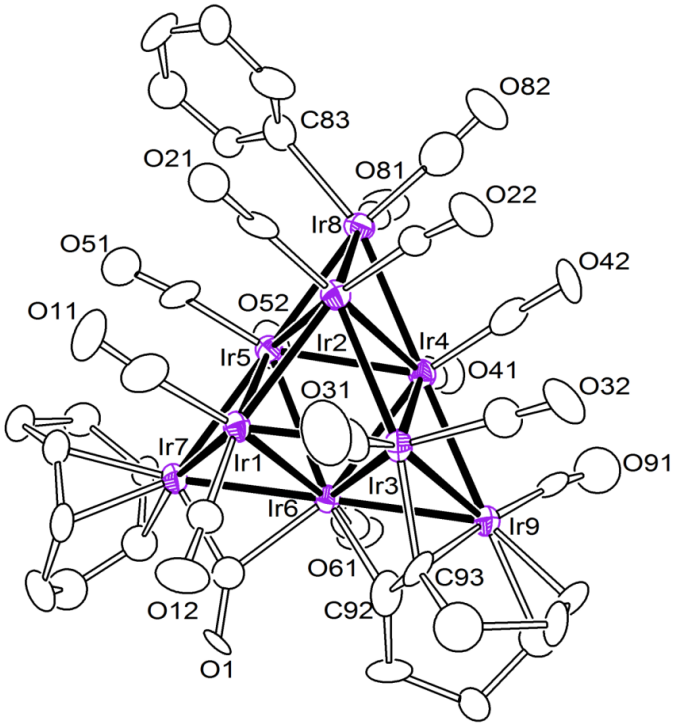


**Figure 4.8.** An ORTEP diagram of the molecular structure of $Ir_9(CO)_{15}(Ph)(COD)(\mu_3\text{-}C_8H_{10})$, **4.8** showing 30% thermal ellipsoid probability.

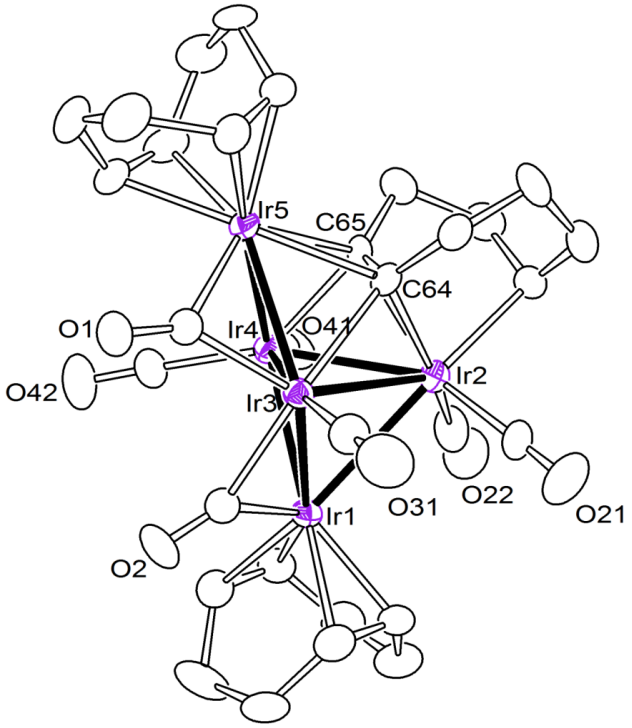


**Figure 4.9.** An ORTEP diagram of the molecular structure of $Ir_5(CO)_7(COD)_2(\mu_4\text{-}\eta^2\text{–}\eta^1\text{-}C_8H_{11})$, **4.9** showing 30% thermal ellipsoid probability.

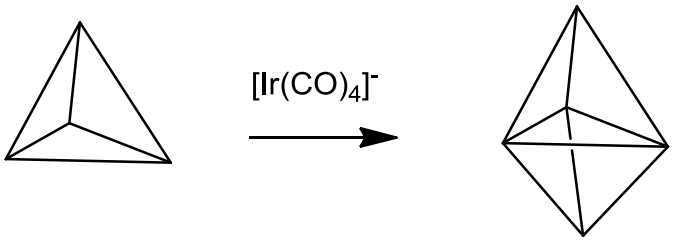


$[HIr_4(CO)_{11}]^-$ $[HIr_5(CO)_{12}]^{2-}$ **4.1**

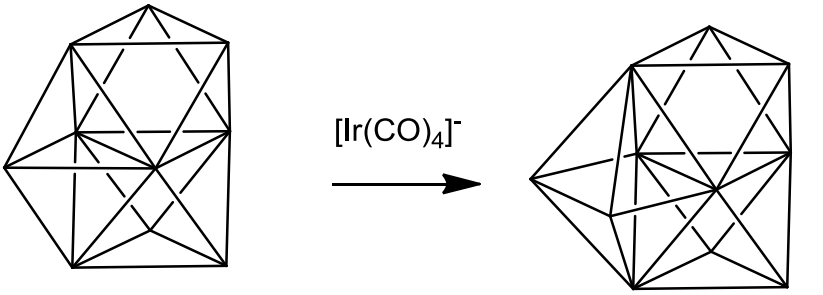


$[Ir_{10}(CO)_{21}]^{2-}$ $[Ir_{11}(CO)_{23}]^{3-}$ **4.2**

Equation 4.1 & 4.2 Chini's successful synthesis of large iridium carbonyl cluster complexes.

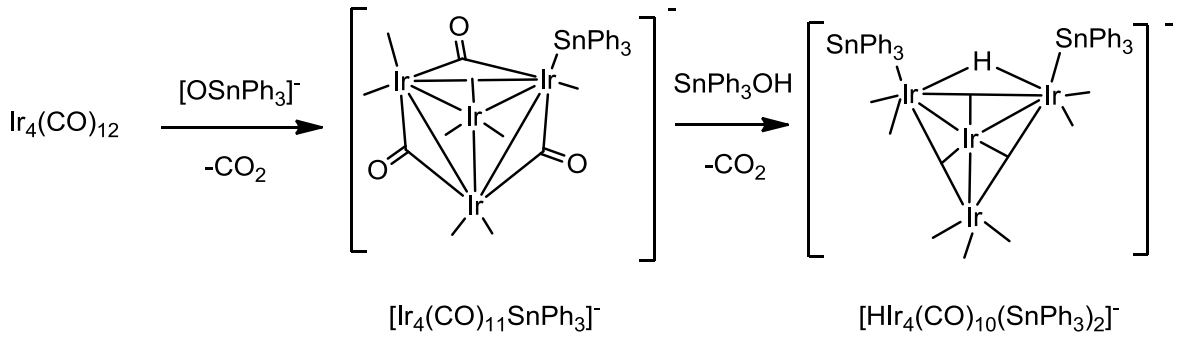


Equation 4.3 Reaction of $Ir_4(CO)_{12}$ with $SnPh_3OH$ in the presence of $[OH]^-$.

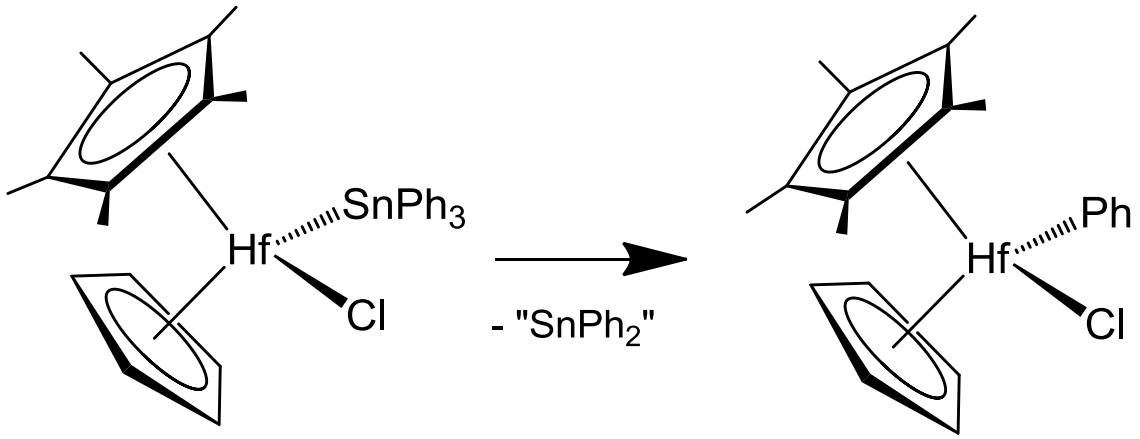


Equation 4.4 Example of Stille coupling reactions showing elimination of a $SnPh_2$ group to form σ-phenyl coordinated complexes.

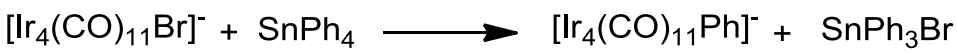


Equation 4.5 Formation of compound **4.1** by transmetalation reaction of $[Et_4N][Ir_4(CO)_{11}Br]$ with $SnPh_4$.

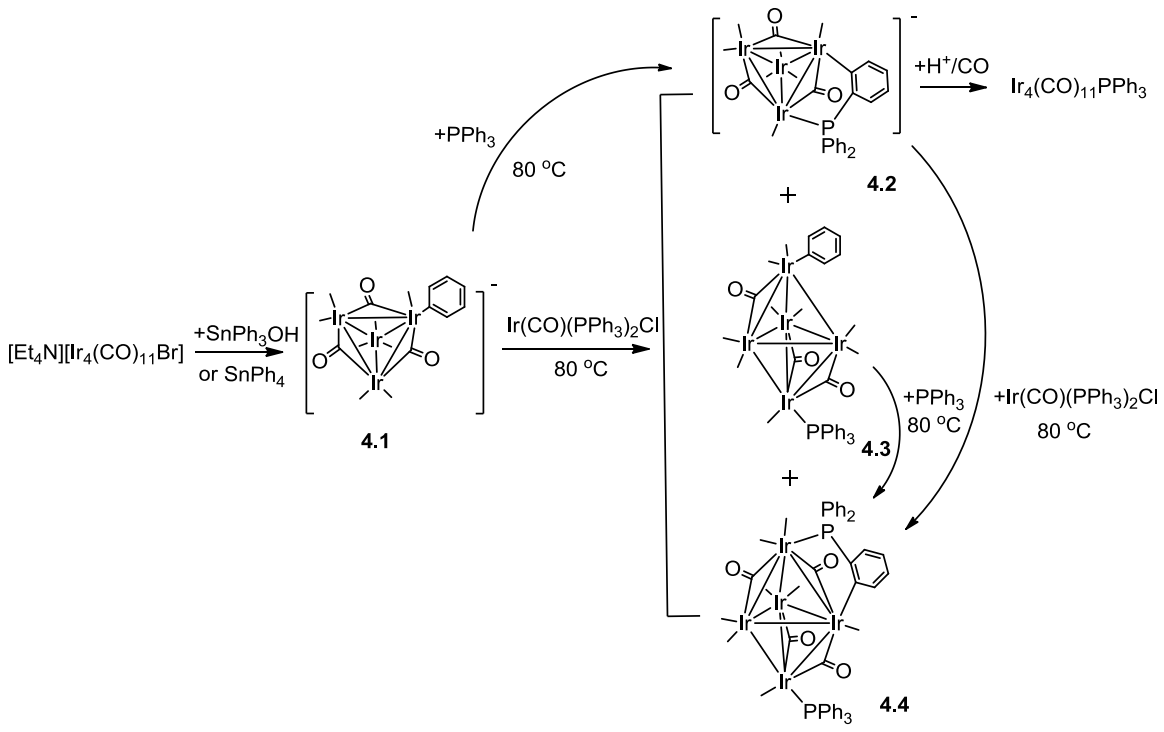


Scheme 4.1 Schematic diagram of reactions of $[Ir_4(CO)_{11}(\sigma\text{-Ph})]^-$ with Vaska complex $Ir(CO)(PPh_3)Cl$.

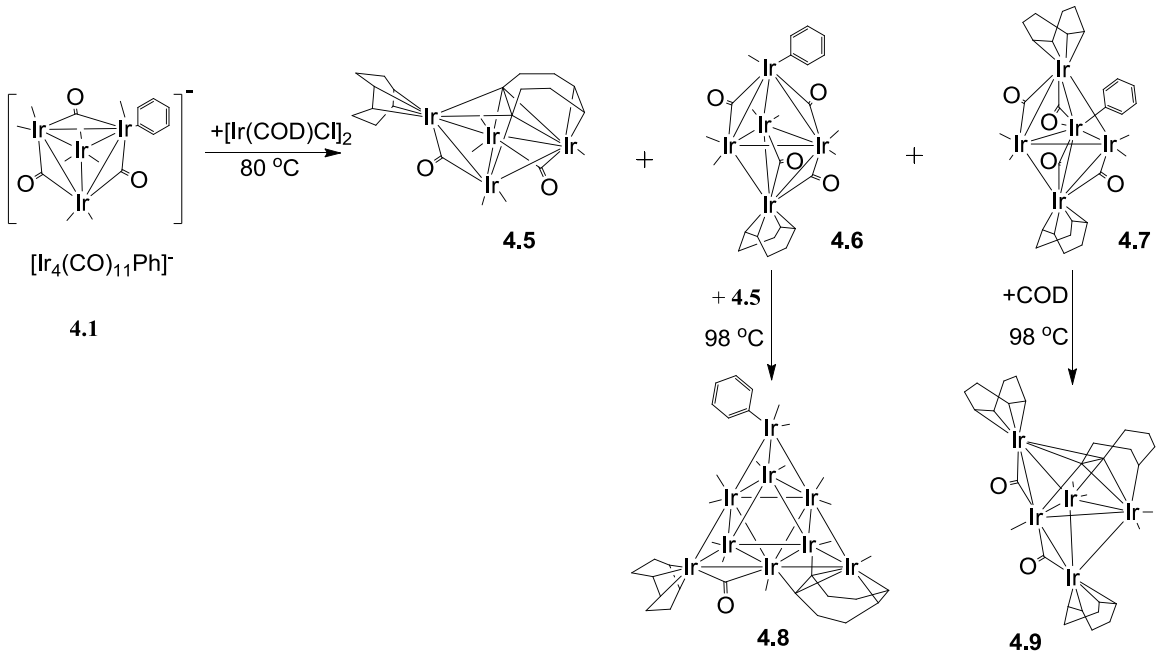


Scheme 4.2 Schematic diagram of reactions of $[Ir_4(CO)_{11}(\sigma\text{-Ph})]^-$ with $[Ir(COD)Cl]_2$ (COD = 1,5-cyclooctadiene).

**Table 4.1. Crystallographic Data for Compounds 4.1 - 4.9.**

| Compound | **4.1** | **4.2** | **4.3** |
|---|---|---|---|
| Empirical formula | $Ir_4NC_{25}H_{25}O_{11}$ | $Ir_4PNC_{36}H_{34}O_{10}$ | $Ir_5PC_{36}H_{20}O_{12}$ |
| Formula weight | 1284.33 | 1440.49 | 1636.59 |
| Crystal system | Monoclinic | Monoclinic | Monoclinic |
| Lattice parameters | | | |
| *a* (Å) | 15.6537(8) | 33.565(4) | 18.5348(4) |
| *b* (Å) | 13.4349(7) | 13.5442(18) | 13.0734(3) |
| *c* (Å) | 16.4958(9) | 19.622(3) | 15.9317(4) |
| α (deg) | 90 | 90 | 90 |
| β (deg) | 113.836(1) | 103.262(3) | 103.922(1) |
| γ (deg) | 90 | 90 | 90 |
| V ($Å^3$) | 3173.3(3) | 8683(2) | 3747.05(15) |
| Space group | $P2_1/n$, 14 | $C2/c$, 15 | $P2_1/c$, 14 |
| Z value | 4 | 8 | 4 |
| $\rho_{calc}$ (g / $cm^3$) | 2.688 | 2.270 | 2.901 |
| μ (Mo Kα) ($mm^{-1}$) | 16.775 | 12.312 | 17.798 |
| Temperature (K) | 294(2) | 294(2) | 294(2) |
| $2\Theta_{max}$ (°) | 48.88 | 56.68 | 56.58 |
| No. Obs. ( I > 2σ(I)) | 6457 | 7679 | 6609 |
| No. Parameters | 332 | 474 | 487 |
| Goodness of fit (GOF) | 1.085 | 1.059 | 0.999 |
| Max. shift in cycle | 0.001 | 0.001 | 0.001 |
| Residuals*: R1; wR2 | 0.0477; 0.1266 | 0.0432; 0.1261 | 0.0453; 0.1339 |
| Absorption Correction, | Multi-scan | Multi-scan | Multi-scan |
| Trans. Max/min | 1.000 / 0.417 | 1.000 / 0.531 | 1.000 / 0.540 |
| Largest peak in Final Diff. Map ($e^-$ /$Å^3$) | 2.70 | 2.08 | 1.15 |

*$R = \Sigma_{hkl}(||F_{obs}| - |F_{calc}||)/\Sigma_{hkl}|F_{obs}|$; $R_w = [\Sigma_{hkl} w(|F_{obs}| - |F_{calc}|)^2/\Sigma_{hkl} wF^2_{obs}]^{1/2}$; $w = 1/\sigma^2(F_{obs})$; GOF = $[\Sigma_{hkl} w(|F_{obs}| - |F_{calc}|)^2/(n_{data} - n_{vari})]^{1/2}$

**Table 4.1 (continue). Crystallographic Data for Compounds 4.1 - 4.9.**

| Compound | **4.4** | **4.5** | **4.6** |
|---|---|---|---|
| Empirical formula | $Ir_5P_2C_{47}H_{29}O_{11}$ | $Ir_4C_{23}H_{22}O_7$ | $Ir_5C_{25}H_{17}O_{11}$ |
| Formula weight | 1792.75 | 1179.28 | 1454.48 |
| Crystal system | Monoclinic | Monoclinic | Monoclinic |
| Lattice parameters | | | |
| *a* (Å) | 16.2096(8) | 10.1295(3) | 13.4948(4) |
| *b* (Å) | 19.9166(10) | 16.7531(5) | 13.5381(4) |
| *c* (Å) | 16.9894(8) | 14.8948(4) | 16.3963(5) |
| α (deg) | 90 | 90 | 90 |
| β (deg) | 108.529(1) | 104.342(1) | 103.802(1) |
| γ (deg) | 90 | 90 | 90 |
| V (Å$^3$) | 5200.5(4) | 2448.88(12) | 2909.01(15) |
| Space group | $P2_1/n$, 14 | $P2_1/n$ | $P2_1/n$ |
| Z value | 4 | 4 | 4 |
| $\rho_{calc}$ (g / cm$^3$) | 2.448 | 3.198 | 3.321 |
| μ (Mo Kα) (mm$^{-1}$) | 12.971 | 21.709 | 22.847 |
| Temperature (K) | 294(2) | 294(2) | 294(2) |
| $2\Theta_{max}$ (°) | 56.78 | 56.56 | 56.62 |
| No. Obs. ( I > 2σ(I)) | 7459 | 6105 | 7252 |
| No. Parameters | 529 | 307 | 370 |
| Goodness of fit (GOF) | 1.097 | 1.001 | 1.058 |
| Max. shift in cycle | 0.001 | 0.001 | 0.001 |
| Residuals*: R1; wR2 | 0.0622; 0.2054 | 0.0261; 0.0743 | 0.0359; 0.0945 |
| Absorption Correction, | Multi-scan | Multi-scan | Multi-scan |
| Trans. Max/min | 1.000 / 0.426 | 1.000 / 0.584 | 1.000 / 0.345 |
| Largest peak in Final Diff. Map (e$^-$ /Å$^3$) | 2.38 | 0.77 | 3.99 |

*$R = \Sigma_{hkl}(||F_{obs}| - |F_{calc}||)/\Sigma_{hkl}|F_{obs}|$; $R_w = [\Sigma_{hkl}w(|F_{obs}| - |F_{calc}|)^2/\Sigma_{hkl}wF^2_{obs}]^{1/2}$; $w = 1/\sigma^2(F_{obs})$; GOF = $[\Sigma_{hkl}w(|F_{obs}| - |F_{calc}|)^2/(n_{data} - n_{vari})]^{1/2}$

**Table 4.1 (continue). Crystallographic Data for Compounds 4.1 - 4.9.**

| Compound | **4.7** | **4.8** | **4.9** |
|---|---|---|---|
| Empirical formula | $Ir_5C_{31}H_{29}O_9$ | $Ir_9C_{37}H_{27}O_{15}$ | $Ir_5C_{31}H_{35}O_7$ |
| Formula weight | 1506.64 | 2441.55 | 1480.69 |
| Crystal system | Monoclinic | Monoclinic | Monoclinic |
| Lattice parameters | | | |
| *a* (Å) | 15.6500(7) | 13.0530(5) | 14.0036(5) |
| *b* (Å) | 12.4570(6) | 13.2170(5) | 12.9445(4) |
| *c* (Å) | 18.2221(8) | 28.3850(11) | 17.9786(6) |
| α (deg) | 90 | 90 | 90 |
| β (deg) | 97.822(1) | 98.105(1) | 105.476(1) |
| γ (deg) | 90 | 90 | 90 |
| V ($Å^3$) | 3519.4(3) | 4848.1(3) | 3140.81(18) |
| Space group | $P2_1/c$ | $P2_1/n$ | $P2_1/c$ |
| Z value | 4 | 4 | 4 |
| $\rho_{calc}$ (g / $cm^3$) | 3.004 | 3.156 | 3.131 |
| μ (Mo Kα) ($mm^{-1}$) | 19.042 | 21.642 | 21.155 |
| Temperature (K) | 294(2) | 294(2) | 294(2) |
| $2\Theta_{max}$ (°) | 56.62 | 56.42 | 56.56 |
| No. Obs. ( $I > 2\sigma(I)$) | 8810 | 6818 | 5548 |
| No. Parameters | 418 | 534 | 402 |
| Goodness of fit (GOF) | 1.074 | 1.092 | 1.078 |
| Max. shift in cycle | 0.001 | 0.001 | 0.001 |
| Residuals*: R1; wR2 | 0.0372; 0.1027 | 0.0796; 0.2519 | 0.0369; 0.1005 |
| Absorption Correction, | Multi-scan | Multi-scan | Multi-scan |
| Trans. Max/min | 1.000 / 0.346 | 1.000/0.598 | 1.000/0.535 |
| Largest peak in Final Diff. Map ($e^-$ /$Å^3$) | 2.01 | 2.08 | 1.97 |

*$R = \Sigma_{hkl}(||F_{obs}|-|F_{calc}||)/\Sigma_{hkl}|F_{obs}|$; $R_w = [\Sigma_{hkl}w(|F_{obs}|-|F_{calc}|)^2/\Sigma_{hkl}wF^2_{obs}]^{1/2}$;
$w = 1/\sigma^2(F_{obs})$; GOF = $[\Sigma_{hkl}w(|F_{obs}|-|F_{calc}|)^2/(n_{data} - n_{vari})]^{1/2}$

Table 4.2 Selected intramolecular angles and bond distances for compound **4.1**.[a]

| **Distances** | | | **Angles** | | | |
|---|---|---|---|---|---|---|
| Atom | Atom | Distance (Å) | Atom | Atom | Atom | Angle(deg) |
| Ir1 | Ir2 | 2.7494(7) | C44 | Ir1 | Ir4 | 160.0(4) |
| Ir1 | Ir3 | 2.7393(7) | | | | |
| Ir1 | Ir4 | 2.7515(7) | | | | |
| Ir1 | C44 | 2.125(13) | | | | |
| Ir2 | Ir3 | 2.7015(7) | | | | |
| Ir2 | Ir4 | 2.7235(7) | | | | |
| Ir3 | Ir4 | 2.7317(7) | | | | |

[a] Estimated Standard deviations in the least significant figure are given in parentheses.

Table 4.3 Selected intramolecular angles and bond distances for compound **4.2**.[a]

| **Distances** | | | **Angles** | | | |
|---|---|---|---|---|---|---|
| Atom | Atom | Distance (Å) | Atom | Atom | Atom | Angle(deg) |
| Ir1 | Ir2 | 2.7367(6) | P1 | Ir1 | Ir2 | 97.57(7) |
| Ir1 | Ir3 | 2.6633(6) | P1 | Ir1 | Ir3 | 90.32(8) |
| Ir1 | Ir4 | 2.7434(7) | P1 | Ir1 | Ir4 | 149.50(7) |
| Ir1 | P1 | 2.286(3) | C56 | Ir3 | Ir1 | 93.3(3) |
| Ir3 | C56 | 2.096(12) | | | | |

[a] Estimated Standard deviations in the least significant figure are given in parentheses.

Table 4.4 Selected intramolecular angles and bond distances for compound **4.3**.[a]

| **Distances** | | | **Angles** | | | |
|---|---|---|---|---|---|---|
| Atom | Atom | Distance (Å) | Atom | Atom | Atom | Angle(deg) |
| Ir1 | Ir2 | 2.7303(8) | P1 | Ir1 | Ir3 | 171.83(9) |
| Ir1 | Ir3 | 2.8268(8) | C4 | Ir5 | Ir4 | 160.3(4) |
| Ir1 | Ir4 | 2.7215(8) | | | | |
| Ir2 | Ir3 | 2.6848(8) | | | | |
| Ir2 | Ir4 | 2.7988(8) | | | | |
| Ir2 | Ir5 | 2.7765(8) | | | | |
| Ir3 | Ir4 | 2.7021(8) | | | | |
| Ir3 | Ir5 | 2.7629(8) | | | | |
| Ir4 | Ir5 | 2.7912(8) | | | | |
| Ir1 | P1 | 2.311(4) | | | | |
| Ir5 | C4 | 2.116(16) | | | | |

[a] Estimated Standard deviations in the least significant figure are given in parentheses.

Table 4.5 Selected intramolecular angles and bond distances for compound **4.4**.[a]

| **Distances** | | | **Angles** | | | |
|---|---|---|---|---|---|---|
| Atom | Atom | Distance (Å) | Atom | Atom | Atom | Angle(deg) |
| Ir1 | Ir2 | 2.7555(12) | P1 | Ir1 | Ir3 | 170.05(15) |
| Ir1 | Ir3 | 2.7932(12) | C70 | Ir2 | Ir3 | 103.8(6) |
| Ir1 | Ir4 | 2.7047(13) | P2 | Ir5 | Ir4 | 154.95(16) |
| Ir2 | Ir5 | 2.6891(12) | | | | |
| Ir3 | Ir5 | 2.6948(12) | | | | |
| Ir4 | Ir5 | 2.7607(14) | | | | |
| Ir2 | C70 | 2.14(2) | | | | |
| Ir1 | P1 | 2.317(6) | | | | |
| Ir5 | P2 | 2.289(7) | | | | |

[a] Estimated Standard deviations in the least significant figure are given in parentheses.

Table 4.6 Selected intramolecular angles and bond distances for compound **4.5**.[a]

| **Distances** | | | **Angles** | | | |
|---|---|---|---|---|---|---|
| Atom | Atom | Distance (Å) | Atom | Atom | Atom | Angle(deg) |
| Ir1 | Ir2 | 2.6909(3) | Ir4 | Ir1 | Ir2 | 93.794(10) |
| Ir1 | Ir3 | 2.7818(3) | Ir4 | Ir3 | Ir2 | 94.543(10) |
| Ir1 | Ir4 | 2.7294(3) | Ir4 | C33 | Ir2 | 122.3(2) |
| Ir2 | Ir3 | 2.6965(3) | Ir4 | C34 | Ir2 | 121.7(3) |
| Ir3 | Ir4 | 2.6911(4) | | | | |
| Ir1 | C34 | 2.128(6) | | | | |
| Ir2 | C33 | 2.205(6) | | | | |
| Ir2 | C34 | 2.264(6) | | | | |
| Ir3 | C33 | 2.147(6) | | | | |
| Ir4 | C33 | 2.312(6) | | | | |
| Ir4 | C34 | 2.267(6) | | | | |
| C33 | C34 | 1.443(8) | | | | |

[a] Estimated Standard deviations in the least significant figure are given in parentheses.

Table 4.7 Selected intramolecular angles and bond distances for compound **4.6**.[a]

| **Distances** | | | **Angles** | | | |
|---|---|---|---|---|---|---|
| Atom | Atom | Distance (Å) | Atom | Atom | Atom | Angle(deg) |
| Ir1 | Ir2 | 2.7150(5) | C43 | Ir1 | Ir4 | 161.4(3) |
| Ir1 | Ir3 | 2.7408(5) | | | | |
| Ir1 | Ir4 | 2.8009(5) | | | | |
| Ir2 | Ir3 | 2.7490(5) | | | | |
| Ir2 | Ir4 | 2.6965(5) | | | | |
| Ir2 | Ir5 | 2.7985(5) | | | | |
| Ir3 | Ir4 | 2.7803(5) | | | | |
| Ir3 | Ir5 | 2.7874(5) | | | | |
| Ir4 | Ir5 | 2.7054(5) | | | | |
| Ir1 | C43 | 2.082(10) | | | | |

[a] Estimated Standard deviations in the least significant figure are given in parentheses.

Table 4.8 Selected intramolecular angles and bond distances for compound **4.7**.[a]

| **Distances** | | | **Angles** | | | |
|---|---|---|---|---|---|---|
| Atom | Atom | Distance (Å) | Atom | Atom | Atom | Angle(deg) |
| Ir1 | Ir2 | 2.7631(5) | C43 | Ir2 | Ir3 | 158.5(2) |
| Ir1 | Ir3 | 2.7952(5) | | | | |
| Ir1 | Ir4 | 2.7206(5) | | | | |
| Ir2 | Ir3 | 2.7794(5) | | | | |
| Ir2 | Ir4 | 2.7796(5) | | | | |
| Ir2 | Ir5 | 2.7741(5) | | | | |
| Ir3 | Ir4 | 2.6968(5) | | | | |
| Ir3 | Ir5 | 2.7567(5) | | | | |
| Ir4 | Ir5 | 2.7972(5) | | | | |
| Ir1 | C43 | 2.120(9) | | | | |

[a] Estimated Standard deviations in the least significant figure are given in parentheses.

Table 4.9 Selected intramolecular angles and bond distances for compound **4.8**.[a]

| **Distances** | | | **Angles** | | | |
|---|---|---|---|---|---|---|
| Atom | Atom | Distance (Å) | Atom | Atom | Atom | Angle(deg) |
| Ir1 | Ir2 | 2.755(2) | C83 | Ir8 | Ir4 | 161.5(11) |
| Ir1 | Ir3 | 2.740(2) | | | | |
| Ir1 | Ir7 | 2.685(2) | | | | |
| Ir2 | Ir8 | 2.656(2) | | | | |
| Ir3 | Ir6 | 2.816(2) | | | | |
| Ir4 | Ir6 | 2.730(2) | | | | |
| Ir4 | Ir9 | 2.820(2) | | | | |
| Ir5 | Ir6 | 2.832(2) | | | | |
| Ir5 | Ir8 | 2.669(2) | | | | |
| Ir6 | Ir7 | 2.717(2) | | | | |
| Ir6 | Ir9 | 2.806(2) | | | | |
| Ir3 | C93 | 2.10(4) | | | | |
| Ir6 | C92 | 2.13(5) | | | | |
| Ir8 | C83 | 2.17(5) | | | | |
| Ir9 | C93 | 2.16(4) | | | | |
| C92 | C93 | 1.33(7) | | | | |

[a] Estimated Standard deviations in the least significant figure are given in parentheses.

Table 4.10 Selected intramolecular angles and bond distances for compound **4.9**.[a]

| **Distances** | | | **Angles** | | | |
|---|---|---|---|---|---|---|
| Atom | Atom | Distance (Å) | Atom | Atom | Atom | Angle(deg) |
| Ir1 | Ir2 | 2.8947(7) | Ir5 | Ir3 | Ir2 | 90.47(2) |
| Ir1 | Ir3 | 2.7008(6) | Ir5 | Ir3 | Ir1 | 120.51(2) |
| Ir1 | Ir4 | 2.6825(6) | | | | |
| Ir2 | Ir3 | 2.7721(7) | | | | |
| Ir2 | Ir4 | 2.7022(7) | | | | |
| Ir3 | Ir4 | 2.6804(6) | | | | |
| Ir3 | Ir5 | 2.7027(6) | | | | |
| Ir4 | Ir5 | 2.7299(6) | | | | |
| Ir2 | C60 | 2.173(13) | | | | |
| Ir5 | C65 | 2.182(12) | | | | |
| Ir4 | C65 | 2.183(13) | | | | |
| Ir2 | C64 | 2.132(15) | | | | |
| Ir3 | C64 | 2.190(14) | | | | |
| Ir5 | C64 | 2.271(12) | | | | |
| C64 | C65 | 1.48(3) | | | | |

[a] Estimated Standard deviations in the least significant figure are given in parentheses.

## References


1. (a) Chini, P. *J. Organomet. Chem.* **1980**, *200*, 37-61. (b) Adams, R. D. in *The Chemistry of Metal Cluster Complexes*, Shriver, D. F.; Kaesz, H. D.; Adams, R. D., VCH Publishers, 1990, Ch. 3, pp 121 – 170. (c) Adams, R. D. in *Comprehensive Organometallic Chemistry*, Abel, E. W.; Stone, F. G. A.; Wilkinson, G.; Pergamon, 1995, Vol. 10, Ch. 1, pp 1 – 22.

2. Della Pergola, R.; Garlaschelli, L.; Manassero, M.; Sansoni, M.; Strumolo, D. *J. Cluster Sci.* **2001**, *12*, 23 – 34.

3. Della Pergola, R.; Garlaschelli, L.; Manassero, M.; Sansoni, M. *J. Cluster Sci.* **1999**, *12*, 109 – 119.

4. Adams, R. D.; Chen, M.; Trufan, E.; Zhang, Q. *Organometallics*, **2011**, *30*, 661-664.

5. (a) Espinet, P.; Echavarren, A. M. *Angew. Chem. Int. Ed.* **2004**, *43*, 4704 – 4734. (b) Yabe,Y.; Maegawa, T.; Monguchi, Y.; Sajiki, H. *Tetrahedron* **2010**, *66*, 8654 – 8660.

6. Neale, N.R.; Tilley T.D., *J. Am. Chem. Soc.* **2005**, *127*, 14745-14755.

7. (a) Adams, R. D.; Chen, M. *Organometallics*, **2011**, 30(21), 5867-5872. (b) Adams, R. D.; Chen, M. *Organometallics*, **2012**, 31(1), 445-450.

8. Chini, P.; Ciani, G.; Garlaschelli, L.; Manassero, M.; Martinengo, S.; Sironi, A.; Canziani, F., *J. Organomet. Chem.*, **1978**, *152*, C35-C38.

9. M. T. Ahmet, A. Houlton, C. S. Frampton, J.R. Miller, R. M. Roberts, J. Silver and B.Yavari, *J. Chem. Soc. Dalton Trans.*, **1993**, 1, 3085-3092.

10. Ros, R.; Scrivanti, A.; Albani, V.G.; Braga, D.; Garlaschelli, L., *J. Chem. Soc., Dalton Trans.*, **1986**, 2411-2421.

11. Stuntz, G. F.; Shapley, J. R.; Pierpont, C. G. *Inorg. Chem.* **1978**, *17*, 2596 – 2603.

12. SAINT+, version 6.2a, Bruker Analytical X-ray Systems, Inc., Madison, WI, 2001.

13. G. M. Sheldrick, SHELXTL, version 6.1, Bruker Analytical X-ray Systems, Inc., Madison, WI, 1997.

14. Ciani, G.; Garlaschelli, L.; Manassero, M.; Martinengo, S.; Sironi, A.; Canziani, F., *J. Organomet. Chem.*, **1980**, *199*, 271-279.

15. Harding, M. M.; Nicholls, B. S.; Smith, A. K., *J. Chem. Soc., Dalton Trans.* **1983**, 1479-1481.

16. Pereira, R.M.S.; Fujiwara, F.Y.; Vargas, M. D. *Organometallics* **1997**, *16*, 4833-4838.

17. de Araujo M. H.; M. D.; Braga, D.; Grepioni, F. *Polyhedron* **1998**, *17*, 2865-2875.

18. (a) Eaborn, C.; Odell, K. J.; Pidcock, A. *J. Chem. Soc. Dalton Trans.* **1979**, 134-138. (b) Eaborn, C.; Odell, K. J.; Pidcock, A. *J. Chem. Soc. Dalton Trans.* **1979**, 758-760. (c) Eaborn, C.; Kundu, K.; Pidcock, A. *J. Organomet. Chem.* **1979**, *170*, C18-C20. (d) Eaborn, C.; Odell, K. J.; Pidcock, A. *J. Chem. Soc. Dalton Trans.* **1978**, 1288-1294. (e) Eaborn, C.; Odell, K. J.; Pidcock, A. *J. Chem. Soc. Dalton Trans.* **1978**, 357-368. (f) Eaborn, C.; Odell, K. J.; Pidcock, A. *J. Organomet. Chem.* **1978**, *146*, 17-21. (g) Eaborn, C.; Odell, K. J.; Pidcock, A. *J. Organomet. Chem.* **1975**, *96*, C38-C40. (h) Weisemann, C.; Schmidtberg, G.; Brune, H.A. *J. Organomet. Chem.* **1989**, *362*, 63-76. (i) Weisemann, C.; Schmidtberg, G.; Brune, H.A. *J. Organomet. Chem.* **1989**, *365*, 403-412. (j) Brune, H.A.; Schmidtberg, G.; Weisemann, C. *J. Organomet. Chem.* **1989**, *371*, 121-127.

19. (a) Suggs, J. W.; Lee, K. S. *J. Organomet. Chem.* **1986**, *299*, 297-309. (b) Molter, A.; Mohr, F. *Z. Anorg, Allg. Chem.* **2009**, *635*, 134-138.

20. (a) Meyer, N.; Sivanathan, S.; Mohr, F. *J. Organomet. Chem.* **2011**, *696*, 1244-1247. (b) Meyer, N.; Lehmann, C. W.; Lee, T. K. M.; Rust, J.; Yam, V. W. W.; Mohr, F. *Organometallics* **2009**, *28*, 2931-2934. (c) Bojan, R. V.; López-de-Luzuriaga, J. M.; Monge, M.; Olmos, M. E. . *J. Organomet. Chem.* **2010**, *696*, 2385 – 2393.

21. Shi, L. L .; Zhao, S. S .; Zhao, S. S .; Li, H .; Su, Z. *Theor. Chem. Acc.* **2009**, *124*, 29-36.

22. Harding, M. M.; Nicholls, B. S.; Smith, A. K., *J. Chem. Soc., Dalton Trans.* **1983**, 1479-1481.

23. Pereira, R.M.S.; Fujiwara, F.Y.; Vargas, M. D. *Organometallics* **1997**, *16*, 4833-4838.

24. de Araujo M. H.; M. D.; Braga, D.; Grepioni, F. *Polyhedron* **1998**, *17*, 2865-2875.

25. (a) Braga, D.; Grepioni, F.; Righi, S.; Johnson, B. F. G.; Frediani, P.; Bianchi, M.; Piacenti, F.; Lewis, J. *Organometallics*, 1992, **11**, 706 - 711. (b) Jackson, P. F.; Johnson, B. F. G.; Lewis, J.; Nelson, W. J. H.; McPartlin, M. *J. Chem. Soc., Dalton Trans.*, 1982, 2099. (c) Bailey, P. J.; Conole, G.; Johnson, B. F. G.; Lewis, J.; McPartlin, M.; Moule, A.; Powell, H. R.; Wilkinson, D. A. *J. Chem. Soc., Dalton Trans.*, **1995**, 741 - 751. (d) Chihara, T.; Komoto, R.; Kobayashi, K.; Yamazaki, H.; Matsuura, and Y. *Inorg. Chem.*, 1989, **28**, 964 - 967. (e) Brivio, E.; Alessandro Cerrioti, A.; Della Pergola, R.; Garlaschelli, L.; Demartin, F.; Manassero, M.; Sansoni, M.; Zanello, P.; Laschi, F.; Heaton, B. T. *J. Chem. Soc., Dalton Trans.*, **1994**, 3237 - 3242. (f) Femoni C.; Iapalucci, M. C.; Longoni G.; Svensson, P. H. *Inorg. Chim. Acta* **2002**, 330, 111 - 117.

26. Chihara, T.; Sato M.; Konomoto, H.; Kamiguchi, S.; Ogawa, H.; Wakatsuki, Y. *J. Chem. Soc., Dalton Trans.* **2000**, 2295 - 2299.

27. Cerrioti, A.; Della Pergola, R.; Garlaschelli, L. *Organometallics* **1995**, *14*, 186 - 193.

28. Amoroso, A. J.; Johnson, B. F. G.; Lewis, J.; Raithby, P. R.; Wong, W.-T. *J. Chem. Soc., Chem. Commun.* **1991**, 814 – 815.

29. Mingos, D. M. P. *Acc. Chem. Res.* **1984**, *17*, 311 – 319.

30. Della Pergola, R.; Demartin, F.; Garlaschelli, L.; Manassero, M.; Martinengo, S.; Masciocchi, N.; Zanello, P. *Inorg. Chem.* **1993**, *32*, 3670 – 3674.

# CHAPTER FIVE

# Iridium-Gold Cluster Compounds: Syntheses, Structures, Theoretical Studies and an Unusual Ligand-Induced Skeletal Rearrangement.

## Introduction

Applications for iridium in catalysis continue to grow.[1] Although most catalytic applications are of a homogeneous type,[2] it has been shown that iridium clusters can serve as precursors to heterogeneous nanoscale catalysts that exhibit good activity for the hydrogenation of aromatics and olefins.[3] Years ago, Sinfelt showed that the addition of iridium to platinum greatly improved its activity for the catalytic reforming of petroleum.[4] Heterogeneous iridium-iron catalysts derived from bimetallic cluster complexes have been shown to exhibit exceptional catalytic activity for the formation of methanol from synthesis gas.[5]

Recently, gold nanoparticles have been shown to exhibit significant catalytic activity for the oxidation of CO and certain olefins.[6] Combining transition metals with gold has led to interesting new bimetallic catalysts for the oxidation of hydrocarbons.[7] There have been few studies of the chemistry of iridium-gold carbonyl cluster complexes.[8-9] A recent report shows that an Ir(III)-Au(I) complex exhibits better catalytic activity for the transfer hydrogenation of nitrobenzene than di-Ir(III) and di-Au(I) complexes.[10]

We have recently reported the synthesis and structural characterization of the tetrairidium anion, $[Ir_4(CO)_{11}(Ph)]^-$.[11] $[Ir_4(CO)_{11}(Ph)]^-$ has been shown to react with $Ir(CO)(PPh_3)_2Cl$ to form the pentairidium complex $Ir_5(CO)_{12}Ph(PPh_3)$ by halide displacement combined with the elimination of one $PPh_3$ ligand. It also reacts with $[(COD)Ir(Cl)]_2$ to form a series of higher nuclearity iridium carbonyl cluster complexes containing COD and COD transformed ligands, Scheme 5.1.[11] We have now investigated the reaction of $[Ir_4(CO)_{11}(Ph)]^-$ with $[Au(PPh_3)][NO_3]$ and have obtained the gold-tetrairidium cluster complex $Ir_4(CO)_{11}(Ph)(\mu\text{-}AuPPh_3)$, **5.1**.

For comparisons, we have investigated the reaction of $[HIr_4(CO)_{11}]^-$ with $[Au(PPh_3)][NO_3]$ and have obtained two new iridium-gold carbonyl cluster complexes $Ir_4(CO)_{10}(AuPPh_3)_2$, **5.2** and $Ir_4(CO)_{11}(AuPPh_3)_2$, **5.3**. Compound **5.2** can be converted to **5.3** by a reversible CO addition involving an interesting metal-framework transformation that does not result in a change in the total number of metal – metal bonds. The addition of two electron donors, such as CO or $PR_3$, to polynuclear metal carbonyl complexes generally induces the cleavage of a metal – metal bond to form a more open structure as shown, for example, in the reversible addition of CO or $PPh_3$ to $CpMnFe_2(CO)_8(\mu_3\text{-}PPh)$ to form $CpMnFe_2(CO)_8(L)(\mu\text{-}PPh)$,[12] L = CO or $PPh_3$, in Scheme 5.2 (1) or in the reversible addition of CO to $Os_4(CO)_{12}(\mu_3\text{-}S)_2$ to form $Os_4(CO)_{13}(\mu_3\text{-}S)_2$ in Scheme 5.2 (2).[13]

The bromo ligand in the anion $[Ir_4(CO)_{11}Br]^-$ is also readily replaced and is a good reagent for the synthesis of new $Ir_4(CO)_{11}L$ complexes.[14] We have also investigated the reaction of $[Ir_4(CO)_{11}Br]^-$ and $[HIr_4(CO)_{11}]^-$ with the gold compounds $ArAu(PPh_3)$, Ar =

$CH_3$, $C_6H_5$, 2-$C_{16}H_9$ and obtained a series of new iridium-gold carbonyl cluster compounds containing methy and σ-Aryl Ligands.

**Experimental Section**

**General Data**. Reagent grade solvents were dried by the standard procedures and were freshly distilled prior to use. Infrared spectra were recorded on a Thermo Nicolet Avatar 360 FT-IR spectrophotometer. $^1$H NMR spectra were recorded on a Varian Mercury 300 spectrometer operating at 300.1 MHz. Mass spectrometric (MS) measurements performed by a direct-exposure probe using electron impact ionization (EI) or by electrospray ionization (ESI) were made on a VG 70S instrument. $Ir_4(CO)_{12}$, $(CH_3)Au(PPh_3)$ and $Au(PPh_3)Cl$ were obtained from STREM and were used without further purification. $[Au(PPh_3)][NO_3]$,[15] $PhAu(PPh_3)$,[16] $Au(PPh_3)(1\text{-}C_{16}H_9)$,[17] $[Et_4N][Ir_4(CO)_{11}Ph]$[10] and $[PPN][HIr_4(CO)_{11}]$ PPN = $[(Ph_3P)N(PPh_3)]^+$ [18],$[Et_4N][Ir_4(CO)_{11}Br]$,[19] were prepared according to the published procedures. Product separations were performed by TLC in air on Analtech 0.25 and 0.5 mm silica gel 60 Å $F_{254}$ glass plates.

**Synthesis of $Ir_4(CO)_{11}(Ph)(\mu\text{-}AuPPh_3)$, 5.1**.

A 9.6 mg (0.0075 mmol) portion of $[NEt_4][Ir_4(CO)_{11}Ph]$ was dissolved in 15 mL $CH_2Cl_2$. 7.2 mg (0.0138 mmol) of $[Au(PPh_3)][NO_3]$ was added and the solution was stirred for 5 min. The solvent was removed in vacuo, and the products were then isolated by TLC by using a 3:1 hexane/methylene chloride solvent mixture to yield 11.0 mg (91%) of $Ir_4(CO)_{11}(Ph)(\mu\text{-}AuPPh_3)$, **5.1**. Spectral data for **5.1**: IR CO ($cm^{-1}$ in $CH_2Cl_2$): 2088(m), 2057(vs), 2044(m), 2017(s), 1843(m), 1819(m). $^1$H NMR ($CDCl_3$, in ppm) δ = 7.30-7.67

(m, 15H, PPh3), 6.70-6.99 (m, 5H, σ-Ph); $^{31}$P NMR (in $CDCl_3$) δ= 73.21. Mass Spec. EI/MS for **5.1**: 1614 (M) plus ions corresponding to the loss of each of eleven CO ligands.

**Synthesis of $Ir_4(CO)_{10}(AuPPh_3)_2$, 5.2 and $Ir_4(CO)_{11}(AuPPh_3)_2$, 5.3.**

A 22.0 mg (0.0136 mmol) portion of freshly-made [PPN][$HIr_4(CO)_{11}$] was dissolved in 10 mL of $CH_2Cl_2$. 15 mg (0.0288 mmol) of [$AuPPh_3$]$NO_3$ was added to the above solution. The reaction was stirred at 25 $^oC$ for 30 min. The solution turned from yellow to dark red. The solvent was then removed *in vacuo*, and the products were then isolated by TLC by using a 2:1 hexane/methylene chloride solvent mixture. In order of elution they were: 1.3 mg (5 % yield) of black $Ir_4(CO)_{10}(AuPPh_3)_2$, **5.2**, 19.9 mg (73 % yield) of red $Ir_4(CO)_{11}(AuPPh_3)_2$, **5.3**. Spectral data for **5.2**: IR $\nu_{CO}$ ($cm^{-1}$ in $CH_2Cl_2$): 2056(m), 2023(vs), 2007(vs), 1975(m), 1844(m), 1824(m). $^1$H NMR ($CDCl_3$, in ppm) δ = 6.95-7.28 (m, 30H, Ph). $^{31}P\{^1H\}$ NMR ($CDCl_3$) δ = 56.69 ppm (s, 2P). Mass Spec. ES(positive)/MS for **5.2:** 1969 (M+H). Spectral data for **5.3**: IR $\nu_{CO}$ ($cm^{-1}$ in $CH_2Cl_2$): 2075(s), 2033(m), 2019(vs), 1974(m), 1816(m). $^1$H NMR ($CDCl_3$, in ppm) δ = 7.05-7.54 (m, 30H, Ph). $^{31}P\{^1H\}$ NMR ($CDCl_3$): δ = 84.71 ppm (s, 2P). Mass Spec. ES(positive)/MS for **5.3:** 1997 (M+H).

**Synthesis of $Ir_4(CO)_{10}(PPh_3)(AuPPh_3)_2$, 5.4.**

A 7.8 mg (0.004 mmol) portion of $Ir_4(CO)_{10}(AuPPh_3)_2$, **5.2** was dissolved in 10 mL $CH_2Cl_2$ and 1.5 mg (0.0057mmol) of $PPh_3$ was added and the mixture was stirred for 10 min. The color of solution changed from dark red to red. The solvent was then removed *in vacuo*, and the products were isolated by TLC by using a 2:1 hexane/methylene chloride solvent mixture to yield 5.4 mg of $Ir_4(CO)_{10}(PPh_3)(AuPPh_3)_2$, **5.4** (61%

yield). Spectral data for **5.4**: IR $\nu_{CO}$ ($cm^{-1}$ in $CH_2Cl_2$): 2047(m), 2037(w), 2007(vs), 1991(s), 1964(m), 1792(m), 1761(m). $^1H$ NMR ($CDCl_3$, in ppm) $\delta$ = 7.15-7.42 (m, 45H, Ph). $^{31}P\{^1H\}$ NMR ($CDCl_3$) $\delta$ = 75.94 ppm (s, 2P, $AuPPh_3$), 1.38 ppm (s, 1P, $IrPPh_3$). Mass Spec. ES(positive)/MS for **5.5:** 2231 (M+H).

**Conversion of 5.2 to 5.3 by addition of CO.**

A 6.3 mg portion of **5.2** was dissolved in 15 mL $CH_2Cl_2$. When carbon monoxide was purged into the solution, the red solution turned yellow in 5 min. The solvent was removed *in vacuo*, and the product was isolated by TLC by using a 2:1 hexane/methylene chloride solvent mixture to yield 6.0 mg of **5.3** (95% yield).

**Decarbonylation of 5.3 to 5.2.**

A 5.0 mg portion of compound **5.3** was dissolved in 15 mL $CH_2Cl_2$ under nitrogen and the solution was heated to reflux for 30 min. The solvent was removed *in vacuo*, and the products were then isolated by TLC by using a 2:1 hexane/methylene chloride solvent mixture to yield 4.5 mg (91% yield) of **5.2**.

**Transformation of 5.4 to $Ir_4(CO)_9(\mu_3\text{-}PPhC_6H_4)(AuPPh_3)_2$, 5.5.**

A 8.0 mg portion of compound **5.5** was dissolved in 15 mL benzene and heated to reflux for 1.5 h. The solvent was removed *in vacuo*, and the products were then isolated by TLC by using a 2:1 hexane/methylene chloride solvent mixture to yield 6.7 mg (85%) of $Ir_4(CO)_9(\mu_3\text{-}PPhC_6H_4)(AuPPh_3)_2$, **5.5**. Spectral data for **5.5**: IR CO ($cm^{-1}$ in $CH_2Cl_2$): 2047(s), 2022(vs), 2002(vs), 1987(s), 1976(s), 1953(m), 1812(w). $^1H$ NMR ($CDCl_3$, in ppm) = 7.15-7.49 (m, 39H, Ph). Mass Spec. ES(positive)/MS for **5.5**: 2125 (M+H).

**Syntheses of $Ir_4(CO)_{11}(CH_3)(AuPPh_3)$, 5.6.**

A 18.0 mg (0.0140 mmol) portion of $[Et_4N][Ir_4(CO)_{11}Br]$ was dissolved in 15 mL of $CH_2Cl_2$. 10.0 mg (0.0211 mmol) of $(CH_3)Au(PPh_3)$ was added to the above solution. The reaction mixture was stirred at room temperature for 2 h and the solvent was then removed *in vacuo*. The products were then isolated by TLC by using a 3:1 hexane/methylene chloride solvent mixture to yield 12.9 mg (60% yield) of $Ir_4(CO)_{11}(CH_3)(AuPPh_3)$, **5.6**. Spectral data for **5.6**: IR CO ($cm^{-1}$ in $CH_2Cl_2$): 2084(m), 2052(vs), 2037(m), 2013(s), 1847(m), 1824(m). $^1H$ NMR ($CDCl_3$, in ppm) $\delta$ = 7.13-7.35 (m, 15H, $PPh_3$), -0.1352 (s, 3H, $\sigma$-$CH_3$). $^{31}P\{^1H\}$ NMR ($CDCl_3$) $\delta$ = 69.37 ppm (s, $PPh_3$). Mass Spec. ES+/MS for **5.6**: 1552 (M+).

**Reaction of $[Et_4N][Ir_4(CO)_{11}Br]$ with $PhAu(PPh_3)$.**

Compound $Ir_4(CO)_{11}(Ph)(\mu$-$AuPPh_3)$, **5.1** could also be made in yield (71%) by the reaction of $[Et_4N][Ir_4(CO)_{11}Br]$ with $PhAu(PPh_3)$ in $CH_2Cl_2$ at room temperature in 2 h as described for the synthesis of **5.6**.

**Synthesis of $Ir_4(CO)_{11}(2\text{-}C_{16}H_9)(AuPPh_3)$, 5.7 from the reaction of $[Et_4N][Ir_4(CO)_{11}Br]$ with $(1\text{-}C_{16}H_9)Au(PPh_3)$, $1\text{-}C_{16}H_9$ = 1-pyrenyl.**

A 25.0 mg (0.0194 mmol) portion of $[Et_4N][Ir_4(CO)_{11}Br]$ was dissolved in 15 mL of $CH_2Cl_2$. 15.0 mg (0.0227 mmol) of $(1\text{-}C_{16}H_9)(AuPPh_3)$ was added to the above solution. The reaction mixture was stirred at room temperature for 2 h and the solvent was then removed *in vacuo*. The products were then isolated by TLC by using a 3:1 hexane/methylene chloride solvent mixture to yield 8.0 mg (24% yield) of yellow $Ir_4(CO)_{11}(2\text{-}C_{16}H_9)(AuPPh_3)$, **5.7**. Spectral data for **5.7**: IR CO ($cm^{-1}$ in $CH_2Cl_2$):

2088(m), 2058(vs), 2018(s), 1844(m), 1817(m). $^{1}$H NMR ($CDCl_3$, in ppm) δ = 7.18 - 7.45 (m, 15H, $PPh_3$), 7.71 - 8.13 (m, 9H, 2-pyrenyl). $^{31}P\{^{1}H\}$ NMR ($CDCl_3$) δ = 73.23 ppm (s, $PPh_3$). Mass Spec. ES+/MS for **5.7**: 1739 (M+H).

**Reaction of PPN[$HIr_4(CO)_{11}$] with $(CH_3)Au(PPh_3)$: Syntheses of 5.6 and $Ir_4(CO)_9(CH_3)_2(AuPPh_3)_4$, 5.8.**

A 33.0 mg (0.0204 mmol) portion of freshly-made [PPN][$HIr_4(CO)_{11}$] was dissolved in 20 mL of $CH_2Cl_2$. 42.0 mg (0.0886 mmol) of $CH_3Au(PPh_3)$ was added to the above solution. The reaction mixture was heated to reflux with stirring for 3 h and then the solvent was removed *in vacuo*. The products were then isolated by TLC by using a 2:1 hexane/methylene chloride solvent mixture. The following bands were isolated in order of elution: 12.0 mg (38% yield) of yellow $Ir_4(CO)_{11}(CH_3)(AuPPh_3)$, **5.6**, and 4.8 mg (8% yield) of red $Ir_4(CO)_9(CH_3)_2(AuPPh_3)_4$, **5.8**. Spectral data for **5.8**: IR CO ($cm^{-1}$ in $CH_2Cl_2$): 2034(vs), 1974(vs), 1958(s), 1939(w), 1834(w), 1803(m), 1762(m). $^{1}$H NMR ($CDCl_3$, in ppm) δ = 7.10-7.34 (m, 60H, $PPh_3$), -0.1376 (s, 6H, σ-$CH_3$). $^{31}P\{^{1}H\}$ NMR ($CDCl_3$) δ = 69.29, 65.51, 53.35 (2:1:1, 4$AuPPh_3$). Mass Spec. ES+/MS for **5.8**: 2888 (M+), 2911(M+Na).

**Conversion of $Ir_4(CO)_{11}(CH_3)(AuPPh_3)$, 5.6 to $Ir_4(CO)_9(CH_3)_2(AuPPh_3)_4$, 5.8.**

A 10.0 mg (0.006 mmol) portion of $Ir_4(CO)_{11}(CH_3)(AuPPh_3)$, **5.6** dissolved in 10 mL $CH_2Cl_2$ and 12.0 mg (0.0253mmol) of $(CH_3)Au(PPh_3)$ was added to the above solution, and the mixture was then heated to reflux for 3 h. After cooling, the solvent was removed *in vacuo*, and the products were then isolated by TLC by using a 2:1 hexane/methylene chloride solvent mixture to yield 3.8 mg (21% yield) of $Ir_4(CO)_9(CH_3)_2(AuPPh_3)_4$, **5.8**.

**Reaction of PPN[$HIr_4(CO)_{11}$] with $(C_6H_5)Au(PPh_3)$.**

A 37.0 mg (0.0229 mmol) portion of freshly-made PPN[$HIr_4(CO)_{11}$] was dissolved in 20 mL of $CH_2Cl_2$. 46 mg (0.0858 mmol) of $Au(PPh_3)Ph$ was added to the above solution. The reaction mixture was heated to reflux with stirring for 4 h. After cooling, the solvent was removed *in vacuo* and, the products were then isolated by TLC by using a 1:1 hexane/methylene chloride solvent mixture. The following bands were isolated in order of elution: 7.9 mg (22 % yield) of yellow $Ir_4(CO)_{11}(Ph)(AuPPh_3)$, **5.1**, 4.4 mg of yellow $Ir_4(CO)_{10}(PPh_3)_2$, 2.5 mg (4% yield) of red $Ir_4(CO)_9(PPh_3)(Ph)(AuPPh_3)_3$, **5.9**and 8.6 mg (13 % yield) of red $Ir_4(CO)_9(Ph)_2(AuPPh_3)_4$, **5.10**. Spectral data for **5.9**: IR CO ($cm^{-1}$ in $CH_2Cl_2$): 2029(m), 1998(vs), 1985(s), 1972(m), 1932(w), 1809(m), 1771(m). $^1H$ NMR ($CDCl_3$, in ppm) $\delta$ = 7.16-7.41 (m, 45H, $PPh_3$), 6.96-7.01 (m, 5H, $\sigma$-Ph). $^{31}P\{^1H\}$ NMR ($CDCl_3$) $\delta$ = 33.31 (s, $3AuPPh_3$), 12.91 (s, $1Ir\text{-}PPh_3$). Mass Spec. ES+/MS for **5.9**: 2739 (M+). Spectral data for **5.10**: IR CO ($cm^{-1}$ in $CH_2Cl_2$): 2045(vs), 1984(vs), 1966(s), 1932(w), 1844(w), 1802(m), 1771(m). $^1H$ NMR ($CDCl_3$, in ppm) $\delta$ = 6.81-7.10 (m, 60H, $4PPh_3$), 6.34-6.47 (m, 10H, $2\sigma$-Ph). $^{31}P\{^1H\}$ NMR ($CDCl_3$) $\delta$ = 65.25, 56.89, 53.37 (2:1:1, 4 $AuPPh_3$). Mass Spec. ES+/MS for **5.10**: 3013 (M+H), 3035(M+Na), 3051(M+K).

**Conversion of $Ir_4(CO)_{11}(Ph)(AuPPh_3)$, 5.1 to $Ir_4(CO)_9(Ph)_2(AuPPh_3)_4$, 5.10.**

A 8.0 mg (0.005 mmol) portion of **5.1** was dissolved in 10 mL $CH_2Cl_2$. Then 10.0 mg (0.0186 mmol) of $PhAu(PPh_3)$ was added to the solution and the mixture was heated to reflux for 2 h. After cooling, the solvent was removed *in vacuo*, and the product was then

isolated by TLC by using a 2:1 hexane/methylene chloride solvent mixture to yield 1.3 mg (9% yield) of $Ir_4(CO)_9(Ph)_2(AuPPh_3)_4$, **5.10**.

**Improved Synthesis of $Ir_4(CO)_9(CH_3)_2(AuPPh_3)_4$, 5.8.**

A 14.0 mg (0.007 mmol) portion of $Ir_4(CO)_{11}(AuPPh_3)_2$, **5.3** dissolved in 15 mL $CH_2Cl_2$ and 16.0 mg (0.0337mmol) of $(CH_3)Au(PPh_3)$ was added to the above solution. The mixture was heated to reflux for 1 h. Then the solvent was removed *in vacuo*, and the products were then isolated by TLC by using a 2:1 hexane/methylene chloride solvent mixture to yield 12.7 mg (63% yield) of **5.8**.

**Improved Synthesis of $Ir_4(CO)_9(Ph)_2(AuPPh_3)_4$, 5.10**.

A 15.0 mg (0.008 mmol) portion of $Ir_4(CO)_{11}(AuPPh_3)_2$, **5.3** dissolved in 15 mL $CH_2Cl_2$ and 16.0 mg (0.0298 mmol) of $PhAu(PPh_3)$ was added to the above solution. The mixture was heated to reflux for 1 h. Then the solvent was removed *in vacuo*, and the products were then isolated by TLC by using a 2:1 hexane/methylene chloride solvent mixture to yield 15.5 mg (69% yield) of **5.10**.

**Improved yield of $Ir_4(CO)_9(PPh_3)(Ph)(AuPPh_3)_3$, 5.9 from reaction of $Ir_4(CO)_{10}(PPh_3)(AuPPh_3)_2$, 5.4 with $Au(PPh_3)Ph$.**

A 7.0 mg (0.003 mmol) portion of $Ir_4(CO)_{10}(PPh_3)(AuPPh_3)_2$, **5.4** dissolved in 10 mL $CH_2Cl_2$ and 4.0 mg (0.007 mmol) of $Au(PPh_3)Ph$ was added to the above solution. The mixture was heated to reflux for 1 h. Then the solvent was removed *in vacuo*, and the products were then isolated by TLC by using a 2:1 hexane/methylene chloride solvent mixture to yield 6.9 mg (80% yield) of **5.9**.

**Synthesis of $Ir_4(CO)_9[\mu\text{-}\eta^3\text{-}O{=}C(C_{16}H_8)](\mu\text{-}AuPPh_3)(\mu_3\text{-}AuPPh_3)$, 5.11.**

A 9.0 mg (0.0052 mmol) portion of compound **5.7** was dissolved in 10 mL $CH_2Cl_2$. 10.0 mg (0.021 mmol) of $(CH_3)AuPPh_3$ was added to the above solution. The reaction mixture was heated to reflux for 2 h. After cooling, the solvent was then removed *in vacuo*, and the product was isolated by TLC by using a 3:1 hexane/methylene chloride solvent mixture to yield 2.8 mg (25 % yield) of yellow $Ir_4(CO)_9(\mu\text{-}\eta^3\text{-}O{=}CC_{16}H_8)(\mu\text{-}AuPPh_3)(\mu_3\text{-}AuPPh_3)$, **5.11**. Spectral data for **5.11**: IR CO ($cm^{-1}$ in $CH_2Cl_2$): 2060(s), 2021(s), 2010(vs), 1995(s), 1985(m) 1963(w), 1834(w). $^1$H NMR ($CDCl_3$) $\delta$ = 7.14-7.36 (m, 30H, $PPh_3$), 7.96-8.52 (m, 8H, 1,10-pyrene). Mass Spec. ES+/MS for **5.11**: 2169 (M+H).

**Crystallographic Analyses:** Yellow crystals of **5.1**, black crystals of **5.2**, red crystals of **5.3** and **5.5** suitable for x-ray diffraction analyses were each obtained by slow evaporation of solvent from a solution of the compound in a benzene/methylene chloride solvent mixture by slow evaporation of the solvent at room temperature. Yellow crystals of **5.6** and **5.7**, red crystals of **5.8**, **5.9** and **5.10** suitable for x-ray diffraction analyses were obtained by slow evaporation of solvent from solutions of the pure compounds in benzene/octane solvent mixtures at room temperature. Red crystals of **5.4** and **5.11** suitable for x-ray diffraction analysis were obtained by slow evaporation of solvent from solutions in hexane/methylene chloride solvent mixtures at -25 ℃. Each data crystal was glued onto the end of a thin glass fiber. X-ray intensity measurements were performed on a Bruker SMART APEX CCD-based diffractometer with Mo K$\alpha$ radiation ($\lambda$ = 0.71073 Å). The raw data frames were integrated with the SAINT+ program by using a narrow-frame integration algorithm.[20] Corrections for Lorentz and polarization effects were also applied by using the program SAINT+.[20] An empirical absorption correction based on

the multiple measurement of equivalent reflections was applied by using the program SADABS. All structures were solved by a combination of direct methods and difference Fourier syntheses, and were refined by full-matrix least-squares on $F^2$ by using the SHELXTL software package.[21] All non-hydrogen atoms were refined with anisotropic displacement parameters. Hydrogen atoms were placed in geometrically idealized positions and included as standard riding atoms during the least-squares refinements. Crystal data, data collection parameters, and results of the analyses are listed in Tables 5.1. Compounds **5.1, 5.4** and **5.8** crystallized in the monoclinic crystal system. For all these the space group $P2_1/c$ was established by the pattern of systematic absences observed in the data. Two half-molecules of benzene cocrystallized with **5.8** in the asymmetric crystal unit. Compound **5.2, 5.9** and **5.10** crystallized in the triclinic crystal system. The space group *P-1* was assumed and confirmed by the successful solution and refinement of the structure. Two molecules of benzene cocrystallized with **5.2** in the asymmetric crystal unit. Two molecules of benzene cocrystallized with **5.9** in the asymmetric crystal unit. Three molecules of benzene cocrystallized with **5.10** in the asymmetric crystal unit. Compound **5.3** crystallized in the hexagonal crystal system. The systematic absences in the intensity data were consistent with either of the space groups $P6_1$ or $P6_5$. The structure was solved in the space $P6_5$. Attempts to refine in the enantiomeric space group $P6_1$ gave a poorer agreement than $P6_5$, so the $P6_5$ setting was used in the final analysis. Compound **5.5** crystallized in the space group *P*-1. A half molecule of benzene located on a center of symmetry was found cocrystallized with the complex in the asymmetric crystal unit. Compound **5.6** crystallized in the monoclinic crystal system. The space group $P2_1/n$ was established uniquely on the basis of

systematic absences observed in the data. Compounds **5.7** and **5.11** both crystallized in the monoclinic crystal system. The systematic absences were consistent with either of the space groups *C*c or *C*2/c. The centrosymmetric space group *C*2/c was assumed and confirmed by the successful solution and refinement for both of these structural analyses. One molecule of benzene cocrystallized with **5.7** in the asymmetric crystal unit. Two molecules of methylene chloride cocrystallized with **5.11** in the asymmetric crystal unit.

**Computational Details:** All density functional theory (DFT) calculations were performed using the Gaussian 09 suite of *ab initio* programs[22] at the non-empirical meta-GGA Tao-Perdew-Staroverov-Scuseria (TPSS) functional[23] in conjunction with all-electron 6-31G(d,p) basis set for H, C, O and P atoms and Stuttgart quasi-relativistic effect core potential basis set (ECP60MWB) for Ir and Au atoms.[24] We believe such basis sets (1324 basis functions for **5.2**) are sufficient for accurate DFT calculations. All structures studied in this paper were fully optimized as gas-phase without any restriction. Experimental $PPh_3$ groups were employed without any simplification in the geometry optimization and molecular orbital analysis of **5.2** and **5.3**. Simplified structure models, $Ir_4(CO)_{10}(AuPMe_3)_2$, **5.2*** and $Ir_4(CO)_{11}(AuPMe_3)_2$, **5.3***, was used to study the reaction mechanisms in the ligand-induced skeletal rearrangements.

**Results and Discussion**

The reaction of $[NEt_4][Ir_4(CO)_{11}(Ph)]$ with $[Au(PPh_3)][NO_3]$ provided the compound $Ir_4(CO)_{11}(Ph)(\mu\text{-}AuPPh_3)$, **5.1** in 91% yield, Scheme 5.3. Compound **5.1** was characterized by a combination of of IR, $^1H$ and $^{31}P$ NMR, mass spec and a single crystal X-ray diffraction analyses. An ORTEP diagram of the molecular structure of compound

**5.1** is shown in Figure 5.1. Compound **5.1** contains a tetrahedral cluster of four iridium atoms with a bridging $Au(PPh_3)$ group on the Ir(1) – Ir(2) edge of $Ir_4$ cluster and a σ-phenyl group terminally coordinated to atom Ir(2). This is the same Ir – Ir bond that lies trans to the phenyl ligand in the anion $[Ir_4(CO)_{11}(Ph)]^-$. The most structurally similar complex in the literature is the compound $Ir_4(CO)_{10}(\mu\text{-}PPh_2)(AuPPh_3)$, **5.12**.[9c] The Ir – Au bond distances in **5.12** are 2.731(2) Å and 2.788(2) Å. The Ir – Au bond distances in **5.1** are similar to those in **5.12**, but are themselves significantly different, Ir(1) – Au(1) = 2.7332(4) Å and Ir(2) – Au(1) = 2.8056(4) Å. The longer length of the Ir(2) – Au(1) bond distance may be due to steric effects, because atom Ir(2) contains bonds to four ligands, the σ-phenyl group, a terminal CO ligand and two bridging CO ligands while Ir(1) has only three CO ligands coordinated to it.

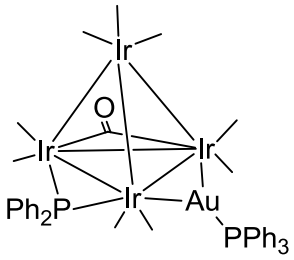


**5.12**

The Ir – Ir bond distances in **5.1**, 2.6968(5) Å - 2.7460(4) Å are similar to those in **5.12**, 2.689(2) Å - 2.832(2) Å except for the Au bridged Ir – Ir bond which is Ir(1) – Ir(2) = 2.9143(4) Å. This may also be due to the steric crowding about Ir(2). The Ir - C distance to the σ-phenyl group, 2.100(7) Å, is similar to that found in $[NEt_4][Ir_4(CO)_{11}(Ph)]$, 2.125(13) Å.

Two new iridium-gold cluster complexes: $Ir_4(CO)_{10}(AuPPh_3)_2$, **5.2**, 5 % yield and $Ir_4(CO)_{11}(AuPPh_3)_2$, **5.3**, 73 % yield were obtained from the reaction of $[HIr_4(CO)_{11}]^-$

with $[Au(PPh_3)][NO_3]$. Both of the complexes are new and were characterized by a combination of IR, $^1H$ NMR, mass spec and a single-crystal X-ray diffraction analysis, See Scheme 5.4.

An ORTEP diagram of the molecular structure of compound **5.2** is shown in Figure 5.2. The basic framework of the cluster in **5.2** can be described as an $Ir_4$ butterfly tetrahedron with two mutually bonded Au atoms bridging in the fold of the butterfly to form an $Ir_4Au_2$ six metal cluster in the shape of an octahedron. The Au – Au bond distance, Au(1) – Au(2) = 3.1405(10) Å is slightly longer than Au – Au bond distances in the cationic octahedral gold cluster $[Au_6\{P\text{-}p\text{-}tolyl_3\}][BPh_4]_2$, 2.932(2) Å – 3.091(2) Å,[25] and significantly longer that the Au – Au bond distance, 2.8530(8) Å, found in the complex $Ir_6(CO)_{15}(AuPPh_3)_2$[8a] where the two $Au(PPh_3)$ groups are mutually-bonded capping groups. The Au – Au distances in the octahedral $Au_6$-($\mu_6$-C) carbido cluster complex, $[Au_6\{PPh_3\}_6(\mu_6\text{-}C)][BPh_4]_2$, range from 2.887(1) Å – 3.226(1) Å.[26] The Ir – Au distances in **5.2** range from 2.7299(10) Å to 2.9031(10) Å and are similar to those found in $Ir_6(CO)_{15}(AuPPh_3)_2$, 2.6569(6) Å – 2.9347(5) Å. The Ir – Ir bond distances in **5.2** range from 2.7127(10) Å - 2.7676(11) Å and are slightly shorter than the Ir – Ir distances in the hexairidiumdigold cluster complex $Ir_6(CO)_{15}(AuPPh_3)_2$, 2.760(1) Å – 2.9325(7) Å. Each Au atom in **5.2** contains one $PPh_3$ ligand. There are ten CO ligands; two of these are bridging ligands across the Ir(1) – Ir(3) and Ir(2) – Ir(4) bonds. The other CO ligands are linear terminal ligands.

The Au – Au bond in **5.2** may be weak, but DFT molecular orbital calculations indicate that there are significant direct Au – Au orbital interactions. In the DFT optimized structure of $Ir_4Au_2(CO)_{10}(PPh_3)_2$, the Au – Au distance is 3.142 Å, which is

very close to the experimentally measured value of 3.1405(10) Å. Selected molecular orbitals (MOs) that show the most significant Au - Au interactions are presented in Figure 5.12. HOMO-33, HOMO-35, HOMO-37, HOMO-50, HOMO-54 and HOMO-62 show the bonding between two gold atoms through the interaction of their d orbitals, which are combined with the d-orbitals of iridium atoms and the p-orbitals of the P atoms.

It is worthwhile to compare and contrast the structure of **5.2** with that of the isoelectronic tetraosmium compound $Os_4(CO)_{12}(\mu_3\text{-}AuPPh_3)_2$, **5.13**.[27] Compound **5.13** contains a butterfly cluster of four osmium atoms, but differs from **5.2** in that it contains twelve linear terminal carbonyl ligands, three on each osmium atom. Compound **5.13** contains two triply-bridging $Au(PPh_3)$ groups, but there is no bond between the two Au atoms, Au – Au = 4.045 Å. The reason for this could be steric in nature, namely the increase in ligand repulsions in going from **5.2** which has ten CO ligands to **5.13** which has twelve CO ligands may be sufficient to prevent that the formation of an Au – Au bond in **5.13**. The $Os_4$ cluster in compound **5.13** has only 58 valence electrons and is formally electron deficient.[27] Compound **5.2** also has only 58 cluster valence electrons, but it contains an Au – Au bond that is not present in **5.13**, see above.

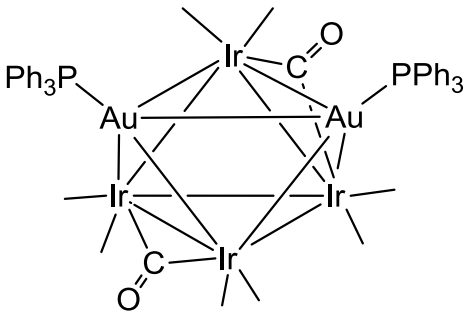


**5.2**

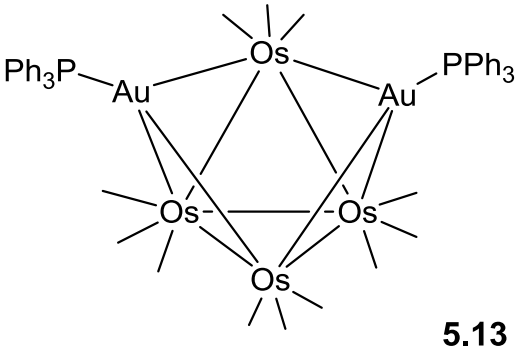


**5.13**

An ORTEP diagram of the molecular structure of compound **5.3** is shown in Figure 5.3. The metal cluster can be described as a doubly $Au(PPh_3)$ capped $Ir_4$ tetrahedron or as a mono- $Au(PPh_3)$ capped $Ir_4Au$ trigonal bipyramid. By the former description, one $Au(PPh_3)$ cap bridges three iridium atoms: Ir(2), Ir(3) and Ir(4). The other $Au(PPh_3)$ cap bridges the two iridium atoms: Ir(2), Ir(3) and the other Au atom, Au(1). The $Au(PPh_3)$ groups are mutually bonded in **5.3**. The Au – Au bond distance in **5.3** is longer than that in **5.2**, 3.2464(13) Å. This cluster is structurally similar to the $Ir_4Au_2$ cluster found in the complex $Ir_4(CO)_{11}(\mu_4\text{-PhPPh})Ir_4(CO)_9(AuPEt_3)_2$, which has an Au – Au bond distance of 3.052(2) Å.[9a] The Au-bridged, equatorial Ir – Ir bond in **5.3**, Ir(2) – Ir(3) = 3.1013(10) Å is significantly longer than the all of the other Ir – Ir bond distances, 2.7107(12) Å - 2.8196(12) Å. There are eleven CO ligands in **5.3**. One of these, C(2) – O(2), is a bridging ligand across the Ir(2 – Ir(4) bond and one other, C(1) – O(1), is a semi-bridging ligand from Ir(3) to Ir(4), Ir(3) – C(1) – O(1) = 157(3)$^o$, Ir(4)$\cdots$C(1) = 2.56(3)Å. All the other CO ligands are linear terminal ligands. The $^{31}P\{^1H\}$ NMR of **5.3** exhibits only one resonance at $\delta$ = 84.71 ppm. This is inconsistent with the solid state structure in which the two $PPh_3$ ligands are inequivalent. Studies of other $AuPR_3$ capped trigonal bipyramidal digold complexes have been reported to show only a single phosphorus resonance at room temperature.[28] Variable temperature NMR studies of these complexes have shown that the $AuPR_3$ groups are dynamically active in solution and are exchanging sites rapidly on the NMR timescale at room temperature. We believe that a similar type of exchange is also occurring in **5.3** and that leads to an averaging of the two resonances expected for the $PPh_3$ ligands. The $AuPR_3$ groups are generally regarded as one electron donors similar to hydrogen, e. g. compare $Ph_3PAuCl$ and HCl.[29] Assuming

that each $AuPR_3$ group formally donates only one electron to the $Ir_4$ cluster in **5.3**, then the $Ir_4$ cluster contains a total of 60 electrons which means that each iridium atom formally has an 18-electron configuration.

DFT molecular orbital calculations were also performed for compound **5.3**. Interestingly, the ligand structure for the geometry-optimized structure of **5.3** is slightly different from that of the structure of **5.3** found in crystal. In particular, the DFT structure contains two full bridging CO ligands to atom Ir(4) as shown in Figure 5.3. The DFT structure is formed simply by moving the semibridging CO ligand C(1) – O(1) on atom Ir(3) in the solid state structure of **5.3** to a bridging position across the Ir(3) – Ir(4) bond. The metal atoms and CO ligands are very close to the $C_s$ symmetry in the optimized structure of **5.3**. The difference between the DFT structure and the solid state structure is very small and may be due simply to the existence of packing effects that exist between molecules in the solid state. Selected molecular orbitals for **5.3** are shown in Figure 5.13. The HOMO-29, HOMO-34, HOMO-51 and HOMO-63 show that there is significant d-d Au – Au bonding interactions.

Interestingly, compounds **5.2** and **5.3** were found to be readily interconvertible by the addition and elimination of CO. When **5.2** was treated with CO at 25 $^oC$/1 atm, it was converted to **5.3** in 95 % isolated yield within 5 min. Conversely, when a solution of **5.2** in a $CH_2Cl_2$ solution was heated to reflux under nitrogen, it was converted back to **5.2** in 91% yield within 30 min. Interestingly, compound **5.2** also reacted with $PPh_3$ by ligand addition at 25 $^oC$ to yield the $PPh_3$ addition product $Ir_4(CO)_{10}(PPh_3)(AuPPh_3)_2$, **5.4** in 61% yield within 10 min. An ORTEP diagram of the molecular structure of compound **5.4** is shown in Figure 5.4. The molecular structure of **5.4** is similar to that of **5.3**, (i. e. a doubly

$Au(PPh_3)$ capped $Ir_4$ tetrahedron), except that there is a $PPh_3$ on the iridium atom Ir(4). The Au – Au bond distance in **5.4**, 2.7695(5) Å, is considerably shorter than that in **5.3** despite the fact that **5.4** contains an additional bulky $PPh_3$ ligand. Indeed, the shortening of the Au – Au distance might be due to increased sterics about the $Ir_4$ tetrahedron caused by the bulky $PPh_3$ ligand, and the CO ligands C(11) – O(11) and C(32) – O(32) on atoms Ir(1) and Ir(3), respectively, are pushed toward the group Au(2) – P(2) which in turn moves toward the group Au(1) – P(1) and this could explain the observed shortening of the Au – Au bond distance. There are also other effects on the ligand geometry. In particular, compound **5.4** contains two full bridging CO ligands while **5.3** had only one bridge and one semibridge in different locations. The Ir – Ir bond distances in **5.4** are similar to those in **5.3**, range 2.7459(4) Å – 2.8363(4) Å, except for the Ir(1) – Ir(3) bond 2.8363(4) Å, which is much shorter than the corresponding bond in **5.3**, Ir(2) – Ir(3) = 3.1013(10) Å. Assuming that each $AuPR_3$ group formally donates only one electron to the $Ir_4$ cluster, the $Ir_4$ cluster in **5.4** then contains a total of 60 electrons which means that each iridium atom in **5.4** has an 18-electron configuration.

Although there are other possible mechanisms, based on the location of the $PPh_3$ ligand found in **5.5**, it is proposed that the ligand additions to **5.2** occur at one of the Ir atoms in the "hinge" of the $Ir_4$ butterfly, see L in Scheme 5.5. The conversions to **5.3** or **5.4** are then as simple as the cleavage of the Ir – Au bond to the Ir atom that accepted the ligand and the formation of an Ir – Ir bond between two "wingtip" Ir atoms, see the conversions of **5.2** to **5.3** and **5.2** to **5.4** in Scheme 5.5. Most interestingly, the number of metal – metal bonds in **5.2** and **5.3** is the same at 12.

To establish further details of the mechanism of this transformation, we have investigated the loss of CO from the model compound $Ir_4(CO)_{11}(AuPMe_3)_2$, **5.3*** and traced its transformation back to the structure $Ir_4(CO)_{10}(AuPMe_3)_2$, **5.2*** computationally. The geometry optimized structure of **5.3*** is not significantly different from that of **5.3**. Since the addition and loss of a CO ligand happen on the Ir atom, Ir(1), far removed from the $PPh_3$ ligands, the difference in steric effects between phenyl groups in **5.3** and methyl groups in **5.3*** for this transformation should be insignificant. To initiate the **5.3*** to **5.2*** transformation, a CO ligand was removed from atom Ir(1) in the structure **5.3***. Dissociation of CO from Ir(1) can occur in either of two ways: 1) removal of one of the two symmetry equivalent CO ligands C(11) or C(12) on Ir(1) or 2) the removal of the unique CO ligand C(13) on Ir(1). Both processes were tested computationally. Figure 5.14 shows the sequence of structures that were traversed in the course of the geometry optimization of the structure **B** formed by the removal of the CO ligand C(12) in the structure of **5.3***. A transition state was encountered as the CO ligand was expelled from Ir(1). Following this, there was a smooth transformation from **5.3*** to the structure **5.2*** that involves a weakening and cleavage of the Ir(2) – Ir(3) bond and a shift of the bridging CO ligand C(10) to a terminal position on Ir(2), **B** $\rightarrow$ **C**. Next a Au – Ir bond is formed between Ir(1) and Au(6), structure **D** and the CO ligand C(14) in Ir(2) moves into a bridging position across the Ir(1) – Ir(2) bond, structure **E**. The transformation concludes with the formation of the structure **5.2*** which is the homolog of **5.2**. This is approximately the same as the reverse of the transformation of **5.2** to **5.3** shown in Scheme 5.5.

The transformation of **5.3*** to **5.2*** by loss of the unique CO ligand C(13) on Ir(1) was also studied computationally and follows a similar pathway with a few modifications as described below. The structures traversed in this transformation are shown in Figure 8. Upon loss of the CO ligand C(13) on Ir(1), the initial structure **B′** is transformed into a discrete intermediate **5.2′*** by a cleavage of the Au − Au bond via  to the structure **C′**, Au···Au = 4.250 Å, and the formation of an Ir – Au bond between Au(6) and Ir(1), 2.788 Å via **D'**.  The intermediate **5.2′*** is then transformed in to **5.2*** via the transition state $\mathbf{TS_{5.2'*,5.2*}}$, which is only 3.6 kcal/mol higher than **5.2′*** in free energy, by a repositioning of the bridging CO ligand between Ir(4) and Ir (1), cleavage of the Ir(2) – Ir(3) bond and a reformation of the Au – Au bond. Such a low barrier indicates that the formation of **5.2*** is rapid once the CO ligand C(13) is dissociated from Ir(1).

Figure 5.16 shows and compares the calculated free-energy profiles for the transformation between **5.3*** to **5.2*** through the loss of the CO ligand C(12) and loss of the CO ligand C(13). The transition state for the dissociation of the CO ligand C(13) $\mathbf{TS_{CO\text{-}13}}$ is only 0.2 kcal/mol higher than the transition state for the dissociation of the CO ligand C(12) $\mathbf{TS_{CO\text{-}12}}$. Therefore, we predict that these two reaction pathways are competitive.

When compound **5.4** was heated to reflux for 1.5 h in a benzene solution, it expelled one CO ligand and was converted to the new compound $Ir_4(CO)_9(\mu_3\text{-}PPhC_6H_4)(AuPPh_3)_2$, **5.5** in 85% yield. The structure of **5.5** was established by a single-crystal x-ray diffraction analysis and an ORTEP diagram of its molecular structure is shown in Figure 5.5. The arrangement of the metal atoms can be described as a doubly $Au(PPh_3)$ capped $Ir_4$ tetrahedron similar to that found in **5.3** and **5.4**. The Au – Au bond,

3.2071(10) Å, is long as found in **5.3**. The Ir – Ir and Ir – Au bond distances are similar to those found in **5.2**. The $PPh_3$ ligand was converted a triply-bridging $P(Ph)C_6H_4$ ligand by the loss of a phenyl group and an ortho-metallation at one of its remaining phenyl groups. The phosphorus atom bridges two of the Ir atoms that are bonded to the gold atoms Ir(2) and Ir(3), Ir(2) – P(3) = 2.285(4) Å and Ir(4) – P(3) = 2.303(4) Å, so either the gold atoms changed sites, which is likely given the known fluxionality of these atoms, or the phosphorus atom changed sites, which seems less likely since tertiary phosphines do not easily move been metal atoms. The Ir – C distance to the metallated phenyl ring, Ir(3) – C(86) = 2.121(17) Å, is similar in length to those found in other iridium clusters containing σ–bonded aryl rings: $[Et_4N][Ir_4(CO)_{11}Ph]$,[11a] 2.125(13) Å; $[Et_4N][Ir_4(CO)_{11}(PPh_2C_6H_4)]$,[11a] 2.096(12) Å; $Ir_5(CO)_{11}(PPh_3)(PPh_2C_6H_4)$,[11a] 2.14(2) Å; $Ir_3(CO)_9(Ph)(\mu_3\text{-}PPh)(\mu\text{-dppm})$, 2.084(16) Å,[30] and $Ir_4(CO)_8(\eta^1\text{-}Ph)[\mu_4\text{-}\eta^3\text{-}PhPC(H)CPh](\mu\text{-}PPh_2)$, 2.09(1) Å.[31] There are no hydride ligands in **5.5**, so it is assumed that the hydrogen atom that was cleaved from the phenyl ring in the ortho-metallation process was combined with the phenyl group that was also cleaved from the phosphorus atom and the two were subsequently eliminated from the complex in the form of benzene. The $\mu_3\text{-}P(Ph)C_6H_4$ ligand serves as a four electron donor, so the $Ir_4$ cluster in **5.5** contains a total of 60 valence electrons and each iridium atom formally has an 18-electron configuration.

The compounds $Ir_4(CO)_{11}R(\mu\text{-}AuPPh_3)$, **5.1**, R = $C_6H_5$, **5.6**, R = $CH_3$, and **5.7**, R = 2-$C_{16}H_{10}$, were obtained from the reactions of $[NEt_4][Ir_4(CO)_{11}Br]$ with $RAu(PPh_3)$, R = $C_6H_5$, $CH_3$, and 1-$C_{16}H_{10}$ at room temperature in 2 h in the yields, 71%, 60% and 24%, respectively, see Scheme 5.6.

Compounds **5.1, 5.6** and **5.7** were formed by the loss of $Br^-$ from the $Ir_4$ cluster and the oxidative addition of the Au-C bond of the $RAu(PPh_3)$. Compound **5.1** was obtained by us previously from the reaction of $[Ir_4(CO)_{11}(Ph)]^-$ reacts with $[Au(PPh_3)][NO_3]$, see Scheme 5.3. Compounds **5.6** and **5.7** are new and both of these products have been characterized crystallographically. ORTEP diagrams of the molecular structures of **5.6** and **5.7** are shown in Figures 5.6 and 5.7, respectively.

Except for the substitution of the phenyl group by a methyl group, the structure of **5.6** is virtually the same as that of **5.1**. The molecule consists of a tetrahedral $Ir_4$ cluster with an $AuPPh_3$ group bridging one of the six Ir – Ir bonds. The gold-bridged Ir – Ir bond in **5.6**, Ir(1) – Ir(2) = 2.9158(4) Å, is substantially longer than all of the other Ir – Ir bonds in the molecule, Ir(1) – Ir(4) = 2.7340(5) Å, Ir(1) – Ir(3) = 2.7411(4) Å, Ir(3) – Ir(4) = 2.7126(5) Å, Ir(2) – Ir(3) = 2.7212(5) Å, Ir(2) – Ir(4) = 2.7289(5) Å. This may be due in part to the strong structural trans-effect that is exhibited by methyl groups. The Au-bridged bond in **5.1** is also similarly long, 2.9143(4) Å. The Au-bridged bond of **5.7** is also significantly longer than the other Ir – Ir bonds, Ir(1) – Ir(2) = 2.9129(12) Å versus Ir(1) – Ir(4) = 2.7502(11) Å, Ir(1) – Ir(3) = 2.7248(13) Å, Ir(3) – Ir(4) = 2.7064(11) Å, Ir(2) – Ir(3) = 2.7379(12) Å, Ir(2) – Ir(4) = 2.7233(14) Å. It is notable that the σ-bonded pyrenyl ligand in **5.7** is coordinated to the $Ir_4$ cluster at the 2-position, whereas as it was bonded at the 1-position in the gold reagent that was used to make.[32] Evidently, there was a 1,2-shift of the hydrogen atom at the 2-position to the 1-position somewhere in the course of the reaction. A similar 1,2 aryl-hydrogen shift was also observed in the formation of the compound $Os_3(CO)_{10}(\mu\text{-}2\text{-}Np)(\mu\text{-}AuPPh_3)$, Np = $C_{10}H_7$ in the reaction of $Os_3(CO)_{10}(NCMe)_2$ with the compound $(1\text{-}Np)Au(PPh_3)$.[33] The Ir – C bond to the 2-

pyrenyl ligand in **5.7** is 2.083(16) Å in length. It is similar to the Ir – C distance to the phenyl ligand in **5.1**, 2.100(7) Å. These are both similar to the Ir - C distance to the σ-phenyl group found in $[NEt_4][Ir_4(CO)_{11}(Ph)]$, 2.125(13) Å, but the Ir – C bond distance to the methyl ligand in **5.6**, Ir(2) – C(4), is significantly longer at 2.166(8) Å.

When $(CH_3)Au(PPh_3)$ was allowed to react with $[PPN][HIr_4(CO)_{11}]$, compound **5.6** and the new compound $Ir_4(CO)_9(CH_3)_2(AuPPh_3)_4$, **5.8** were obtained in 38 % and 8 % yields, respectively. Compound **5.8** was characterized crystallographically and an ORTEP diagram of its molecular structure is shown in Figure 5.8. This eight metal cluster can be viewed as a butterfly cluster of four gold atoms, each with one $PPh_3$ ligand, bridging one triangular face (Ir1-Ir2-Ir3) of a tetrahedral $Ir_4$ cluster. All four gold atoms are bonded to the iridium atom Ir(2), Ir(2) – Au(3) = 2.6978(5) Å, Ir(2) – Au(1) = 2.7223(5) Å, Ir(2) – Au(2) = 2.7419(5) Å, Ir(2) – Au(4) = 2.7131(5) Å. The Ir – Au bonds, Ir(1) – Au(4) = 3.0758(5) and Ir(3) – Au(1) = 3.0176(5), are significantly longer. The two longest distances, Ir(1) – Au(2) = 3.2905(5) Å and Ir(3) – Au(2) = 3.2503(5) Å are probably nonbonding contacts. There are five Au – Au bonds, Au(1) – Au(2) = 2.8221(5) Å, Au(1) – Au(3) = 3.1032(5) Å, Au2 - Au4 = 2.8096(5) Å, Au(2) – Au(3) = 2.8560(5) Å and Au(3) – Au(4) = 3.0738(5) Å. Two of these, Au(1) – Au(3) and Au(3) – Au(4), are significantly longer than the others. There are methyl groups coordinated in Ir(1) and Ir(3). The Ir – C distances to the methyl groups, Ir(1) – C(4) = 2.132(9) Å, Ir(3) – C(5) = 2.133(9) Å, are similar to that found in **5.6**. The Ir – Ir bond distances span a considerable range: 2.7212(5) Å -3.0038(5) Å. There are two long Ir – Ir bonds, Ir(1) – Ir(2) = 2.9991(5) Å and Ir(2) – Ir(3) = 3.0038(5) Å, that are bridged by gold atoms and also lie trans to a methyl group.

The analogous phenyl-substituted compounds **5.1** (22 % yield, described above) and $Ir_4(CO)_9(CH_3)_2(AuPPh_3)_4$, **5.10** (13 % yield) and a trigoldtetrairidium complex $Ir_4(CO)_9(PPh_3)(Ph)(AuPPh_3)_3$, **5.9** (4 % yield) were obtained from the reaction of $PhAu(PPh_3)$ with $[PPN][HIr_4(CO)_{11}]$ at room temperature. Compound **5.10** is structurally analogous to **5.8**, see Figure 5.10, but has phenyl groups σ–coordinated to two adjacent iridium atoms in the place of the methyl groups found in **5.8**.

The $M_4Au_4$ composition of compounds **5.8** and **5.10** is similar to that of the compounds $Os_4(CO)_{11}H_2(AuPPh_3)_4$,[34] **5.14** and $Os_4(CO)_{11}H_2[Au_4(dppm)_2]$,[35] **5.15** that were reported a number of years ago. Compound **5.14** contains a butterfly cluster of four $Au(PPh_3)$ groups coordinated to an edge of a tetrahedral $Os_4$ cluster. Compound **5.15** contains an open cluster of four Au groups bridging a triangular face of a tetrahedral $Os_4$ cluster.

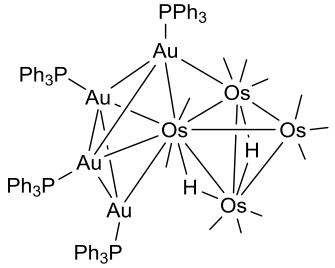


**5.14**

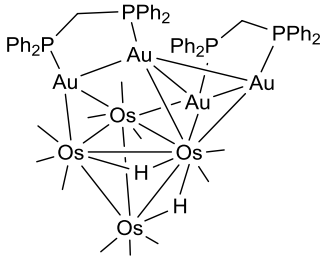


**5.15**

The molecular structure of compound **5.9** is shown in Figure 5.9. The structure of **5.9** consists of an $Ir_4$ tetrahedron with a triangle of gold atoms occupying one triangular face (Ir1-Ir2-Ir3) of the $Ir_4$ tetrahedron. Each gold atom contains one $PPh_3$ ligand. There is additional $PPh_3$ ligand coordinated to Ir(4) in the $Ir_4$ tetrahedron. Compound **5.9** contains one σ–phenyl ligand that is coordinated to Ir(3), Ir(3) – C(4) = 2.09(2) Å. The Ir – Ir bond distances are similar to those in **5.1**, **5.6**, **5.8** and **5.10**, Ir(1) – Ir(2) = 2.7814(11)

Å, Ir(1) – Ir(4) = 2.7479(11) Å, Ir(2) – Ir(3) = 2.7295(12) Å, Ir(2) – Ir(4) = 2.7851(11) Å, Ir(3) – Ir(4) = 2.7653(11) Å, except for the long Ir(1) – Ir(3) bond, 2.8962(11) Å, which lies trans to the σ–phenyl ligand. The Au – Au bond distances span a considerable range, 2.7865(11) Å to 2.9888(11) Å. The reason for this is not clear. All three gold atoms are bonded to Ir(1), Ir(1) – Au(2) = 2.7205(11) Å, Ir(1) – Au(3) = 2.6790(10) Å, Ir(1) – Au(1) = 2.6831(10) Å, but Au(1) and Au(3) are also bonded to Ir(2) and Ir(3), respectively, although these Ir – Au distances are significantly longer, Ir(2) – Au(1) = 3.0157(12) Å, Ir(3) – Au(3) = 2.9639(11) Å than the others.

The tetranuclear gold compounds **5.8** and **5.10** were also obtained from the reactions **5.6** and **5.1** with $(CH_3)Au(PPh_3)$ and $PhAu(PPh_3)$, respectively, but the best routes to **5.8** and **5.10** were by using iridium clusters that already contain some $Au(PPh_3)$ groups. For example, the reactions of $Ir_4(CO)_{11}(AuPPh_3)_2$, **5.3** with $(CH_3)Au(PPh_3)$ and $PhAu(PPh_3)$ provided **5.8** and **5.10** in 63 % and 69 % yields, respectively, see Scheme 5.7. Similarly, the trigold compound **5.9** was obtained in a high yield (80%) from the reaction of $Ir_4(CO)_{10}(PPh_3)(AuPPh_3)_2$, **5.4** with $PhAu(PPh_3)$, see Scheme 5.8.

Finally, the reaction of **5.7** with $(CH_3)Au(PPh_3)$ was found to yield the digold compound **5.11** in 25% yield, see Scheme 5.9. An ORTEP diagram of the molecular structure of **5.11** is shown in Figure 5.11. The cluster of compound **5.11** consists of an $Ir_4$ tetrahedron with two bridging $Au(PPh_3)$ groups. One of the $Au(PPh_3)$ groups, Au(1), is a triple bridge on the Ir2-Ir3-Ir4 face of the cluster. The other is an edge-bridging group, Au(2), that is bonded only to the metal atoms Ir(2) and Ir(3). The Au(1)···Au(2) distance, 3.501(1) Å, is too long to allow a significant bonding interaction in this molecule. The Ir – Ir bond distances are normal, 2.7073(6) Å - 2.8368(6) Å, except for the long Ir(2) – Ir(3)

bond, 2.9898(5) Å, that is bridged by the second Au($PPh_3$) group, Au(2). The 2-pyrenyl ligand has formed a bonding interaction to one of the CO ligands at its 1-position and has become metallated at the 10-position. The associated CO group has become a bridge across the Ir(2) – Ir(4) bond with the oxygen atom coordinated to Ir(2), Ir(2) – O(1) = 2.340(5) Å, and the carbon atom coordinated to Ir(4), Ir(4) – C(1) = 2.005(8) Å. The pyrenyl ring is coordinated to Ir(4) via the ring carbon C(43), Ir(4) – C(43) = 2.102(8) Å. The transformation of the 2-pyrenyl ligand into the bridging 1-carbonyl-10-pyrenyl ligand must have involved a 1,2-hydrogen shift, a CO insertion and an oxidative-addition of a CH bond at the 10-position, all accompanied by the oxidative addition of the Au-C bond of the incoming molecule of ($CH_3$)Au($PPh_3$), the reductive elimination of methane and the loss of two CO ligands. The sequence of these steps cannot be ascertained from this work.

**Conclusions**

New polynuclear iridium-gold carbonyl cluster complexes have been obtained from reactions of the iridium anions: $[Ir_4(CO)_{11}(Ph)]^-$ and $[HIr_4(CO)_{11}]^-$ with [Au($PPh_3$)][$NO_3$]. The tetrairidium cluster complexes **5.2** and **5.3** engage in a facile interconversion via the reversible addition and elimination of CO. The interconversion involves a transformation of the metal framework of the clusters but it does not result in a change in the total number of metal – metal bonds. Calculations indicate that there is a significant bonding interaction between the gold atoms in compounds **5.2** and **5.3**. The addition of $PPh_3$ to **5.2** to form **5.4** is not reversible. However, **5.4** does eliminate CO when heated in a process that leads to a transformation and degradation of the $PPh_3$ ligand into a triply-bridging PPh($C_6H_4$) ligand to yield compound **5.5**.

The organogoldphosphine compounds $RAu(PPh_3)$, R = $CH_3$, Ph and 2-$C_{16}H_{10}$ ($C_{16}H_{10}$ = pyrenyl) react with the iridium anions, $[Ir_4(CO)_{11}Br]^-$ and $[HIr_4(CO)_{11}]^-$, to form iridium-gold cluster complexes. The primary products are the monogold compounds **5.1, 5.6** and **5.7**. The $[Ir_4(CO)_{11}Br]^-$ is more reactive and gives higher yields of **5.1** and **5.6** than the $[HIr_4(CO)_{11}]^-$ anion. Low yields of tri- and tetragold **5.8** – **5.10** were also obtained in the reaction using the anion $[HIr_4(CO)_{11}]^-$. The higher nuclearity gold compounds **5.8** and **5.10** were obtained in much better yields from reactions of the appropriate $RAu(PPh_3)$ reagents with the iridium-gold cluster complexes **5.3** and **5.9** was obtained in a high yield from the reaction of $PhAu(PPh_3)$ with **5.5**. Treatment of **5.7** with $(CH_3)Au(PPh_3)$ provided the digold complex **5.11** which was formed after considerable transformation/modification(s) of the pyrenyl ligand.

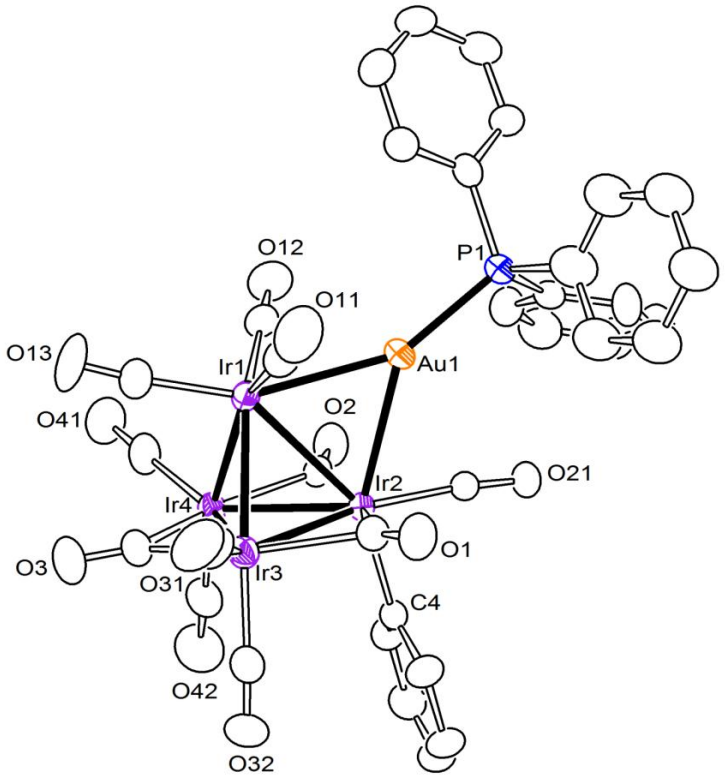


**Figure 5.1.** An ORTEP diagram of the molecular structure of $Ir_4(CO)_{11}(Ph)(\mu\text{-}AuPPh_3)$, **5.1** showing 30% thermal ellipsoid probability.

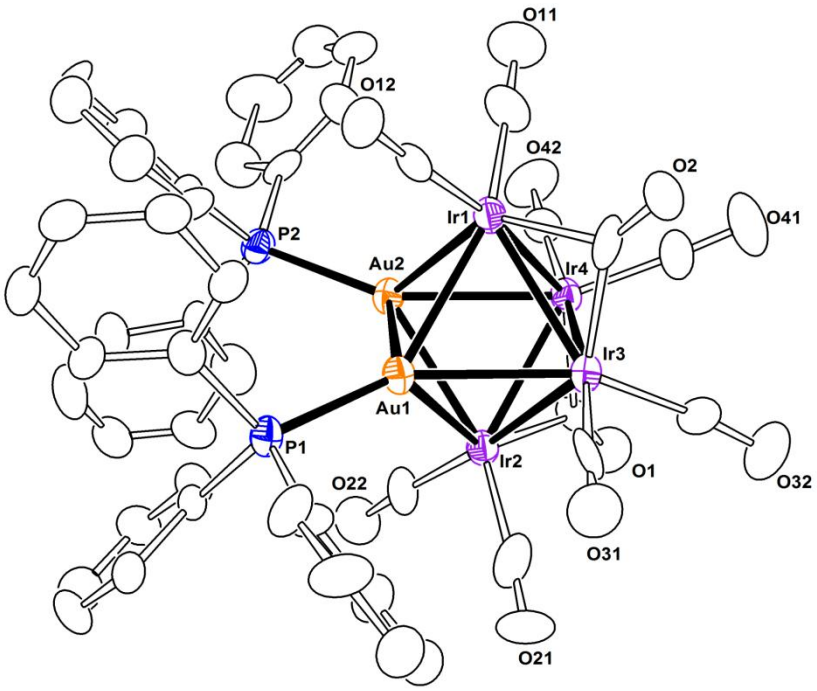


**Figure 5.2.** An ORTEP diagram of the molecular structure of $Ir_4(CO)_{10}(AuPPh_3)_2$, **5.2** showing 30% thermal ellipsoid probability.

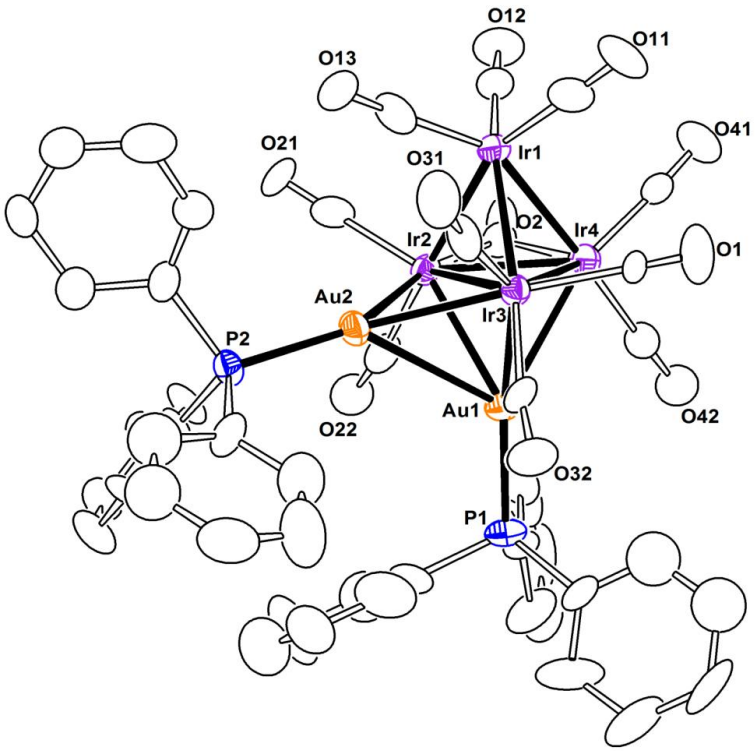


**Figure 5.3.** An ORTEP diagram of the molecular structure of $Ir_4(CO)_{11}(AuPPh_3)_2$, **5.3**, showing 30% thermal ellipsoid probability.

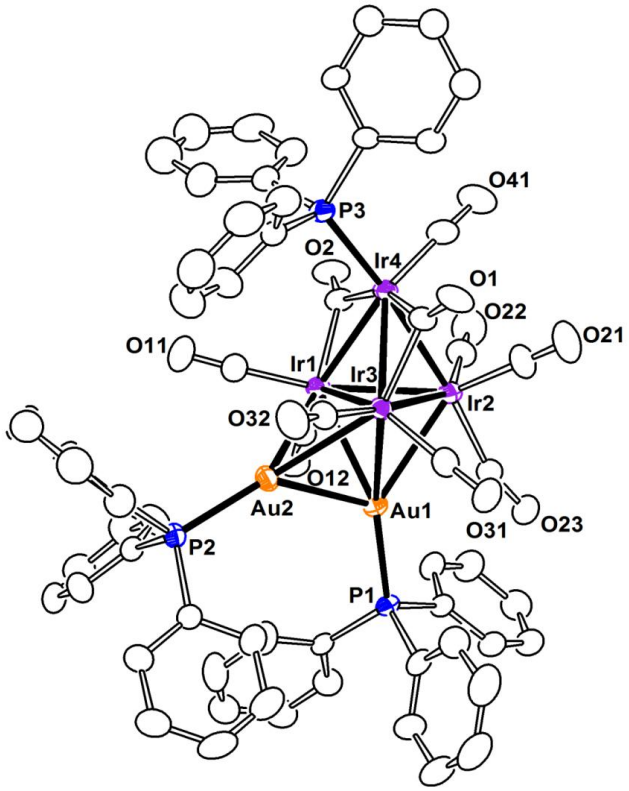


**Figure 5.4.** An ORTEP diagram of the molecular structure of $Ir_4(CO)_{10}(PPh_3)(AuPPh_3)_2$, **5.4** showing 30% thermal ellipsoid probability.

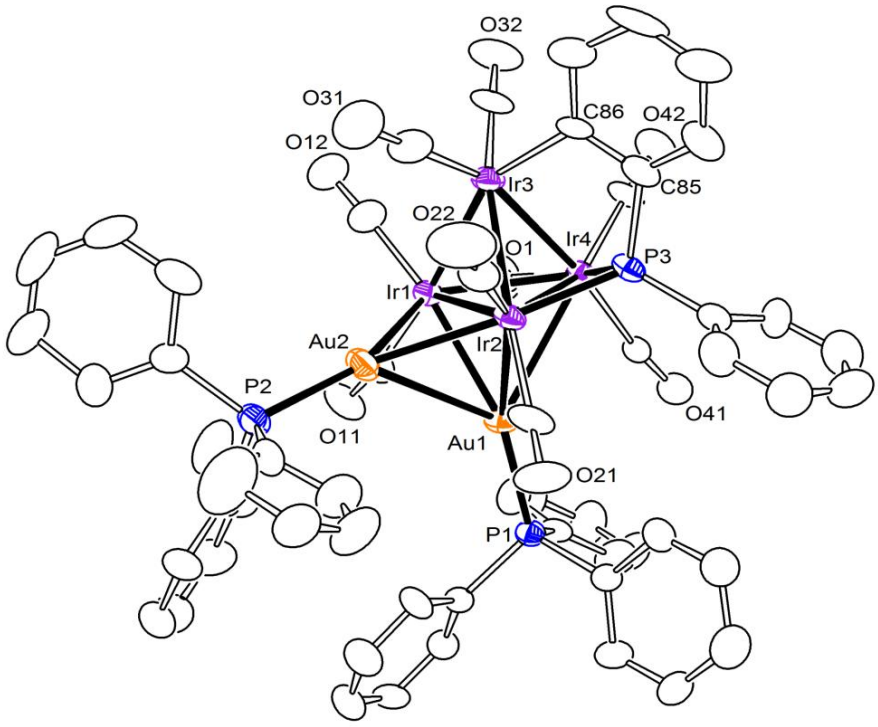


**Figure 5.5.** An ORTEP diagram of the molecular structure of $Ir_4(CO)_9(PPhC_6H_4)(AuPPh_3)_2$, **5.5** showing 30% thermal ellipsoid probability.

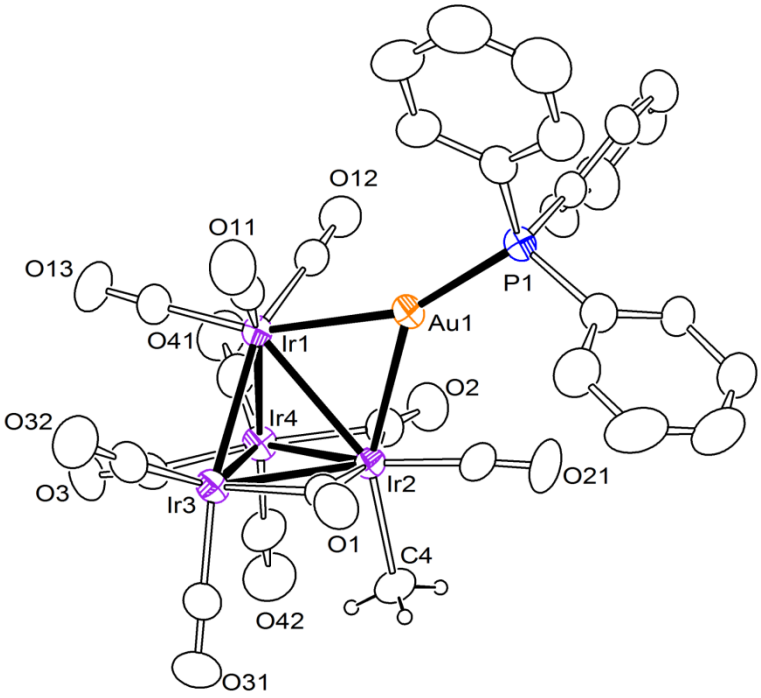


**Figure 5.6.** An ORTEP diagram of the molecular structure of $Ir_4(CO)_{11}(CH_3)(AuPPh_3)$, **5.6** showing 30% thermal ellipsoid probability.

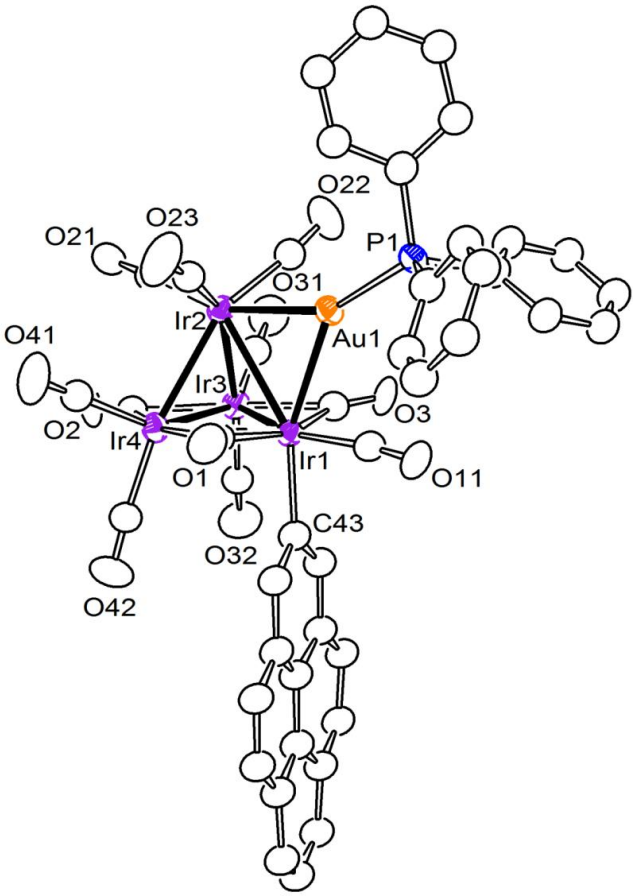


**Figure 5.7.** An ORTEP diagram of the molecular structure of $Ir_4(CO)_{11}(2\text{-}C_{16}H_9)(AuPPh_3)$, **5.7** showing 30% thermal ellipsoid probability.

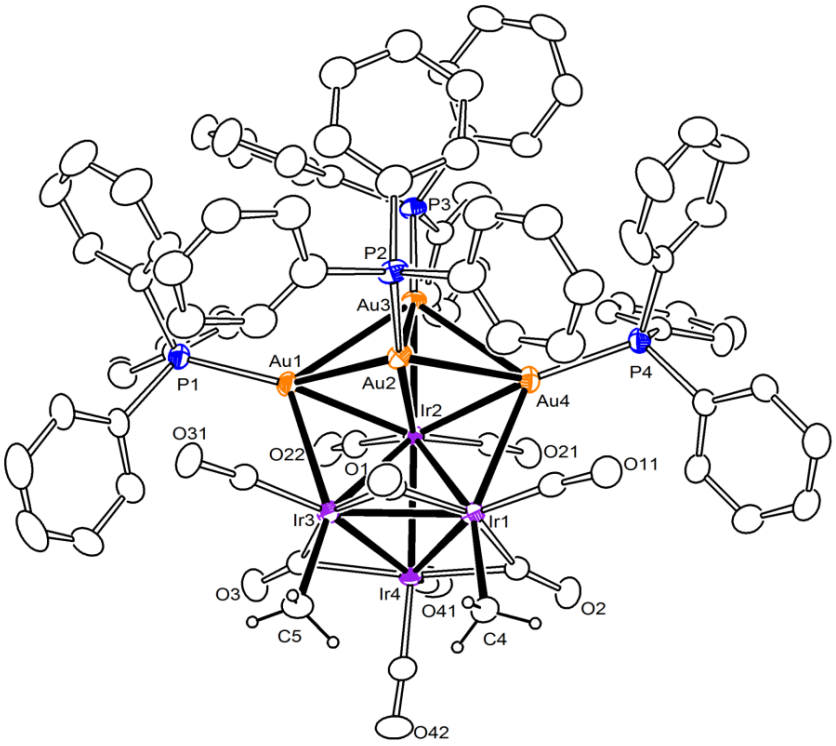


**Figure 5.8.** An ORTEP diagram of the molecular structure of $Ir_4(CO)_9(CH_3)_2(AuPPh_3)_4$, **5.8** showing 30% thermal ellipsoid probability.

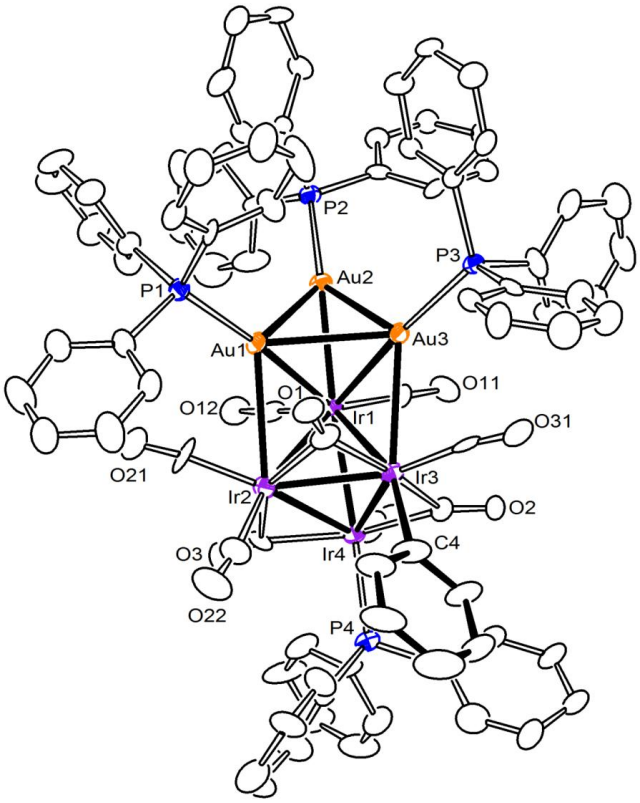


**Figure 5.9.** An ORTEP diagram of the molecular structure of $Ir_4(CO)_9(PPh_3)(Ph)(AuPPh_3)_3$, **5.9**, showing 20% thermal ellipsoid probability.

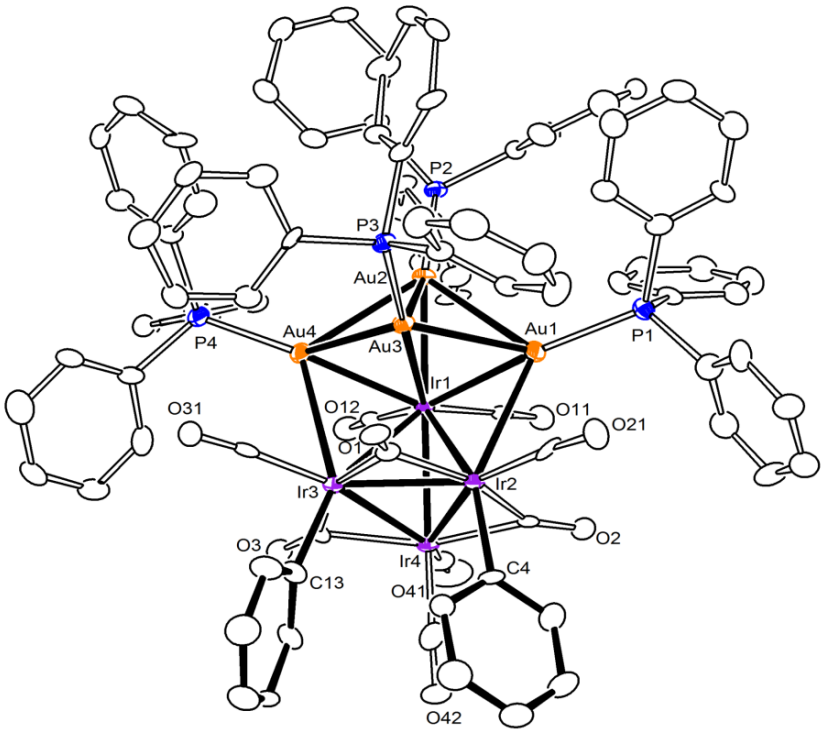


**Figure 5.10.** An ORTEP diagram of the molecular structure of $Ir_4(CO)_9(Ph)_2(AuPPh_3)_4$, **5.10** showing 50% thermal ellipsoid probability.

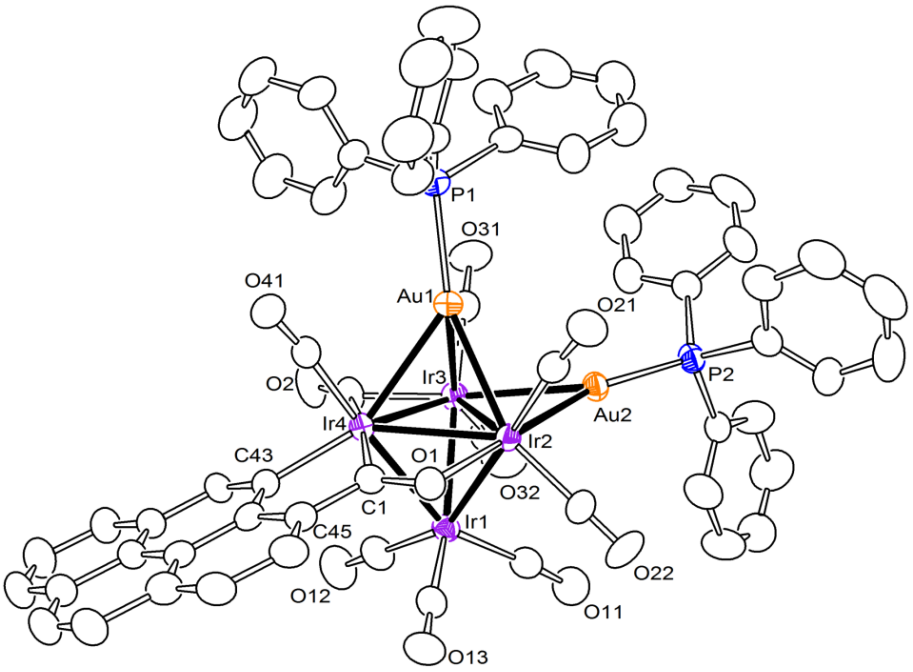


**Figure 5.11.** An ORTEP diagram of the molecular structure of $Ir_4(CO)_9(\mu\text{-}\eta^3\text{-}O{=}CC_{16}H_8)(\mu\text{-}AuPPh_3)(\mu_3\text{-}AuPPh_3)$, **5.11** showing 30% thermal ellipsoid probability.

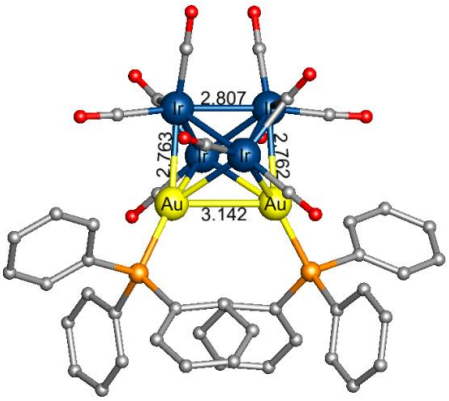


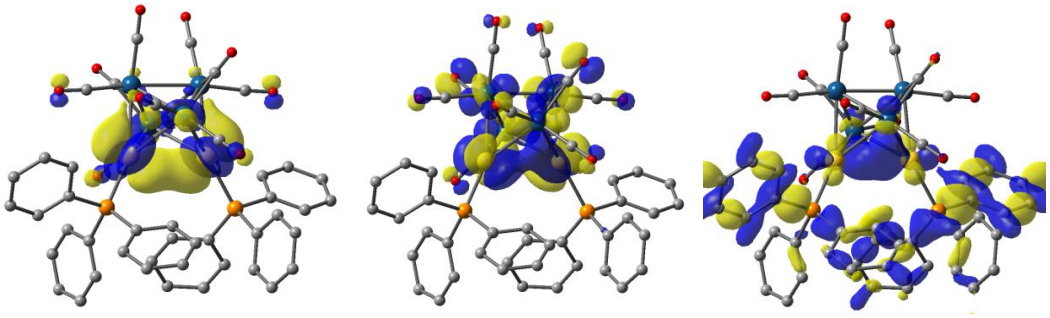

HOMO-33, -9.81 eV HOMO-35, -10.00 eV HOMO-37, -10.19 eV

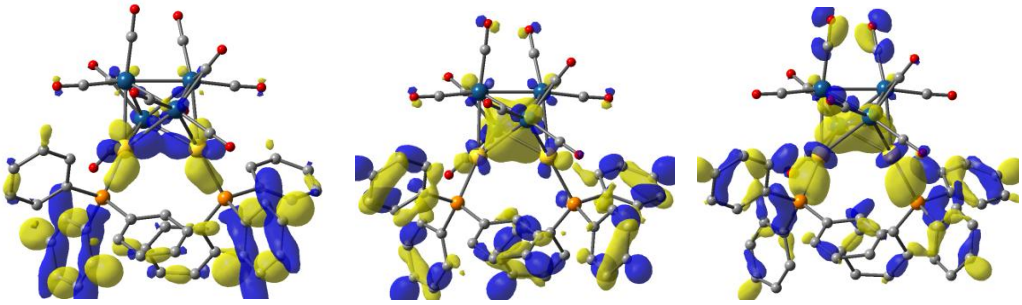

HOMO-50, -11.04 eV HOMO-54, -11.55 eV HOMO-62, -12.82 eV

**Figure 5.12.** Selected molecular orbitals, HOMO-33, HOMO-35, HOMO-37, HOMO-50, HOMO-54, HOMO-62, with calculated energies showing metal-metal bonding particularly for the Au – Au interactions in **5.2**.

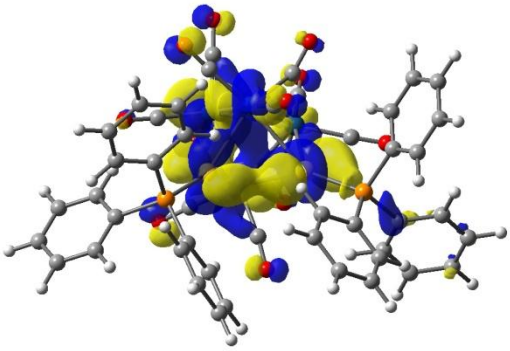

HOMO-29,-7.32 eV

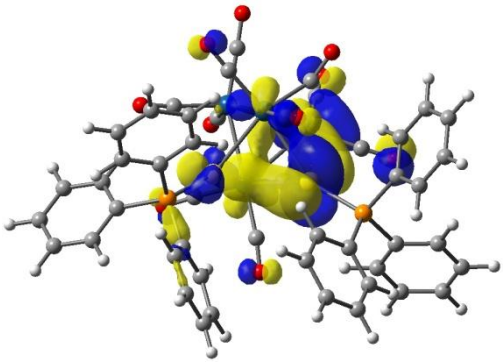

HOMO-34, -7.89 eV

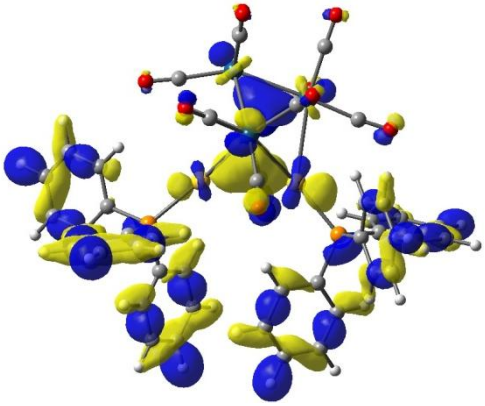

HOMO-51, -9.10 eV

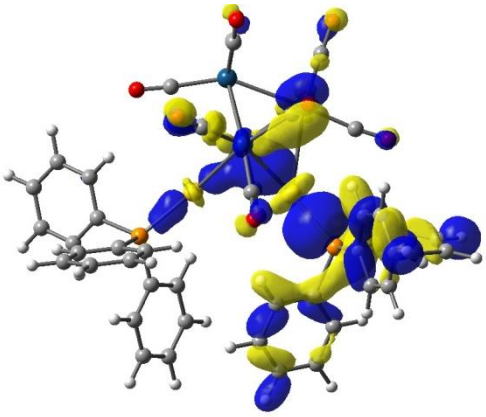

HOMO-63, -10.11 eV

**Figure 5.13.** Selected molecular orbitals HOMO-29, HOMO-34, HOMO-51 and HOMO-63 with calculated energies showing the existence of Au - Au bonding interactions in **5.3**.

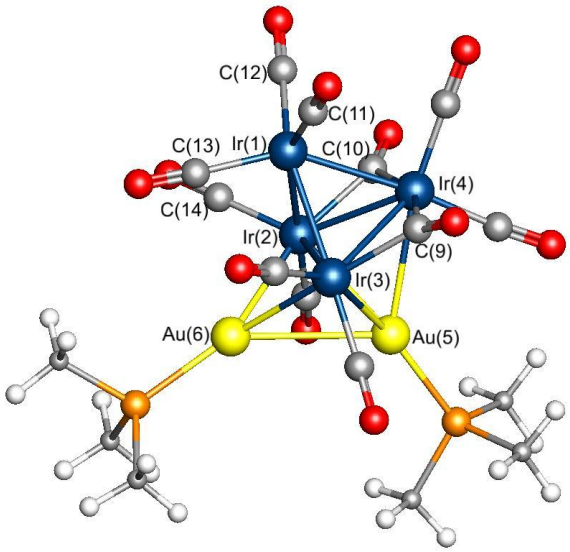


**A = 5.3***

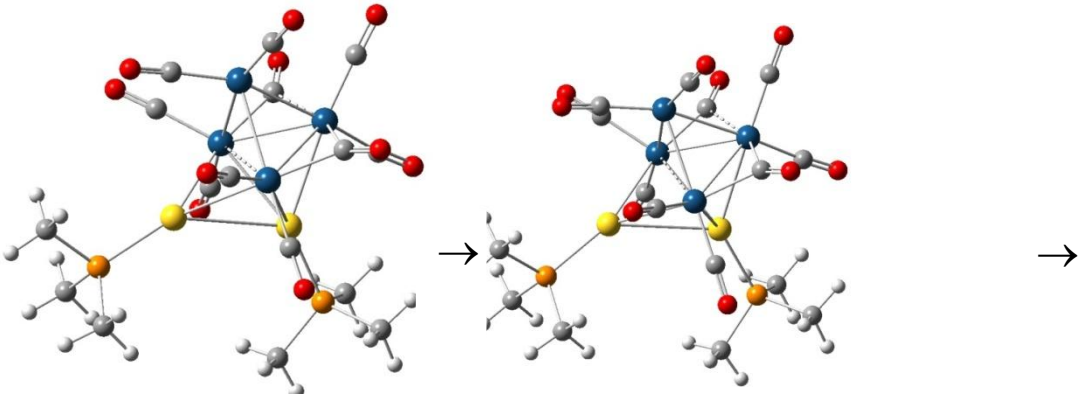

**B** **C**

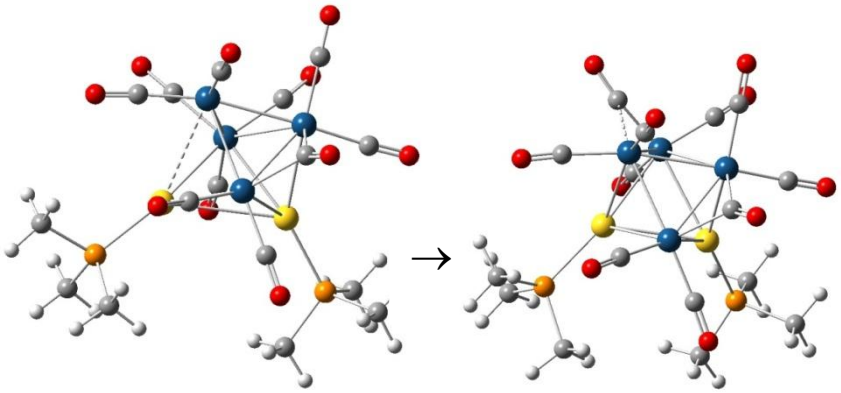

**D** **E**

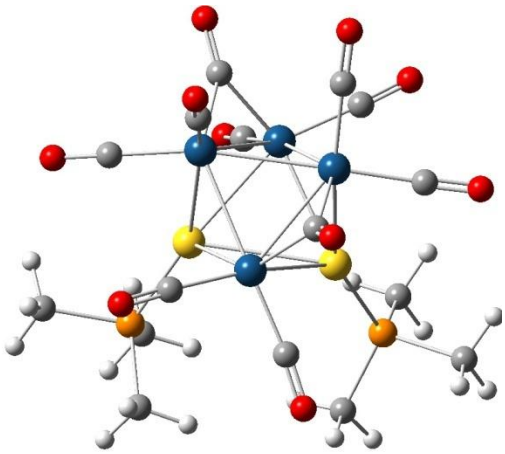

**5.2***

**Figure 5.14.** A series of structures showing the transformations B → C → D → E → **5.2*** of **5.3*** to **5.2*** upon the loss of the CO ligand C(12) on atom Ir(1). Structure **A** is **5.3*** with atom labels. Structures **B** and **C** are **5.3*** with CO ligand C(12) removed. The dashed lines in structures **B** and **C** show where bonds are being broken. The dashed lines in structures **D** and **E** show where the Ir – Au bond and the final bridging CO ligand are being formed, respectively, to yield **5.2***.

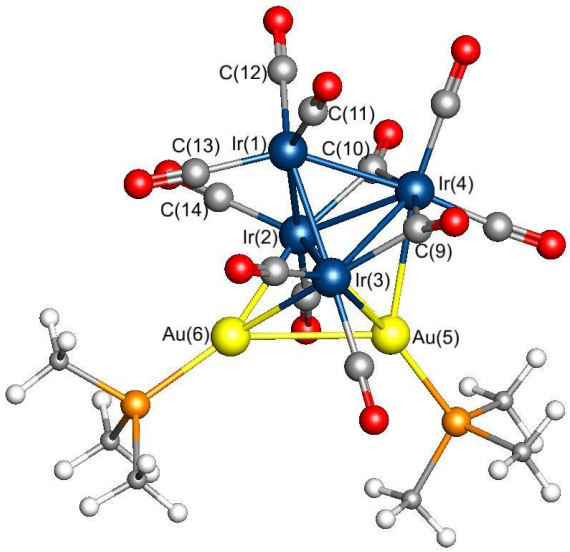


**A = 5.3***

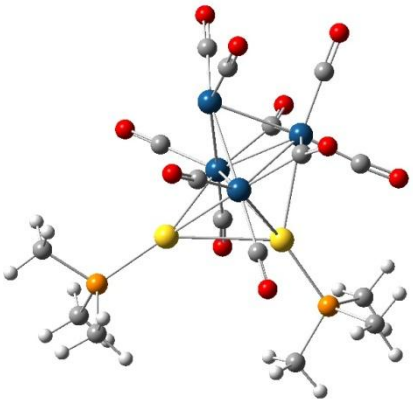

**B′**

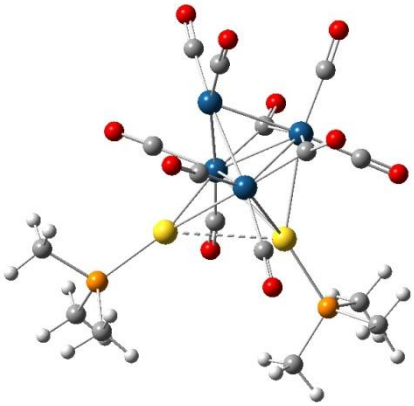

**C′**

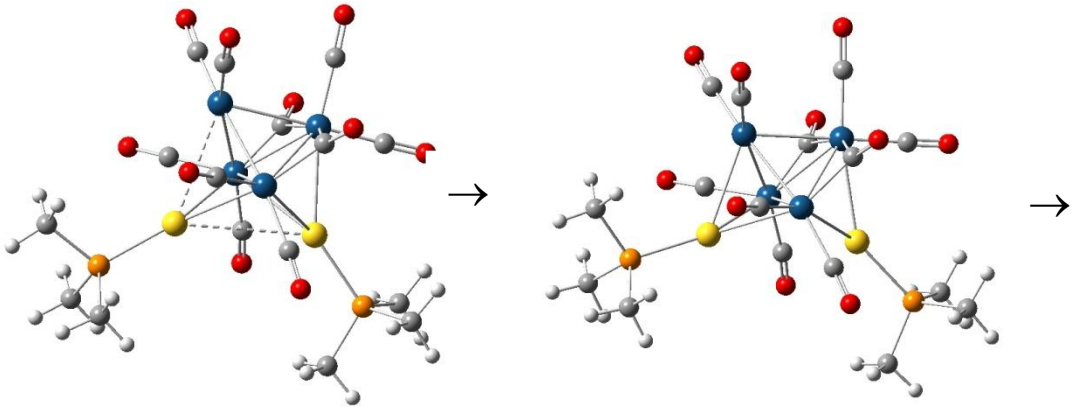

**D′** **5.2′***

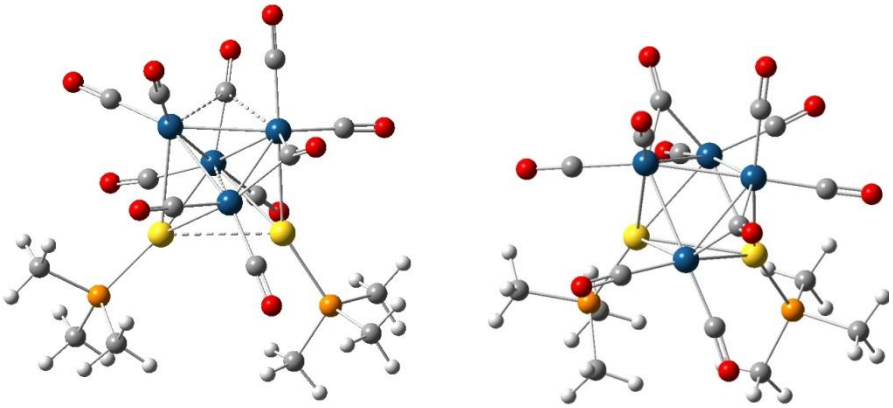

**$TS_{5.2'*,5.2*}$** **5.2***

**Figure 5.15.** A series of structures showing the transformations **B′** → **C′** → **D′** → **5.2′*** of **5.3*** to **5.2*** upon the loss of the CO ligand C(13) on atom Ir(1). Structure **A** is **5.3*** with atom labels. Structure **B′** is **5.3*** with CO ligand C(13) removed. The dashed lines in structures **C′** and **D′** show the Ir – Au bond formation and the Au – Au bond breaking. **5.2′*** is a less stable isomer of **5.2***. **$TS_{5.2'*,5.2*}$** is the transition state for the transformation between **5.2′*** and **5.2***.

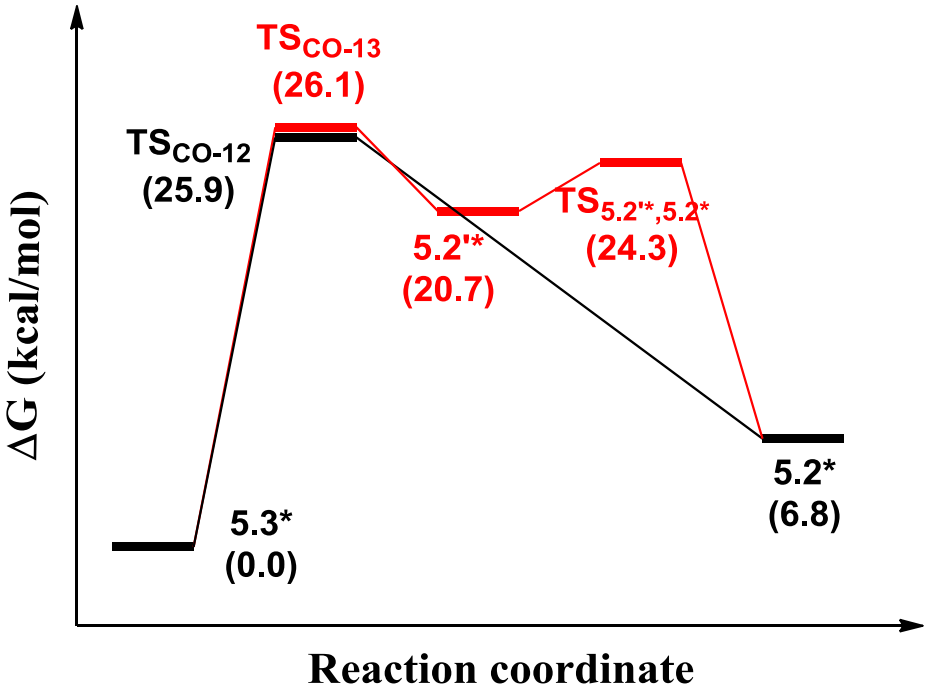


**Figure 5.16.** Calculated gas-phase free energy profile for the transformation between **5.3*** to **5.2*** through the loss of the CO ligand from Ir(1). Black corresponds to the pathway via loss of C(12). Red corresponds to the pathway via loss of C(13).

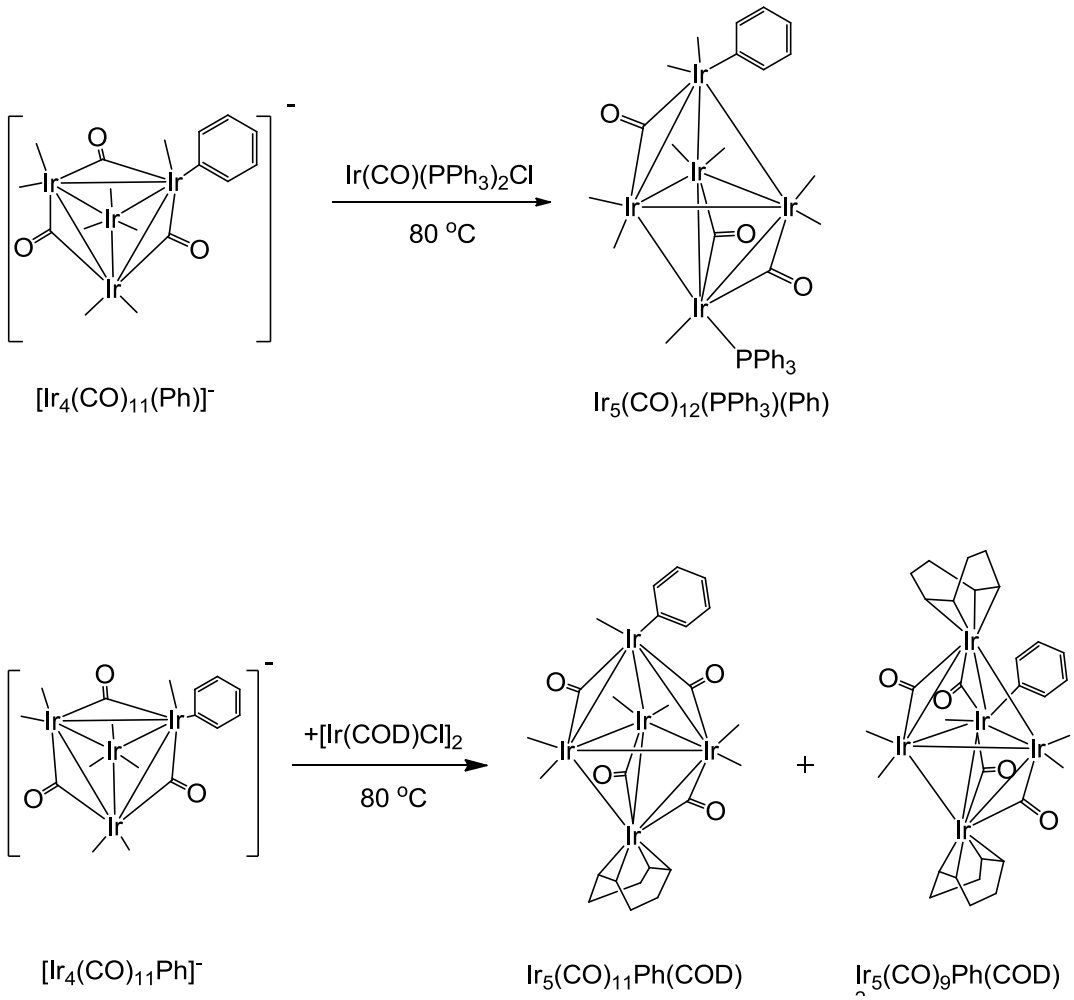


Scheme 5.1 Schematic diagram of reactions of $Ir(CO)(PPh_3)Cl$ and $[Ir(COD)Cl]_2$ to form pentairidium complexes containing σ-phenyl ligand.

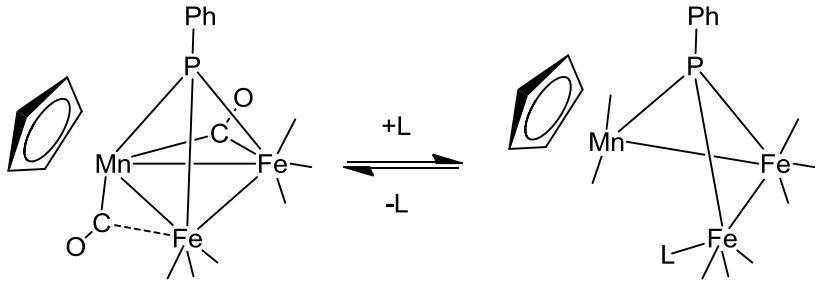


(1)

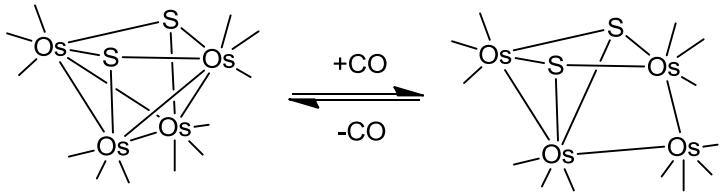


(2)

Scheme 5.2 Schematic diagrams of open structures form by addition of electron donors, such as CO or $PR_3$.

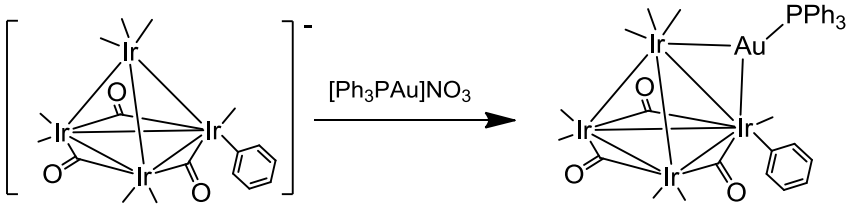


$[PhIr_4(CO)_{11}]^-$ **4.1** **5.1**

Scheme 5.3 Schematic diagrams of reaction of $[Et_4N][PhIr_4(CO)_{11}]$, 4.1 with $[Ph_3PAu]NO_3$.

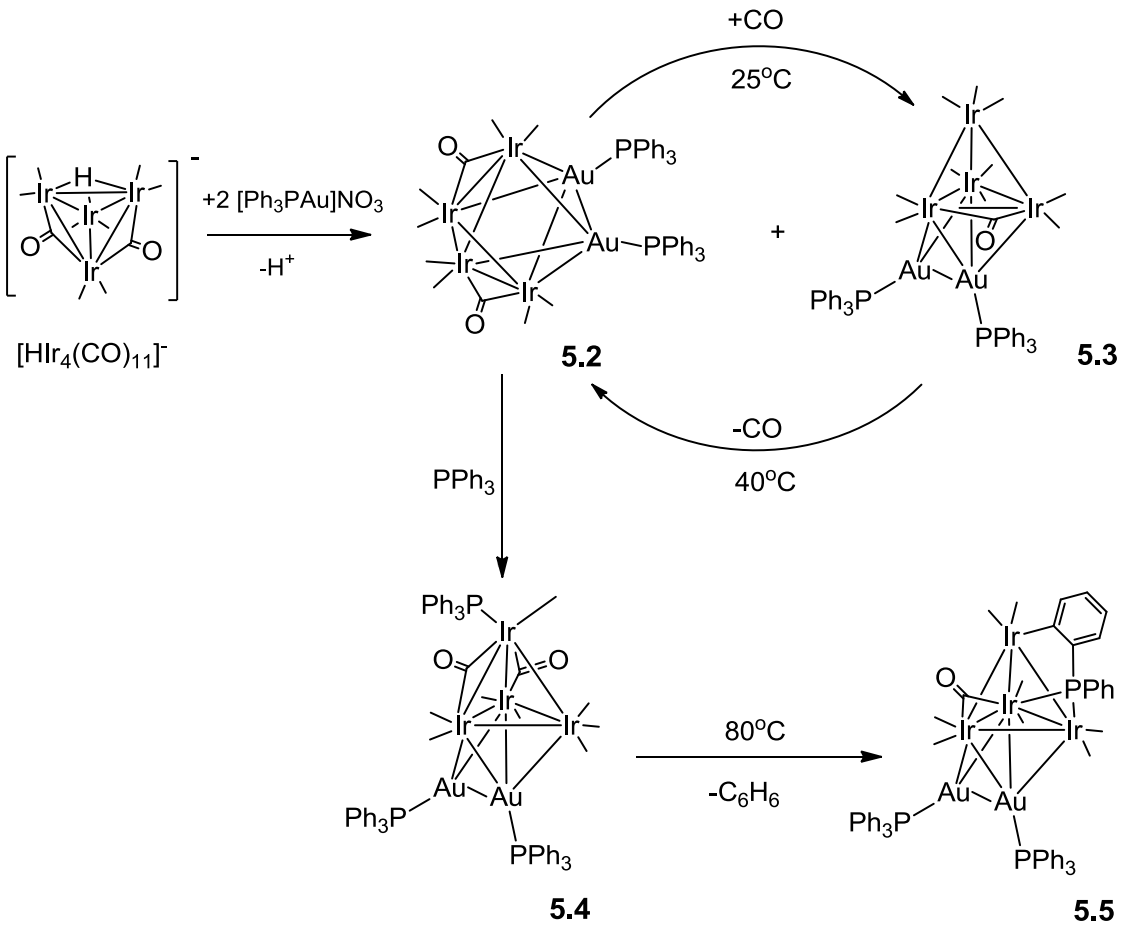


Scheme 5.4 Schematic diagram of reactions of $[HIr_4(CO)_{11}]^-$ with $[AuPPh_3][NO_3]$.

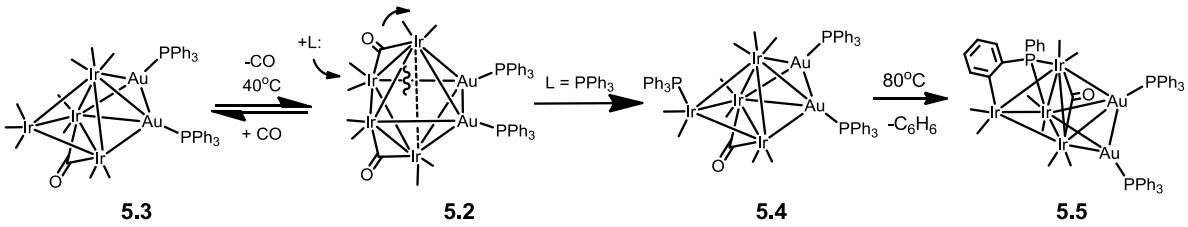


**5.3** **5.2** **5.4** **5.5**

Scheme 5.5 Schematic diagram of ligand-induced skeletal rearrangement.

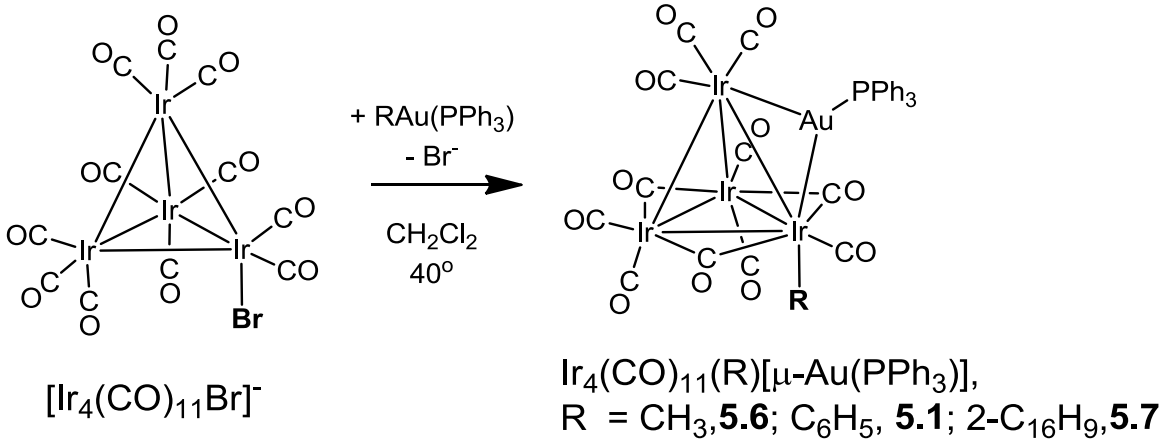


Scheme 5.6 Schematic diagram of reactions of $[Ir_4(CO)_{11}Br]^-$ with $(R)Au(PPh_3)$ (R = $C_6H_5$, $CH_3$, 1-$C_{16}H_{10}$).

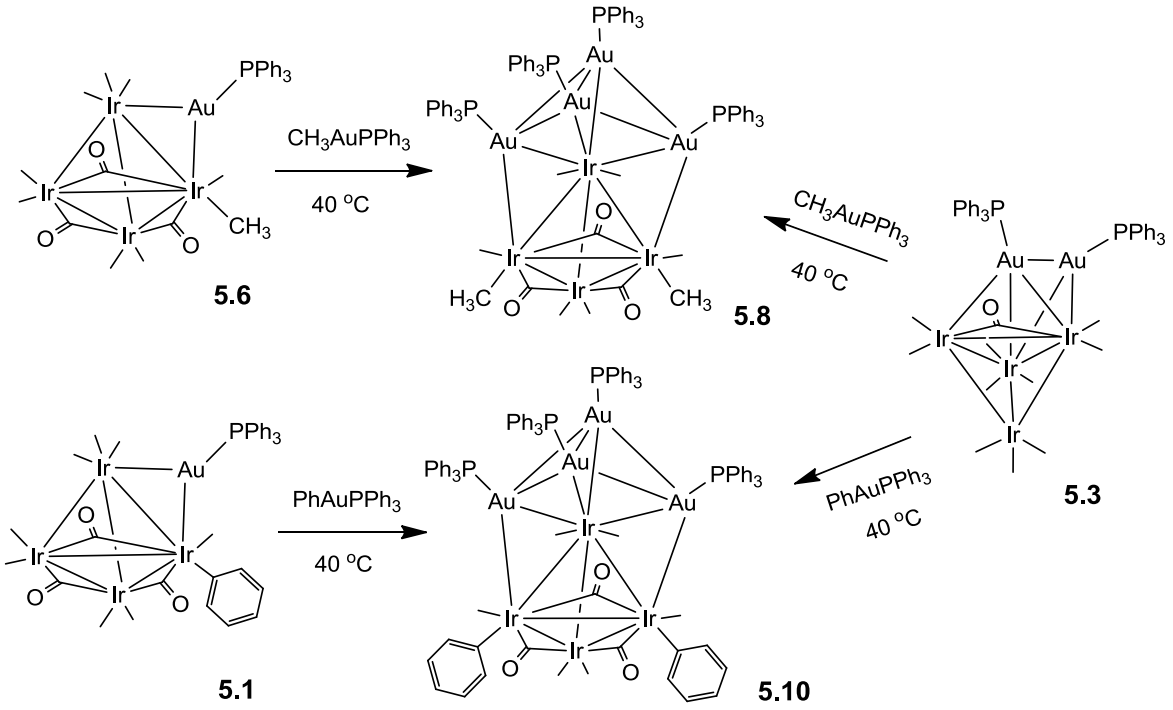


Scheme 5.7 Schematic diagram of improved synthesis of compound **5.8** and **5.10** from **5.6**, **5.3** and **5.1**.

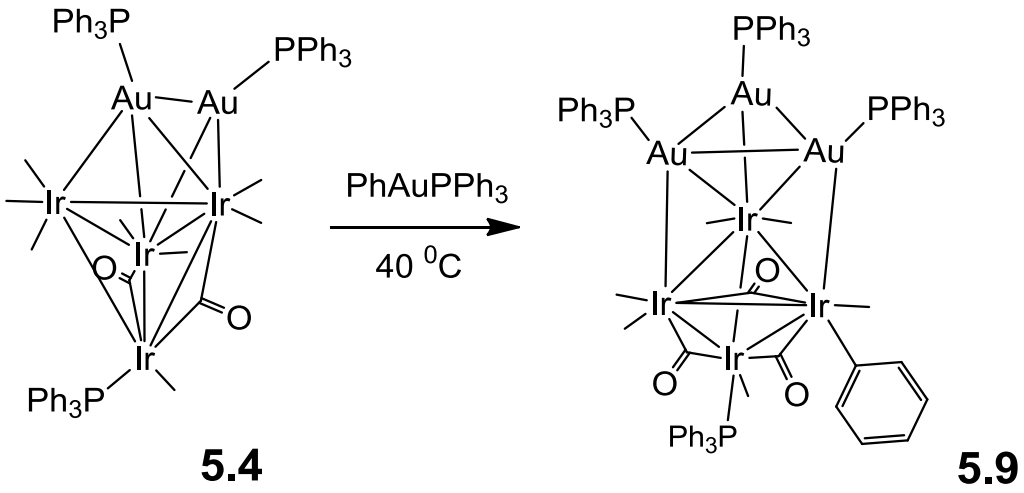


**5.4** **5.9**

Scheme 5.8 Schematic diagram of improved synthesis of compound **5.9** from **5.4**.

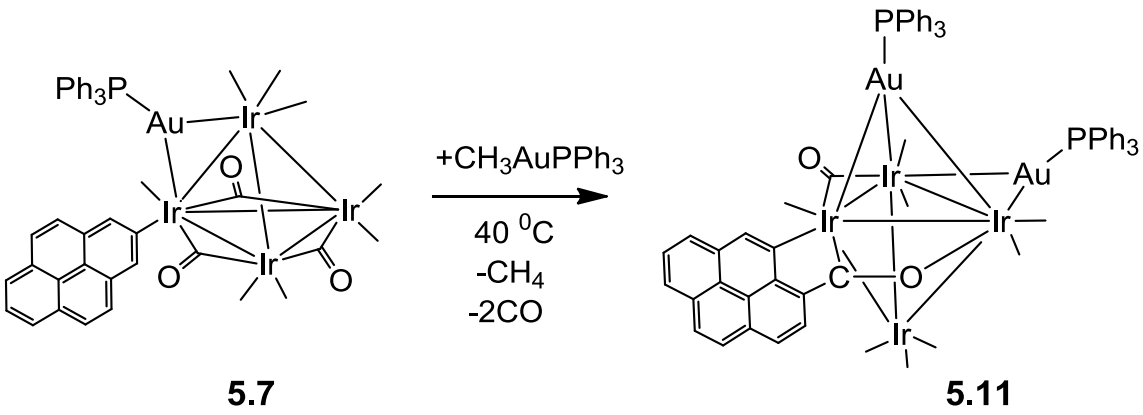


Scheme 5.9 Schematic diagram of synthesis of compound **5.11** from **5.7**.

**Table 5.1. Crystallographic Data for Compounds 5.1 - 5.11.**

| Compound | **5.1** | **5.2** | **5.3** |
|---|---|---|---|
| Empirical formula | $Ir_4AuC_{35}H_{20}O_{11}P$ | $Ir_4Au_2C_{46}H_{30}O_{10}P_2$ | $Ir_4Au_2C_{47}H_{30}O_{11}P_2$ |
| Formula weight | 1613.33 | 1967.47 | 1995.48 |
| Crystal system | Monoclinic | Triclinic | Hexagonal |
| Lattice parameters | | | |
| *a* (Å) | 13.5055(6) | 10.2250(4) | 13.3377(3) |
| *b* (Å) | 16.7314(8) | 15.1704(6) | 13.3377(3) |
| *c* (Å) | 17.2324(8) | 19.2345(7) | 48.755(2) |
| α (deg) | 90 | 94.858(1) | 90 |
| β (deg) | 97.638(1) | 102.439(1) | 90 |
| γ (deg) | 90 | 98.277(1) | 120 |
| V ($Å^3$) | 3859.4(3) | 2862.48(19) | 7511.2(4) |
| Space group | $P2_1/c$ | P-*1* | $P6_5$ |
| Z value | 4 | 2 | 6 |
| $\rho_{calc}$ (g / $cm^3$) | 2.776 | 2.464 | 2.647 |
| μ (Mo Kα) ($mm^{-1}$) | 17.628 | 14.480 | 16.546 |
| Temperature (K) | 294(2) | 294(2) | 294(2) |
| $2\Theta_{max}$ (°) | 51.36 | 56.14 | 56.02 |
| No. Obs. ( $I > 2\sigma(I)$) | 7330 | 10096 | 8761 |
| No. Parameters | 427 | 625 | 547 |
| Goodness of fit (GOF) | 1.002 | 1.081 | 1.058 |
| Max. shift in cycle | 0.001 | 0.001 | 0.001 |
| Residuals*: R1; wR2 | 0.0297; 0.0727 | 0.0613; 0.1634 | 0.0519; 0.1146 |
| Absorption Correction, | Multi-scan | Multi-scan | Multi-scan |
| Max/min | 1.000 / 0.435 | 1.000 /0.686 | 1.000 / 0.522 |
| Largest peak in Final Diff. Map ($e^-$ / $Å^3$) | 2.11 | 1.08 | 1.29 |

[a] $R = \Sigma_{hkl}(||F_{obs}| - |F_{calc}||)/\Sigma_{hkl}|F_{obs}|$; $R_w = [\Sigma_{hkl}w(|F_{obs}| - |F_{calc}|)^2/\Sigma_{hkl}wF^2_{obs}]^{1/2}$; $w = 1/\sigma^2(F_{obs})$; $GOF = [\Sigma_{hkl}w(|F_{obs}| - |F_{calc}|)^2/(n_{data} - n_{vari})]^{1/2}$.

**Table 5.1(continue). Crystallographic Data for Compounds 5.1 – 5.11.**

| Compound | **5.4** | **5.5** |
|---|---|---|
| Empirical formula | $Ir_4Au_2C_{65}H_{45}O_{11}P_3$ | $Ir_4Au_2C_{57}H_{39}O_9P_3$ |
| Formula weight | 2257.76 | 2123.63 |
| Crystal system | Monoclinic | Triclinic |
| Lattice parameters | | |
| *a* (Å) | 15.8580(8) | 13.7892(14) |
| *b* (Å) | 23.8550(13) | 13.9054(14) |
| *c* (Å) | 17.3821(9) | 17.8443(18) |
| α (deg) | 90 | 85.321(2) |
| β (deg) | 95.644(1) | 75.087(2) |
| γ (deg) | 90 | 65.024(2) |
| V ($Å^3$) | 6543.6(6) | 2995.7(5) |
| Space group | $P2_1/c$ | P-*1* |
| Z value | 4 | 2 |
| $\rho_{calc}$ ($g / cm^3$) | 2.348 | 2.397 |
| μ (Mo Kα) ($mm^{-1}$) | 12.781 | 13.863 |
| Temperature (K) | 294(2) | 294(2) |
| $2\Theta_{max}$ (°) | 56.86 | 56.48 |
| No. Obs. ( $I > 2\sigma(I)$) | 16466 | 9873 |
| No. Parameters | 735 | 688 |
| Goodness of fit (GOF) | 1.061 | 1.087 |
| Max. shift in cycle | 0.001 | 0.001 |
| Residuals*: R1; wR2 | 0.0432; 0.1065 | 0.0580; 0.1280 |
| Absorption Correction, | Multi-scan | Multi-scan |
| Max/min | 1.000 / 0.382 | 1.000 / 0.388 |
| Largest peak in Final Diff. Map ($e^- / Å^3$) | 2.71 | 2.36 |

[a] $R = \Sigma_{hkl}(\,|\,|F_{obs}|-|F_{calc}|\,|)/\Sigma_{hkl}|F_{obs}|$; $R_w = [\Sigma_{hkl}w(|F_{obs}|-|F_{calc}|)^2/\Sigma_{hkl}wF^2_{obs}]^{1/2}$; $w = 1/\sigma^2(F_{obs})$;
GOF = $[\Sigma_{hkl}w(|F_{obs}|-|F_{calc}|)^2/(n_{data} - n_{vari})]^{1/2}$.

**Table 5.1(continue). Crystallographic Data for Compounds 5.1 - 5.11.**

| Compound | **5.6** | **5.7** | **5.8** |
|---|---|---|---|
| Empirical formula | $Ir_4$ $Au_1C_{30}H_{18}O_{11}P_1$ | $Ir_4$ $Au_4C_{83}H_{66}O_9P_4$ | $Ir_4$ $Au_3C_{87}H_{65}O_9P_4$ |
| Formula weight | 1551.26 | 2888.03 | 2738.10 |
| Crystal system | Monoclinic | Monoclinic | Triclinic |
| Lattice parameters | | | |
| *a* (Å) | 16.8530(5) | 23.4673(12) | 13.1907(8) |
| *b* (Å) | 9.4850(3) | 15.1658(8) | 14.1090(8) |
| *c* (Å) | 22.4374(6) | 26.0618(13) | 25.7346(15) |
| α (deg) | 90.00 | 90.00 | 87.8110(10) |
| β (deg) | 97.1090(10) | 112.8570(10) | 79.1250(10) |
| γ (deg) | 90.00 | 90.00 | 79.8250(10) |
| V ($Å^3$) | 3559.06(18) | 8547.1(8) | 4629.4(5) |
| Space group | *P2(1)/n* | *P2(1)/c* | *P-1* |
| Z value | 4 | 4 | 2 |
| $\rho_{calc}$ (g / $cm^3$) | 2.895 | 2.305 | 2.076 |
| μ (Mo Kα) ($mm^{-1}$) | 19.109 | 13.169 | 10.585 |
| Temperature (K) | 294(2) | 294(2) | 294(2) |
| $2\Theta_{max}$ (°) | 55.64 | 46.02 | 47.30 |
| No. Obs. ( I > 2σ(I)) | 6273 | 15089 | 13079 |
| No. Parameters | 425 | 849 | 1049 |
| Goodness of fit (GOF) | 1.046 | 1.012 | 1.095 |
| Max. shift in cycle | 0.001 | 0.001 | 0.001 |
| Residuals*: R1; wR2 | 0.0306; 0.0738 | 0.0347; 0.0767 | 0.0689; 0.1304 |
| Absorption Correction, | Multi-scan | Multi-scan | Multi-scan |
| Max/min | 1.000 / 0.345682 | 1.000 / 0.706079 | 1.000 / 0.478702 |
| Largest peak in Final Diff. Map ($e^-$ / $Å^3$) | 1.03 | 1.43 | 1.87 |

[a] $R = \Sigma_{hkl}(||F_{obs}| - |F_{calc}||)/\Sigma_{hkl}|F_{obs}|$; $R_w = [\Sigma_{hkl}w(|F_{obs}| - |F_{calc}|)^2/\Sigma_{hkl}wF^2_{obs}]^{1/2}$; $w = 1/\sigma^2(F_{obs})$; $GOF = [\Sigma_{hkl}w(|F_{obs}| - |F_{calc}|)^2/(n_{data} - n_{vari})]^{1/2}$.

**Table 5.1(continue). Crystallographic Data for Compounds 5.1 - 5.11.**

| Compound | **5.9** | **5.10** | **5.11** |
|---|---|---|---|
| Empirical formula | $Ir_4\ Au_4C_{93}H_{70}O_9P_4$ | $Ir_4\ Au_1C_{45}H_{24}O_{11}P_1$ | $Ir_4Au_2C_{62}H_{38}O_{10}P_2$ |
| Formula weight | 3012.17 | 1737.47 | 2167.70 |
| Crystal system | Triclinic | Monoclinic | Monoclinic |
| Lattice parameters | | | |
| *a* (Å) | 13.8353(15) | 36.675(15) | 35.589(7) |
| *b* (Å) | 19.656(2) | 15.048(6) | 13.438(2) |
| *c* (Å) | 19.870(2) | 17.918(7) | 26.826(5) |
| α (deg) | 75.375(2) | 90.00 | 90.00 |
| β (deg) | 74.007(2) | 99.710(9) | 99.087(7) |
| γ (deg) | 75.261(2) | 90.00 | 90.00 |
| V ($Å^3$) | 4925.8(9) | 9747(7) | 12668(4) |
| Space group | *P-1* | *C2/c* | *C2/c* |
| Z value | 2 | 8 | 8 |
| $\rho_{calc}$ (g / $cm^3$) | 2.189 | 2.466 | 2.407 |
| μ (Mo Kα) ($mm^{-1}$) | 11.436 | 13.975 | 13.219 |
| Temperature (K) | 100(2) | 294(2) | 294(2) |
| $2\Theta_{max}$ (°) | 54.18 | 39.18 | 56.58 |
| No. Obs. ( I > 2σ(I)) | 17428 | 8613 | 11179 |
| No. Parameters | 1189 | 571 | 772 |
| Goodness of fit (GOF) | 1.025 | 1.080 | 1.050 |
| Max. shift in cycle | 0.001 | 0.001 | 0.001 |
| Residuals*: R1; wR2 | 0.0363; 0.0791 | 0.0581; 0.1043 | 0.0317; 0.0706 |
| Absorption Correction, | Multi-scan | Multi-scan | Multi-scan |
| Max/min | 1.000 / 0.625400 | 1.000 / 0.639576 | 1.000 / 0.410727 |
| Largest peak in Final Diff. Map ($e^-$ / $Å^3$) | 2.16 | 1.59 | 2.62 |

[a] $R = \Sigma_{hkl}(||F_{obs}| - |F_{calc}||)/\Sigma_{hkl}|F_{obs}|$; $R_w = [\Sigma_{hkl}w(|F_{obs}| - |F_{calc}|)^2/\Sigma_{hkl}wF^2_{obs}]^{1/2}$; $w = 1/\sigma^2(F_{obs})$; $GOF = [\Sigma_{hkl}w(|F_{obs}| - |F_{calc}|)^2/(n_{data} - n_{vari})]^{1/2}$.

Table 5.2 Selected intramolecular angles and bond distances for compound **5.1**.[a]

| **Distances** | | | **Angles** | | | |
|---|---|---|---|---|---|---|
| Atom | Atom | Distance (Å) | Atom | Atom | Atom | Angle(deg) |
| Ir1 | Ir2 | 2.9143(4) | Ir1 | Au1 | Ir2 | 63.476(10) |
| Ir1 | Ir3 | 2.7460(4) | C4 | Ir2 | Ir1 | 152.0(2) |
| Ir1 | Ir4 | 2.7332(4) | | | | |
| Ir2 | Ir3 | 2.7280(4) | | | | |
| Ir2 | Ir4 | 2.7420(4) | | | | |
| Ir3 | Ir4 | 2.6968(5) | | | | |
| Ir1 | Au1 | 2.7332(4) | | | | |
| Ir2 | Au1 | 2.8056(4) | | | | |
| Ir2 | C4 | 2.100(7) | | | | |
| Au1 | P1 | 2.274(2) | | | | |

[a] Estimated Standard deviations in the least significant figure are given in parentheses.

Table 5.3 Selected intramolecular angles and bond distances for compound **5.2**.[a]

| **Distances** | | | **Angles** | | | |
|---|---|---|---|---|---|---|
| Atom | Atom | Distance (Å) | Atom | Atom | Atom | Angle(deg) |
| Ir1 | Ir3 | 2.7157(10) | Ir1 | Au1 | Au2 | 57.30(2) |
| Ir1 | Ir4 | 2.7127(10) | Ir1 | Au1 | Ir2 | 84.31(3) |
| Ir2 | Ir3 | 2.7031(10) | Au2 | Au1 | Ir3 | 85.61(3) |
| Ir2 | Ir4 | 2.7217(10) | Au1 | Ir3 | Ir4 | 94.59(3) |
| Ir3 | Ir4 | 2.7676(11) | | | | |
| Ir1 | Au1 | 2.7864(10) | | | | |
| Ir2 | Au1 | 2.9031(10) | | | | |
| Ir1 | Au2 | 2.8587(10) | | | | |
| Ir2 | Au2 | 2.7876(10) | | | | |
| Au1 | Au2 | 3.1405(10) | | | | |
| Au1 | P1 | 2.319(5) | | | | |
| Au2 | P2 | 2.322(5) | | | | |
| Ir3 | Au1 | 2.7299(10) | | | | |
| Ir4 | Au2 | 2.7404(10) | | | | |

[a] Estimated Standard deviations in the least significant figure are given in parentheses.

Table 5.4 Selected intramolecular angles and bond distances for compound **5.3**.[a]

| **Distances** | | | **Angles** | | | |
|---|---|---|---|---|---|---|
| Atom | Atom | Distance (Å) | Atom | Atom | Atom | Angle(deg) |
| Ir1 | Ir2 | 2.7206(11) | Ir1 | Ir2 | Ir3 | 55.73(3) |
| Ir1 | Ir3 | 2.7416(11) | Au1 | Ir2 | Ir3 | 55.28(3) |
| Ir1 | Ir4 | 2.7107(12) | Au2 | Au1 | Ir3 | 53.57(3) |
| Ir2 | Ir3 | 3.1013(10) | | | | |
| Ir2 | Ir4 | 2.7527(12) | | | | |
| Ir3 | Ir4 | 2.8196(12) | | | | |
| Ir2 | Au1 | 2.8002(11) | | | | |
| Ir3 | Au1 | 2.7786(11) | | | | |
| Ir4 | Au1 | 2.9160(13) | | | | |
| Ir2 | Au2 | 2.7896(13) | | | | |
| Ir3 | Au2 | 2.7469(12) | | | | |
| Au1 | Au2 | 3.2464(13) | | | | |
| Au1 | P1 | 2.280(6) | | | | |
| Au2 | P2 | 2.292(5) | | | | |

[a] Estimated Standard deviations in the least significant figure are given in parentheses.

Table 5.5 Selected intramolecular angles and bond distances for compound **5.4**.[a]

| **Distances** | | | **Angles** | | | |
|---|---|---|---|---|---|---|
| Atom | Atom | Distance (Å) | Atom | Atom | Atom | Angle(deg) |
| Ir1 | Ir2 | 2.8320(5) | P3 | Ir4 | Ir2 | 172.96(6) |
| Ir1 | Ir3 | 2.8363(4) | Ir1 | Au1 | Ir2 | 59.227(11) |
| Ir1 | Ir4 | 2.7459(4) | Au1 | Au2 | Ir1 | 60.474(12) |
| Ir2 | Ir4 | 2.7471(5) | | | | |
| Ir3 | Ir4 | 2.7968(4) | | | | |
| Ir1 | Au1 | 2.8326(4) | | | | |
| Ir1 | Au2 | 2.8536(5) | | | | |
| Ir3 | Au2 | 2.8494(5) | | | | |
| Ir3 | Au1 | 2.9371(5) | | | | |
| Ir4 | P3 | 2.308(2) | | | | |
| Au1 | Au2 | 2.7695(5) | | | | |
| Au1 | P1 | 2.297(2) | | | | |
| Au2 | P2 | 2.292(5) | | | | |

[a] Estimated Standard deviations in the least significant figure are given in parentheses.

Table 5.6 Selected intramolecular angles and bond distances for compound **5.5**.[a]

| **Distances** | | | **Angles** | | | |
|---|---|---|---|---|---|---|
| Atom | Atom | Distance (Å) | Atom | Atom | Atom | Angle(deg) |
| Ir1 | Ir2 | 2.9401(10) | P3 | Ir4 | Ir2 | 51.22(10) |
| Ir1 | Ir3 | 2.7207(9) | Ir1 | Au1 | Ir2 | 64.57(2) |
| Ir1 | Ir4 | 2.8438(9) | Au1 | Au2 | Ir1 | 53.57(2) |
| Ir2 | Ir4 | 2.8556(8) | | | | |
| Ir3 | Ir4 | 2.7347(9) | | | | |
| Ir1 | Au1 | 2.7397(9) | | | | |
| Ir1 | Au2 | 2.8256(10) | | | | |
| Ir2 | Au2 | 2.7223(10) | | | | |
| Ir2 | Au1 | 2.7649(9) | | | | |
| Ir4 | Au1 | 3.0853(8) | | | | |
| Ir2 | P3 | 2.285(4) | | | | |
| Ir4 | P3 | 2.303(4) | | | | |
| Ir3 | C86 | 2.121(17) | | | | |
| Au1 | Au2 | 3.2071(10) | | | | |
| Au1 | P1 | 2.273(4) | | | | |
| Au2 | P2 | 2.290(5) | | | | |

[a] Estimated Standard deviations in the least significant figure are given in parentheses.

Table 5.7 Selected intramolecular angles and bond distances for compound **5.6**.[a]

| **Distances** | | | **Angles** | | | |
|---|---|---|---|---|---|---|
| Atom | Atom | Distance (Å) | Atom | Atom | Atom | Angle(deg) |
| Ir1 | Ir2 | 2.9158(4) | Ir1 | Au1 | Ir2 | 63.553(12) |
| Ir1 | Ir3 | 2.7411(4) | C4 | Ir2 | Ir1 | 149.6(3) |
| Ir1 | Ir4 | 2.7340(5) | | | | |
| Ir2 | Ir3 | 2.7212(5) | | | | |
| Ir2 | Ir4 | 2.7289(5) | | | | |
| Ir3 | Ir4 | 2.7126(5) | | | | |
| Ir1 | Au1 | 2.7414(5) | | | | |
| Ir2 | Au1 | 2.8056(4) | | | | |
| Ir2 | C4 | 2.7949(5) | | | | |
| Au1 | P1 | 2.286(2) | | | | |

[a] Estimated Standard deviations in the least significant figure are given in parentheses.

Table 5.8 Selected intramolecular angles and bond distances for compound **5.7**.[a]

| **Distances** | | | **Angles** | | | |
|---|---|---|---|---|---|---|
| Atom | Atom | Distance (Å) | Atom | Atom | Atom | Angle(deg) |
| Ir1 | Ir2 | 2.9129(12) | Ir1 | Au1 | Ir2 | 63.30(3) |
| Ir1 | Ir3 | 2.7248(13) | C43 | Ir1 | Ir3 | 95.0(4) |
| Ir1 | Ir4 | 2.7502(11) | | | | |
| Ir2 | Ir3 | 2.7379(12) | | | | |
| Ir2 | Ir4 | 2.7233(14) | | | | |
| Ir3 | Ir4 | 2.7064(11) | | | | |
| Ir1 | Au1 | 2.7944(12) | | | | |
| Ir2 | Au1 | 2.7564(13) | | | | |
| Ir1 | C43 | 2.083(16) | | | | |
| Au1 | P1 | 2.283(4) | | | | |

[a] Estimated Standard deviations in the least significant figure are given in parentheses.

Table 5.9 Selected intramolecular angles and bond distances for compound **5.8**.[a]

| **Distances** | | | **Angles** | | | |
|---|---|---|---|---|---|---|
| Atom | Atom | Distance (Å) | Atom | Atom | Atom | Angle(deg) |
| Ir1 | Ir2 | 2.9991(5) | Ir2 | Ir1 | Ir3 | 62.890(12) |
| Ir2 | Ir3 | 3.0038(5) | Ir1 | Au4 | Au2 | 67.811(13) |
| Ir2 | Ir4 | 2.7447(5) | C4 | Ir1 | Ir3 | 99.2(3) |
| Ir1 | C4 | 2.132(9) | Au1 | Ir2 | Au2 | 62.191(13) |
| Ir3 | C5 | 2.133(9) | | | | |
| Ir1 | Au2 | 3.2905(5) | | | | |
| Ir1 | Au4 | 3.0758(5) | | | | |
| Ir2 | Au1 | 2.7223(5) | | | | |
| Ir2 | Au3 | 2.6978(5) | | | | |
| Ir3 | Au1 | 3.0176(5) | | | | |
| Ir3 | Au2 | 3.2503(5) | | | | |
| Au1 | Au3 | 3.1032(5) | | | | |
| Au2 | Au3 | 2.8560(5) | | | | |
| Au3 | Au4 | 3.0738(5) | | | | |
| Au2 | Au4 | 2.8096(5) | | | | |
| Au1 | P1 | 2.291(2) | | | | |

[a] Estimated Standard deviations in the least significant figure are given in parentheses.

Table 5.10 Selected intramolecular angles and bond distances for compound **5.9**.[a]

| **Distances** | | | **Angles** | | | |
|---|---|---|---|---|---|---|
| Atom | Atom | Distance (Å) | Atom | Atom | Atom | Angle(deg) |
| Ir1 | Ir2 | 2.7814(11) | C4 | Ir3 | Ir1 | 157.1(6) |
| Ir1 | Ir3 | 2.8962(11) | P4 | Ir4 | Ir1 | 177.21(15) |
| Ir1 | Ir4 | 2.7479(11) | Au1 | Ir1 | Au2 | 62.08(3) |
| Ir2 | Ir3 | 2.7295(12) | Au1 | Au2 | Au3 | 63.76(3) |
| Ir2 | Ir4 | 2.7851(11) | | | | |
| Ir3 | C4 | 2.09(2) | | | | |
| Ir1 | Au1 | 2.6831(10) | | | | |
| Ir2 | Au1 | 3.0157(12) | | | | |
| Ir3 | Au3 | 2.9639(11) | | | | |
| Au1 | Au2 | 2.7865(11) | | | | |
| Au1 | Au3 | 2.9888(11) | | | | |
| Au2 | Au3 | 2.8713(11) | | | | |
| Ir4 | P4 | 2.320(5) | | | | |
| Au1 | P1 | 2.285(5) | | | | |

[a] Estimated Standard deviations in the least significant figure are given in parentheses.

Table 5.11 Selected intramolecular angles and bond distances for compound **5.10**.[a]

| **Distances** | | | **Angles** | | | |
|---|---|---|---|---|---|---|
| Atom | Atom | Distance (Å) | Atom | Atom | Atom | Angle(deg) |
| Ir1 | Ir2 | 3.0192(6) | Ir2 | Ir1 | Ir3 | 54.652(13) |
| Ir1 | Ir3 | 3.0054(6) | Ir2 | Au1 | Au2 | 110.385(16) |
| Ir1 | Ir4 | 2.7402(6) | C4 | Ir2 | Ir4 | 93.7(3) |
| Ir2 | Ir4 | 2.6944(6) | Au1 | Ir1 | Au2 | 72.110(15) |
| Ir2 | C4 | 2.109(9) | | | | |
| Ir3 | C13 | 2.102(9) | | | | |
| Ir1 | Au2 | 2.6781(6) | | | | |
| Ir1 | Au4 | 2.7144(5) | | | | |
| Ir2 | Au1 | 3.0497(6) | | | | |
| Ir3 | Au4 | 3.1012(6) | | | | |
| Au1 | Au2 | 3.1826(6) | | | | |
| Au1 | Au3 | 2.7815(5) | | | | |
| Au2 | Au3 | 2.8727(6) | | | | |
| Au3 | Au4 | 2.8090(6) | | | | |
| Au2 | Au4 | 3.0273(6) | | | | |
| Au1 | P1 | 2.289(3) | | | | |

[a] Estimated Standard deviations in the least significant figure are given in parentheses.

Table 5.12 Selected intramolecular angles and bond distances for compound **5.11**.[a]

| **Distances** | | | **Angles** | | | |
|---|---|---|---|---|---|---|
| Atom | Atom | Distance (Å) | Atom | Atom | Atom | Angle(deg) |
| Ir1 | Ir2 | 2.7357(7) | C1 | Ir4 | C43 | 80.5(3) |
| Ir1 | Ir3 | 2.7073(6) | Au1 | Ir4 | Ir2 | 58.124(12) |
| Ir1 | Ir4 | 2.7244(6) | Ir2 | Au2 | Ir3 | 65.517(15) |
| Ir2 | Ir3 | 2.9898(5) | Ir2 | Au1 | Ir3 | 63.600(13) |
| Ir2 | Ir4 | 2.8368(6) | | | | |
| Ir4 | C1 | 2.005(8) | | | | |
| Ir4 | C43 | 2.102(8) | | | | |
| Ir2 | Au1 | 2.7564(5) | | | | |
| Ir2 | Au2 | 2.6282(8) | | | | |
| Ir2 | O1 | 2.340(5) | | | | |
| Ir3 | Au1 | 2.9117(7) | | | | |
| Ir3 | Au2 | 2.8829(10) | | | | |
| Ir4 | Au1 | 2.8377(6) | | | | |
| Au1 | Au2 | 3.501(1) | | | | |
| Ir1 | P1 | 2.287(2) | | | | |
| Au2 | P2 | 2.280(2) | | | | |

[a] Estimated Standard deviations in the least significant figure are given in parentheses.

## References


1. (a) Crabtree, R. H. *Topics Organomet. Chem.* **2011**, *34*, 1-10. (b) Montserrat, D.; Oscar, P.; Claver, C. *Topics Organomet. Chem.* **2011**, *34*, 11-29. (c) Woodmansee, D. H.; Pfaltz, A. *Topics Organomet. Chem.* **2011**, *34*, 31-76. (d) Choi, J.; Goldman, A. S. *Topics Organomet. Chem.* **2011**, *34*, 139-167. (e) Hartwig, J. F.; Pouy, M. J. *Topics Organomet. Chem.* **2011**, *34*, 169-208. (f) Choi, J.; MacArthur, A. H. R.; Brookhart, M.; Goldman, A. S. *Chem. Rev.* **2011**, *111*, 1761 – 1779.

2. (a) Jensen, C. M. *Chem. Commun.* **1999**, 2443 – 2449. (b) César, V.; Bellemin-Laponnaz, S.; Gade, L. H. *Chem. Soc. Rev.* **2004**, *33*, 619 – 636. (c) Lu, S.-M.; Han, X.-W.; Zhou, Y.-G. *Adv. Synth. Catal.* **2004**, *346*, 909 – 912. (d) Matthias, W.; Haenel, M. W.; Oevers, S.; Angermund, K.; Kaska, W. C.; Fan, H.-J.; Hall, M. B. *Angew. Chem. int. Ed.* **2001**, *40*, 3596 – 3600. (e) Jones, J. H. *Platinum Metals Rev.* **2000**, *44*, 94 – 105. (f) Church, T. L.; Andersson, P. G. *Coord. Chem. Rev.* **2008**, *252*, 513 – 531. (g) Hartwig, J. F.; Stanley, L. M. *Acc. Chem Res.* **2010**, *43*, 1461 – 1475. (h) Iwai, T.; Fujihara, T.; Terao, J.; Tsuji, Y. *J. Am. Chem. Soc.* **2012**, *134*, 1268 – 1274. (i) Perry, M. C.; Cui, X. H.; Powell, M. T.; Hou, D. R.; Reibenspies, J. H.; Burgess, K. *J. Am. Chem. Soc.* **2003**, *125*, 113 – 123. (j) Tanaka, R.; Yamashita, M.; Nozaki, K**.** *J. Am. Chem. Soc.* **2009**, *131*, 14168 - 14169. (k) Yang, X. *ACS Catal.* **2011,** *8*, 849 - 854.

3. (a) Lu, J.; Pedro Serna, P.; Aydin, C.; Browning, N. D.; Gates, B. C. *J. Am. Chem. Soc.* **2011**, *133*, 16186 – 16195**.** (b) Gates, B. C., *Chem. Rev.* **1995**, *95*, 511 – 522. (c) Bayram, E.; Zahmakiran, M.; Ozkar S.; Finke, R. G. *Langmuir*, **2010**, *26*, 12455 – 12464. (d) Uzun, A.; Dixon, D. A.; Gates, B. C. *ChemCatChem* **2011**, *3*, 95 – 107. (e) Fonseca, G. S.; Umpierre, A.P.; Fichtner, P. F. P.; Teixeira, S. R.; Dupont, J. *Chem. Eur. J.* **2003**, *9*, 3263 – 3269. (f) Gates, B. C. in *Catalysis by Di- and Polynuclear Metal Complexes*, Adams, R. D. and Cotton, F. A. Eds., Wiley-VCH Publishers, New York, 1998, Ch. 14.

4. Sinfelt J. H. *Bimetallic Catalysts: Discoveries, Concepts, and Applications;* John Wiley & Sons, New York, 1983.

5. Psaro, R.; Dossi, C.; Della Pergola, R.; Garlaschelli, L.; Calmotti, S.; Marngo, S.; Bellatreccia, M.; Zanoni, R., *Appl. Catal. A: Gen.* **1995**, *121*, L19-L23.

6. (a) Haruta, M. *Catal. Today* **1997**, *36*, 153 – 166. (b) Haruta, M.; Date, M. *Appl. Catal. A: Gen.* **2001**, *222*, 427 – 437. (c) Hashmi, A. S. K.; Hutchings, G. J. *Angew. Chem. int. Ed.* **2006**, *45*, 7896 – 7936. (d) Della Pina, C.; Falletta, E.; Prati, L.; Rossi, M. *Chem. Soc. Rev.* **2008**, *37*, 2077 – 2095.

7. (a) Hutchings, G. J. *Chem. Commun.* **2008**, 1148 – 1164. (b) Lopez-Sanchez, J. A.; Dimitratos, N.; Glanvilla, N,; Kesavan, L.; Hammond, C.; Edwards, J. K.; Carley, A. F.; Kiely, C. J.; Hutchings, G. J. *Catal. Today* **2011**, *391*, *400 – 406.* (c) Enache, D. I.; Edwards, J. K.; Landon, P.; Solsona-Espriu, B.; Carley, A. F.; Herzing, A. A.; Watanabe, M.; Kiely, C. J.; Knight, D. W.; Hutchings, G. J. *Science* **2006**, *311*, 362 –

365. (d) Ortiz-Soto, L. B.; Alexeev, O. S.; Amiridis, M. D. *Langmuir* **2006,** *22*, 3112-3117. (e) Evans, J.; Gao, J. *J. Chem. Soc., Chem. Commun.* **1985**, 39 - 40. (f) Li, Y.; Pan, W.-X.; Wong, W.-T. *J. Cluster Sci*. **2002**, *13*, 223 – 233.

8. a) Ceriotti, A.; Della Pergola, R.; Garlaschelli, L.; Manassero, M.; Masciocchi, N. *Organometallics* **1995**, *14*, 186 – 193. b) Della Pergola, R.; Demartin, F.; Garlaschelli, L.; Manassero, M.; Martinengo, S.; Masciocchi, N.; Sansoni, M. *Organometallics* **1991**, *10*, 2239 – 2247.

9. a) Nicholls, J. N.; Raithby, P. R.; Vargas, M. D. *J. Chem. Soc., Chem. Commun.* **1986**, 1617 – 1619. b) Braga, D.; Grepioni, F.; Livotto, F. S.; Vargas, M. D. *J. Organomet. Chem.* **1990**, *391*, C28 – C32. c) Livotto, F. S.; Vargas, M. D.; Braga, D.; Grepioni, F.; *J. Chem. Soc. Dalton Trans.* **1992**, 577 – 584. Comstock, M. C.; Prussak-Wieckowska, T.; Wilson, S. R.; Shapley, J. R. *Organometallics* **1997**, *16*, 4033 – 4040.

10. Sabater, S.; Mata, J. A.; Peris, E. *Chem. Eur. J.* **2012**, *18*, 6380 – 6385.

11. a) Adams, R. D.; Chen, M. *Organometallics*, **2011**, *30*, 5867 - 5872. b) Adams, R. D.; Chen, M. *Organometallics*, **2012**, *31*, 445 - 450.

12. Huttner, G.; Schneider, J.; Muller, H. D.; Mohr, G.; Seyerl, J. V.; Wohlfahrt, L. *Angew. Chem. int. Ed.* **1979**, *18*, 76 - 77.

13. Adams, R. D.; Yang, L. W. *J. Am. Chem. Soc.* **1983**, *105*, 235 – 240.

14. (a) Ros, R.; Tassan, A.; Rosario Scopelliti, R.; Roulet, R. *Inorg. Chim. Acta* **2005**, *358*, 2327 – 2331. (b) Ros, R.; Scrivanti, A.; Albano, V. G.; Braga, D.; Garlaschelli, L. *J. Chem. Soc., Dalton Trans.*, **1986**, 2411 - 2421. (c) Ros, R.; Canziani, F.; Roulet, R. *J. Organomet. Chem.*, **1984**, *267*, C9 – C12. (d) Ros, R.; Scrivanti, A.; Roulet, R. *J. Organomet. Chem.*, **1986**, *303*, 273 – 282. (e) Nicholls, J. N.; Raithby, P. R.; Vargas, M. D. *J. Chem. Soc., Chem. Commun.*, **1986**, 1617 – 1619. (f) Albano, V. G.; Braga, D.; Ros, R.; Scrivanti, A. *J. Chem. Soc., Chem. Commun.*, **1985**, 866 - 868.

15. L. Malatesta, L. Naldini, G. Simonetta and F. Cariati, *Coord. Chem. Rev.* **1966**, 1, 255-262.

16. Partyka, D. V.; Zeller, M.; Hunter, A. D.; Gray, T. G. *Angew. Chemie*, **2006**, *45(48)*, 8188-8191.

17. Heng, W. Y.; Hu, J.; Yip, J. H. *Organometallics*, **2007**, *26*, 6760-6768.

18. (a) Angoletta, M.; Malatesta, L.; Caglio, G. *J. Organomet. Chem.* **1975**, *94*, 99 – 106. (b) Bau, R.; Chiang, M. Y.; Wei, C.-Y.; Garlaschelli, L.; Martinengo, S.; Koetzle, T. F. *Inorg. Chem.* **1984**, *23*, 4758 – 4762.

19. Chini, P.; Ciani, G.; Garlaschelli, L.; Manassero, M.; Martinengo, S.; Sironi, A.; Canziani, F. *J. Organomet. Chem.*, **1978**, *152*, C35-C38.

20. SAINT+, version 6.2a, Bruker Analytical X-ray Systems, Inc., Madison, WI, 2001.

21. G. M. Sheldrick, SHELXTL, version 6.1, Bruker Analytical X-ray Systems, Inc., Madison, WI, 1997.

22. Gaussian 09, Revision B.01, suite of programs for *ab initio* calculation; Frisch, M. J.; Trucks, G. W.; Schlegel, H. B.; Scuseria, G. E.; Robb, M. A.; Cheeseman, J. R.; Scalmani, G.; Barone, V.; Mennucci, B.; Petersson, G. A.; Nakatsuji, H.; Caricato, M.; Li, X.; Hratchian, H. P.; Izmaylov, A. F.; Bloino, J.; Zheng, G.; Sonnenberg, J. L.; Hada, M.; Ehara, M.; Toyota, K.; Fukuda, R.; Hasegawa, J.; Ishida, M.; Nakajima, T.; Honda, Y.; Kitao, O.; Nakai, H.; Vreven, T.; Montgomery, Jr., J. A.; Peralta, J. E.; Ogliaro, F.; Bearpark, M.; Heyd, J. J.; Brothers, E.; Kudin, K. N.; Staroverov, V. N.; Kobayashi, R.; Normand, J.; Raghavachari, K.; Rendell, A.; Burant, J. C.; Iyengar, S. S.; Tomasi, J.; Cossi, M.; Rega, N.; Millam, N. J.; Klene, M.; Knox, J. E.; Cross, J. B.; Bakken, V.; Adamo, C.; Jaramillo, J.; Gomperts, R.; Stratmann, R. E.; Yazyev, O.; Austin, A. J.; Cammi, R.; Pomelli, C.; Ochterski, J. W.; Martin, R. L.; Morokuma, K.; Zakrzewski, V. G.; Voth, G. A.; Salvador, P.; Dannenberg, J. J.; Dapprich, S.; Daniels, A. D.; Farkas, Ö.; Foresman, J. B.; Ortiz, J. V.; Cioslowski, J.; Fox, D. J. *Gaussian, Inc*., Wallingford CT, 2010.

23. Tao, J. M.; Perdew, J. P.; Staroverov, V. N.; Scuseria, G. E. *Phys. Rev. Lett.*, **2003**, ***91***, 146401.

24. Peterson, K. A.; Figgen, D.; Dolg, M.; Stoll, H. *J. Chem. Phys.* **2007**, *126*, 124101.

25. Bellon, P.; Manassero, M.; Sansoni, M. *J. Chem. Soc., Dalton Trans.* **1973**, 2423 – 2427.

26. Gabbai, F. P.; Schier, A.; Reide, J., Schmidbaur, H. *Chem. Ber./Recueil* **1997**, *130*, 111-113.

27. Hay, C. M.; Johnson, B. F. G.; Lewis, J.; McQueen, R. C. S.; Raithby, P. R.; Sorrell, R. M.; Taylor, M. J. *Organometallics* **1985**, *4*, 202 – 205.

28. (a) Salter, I. D. in *Metal Clusters in Chemistry*, Braunstein, P.; Oro, L. A.; Raithby, P. R., Eds., Wiley-VCH, Weinheim, Ch. 1.27, pp 509 – 534. (b) Freeman, M. J.; Orpen, A. G.; Salter, I. D. *J. Chem. Soc., Dalton Trans.* **1987**, 379 – 390. (c) Orpen, A. G.; Salter, I. D. *Organometallics* **1991**, *10*, 111 – 117.

29. Wade, K. in *Transition Metal Clusters*, Johnson, B. F. G., Ed.; Wiley, New York, 1980, Ch. 3.

30. Harding, M. M.; Nicholls, B. S.; Smith, A. K., *J. Chem. Soc., Dalton Trans.* **1983**, 1479-1481.

31. Pereira, R.M.S.; Fujiwara, F.Y.; Vargas, M. D. *Organometallics* **1997**, *16*, 4833-4838.

32. Heng, W. Y.; Hu, J.; Yip, J. H. *Organometallics*, **2007**, *26*, 6760-6768.

33. Adams, R. D.; Rassolov, V.; Zhang, Q. *Organometallics* **2012**, *31*, 2961 - 2964.

34. Li, Y.; Wong, W. T. *Eur. J. Inorg. Chem.* **2003**, 2651 - 2662.

35. Al-Mandhary, M. R. A.; Lewis, J.; Raithby, P. R. *J. Organomet. Chem.* **1997**, *536-537*, 549 – 551.

# CHAPTER SIX

# Semibridging Phenyl Ligands in Iridium-Copper and -Silver Cluster Compounds: Synthesis, Structures and Bonding

## Introduction

$\eta^1$-bridging aryl ligands **A** are commonly found in polynuclear metal complexes of the coinage metals: Cu, Ag and Au.[1] Aryl copper compounds have been used for a variety of carbon – carbon bond forming cross-coupling reactions.[1a] There are relatively few examples of $\eta^1$-bridging aryl ligands in polynuclear transition metal carbonyl complexes.[2] In most cases, $\eta^1$-bridging aryl ligands bridge two similar metal atoms in a symmetrical fashion and the plane of the ring is approximately perpendicular to the metal – metal bond vector, **A**.[1,2] Although they are much less common, $\eta^1$-aryl ligands bridging heteronuclear pairs of metal atoms are often coordinated asymmetrically, **B**.[1a,3] In these unsymmetrical cases, the plane of the aryl ring is usually not perpendicular to the M – M' bond vector. In analogy to the well known semibridging behavior of carbonyl ligands,[4] we will, hereafter, refer to these asymmetrical bridging phenyl ligands as *semibridging* ligands. Viewed without a charge all $\eta^1$-bridging aryl ligands serve as one-electron donors. $\eta^2$-bridging aryl ligands **C** are also known. These ligands are generally regarded as three-electron donors,[5] and there are still other examples having more extensive interactions of the ring $\pi$-electrons with neighboring metal atoms.[6]

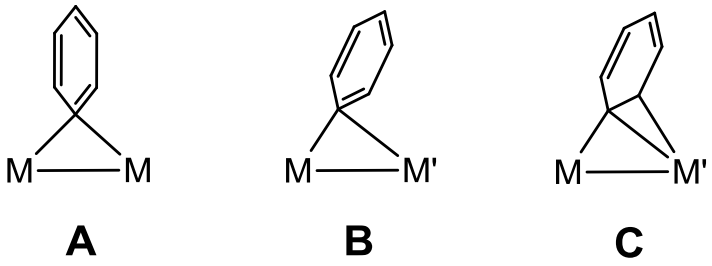


We have recently prepared the tetrairidium anion $[Ir_4(CO)_{11}(Ph)]^-$, **4.1** that contains a terminally coordinated $\eta^1$-σ-phenyl ligand by a trans-metalation reaction between $[Ir_4(CO)_{11}Br]^-$ and $SnPh_3(OH)$ or $SnPh_4$, eq. 4.5.[7] This anion **4.1** was found to react with $Ir(CO)(PPh_3)_2Cl$ to yield higher nuclearity iridium cluster complexes[8] and with $[Au(PPh_3)][NO_3]$ and to yield the gold-tetrairidium complex $Ir_4(CO)_{11}(Ph)(\mu\text{-}AuPPh_3)$ that contains a terminally coordinated σ-phenyl ligand, see Scheme 5.3 (the terminally coordinated CO ligands are indicated only by lines to the Ir atoms in our Scheme).[9,10]

Iridium is well known for its ability to produce highly active homogeneous[11] and heterogeneous[12] catalysts. Recently, gold nanoparticles have been shown to exhibit significant activity for the catalytic oxidation of CO and for the oxidation and transformations of unsaturated hydrocarbons.[13] Certain bimetallic catalysts composed of gold and selected transition metals have been shown to exhibit even higher activity than pure gold for alcohol and hydrocarbon oxidations and for the synthesis of hydrogen peroxide.[14] A recent report shows that an Ir(III)-Au(I) complex exhibits better catalytic activity for the transfer hydrogenation of nitrobenzene than the corresponding pure iridium and pure gold complexes.[15]

Interest in heterometallic transition metal cluster complexes containing copper, silver and gold continues to grow.[16] Nanocrystalline forms of copper and silver have been

used at catalysts for the selective oxidation of alcohols.[17] We have now investigated the reactions of anion **4.1** with $[Cu(NCMe)_4][BF_4]$ and $Ag[NO_3]$ and have obtained the tetrairidium-copper complex $Ir_4(CO)_{11}(\mu\text{-}\eta^1\text{-}Ph)[\mu_3\text{-}Cu(NCMe)]$, **6.2**, and a series of iridium-silver complexes: $[Et_4N][Ir_4(CO)_{11}Ph]_2(\mu_4\text{-}Ag)$, **6.3**, $[Ir_4(CO)_{11}]_2(\mu_4\text{-}Ag)(\mu\text{-}Ag)(\mu_3\text{-}Ph)(\mu\text{-}Ph)$, **6.4**, $Ir_4(CO)_{11}(\eta^1\text{-}Ph)[\mu_3\text{-}Ag(NCMe)]$, **6.5** and $Ir_4(CO)_{11}((\mu\text{-}\eta^1\text{-}Ph)[\mu_3\text{-}Ag(PPh_3)]$, **6.6**. Complexes **6.2**, **6.4** and **6.6** contain unusual σ-π-coordinated, semibridging $\eta^1$-phenyl ligands. Two of them, **6.3** and **6.4**, contain two tetrairidium clusters linked by bridging silver atoms. The bonding of the σ-π-coordinated phenyl ligands in **6.2** and **6.4** were investigated by DFT molecular orbital calculations.

## Experimental

**General Data**. Reagent grade solvents were dried by the standard procedures and were freshly distilled under nitrogen prior to use. Infrared spectra were recorded on a Thermo Nicolet Avatar 360 FT-IR spectrophotometer. $^1H$ NMR spectra were recorded on a Varian Mercury 300 spectrometer operating at 300.1 MHz. Mass spectrometric (MS) measurements were performed by a direct-exposure probe using electron impact ionization (EI) or by electrospray ionization (ESI) by using a VG 70S instrument. $Ag[NO_3]$ and $[Cu(NCMe)_4][BF_4]$ was obtained from SIGMA-ALDRICH and were used without further purification. $[NEt_4][Ir_4(CO)_{11}Ph]$ was prepared according to the published procedure.[6] Product separations were performed by TLC in air on Analtech 0.25 and 0.5 mm silica gel 60 Å $F_{254}$ glass plates. Elemental Analyses were performed by Atlantic Microlab, Norcross, GA.

### Synthesis of $Ir_4(CO)_{11}(\mu\text{-}\eta^1\text{-}Ph)[\mu_3\text{-}Cu(NCMe)]$, 6.2.

A 6.0 mg (0.019 mmol) portion of $[Cu(NCMe)_4][BF_4]$ was added to 12.0 mg (0.009 mmol) of $[NEt_4][Ir_4(CO)_{11}Ph]$ that was dissolved in 15 mL of $CH_2Cl_2$. The reaction solution turned red immediately when $[Cu(NCMe)_4][BF_4]$ was added and the solution was stirred at 25 $^oC$ for 30 min. The solvent was then removed *in vacuo*, and the product was isolated by TLC by eluting with a 3:1 hexane/methylene chloride solvent mixture. This yielded 9.0 mg of red $Ir_4(CO)_{11}(\mu\text{-}\eta^1\text{-}Ph)[\mu_3\text{-}Cu(NCMe)]$, **6.2** (77% yield). Spectral data for **6.2**: IR $\nu_{CO}$ ($cm^{-1}$ in $CH_2Cl_2$): 2082(s), 2044(vs), 2024(s), 2006(s), 1855(m), 1824(m). $^1H$ NMR ($CDCl_3$, in ppm) $\delta$ = 7.542 (d, 2H, $^1J_{H\text{-}H}$=6.6Hz, ortho-H of σ-Ph), 6.911-6.988(m, 3H, meta- & para-H of σ-Ph) 1.84(s, 3H, NCMe). Mass Spec. ES (negative ion) for **6.2:** *m*/*z* = 1263 (M + formate)$^-$. The isotope distribution pattern is consistent with the presence of four iridium atoms and one copper atom.

**Synthesis of $[NEt_4][\{Ir_4(CO)_{11}Ph\}_2(\mu_4\text{-}Ag)]$, 6.3.**

A 6.5 mg (0.038 mmol) portion of $AgNO_3$ was added to 20.0 mg (0.016 mmol) of $[NEt_4][Ir_4(CO)_{11}Ph]$ that was dissolved in 15 mL of $CH_2Cl_2$. The reaction solution was stirred at 25 $^oC$ for 1h. The solvent was then removed *in vacuo*, and the product was isolated by TLC by eluting with a 1:1 hexane/methylene chloride solvent mixture. This yielded 12.7 mg of yellow $[NEt_4][\{Ir_4(CO)_{11}Ph\}_2(\mu_4\text{-}Ag)]$, **6.3** (64% yield). Spectral data for **6.3**: IR $\nu_{CO}$ ($cm^{-1}$ in $CH_2Cl_2$): 2078(m), 2050(vs), 2009(s), 1844(m), 1820(m). $^1H$ NMR ($CDCl_3$, in ppm) $\delta$ = 6.62-6.92 (m, 10H, σ-Ph), 0.83-0.88 (t, 12H, $CH_3$), 1.25-1.30(m, 8H, $CH_2$). Mass Spec. ES (negative ion) *m*/*z* = 2416 = $[\{Ir_4(CO)_{11}Ph\}_2(\mu_4\text{-}Ag)]^-$ and 2389 = $[\{Ir_4(CO)_{11}Ph\}_2(\mu_4\text{-}Ag)]^-$ - CO. The isotope distribution pattern is consistent with the presence of eight iridium atoms and one silver atom.

**Synthesis of $[Ir_4(CO)_{11}]_2(\mu_4\text{-Ag})(\mu\text{-Ag})(\mu_3\text{-Ph})(\mu\text{-Ph})$, 6.4.**

A 11.0 mg (0.004 mmol) portion of **6.3** was dissolved in 10 mL of $CH_2Cl_2$. 2.7 mg (0.016 mmol) of $AgNO_3$ was added and the reaction solution was stirred for 1 h at 25 $^oC$. The solvent was then removed *in vacuo*, and the product was isolated by passing over a short silica column (4 cm) by eluting with a 1:3 hexane/methylene chloride solvent mixture to yield 7.7 mg of yellow $[Ir_4(CO)_{11}]_2(\mu_4\text{-Ag})(\mu\text{-Ag})(\mu_3\text{-Ph})(\mu\text{-Ph})$, **6.4** (71% yield). Spectral data for **6.4**: IR $\nu_{CO}$ ($cm^{-1}$ in $CH_2Cl_2$): 2084(m), 2047(vs), 2006(s), 1841(m), 1821(m). $^1H$ NMR ($CDCl_3$, in ppm) $\delta$ = 7.29-.74 (m, 10H, $\sigma$-Ph). Mass Spec. ES (negative ion) for **6.4:** *m*/*z*=2568 ($M+CO_2H^-$), 2540($M-CO+CO_2H^-$). The isotope distribution pattern is consistent with the presence of eight iridium atoms and two silver atoms.

**Synthesis of 6.4 from $[Et_4N][Ir_4(CO)_{11}Ph]$ and $AgNO_3$.**

A 12.0 mg (0.009 mmol) portion of $[Et_4N][Ir_4(CO)_{11}Ph]$ that was dissolved in 10 mL of $CH_2Cl_2$. 10.0 mg (0.059 mmol) of $Ag[NO_3]$ was added, and the reaction solution was stirred for 1 h at 25 $^oC$. The solvent was then removed *in vacuo*, and the product was isolated through a short silica column (4 cm) by eluting with a 1:3 hexane/methylene chloride solvent mixture to yield 9.2 mg compound **6.4** (78% yield).

**Synthesis of $Ir_4(CO)_{11}(\eta^1\text{-Ph})[\mu_3\text{-Ag(NCMe)}]$, 6.5.**

A 9.8 mg (0.004 mmol) portion of **6.4** was dissolved in 10 mL of MeCN. The solution was stirred at 25 $^oC$ for 1 h. The solvent was then removed *in vacuo*, and the product was isolated by chromatography over a short silica column (4 cm) by eluting with a 1:3 hexane/methylene chloride solvent mixture. This yielded 7.4 mg of yellow $Ir_4(CO)_{11}(\eta^1$-

Ph)[$\mu_3$-Ag(NCMe)], **6.5** (73% yield). Spectral data for **6.5**: IR $\nu_{CO}$ ($cm^{-1}$ in $CH_2Cl_2$): 2082(s), 2043(vs), 2027(s), 2007(s), 1841(m), 1823(m). $^1H$ NMR ($CD_3CN$, in ppm) $\delta$ = 7.338 (d, 2H, $^1J_{H-H}$=6.6Hz, ortho-H of σ-Ph), 6.804-6.848(m, 3H, meta- & para-H of σ-Ph). Analysis: Found (Calc), C 17.26 (17.50); H 0.52 (0.61); N 1.18 (1.07).

**Thermolysis of 6.5.**

A ca. 4.0 mg of **6.5** was dissolved in $CD_3CN$ in NMR tube and was placed in oil bath at 50 ℃ for 48 h. NMR spectra showed the disappearance of phenyl resonance of **6.5** ($\delta$ = 7.338 ppm, doublet; 6.804-6.848 ppm,multiplet) and the appearance of benzene (7.393 ppm, singlet). 1.1mg of $Ir_4(CO)_{12}$ (yield 32%) was separated after the reaction.

**Synthesis of $Ir_4(CO)_{11}(\mu\text{-}\eta^1\text{-Ph})[\mu_3\text{-Ag}(PPh_3)]$, 6.6.**

A 5.0 mg (0.019 mmol) portion of $PPh_3$ was added to 10.5 mg (0.004 mmol) of **6.4** that was dissolved in 15 mL of $CH_2Cl_2$. The reaction solution was stirred for 30 min at 25 $^oC$. The solvent was then removed *in vacuo*, and the product was isolated by TLC by eluting with a 2:1 hexane/methylene chloride solvent mixture. This yielded 9.1 mg of yellow $Ir_4(CO)_{11}(\mu\text{-}\eta^1\text{-Ph})[\mu_3\text{-Ag}(PPh_3)]$, **6.6** (87% yield). Spectral data for **6.6**: IR $\nu_{CO}$ ($cm^{-1}$ in $CH_2Cl_2$): 2081(s), 2042(vs), 2027(s) 2001(s), 1853(m), 1824(m). $^1H$ NMR ($CDCl_3$, in ppm) $\delta$ = 6.31-6.71 (m, 5H, σ-Ph), 6.90-6.95 (m, 15H, $PPh_3$). Analysis: Found (Calc), C 27.76 (27.56); H 1.24 (1.31).

**Crystallographic Analyses:** Single crystals of **6.2** (red)**, 6.3** (brown), **6.4** (yellow) and **6.6** (red) suitable for x-ray diffraction analyses were obtained by slow evaporation of solvent from a hexane/methylene chloride solvent mixture at -25 ℃. Single crystals of

**6.5** (orange) suitable for x-ray diffraction analyses was obtained by slow evaporation of solvent from a MeCN/hexane solvent mixture at -25 ℃. Each data crystal was glued onto the end of a thin glass fiber. X-ray intensity data were measured by using a Bruker SMART APEX CCD-based diffractometer and Mo Kα radiation (λ = 0.71073 Å). The raw data frames were integrated with the SAINT+ program by using a narrow-frame integration algorithm.[18] Corrections for Lorentz and polarization effects were also applied with SAINT+. An empirical absorption correction based on the multiple measurement of equivalent reflections was applied in each analysis by using the program SADABS. All structures were solved by a combination of direct methods and difference Fourier syntheses, and refined by full-matrix least-squares on $F^2$, using the SHELXTL software package.[19] All non-hydrogen atoms were refined with anisotropic displacement parameters. Hydrogen atoms were placed in geometrically idealized positions and included as standard riding atoms during the least-squares refinements. Crystal data, data collection parameters, and results of the analyses are listed in Table 6.1. Compounds **6.2** and **6.5** both crystallized in the monoclinic crystal system. The space group $P2_1/n$ was uniquely identified by the systematic absences in the intensity data and further confirmed by the successful solutions and refinements of the structures. There are two symmetry independent molecules in the asymmetric unit in the crystal of **6.2**. For compound **6.5** the space group $P2_1$ was uniquely identified by the systematic absences in the intensity data and subsequently confirmed by successful solutions and refinements of the structure. There is one symmetry independent molecule in the asymmetric unit in the crystal of **6.5**. Compounds **6.3**, **6.4** and **6.6** crystallized in the triclinic crystal system. The space group *P*-1 was assumed for each analysis and was subsequently confirmed by successful

solution and refinement of the structure in each case. There is one symmetry independent molecule in the asymmetric unit in the crystals of **6.4** and **6.6.** For compound **6.3** there is only one half of symmetry independent molecule in the asymmetric crystal unit.

**Computational details:** All geometry optimizations were performed using the density functional theory (DFT) module in the Gaussian 09 suite of ab initio programs[20] for the range-separated and dispersion-corrected hybrid density functional $\omega$B97X-D.[21] Relativistic effective core potential (ECP) basis sets ECP10MDF_VTZ, ECP28MDF_VTZ and ECP60MDF_VTZ were used for Cu,[22] Ag,[22] and Ir,[23] respectively. All-electron cc-pVDZ basis set was used for H, C, N and O atoms.[24] The $\omega$B97X-D functional was selected for this study because it contains both long-range exchange and empirical dispersion corrections, which are important for the modeling of structures with weak interactions and localized anionic or strongly electron donating sites.[25] We believe such basis sets (789 basis functions, 2207 primitive Gaussians and 900 Cartesian basis functions for **6.2**; 1464 basis functions, 4132 primitive Gaussians and 1680 Cartesian basis functions for **6.4**) used in our study are sufficient for accurate DFT calculations. The geometric structures of **6.2** and **6.4** were fully optimized as gas phase (Cs symmetry for **6.4**). Their ground states were confirmed as singlets through comparison with the optimized high-spin analogs. The fragment analysis for compound **6.2** were performed with the Amsterdam Density Functional (ADF) 2012 suite of programs[26] by using the meta–Generalized Gradient Approximation (meta-GGA) level non-empirical Tao-Perdew-Staroverov-Scuseria (TPSS) functional[27] for the optimized structure of **6.2**. Relativistically optimized Slater-type valence quadruple-ζ + 4 polarization function (QZ4P) basis set was used for Cu and Ir atoms and all-electron double-ζ (DZ) basis set

was used for H, C, N and O atoms in ADF calculations. The topology of electron densities and charge distributions in the optimized structure of complex **6.2** and **6.4** were analyzed using Bader's quantum theory of atoms in molecules (QTAIM),[28] and the AIMAll software package.[29] The Wiberg bond indices[30] were obtained using the NBO 5.0 program.[31] The Mayer bond indices[32] were obtained using Gaussian 09.

**Results and Discussion**

The reaction of the anion $[Ir_4(CO)_{11}(Ph)]^-$, **4.1** with $[Cu(NCMe)_4][BF_4]$ yielded the new iridium-copper complexes $Ir_4(CO)_{11}(\mu\text{-}\eta^1\text{-Ph})[\mu_3\text{-Cu(NCMe)}]$, **6.2** in 77% yield. Compound **6.2** was characterized by single-crystal X-ray diffraction analysis. There are two independent molecules of **6.2** located in the asymmetric crystal unit. Both molecules are structurally similar. An ORTEP diagram of the molecular structure of one of these two molecules is shown in Figure 6.1. The molecule consists of a tetrahedral $Ir_4$ cluster with a Cu atom occupying one of the triangular faces. The Ir – Ir bond distances are similar to those found in the anion **4.1**.[6] The Ir – Ir distances bridged by the Cu atom are slightly longer 2.8077(5) Å, Ir2 – Ir4 = 2.7725(5) Å, Ir3 – Ir4 = 2.7499(5) Å than those that are not, Ir1 – Ir2 = 2.7482(5) Å, Ir1 – Ir3 = 2.7247(5) Å, Ir1 – Ir4 = 2.7307(5) Å. The phenyl ligand serves as a semibridge across the Ir2 – Cu1 bond. It is strongly σ–bonded to Ir(2) but is also π–bonded to the Cu atom, see below. The Ir – C bond distance, Ir2 – C14 = 2.133(9) Å, [Ir6 - C54 = 2.124(9) Å] is slightly shorter than the Cu – C, Cu1 – C14 = 2.171(9) Å, [Cu2 - C54 = 2.201(8) Å] to the bridging phenyl ligand. (The value in brackets is for the second independent molecule in the crystal.) The Ir – C distance to the terminally coordinated σ–phenyl ligand $Ir_4(CO)_{11}(Ph)(\mu\text{-AuPPh}_3)$ is 2.100(7) Å,[8] and in the anion **4.1** itself, 2.125(13) Å.[6] The Cu – C distances to the bridging phenyl ligands in

the complex $Cu_4(\mu\text{-}Ph)_4(SMe_2)_2$, 1.997 (8) Å, 2.010 (6) Å, 2.054 (6) Å, 2.070 (6) Å, are typical of those found for these bridging ligands.[33] Cu – C distances to terminal coordinated Ph ligands are similar in length, e.g. 2.020 (4) Å, as found in (triphos)CuPh.[34] The phenyl-bridged Ir – Cu bond, Ir2 – Cu1 = 2.6628(12) Å, [Ir6 - Cu2 = 2.6730(12) Å], is slightly shorter than the nonbridged Ir – Cu bonds, Ir3 – Cu1 = 2.7400(13) Å, Ir4 – Cu1 = 2.7667(13) Å, [Ir7 - Cu2 = 2.7232(13) Å; Ir8 - Cu2 = 2.7190(15) Å]. The Ir – Cu distances to the triply-bridging Cu(NCMe) group in the complex anion $[Ir_6(CO)_{15}Cu(NCMe)]^-$ are similar: 2.646(4) Å, 2.645(4) Å, 2.617(4) Å.[35] The NCMe ligands lies approximately trans to the Ir(20 – Cu(1) bond, N1– Cu1 – Ir2 = 170.0(3)$^o$. Compound **6.2** contains three bridging carbonyl ligands that circumscribe the $Ir_3$ triangle that contains the bridging Cu atom. Overall, compound **6.2** contains a total of 72 valence electrons, so formally each of the metal atoms can be assigned an 18 electron configuration. Simple electron counting reveals that the uncharged $Ir_4(CO)_{11}(\mu_3\text{-}Cu(NCMe)$ fragment has 71 valence electrons. The 72 electron count is completed by the addition of the one electron from the ipso-carbon atom of the uncharged phenyl ring to the Ir atom to form a simple σ–bond. To a first approximation, the complex should be stable in this form and there is nothing to be gained by having the phenyl ligand adopt the semibridging coordination mode. Indeed such is the structure of compound 6.5, see below. A more detailed account of the bonding of the semibridging phenyl ligand to the metal atoms in 6.2 was provided by a DFT molecular orbital analysis which is described below.

When anion **4.1** was allowed to react with $Ag[NO_3]$, the new iridium-silver complex $[Et_4N][\{Ir_4(CO)_{11}Ph\}_2(\mu_4\text{-}Ag)]$, **6.3** was obtained in 64% yield. Compound **6.3** was characterized by single-crystal X-ray diffraction analysis. Compound **6.3** is a salt

consisting of isolated [$Et_4N$] cations and [{$Ir_4(CO)_{11}Ph$}$_2$($\mu_4$-Ag)] anions. An ORTEP diagram of the molecular structure of the complex anion is shown in Figure 6.2. The molecule consists of two tetrahedral $Ir_4$ clusters of the anion **4.1** that are linked by a single quadruply-bridging Ag atom. The silver atom lies on a crystallographic center of symmetry in the solid state, so the two $Ir_4$ clusters are symmetry related. The silver atom bridges one Ir – Ir bond in each $Ir_4$ cluster. The four Ir atoms exhibit a planar "bow-tie" geometry about the Ag atom. The planar bowtie structure for silver is rare among metal carbonyl cluster complexes, but there are two crystallographically characterized examples, both exist in anionic complexes: [{$Os_3(CO)_{11}H$}$_2$($\mu_4$-Ag)]$^-$ and [{$Rh_6(CO)_{15}(C)$}$_2$($\mu_4$-Ag)]$^{3-}$.[36, 37] The Ag bridged Ir – Ir bond in **6.3**, Ir2 – Ir3 = 2.8909(9) Å, is significantly longer than the other Ir – Ir bonds which range from 2.7129(10) Å to 2.7449(9) Å. The latter are very similar to those found in the anion **4.1**.[6] Each $Ir_4$ cluster contains one terminally coordinated σ–phenyl ligand that lies approximately trans to one of the Ir – Ag bonds. The Ir – C bond distance is similar to that found in **4.1**, Ir3 – C43= 2.128(18) Å.[6] The complex anion has an overall charge of minus one, therefore since each $Ir_4$ cluster is formally minus one, the Ag atom can be viewed formally as having a plus one charge. The two independent Ir – Ag bond distances are significantly different in lengths: Ir2 – Ag1 = 2.8035(7) Å, Ir3 – Ag1 = 3.0060(7) Å. The Ir3 – Ag1 bond that lies approximately trans to the σ–phenyl ligand is the longer of the two. As found in both **4.1** and **6.2**, there are three bridging CO ligands about one of the triangular $Ir_3$ faces, Ir2 – Ir3 – Ir4.

Compound **6.3** reacts with a second equivalent of Ag[$NO_3$] to yield the uncharged complex [$Ir_4(CO)_{11}$]$_2$($\mu_4$-Ag)(μ-Ag)($\mu_3$-Ph)(μ-Ph), **6.4** in 71% yield by the addition of a second $Ag^+$ ion. Compound **6.4** was also obtained in 78 % yield directly by the reaction

of **6.1** with two equivalents of $Ag[NO_3]$. Compound **6.4** was characterized by single-crystal X-ray diffraction analysis. An ORTEP diagram of the molecular structure of the complex anion is shown in Figure 6.3. Compound **6.4** consists of two tetrahedral $Ir_4$ clusters of the anion **4.1** that are linked by bridging Ag atoms. The silver atom Ag1 is a quadruply-bridging atom that is bonded to three Ir atoms, Ir2 – Ir3 – Ir4, of one cluster and one Ir atom, Ir5, of the second cluster. The second silver atom, Ag2 is a bridge across the Ir5 – Ir8 edge of the second cluster. The two phenyl ligands have adopted semibridging coordinations from Ir atoms to the Ag atoms. Phenyl ring, C14 – C19, contains significant interactions with three metal atoms Ir4, Ag1 and Ag2 and could thus be described as a triply-bridging ligand. The ipso carbon atom of this ring is strongly $\eta^1$-bonded to Ir4, Ir4 – C14= 2.11(3) Å but is also weakly bonded to Ag1, Ag1 – C14 = 2.56(3) Å. Most interestingly, the *para*-carbon C17 and to a lesser degree the *meta*-carbon atoms of this ring are also bonded to Ag2. The Ag2 – C17 distance, 2.42(4) Å, is shorter than the Ag1 – C14 distance and implies a fairly strong interaction, see the computational analyses described below. The Ag – C distances to the meta-carbon atoms, Ag2 – C16 = 2.74(9) Å and Ag2 – C18= 2.71(3) Å, suggest some weak bonding between these atoms. We think this ligand is best described as a 1,4-$\eta^2$-triple bridge. Other forms of $\eta^n$-bridging phenyl ligands have been reported, but the 1,4-$\eta^2$-triple bridge found here in compound **6.4** appears to be unique.[3b,5,6] The second phenyl ligand is a simple $\eta^1$-semibridge across the Ir8 – Ag2 bond, Ir8 – C24= 2.13(3) Å, Ag2 – C24= 2.27(3) Å.

When compound **6.4** was dissolved in MeCN, the complex was split in two to yield two $AgIr_4$ clusters and one equivalent of NCMe was added to each half to yield the new complex $Ir_4(CO)_{11}(\eta^1\text{-Ph})[\mu_3\text{-Ag(NCMe)}]$, **6.5** in 73% yield. Compound **6.5** was

characterized by single-crystal X-ray diffraction analysis, and an ORTEP diagram of its molecular structure is shown in Figure 6.4. The molecule consists of a tetrahedral $Ir_4$ cluster with an Ag(NCMe) group occupying one of the triangular faces of the $Ir_4$ cluster. In this sense the molecule is similar to that of **6.2**, but unlike **6.2**, the phenyl ligand in **6.5** is not semibridging ligand. It is instead a terminally coordinated σ–phenyl ligand that lies approximately trans to one of the Ir – Ag bonds, similar to that found for one of the two phenyl ligands in **6.3**. The Ir – C bond distance, Ir2 – C14 = 2.102(16) Å, is similar to that found in **6.3**. The Ag-bridged Ir – Ir bond distances, Ir2 – Ir3 = 2.8141(7) Å, Ir2 – Ir4 = 2.8133(6) Å, Ir3 – Ir4 = 2.7802(8) Å, are significantly longer than the unbridged bonds, Ir1 – Ir2 = 2.7264(8) Å, Ir1 – Ir3 = 2.7217(7) Å, Ir1 – Ir4 = 2.7209(9) Å. The Ir – Ag bond distances, Ir2 – Ag1 = 2.8711(13), Ir3 – Ag1 = 2.8374(10), Ir4 – Ag1 = 2.8724(14), are similar to those found in **6.3** and **6.4**. As found in **6.2** and **6.4**, there are three bridging CO ligands about the $Ir_3$ triangle that supports the triply bridging heterometal atom. The metal cluster in **6.5** contains a total of 72 valence electrons which is formally consistent with 18 electron configurations at each of the metal atoms. Interestingly, when gently heated (reflux in a $CH_2Cl_2$ solution), compound **6.5** did not lose NCMe and reconvert to **6.4** but was instead transformed into $Ir_4(CO)_{12}$ by loss of the Ag metal atom, the NCMe ligand and the Ph ligand and acquisition of a CO ligand. Benzene was also observed to form in this decomposition, apparently derived from the phenyl ligand. The source of the proton need to make the benzene has not been established.

The reaction of **6.4** with $PPh_3$ yielded the new complex $Ir_4(CO)_{11}(\mu\text{-}\eta^1\text{-}Ph)[\mu_3\text{-}Ag(PPh_3)]$, **6.6** in 87% yield. Compound **6.6** was characterized by single-crystal X-ray diffraction analysis, and an ORTEP diagram of its molecular structure is shown in Figure

5. The structure of the $Ir_4Ag$ cluster of **6.6** similar to that of **6.5**, but most interestingly, the phenyl ligand which is terminally coordinated in **6.5** has adopted a semi-bridging coordination mode in **6.6** similar to that observed in **6.2**, Ir3 – C4 = 2.144(11) Å and Ag1 – C4 = 2.506(10) Å. We can only conclude that energetically there is not a big difference between the terminal and semi-bridging coordination modes of the phenyl ligand in these cluster complexes. This is supported by the computational analysis described below. The Ir – Ir distances in **6.6** are similar to those in **6.5**, but the Ir – Ag distances are significantly longer than those in **6.5**, Ir2 – Ag1 = 2.9263(9) Å, Ir3 – Ag1 = 2.9219(9) Å, Ir4 – Ag1 = 2.9382(9) Å. The phosphine ligand is coordinated to the silver atom, Ag1 – P1 = 2.417(3) Å.

*Computational analyses of the bonding in **6.2** and **6.4**.*

To understand the nature of the semibridging bonding of the phenyl ligands in **6.2** and **6.4** in greater detail, geometry-optimized DFT molecular orbital calculations were performed. Selected MOs that pertain to the bonding of the phenyl ligand across the Ir – Cu bond in **6.2** are shown in Figure 6.6. The highest occupied molecular orbital (HOMO) exhibits no significant bonding interactions of the phenyl ring to the $Ir_4Cu$ cluster. The HOMO-1 shows σ–bonding of the ipso carbon atom to the iridium atom. The HOMOs -4, -7, -11 and -12 all show interactions between π–orbitals on the ring with suitably oriented d-orbitals on the copper atom. HOMO-11 and HOMO-12 are clearly ring to metal bonding in character while the orbitals HOMO-4 and HOMO-7 are the corresponding ring to metal antibonding forms.

An ADF fragment analysis reveals the origin of the MOs in Figure 6.7. The fragment MOs were created for the phenyl ring (shown on the right hand side) and the $Ir_4(CO)_{11}[\mu_3\text{-}Cu(NCMe)]$ group (shown on the left hand side) in the combined MO/energy level diagram shown Figure 8. The HOMO-1 of **6.2** is most important orbital for the bonding of the phenyl ring to the metal cluster. The bonding is a combination of the singly-occupied MO (SOMO) of the phenyl ring fragment and the singly-occupied MO of the $Ir_4(CO)_{11}[\mu_3\text{-}Cu(NCMe)]$ fragment. This orbital serves as the basis for what would commonly be referred to as a phenyl – iridium, C – Ir, σ–bond. The HOMO-11 shows the existence of phenyl-copper bonding interactions represented which are derived from the HOMO-1 of the phenyl ring fragment and the HOMO-6 of the $Ir_4(CO)_{11}[\mu_3\text{-}Cu(NCMe)]$ fragment, but there is also an antisymmetric combination of these two fragment orbitals that manifests itself in the HOMO-4. Since both of these orbitals are filled, the phenyl-Cu bonding gained by formation of the HOMO-11 is reduced by the interactions in the HOMO-4. A similar competing relationship is found between the HOMO-12 and the HOMO-7 in **6.2**. The Cu – ring orbital interactions in these two MOs are created by symmetric and antisymmetric combinations of the HOMO-2 ring fragment orbital and the HOMO-10 of the $Ir_4(CO)_{11}[\mu_3\text{-}Cu(NCMe)]$ fragment. Our calculations revealed no significant bonding interactions between the metal atoms and the unoccupied π–orbitals of the phenyl ring. One reason for this is because the ring π–orbitals lie at too high energy, e.g. see the location of the ring lowest unoccupied molecular orbital (LUMO) shown in Figure 6.7.

The bonding in **6.2** was further analyzed by calculating the electron densities at the bond critical points (BCP) in the optimized structure by using the QTAIM method.

Selected electron densities at important BCPs are shown in Figure 8. The electron densities at the BCPs in the C1−Cu and C1−Ir1 bonds are 0.062 and 0.113 e/bohr$^3$, respectively. Such electron densities indicate that the bond strength between C1 and Cu is about half of the bond strength between C1 and Ir1 and support the description as a semi-bridging phenyl ligand between Cu and Ir1. The 0.124 e/bohr$^3$ electron density at the BCP in the C1−Ir1 bond is very similar to the electron densities calculated between Ir atoms and bridging carbonyl ligands in **6.2**, see Figure 6.8.

Before discussing the bonding in **6.4**, it would be appropriate to consider the valence electron count about the metal atoms. First let us consider the stable, related compound $Ir_4(CO)_{11}(Ph)(\mu\text{-}AuPPh_3)$, **6.7** cf. Scheme 6.1.[8] Assuming that the phenyl group and $AuPPh_3$ group in **6.7** each donate one electron to the Ir atoms, then the $Ir_4$ cluster contains a total of 60 valence electrons and each Ir formally achieves an 18 electron configuration. Compound **6.4** can be viewed as a combination of two $AgIr_4(CO)_{11}(Ph)$ fragments. Ag is electronically similar to Au. Electronically, the primary difference between **6.7** and the $AgIr_4(CO)_{11}(Ph)$ fragment is the presence or absence of the $PPh_3$ ligand which serves as a two electron donor to the Au atom. In the absence of a $PPh_3$ ligand or its equivalent, each $AgIr_4(CO)_{11}(Ph)$ fragment is formally electron deficient by the amount of two electrons. Two of those missing electrons in **6.4** are made up by the formation of the Ir – Ag bond between the atoms Ir(5) and Ag(1) linking the two clusters; thus, compound **6.4** itself is only deficient by the amount of two electrons. As can be seen in Figure 6.3, there is an important bonding interaction one of the semibridging phenyl ligands, in particular the $\mu_3$-semibridging Ph ligand represented by

the ipso carbon atom labeled C14 in Figure 6.3 with the atom Ag2. In the absence of this interaction, Ag2 would be the primary site of this electron deficiency.

The DFT optimized structure of **6.4** with the DFT labeling scheme is shown in Figure 6.9. Table 6.3 lists the lengths of some important bonds obtained from DFT optimization and their Wiberg bond indices obtained from NBO analysis. The experimental bond lengths are also listed for comparison. The optimized C1−Ag1, C1−Ir4, C2−Ag2, C3−Ag2 and C3−Ir8 distances are 2.588, 2.134, 2.172 and 2.127 Å, respectively, which are virtually the same as the experimental values. Such small differences validate that the $\omega$B97X-D functional and corresponding basis sets are appropriate for the study of the structure and bonding properties of this complex.

Figure 6.10 shows the QTAIM analyzed bond paths and lists the selected electron densities at the BCPs atomic charges in the optimized structure of **6.4** based on the wavefunction obtained from the DFT calculation. The electron densities at the BCPs in the C1−Ag1 and C1−Ir4 bonds are 0.035 and 0.122 e/bohr$^3$, respectively. Such electron densities indicate that the bond strength between C1 and Ag1 is approximately 30% of the strength of the bond between C1 and Ir4. The electron densities at the BCPs in the C2−Ag2, C3−Ag2 and C3−Ir8 bonds are 0.052, 0.035 and 0.121 e/bohr$^3$, respectively. Such electron densities are very close to the electron densities at the BCPs of the C1−Cu and C1−Ir4 bonds in **6.2**, and confirm that the phenyl groups are asymmetric semi-bridging ligands between Ag and Ir atoms. The calculated QTAIM charges of C1, C2, C3, Ag1, Ag2, Ir4 and Ir8 are −0.182, −0.076, −0.216, +0.284, +0.404, +0.440 and +0.471, respectively, which also indicate significant electron donation from Ag and Ir atoms to the semi-bridging phenyl carbon. In addition, the calculated Wiberg bond indices of

C1−Ag2, C2−Ag2 and C3−Ag2 are 0.07, 0.08 and 0.11, respectively. The Wiberg indices for the C1-Ir4 and C3-Ir8 bonds are considerably larger 0.434 and 0.442, respectively, as expected. Similarly, the corresponding Mayer bond indices are 0.09, 0.25 and 0.28 for C1-Ag2, C2-Ag2 and C3-Ag2 and 0.88 and 0.73, for C1-Ir4 and C3-Ir8 respectively.. These bond indices further confirm that the phenyl ligands are asymmetric semi-bridging between Ag and Ir atoms.

Selected MOs obtained from a geometry-optimized DFT calculation of compound **6.4** that illustrate the bonding interactions between the phenyl rings and the metal atoms implied in the foregoing discussion are shown in Figure 6.11. The DFT calculated energy gap between the HOMO and the LUMO of **6.4** is 6.94 eV. The σ-bonding interactions between the p-orbitals of the semi-bridging phenyl carbon atoms and the iridium atoms to which they are primarily coordinated are shown in HOMO-32 and HOMO-36. Donation from π-orbitals on the ipso-carbon atoms of the rings to the silver atoms are shown in the HOMO-16, HOMO-23, HOMO-56 and the HOMO-59. Most importantly, there is evidence for significant orbital interactions between the para-ring carbon atom of the triply-bridging phenyl ring to the neighboring silver atom Ag2 in the HOMO-28, the HOMO-44, the HOMO-49, the HOMO-51, the HOMO-54, the HOMO-55, and the HOMO-59. The HOMO-43 shows a strong π-backbonding interaction between the ipso carbon of the triply-bridging phenyl ring and Ir4. HOMO-46 and HOMO-49 show weak π-backbonding interactions between the *para*-ring carbon atom of the triply-bridging phenyl ring to the neighboring silver atom Ag2. We were unable to find any significant π-backbonding interactions between the silver atom Ag1 and the C1. Based on the above

analysis, we conclude that the triply-bridging phenyl ligand serves formally as a 3-electron donor.

**Summary and Conclusions**

In this work, we have expanded our syntheses of mixed-metal iridium cluster complexes using the phenyl-containing iridium carbonyl anion **4.1** from gold[9,10] to copper and silver, see Scheme 6.1. In three of the new compounds, **6.2**, **6.4** and **6.6**, the phenyl ligand as adopted a semibridging coordination to the heterometal atom. A molecular orbital analysis of **6.2** revealed the existence of small but significant orbital interactions between the filled π-orbitals ot the semibridging phenyl ring but no significant π-backbonding between the metal atoms and the empty ring π-orbitals. In compound **6.4**, there is a second and rare triply-bridging phenyl ligand that formally serves as a 3-electron donor. Molecular orbital analyses show that in addition to the usual σ-donation of the phenyl rings to the metal atoms, the filled π-orbitals of the ring engage in some π-donation to the metal atoms, but there seems to be very little π-backbonding from the metal atoms into the π*-orbitals of the phenyl rings.

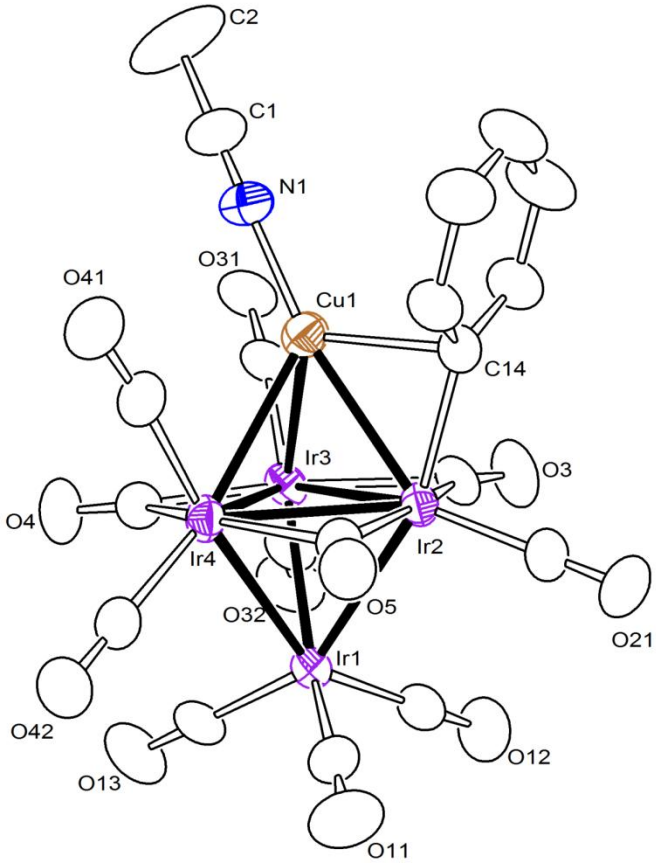


**Figure 6.1.** An ORTEP diagram of the molecular structure of $Ir_4(CO)_{11}(\mu\text{-}\eta^1\text{-}Ph)[\mu_3\text{-}Cu(NCMe)]$, **6.2** showing 30% thermal ellipsoid probability.

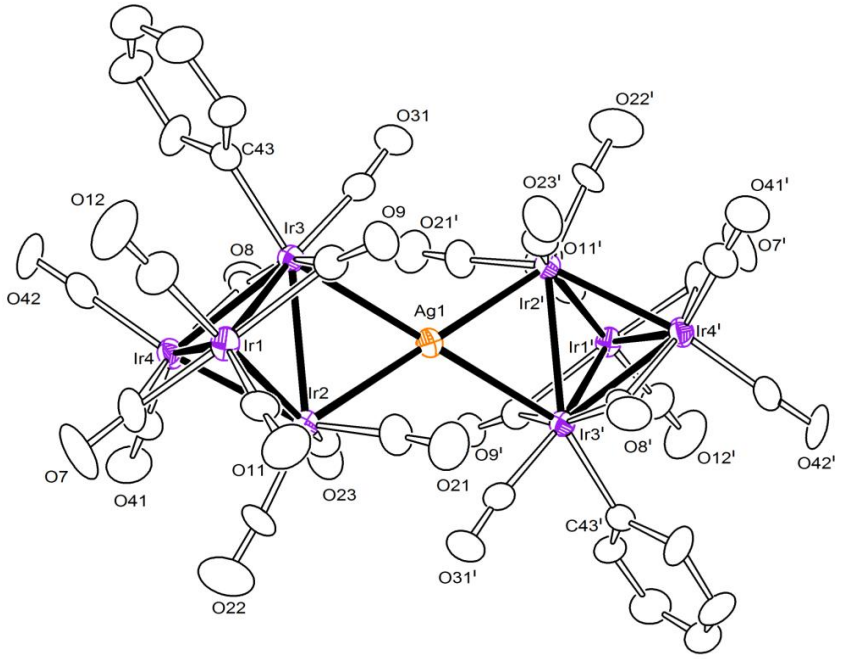


**Figure 6.2.** An ORTEP diagram of the molecular structure of $[NEt_4][\{Ir_4(CO)_{11}Ph\}_2(\mu_4\text{-}Ag)]$, **6.3** showing 30% thermal ellipsoid probability.

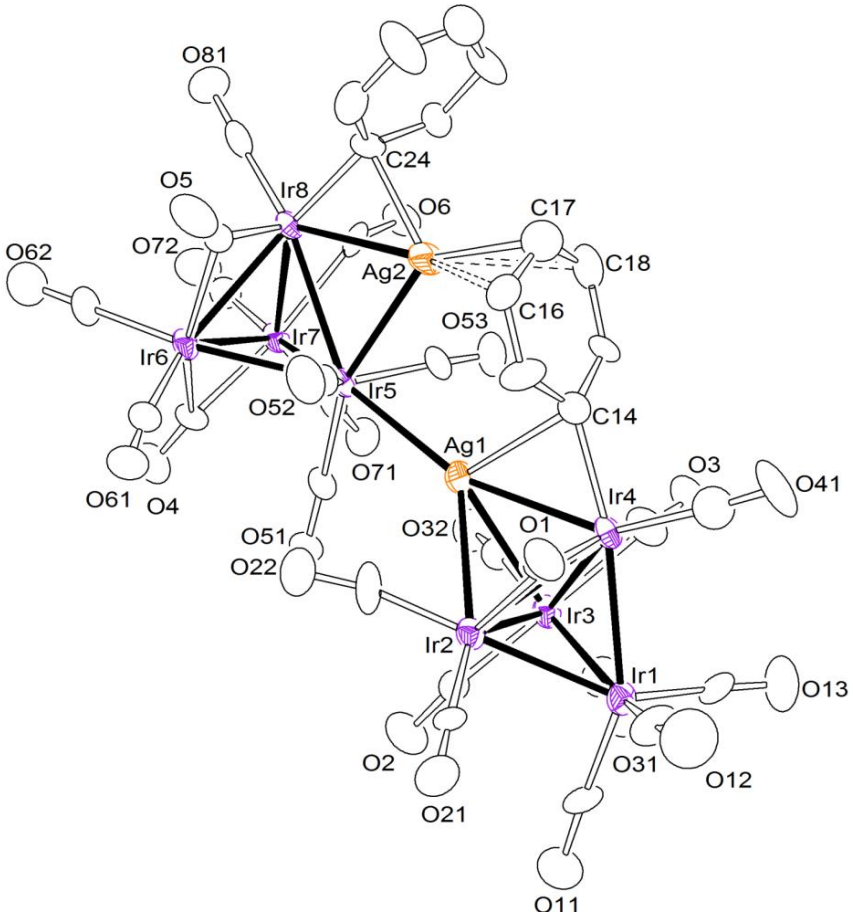


**Figure 6.3**. An ORTEP diagram of the molecular structure of $[Ir_4(CO)_{11}]_2(\mu_4\text{-Ag})(\mu\text{-Ag})(\mu_3\text{-Ph})(\mu\text{-Ph})$, **6.4** showing 30% thermal ellipsoid probability.

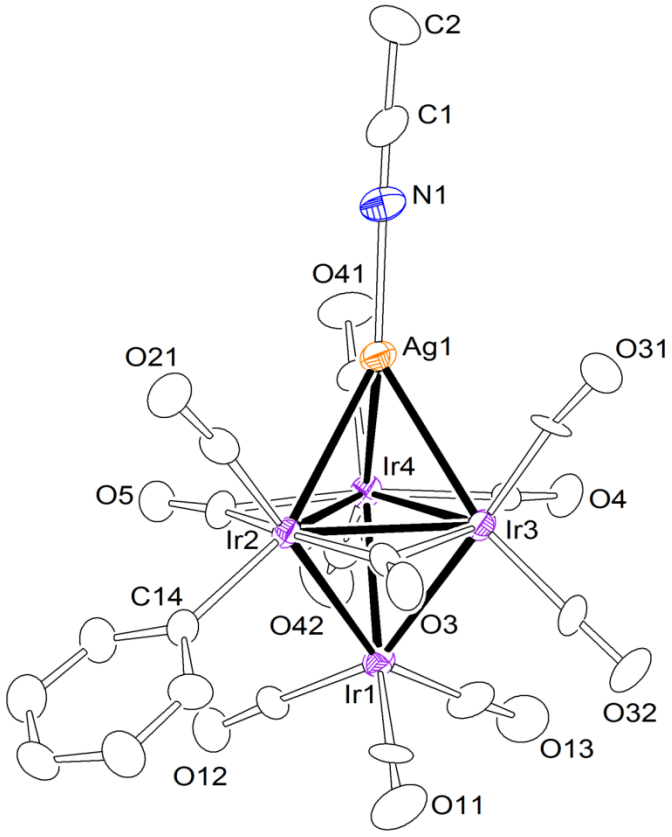


**Figure 6.4.** An ORTEP diagram of the molecular structure of $Ir_4(CO)_{11}(\sigma\text{-Ph})[\mu_3\text{-Ag(NCMe)}]$, **6.5** showing 30% thermal ellipsoid probability.

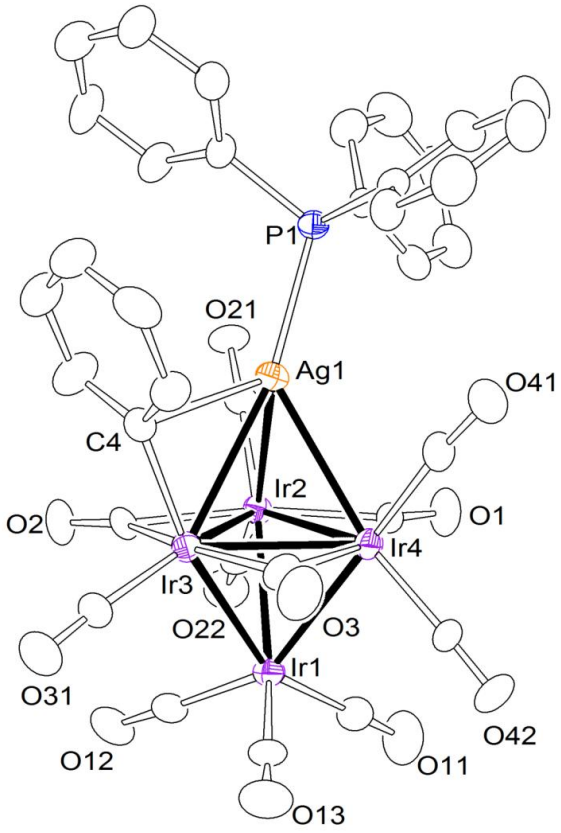


**Figure 6.5**. An ORTEP diagram of the molecular structure of $Ir_4(CO)_{11}(\mu\text{-}\eta^1\text{-}Ph)[\mu_3\text{-}Ag(PPh_3)]$, **6.6** showing 30% thermal ellipsoid probability

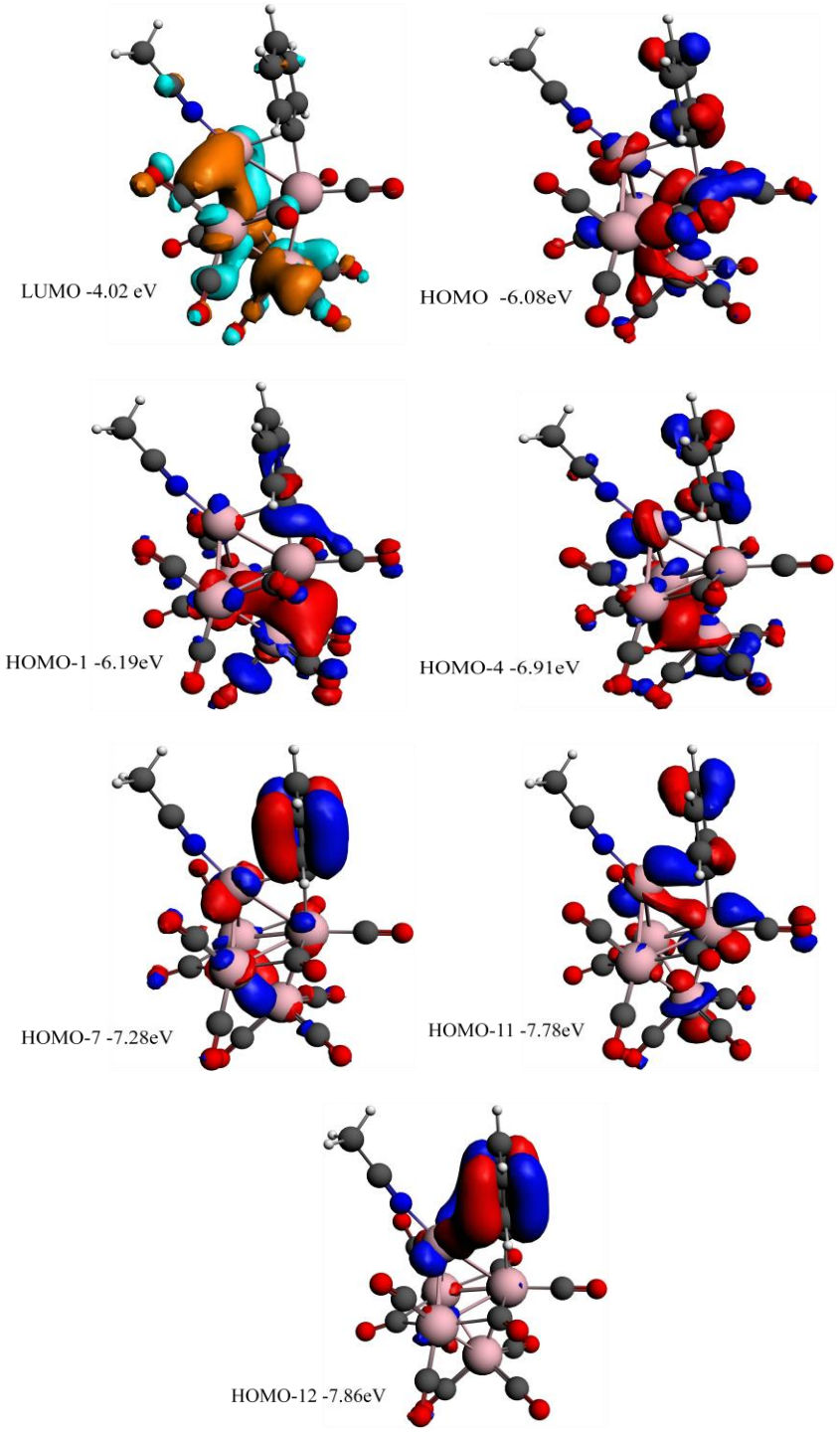


**Figure 6.6**. Selected Molecular Orbitals with calculated energy values for **6.2**.

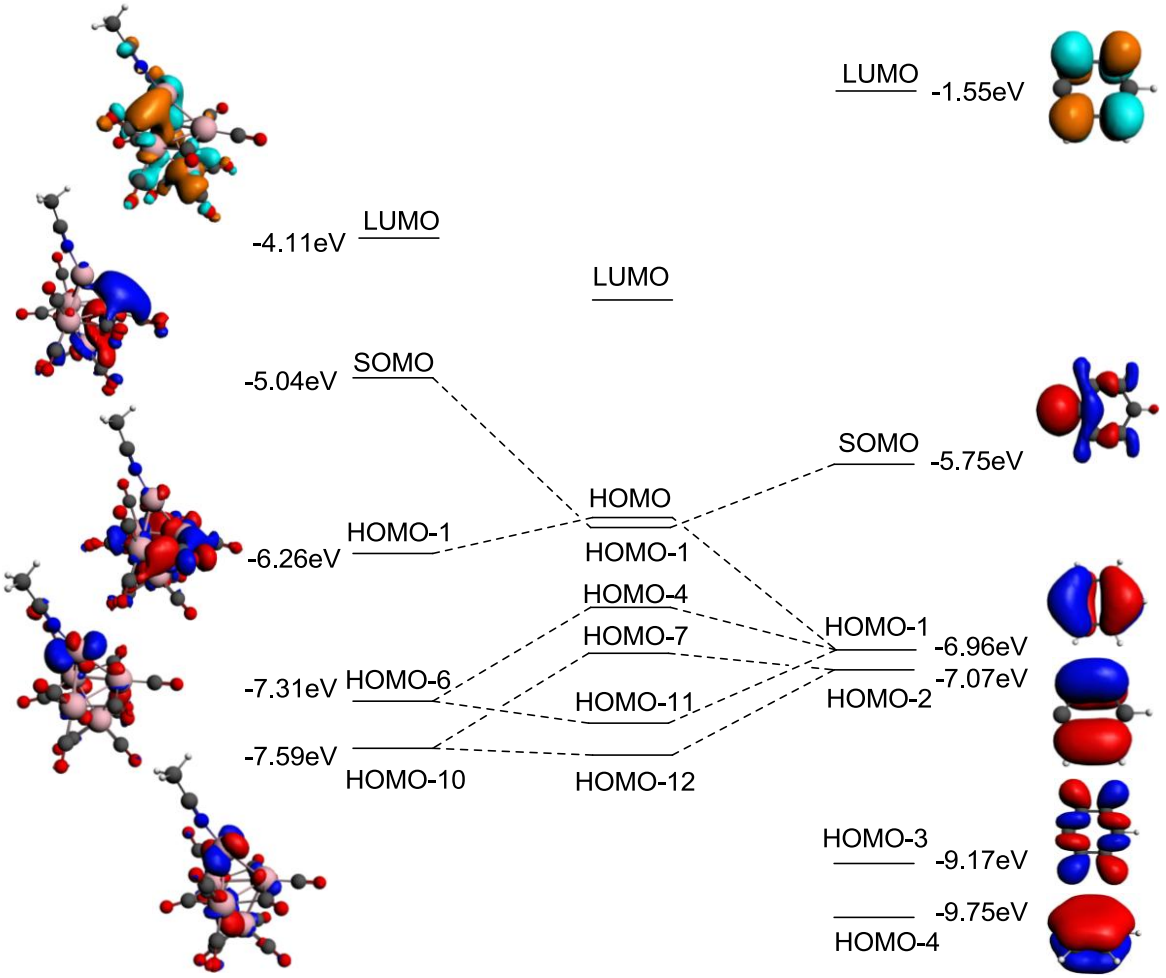


**Figure 6.7**. A molecular orbital energy level diagram for **6.2**.

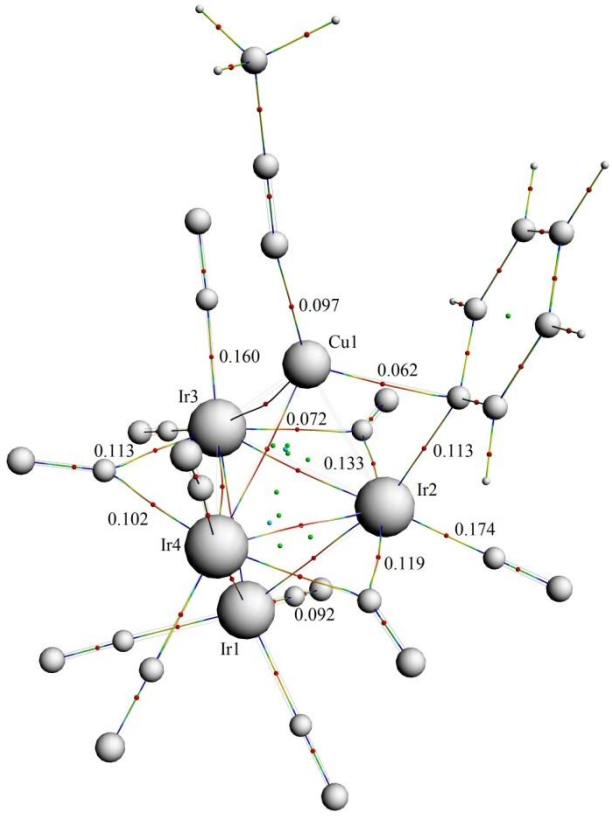


**Figure 6.8**. Selected electron densities at bond critical points calculated by QTAIM using the optimized structure of **6.2**.

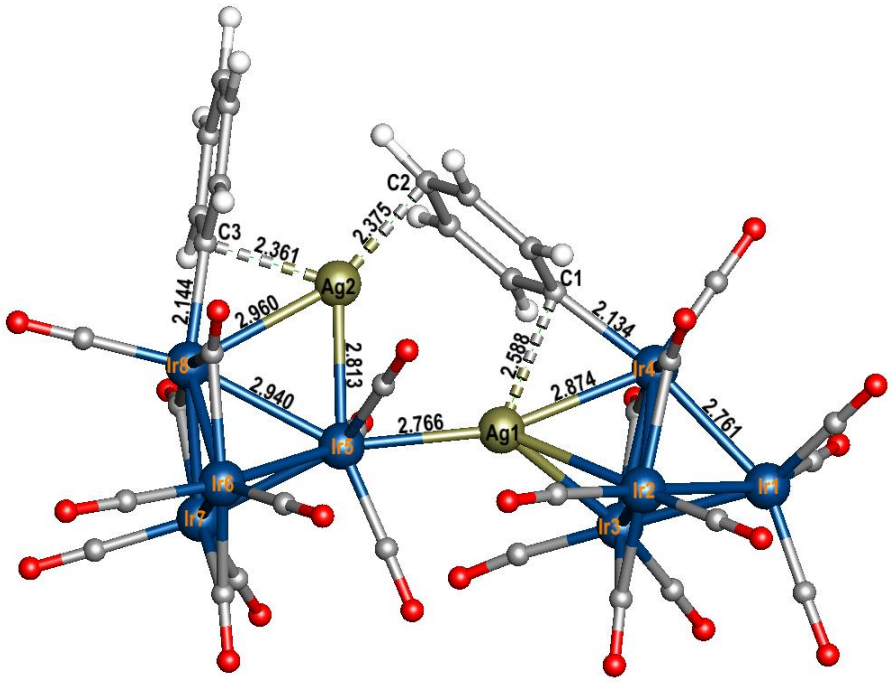


**Figure 6.9**. DFT optimized structure of **6.4**. Bond lengths are given in Å.

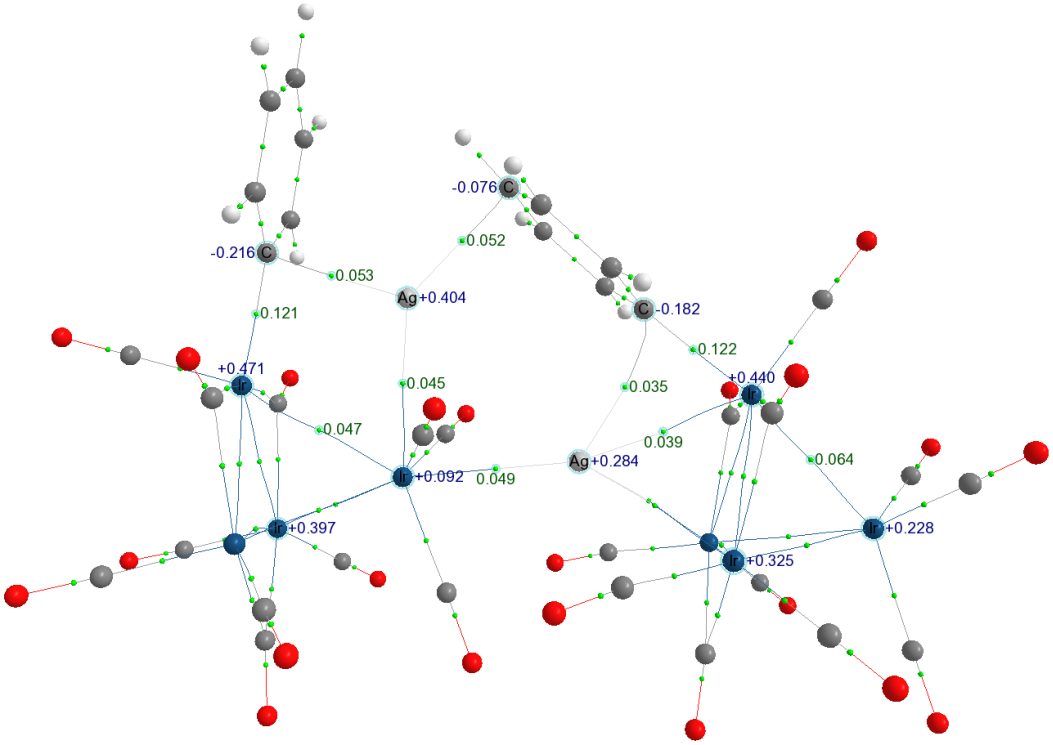


**Figure 6.10**. QTAIM analysis of bond paths with electron densities at selected bond critical points (green) and atomic charges (blue) in the optimized structure of **6.4**.

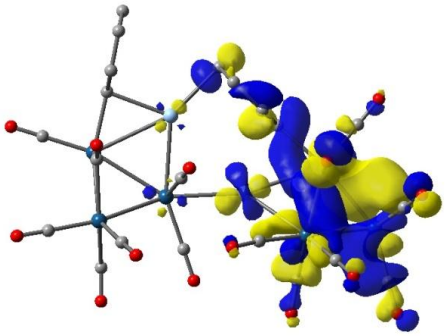

HOMO (−8.02 eV)

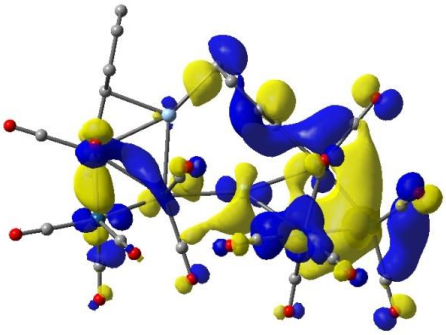

HOMO-4 (−8.72 eV)

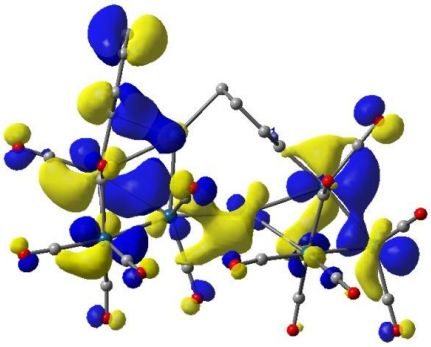

HOMO-16 (−9.82 eV)

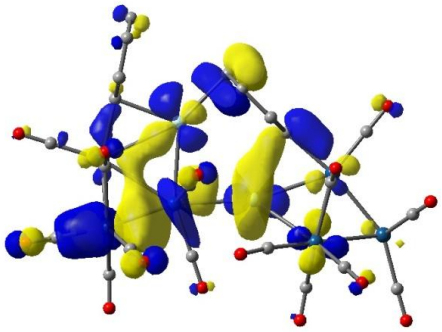

HOMO-23 (−10.74 eV)

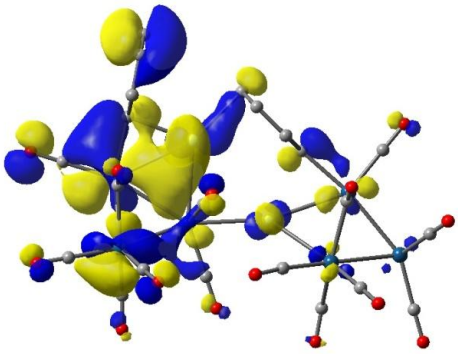

HOMO-28 (−11.14 eV)

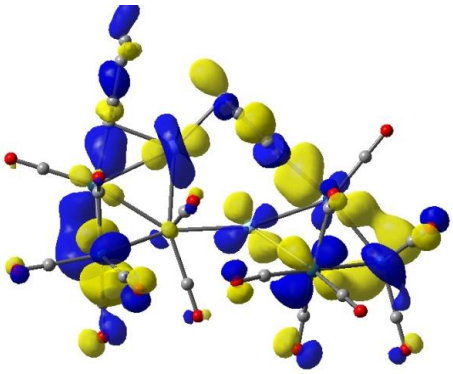

HOMO-32 (−11.42 eV)

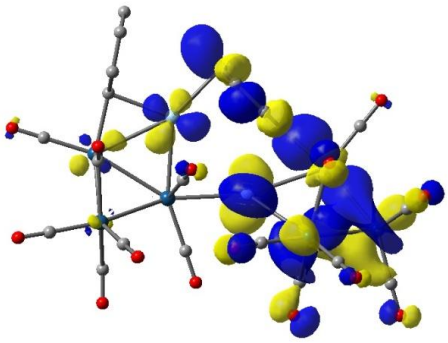

HOMO-36 (−11.86 eV)

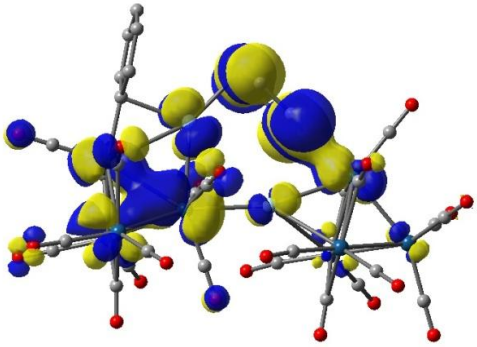

HOMO-43 (−12.27 eV)

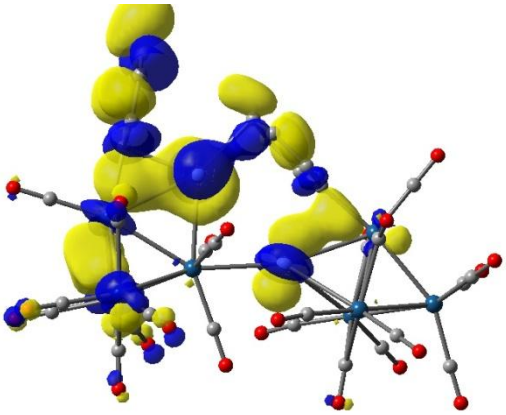

HOMO-44 (−12.30 eV)

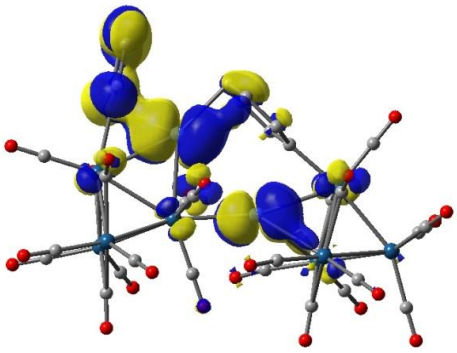

HOMO-46 (−12.48 eV)

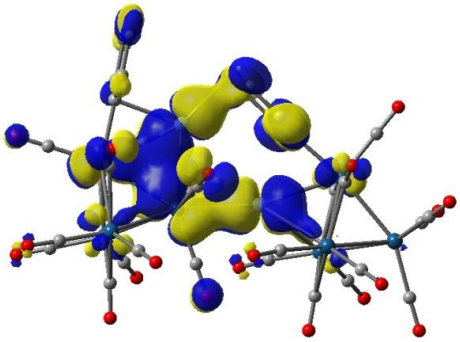

HOMO-49 (−12.70 eV)

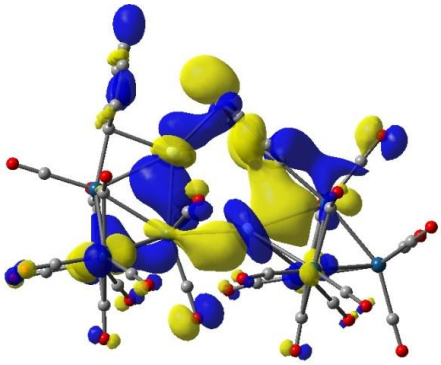

HOMO-51 (−12.91 eV)

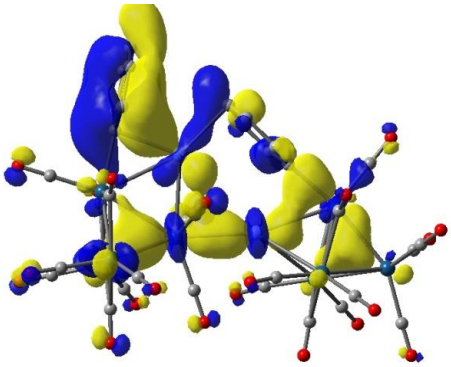

HOMO-53 (−13.58 eV)

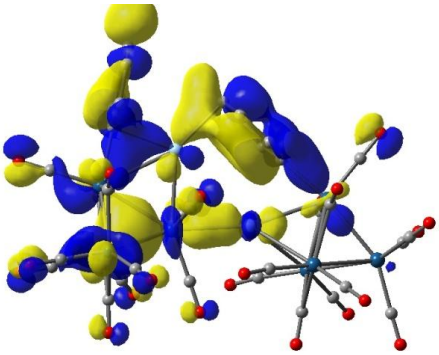

HOMO-54 (−13.69 eV)

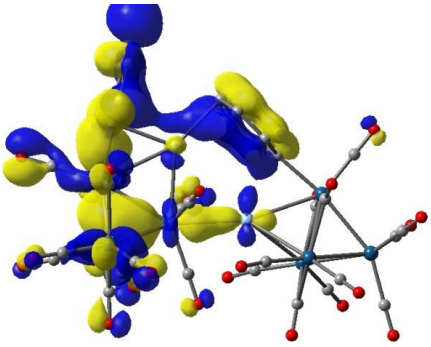

HOMO-55 (−13.98 eV)

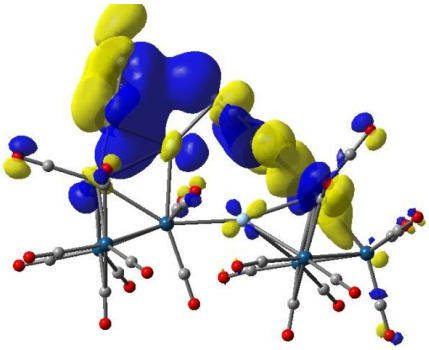

HOMO-56 (−14.03 eV)

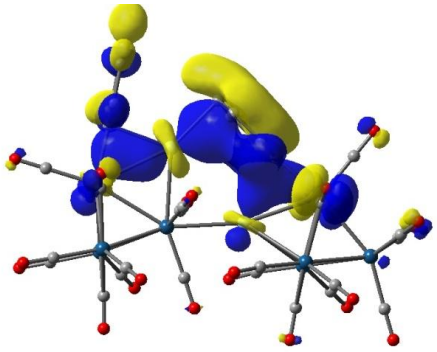

HOMO-59 (−14.25 eV)

**Figure 6.11**. Selected Molecular Orbitals with calculated energy values for **6.4**.

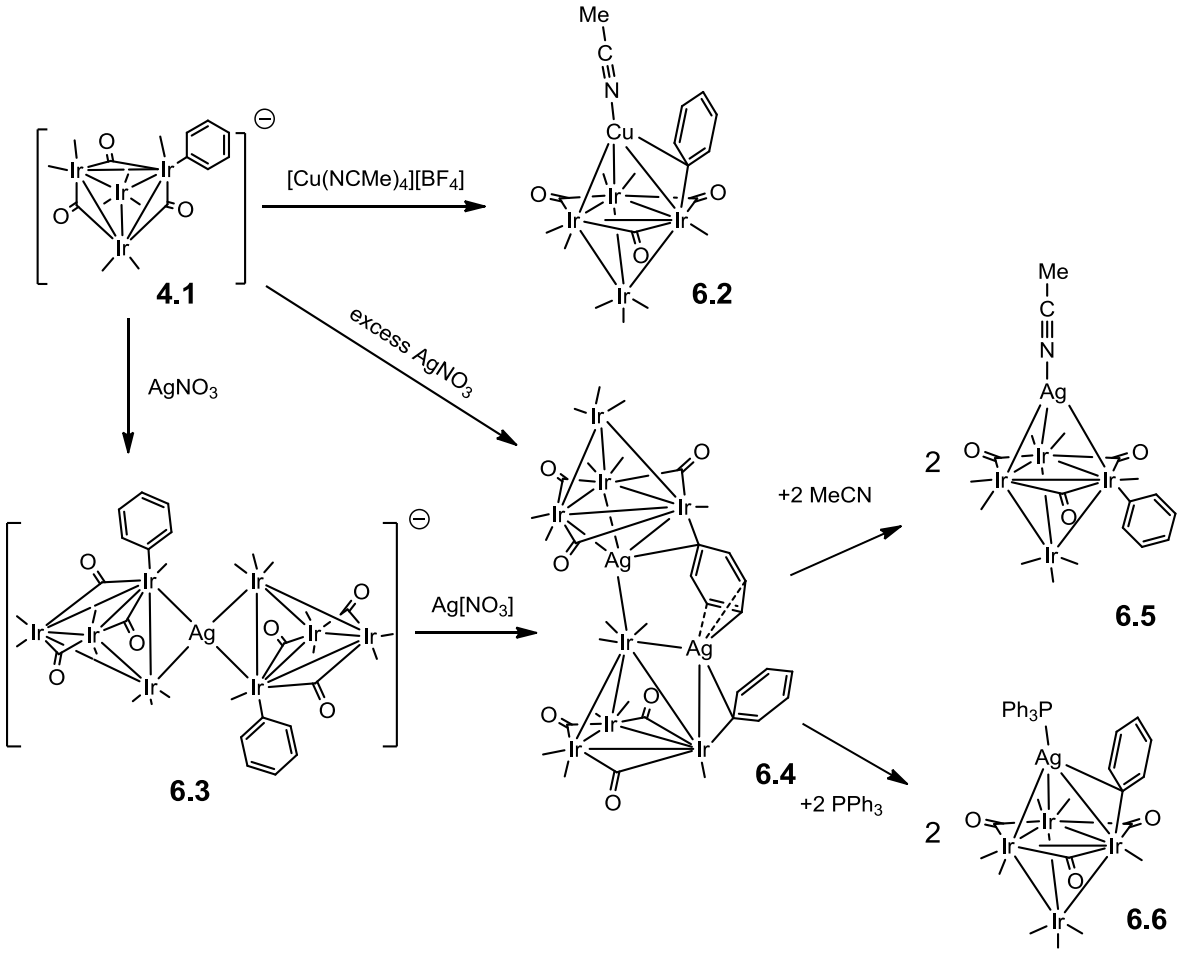


Scheme 6.1 Schematic diagrams of synthesis of iridium-copper and iridium-silver mix-metal complexes by using phenyl-containing iridium carbonyl anion **4.1.**

**Table 6.1. Crystallographic Data for Compounds 6.2 - 6.6.**

| Compound | **6.2** | **6.3** | **6.4** |
|---|---|---|---|
| Empirical formula | $Ir_4Cu_1C_{19}H_8O_{11}N_1$ | $Ir_8Ag_1C_{40}H_{26}O_{22}N_1$ | $Ir_8Ag_2C_{34}H_{10}O_{22}$ |
| Formula weight | 1258.68 | 2518.23 | 2523.90 |
| Crystal system | Monoclinic | Triclinic | Triclinic |
| Lattice parameters | | | |
| *a* (Å) | 9.5872(4) | 9.4395(10) | 9.1167(14) |
| *b* (Å) | 18.1276(9) | 12.3182(13) | 14.120(2) |
| *c* (Å) | 30.2789(14) | 13.4671(15) | 17.939(3) |
| α (deg) | 90.00 | 110.465(2) | 85.205(3) |
| β (deg) | 96.7770(10) | 95.102(2) | 87.131(3) |
| γ (deg) | 90.00 | 108.783(2) | 80.804(3) |
| V ($Å^3$) | 2448.88(12) | 1352.6(3) | 2269.9(6) |
| Space group | *P*2(1)/n | *P*-1 | *P-1* |
| Z value | 8 | 2 | 2 |
| $\rho_{calc}$ (g / $cm^3$) | 3.200 | 3.091 | 3.692 |
| μ (Mo Kα) ($mm^{-1}$) | 21.155 | 20.018 | 24.268 |
| Temperature (K) | 294(2) | 294(2) | 294(2) |
| $2\Theta_{max}$ (°) | 50.64 | 49.94 | 47.64 |
| No. Obs. ( I > 2σ(I)) | 9246 | 4779 | 6742 |
| No. Parameters | 651 | 340 | 595 |
| Goodness of fit (GOF) | 1.022 | 1.030 | 0.981 |
| Max. shift in cycle | 0.000 | 0.000 | 0.000 |
| Residuals*: R1; wR2 | 0.0330; 0.0823 | 0.0471; 0.1417 | 0.0679; 0.1593 |
| Absorption Correction, Max/min | Multi-scan 1.000 / 0.354944 | Multi-scan 1.000 / 0.466344 | Multi-scan 1.000 / 0.478988 |
| Largest peak in Final Diff. Map ($e^-$ / $Å^3$) | 1.68 | 2.02 | 3.41 |

[a] $R = \Sigma_{hkl}(\,|\,|F_{obs}|-|F_{calc}|\,|)/\Sigma_{hkl}|F_{obs}|$; $R_w = [\Sigma_{hkl}w(\,|F_{obs}|-|F_{calc}|\,)^2/\Sigma_{hkl}wF^2_{obs}]^{1/2}$; $w = 1/\sigma^2(F_{obs})$; GOF = $[\Sigma_{hkl}w(\,|F_{obs}|-|F_{calc}|\,)^2/(n_{data}-n_{vari})]^{1/2}$.

**Table 6.1(continue). Crystallographic Data for Compounds 6.2 - 6.6.**

| Compound | **6.5** | **6.6** |
|---|---|---|
| Empirical formula | $Ir_4Ag_1C_{19}H_8O_{11}N_1$ | $Ir_4Ag_1C_{35}H_{20}O_{11}P_1$ |
| Formula weight | 1303.00 | 1524.23 |
| Crystal system | Monoclinic | Triclinic |
| Lattice parameters | | |
| *a* (Å) | 8.4194(6) | 9.6558(4) |
| *b* (Å) | 11.4307(8) | 12.8180(6) |
| *c* (Å) | 13.5542(9) | 15.6027(7) |
| α (deg) | 90.00 | 92.2760(10) |
| β (deg) | 99.7550(10) | 92.2280(10) |
| γ (deg) | 90.00 | 101.4040(10) |
| V ($Å^3$) | 1285.59(15) | 1889.34(15) |
| Space group | *P*2(1) | *P-1* |
| Z value | 2 | 2 |
| $\rho_{calc}$ ($g / cm^3$) | 3.366 | 2.679 |
| μ (Mo Kα) ($mm^{-1}$) | 21.431 | 14.645 |
| Temperature (K) | 294(2) | 294(2) |
| $2\Theta_{max}$ (°) | 56.70 | 56.08 |
| No. Obs. ( I > 2σ(I)) | 4497 | 5803 |
| No. Parameters | 327 | 469 |
| Goodness of fit (GOF) | 1.026 | 1.072 |
| Max. shift in cycle | 0.000 | 0.001 |
| Residuals*: R1; wR2 | 0.0396; 0.1115 | 0.0366; 0.0973 |
| Absorption Correction, | Multi-scan | Multi-scan |
| Max/min | 1.000 / 0.351260 | 1.000 / 0.643451 |
| Largest peak in Final Diff. Map ($e^- / Å^3$) | 2.56 | 0.90 |

[a] $R = \Sigma_{hkl}(||F_{obs}| - |F_{calc}||)/\Sigma_{hkl}|F_{obs}|$; $R_w = [\Sigma_{hkl}w(|F_{obs}| - |F_{calc}|)^2/\Sigma_{hkl}wF^2_{obs}]^{1/2}$; $w = 1/\sigma^2(F_{obs})$; $GOF = [\Sigma_{hkl}w(|F_{obs}| - |F_{calc}|)^2/(n_{data} - n_{vari})]^{1/2}$.

**Table 6.2.** A comparison of selected bond lengths and bond indices of **6.4**.

| Bond | Bond length | | Bond indices | |
|---|---|---|---|---|
| | Calc. (Å) | Expt. (Å) | Wiberg | Mayer |
| C1−Ag1 | 2.588 | 2.557 | 0.0713 | 0.0896 |
| C1−Ir4 | 2.134 | 2.105 | 0.4339 | 0.8846 |
| C2−Ag2 | 2.375 | 2.429 | 0.0777 | 0.2456 |
| C3−Ag2 | 2.361 | 2.262 | 0.1072 | 0.2765 |
| C3−Ir8 | 2.144 | 2.134 | 0.4418 | 0.7324 |
| Ag1−Ir4 | 2.874 | 2.858 | 0.0610 | 0.1214 |
| Ag1−Ir5 | 2.766 | 2.766 | 0.0738 | −0.5082 |
| Ag2−Ir5 | 2.813 | 2.781 | 0.1068 | −0.0262 |
| Ag2−Ir8 | 2.960 | 2.941 | 0.0487 | 0.0248 |
| Ir5−Ir8 | 2.940 | 2.882 | 0.1606 | −0.0529 |
| Ir1−Ir4 | 2.761 | 2.739 | 0.2198 | 0.5353 |

Table 6.3 Selected intramolecular angles and bond distances for compound **6.2**.[a]

| **Distances** | | | **Angles** | | | |
|---|---|---|---|---|---|---|
| Atom | Atom | Distance (Å) | Atom | Atom | Atom | Angle(deg) |
| Ir1 | Ir2 | 2.7482(5) | C14 | Ir2 | Ir1 | 161.7(2) |
| Ir1 | Ir3 | 2.7247(5) | Cu1 | Ir2 | Ir3 | 60.05(3) |
| Ir1 | Ir4 | 2.7307(5) | N1 | Cu1 | Ir2 | 170.0(3) |
| Ir2 | Ir3 | 2.8077(5) | Ir2 | Ir1 | Ir4 | 60.797(13) |
| Ir2 | Ir4 | 2.7725(5) | | | | |
| Ir3 | Ir4 | 2.7499(5) | | | | |
| Ir2 | Cu1 | 2.6628(12) | | | | |
| Ir3 | Cu1 | 2.7400(13) | | | | |
| Ir4 | Cu1 | 2.7667(13) | | | | |
| Ir2 | C14 | 2.133(9) | | | | |
| Cu1 | C14 | 2.171(9) | | | | |
| Cu1 | N1 | 1.907(9) | | | | |
| C1 | N1 | 1.111(13) | | | | |
| C1 | C2 | 1.474(18) | | | | |

[a] Estimated Standard deviations in the least significant figure are given in parentheses.

Table 6.4 Selected intramolecular angles and bond distances for compound **6.3**.[a]

| **Distances** | | | **Angles** | | | |
|---|---|---|---|---|---|---|
| Atom | Atom | Distance (Å) | Atom | Atom | Atom | Angle(deg) |
| Ir1 | Ir2 | 2.7308(10) | C43 | Ir3 | Ir1 | 94.9(5) |
| Ir1 | Ir3 | 2.7449(9) | Ag1 | Ir3 | Ir2 | 56.733(18) |
| Ir1 | Ir4 | 2.7129(10) | Ir2 | Ir1 | Ir4 | 60.37(3) |
| Ir2 | Ir3 | 2.8909(9) | | | | |
| Ir2 | Ir4 | 2.7369(9) | | | | |
| Ir3 | Ir4 | 2.7343(9) | | | | |
| Ir2 | Ag1 | 2.8035(7) | | | | |
| Ir3 | Ag1 | 3.0060(7) | | | | |
| Ir3 | C43 | 2.128(18) | | | | |
| Ir2 | C14 | 2.133(9) | | | | |

[a] Estimated Standard deviations in the least significant figure are given in parentheses.

Table 6.5 Selected intramolecular angles and bond distances for compound **6.4**.[a]

| **Distances** | | | **Angles** | | | |
|---|---|---|---|---|---|---|
| Atom | Atom | Distance (Å) | Atom | Atom | Atom | Angle(deg) |
| Ir1 | Ir2 | 2.7212(18) | C14 | Ir4 | Ir1 | 169.5(8) |
| Ir5 | Ir8 | 2.8817(18) | Ir2 | Ir1 | Ir4 | 61.28(5) |
| Ir6 | Ir7 | 2.6967(18) | C24 | Ir8 | Ir6 | 143.8(10) |
| Ir2 | Ag1 | 2.899(3) | Ag1 | Ir5 | Ir6 | 146.57(8) |
| Ir3 | Ag1 | 2.902(3) | Ag2 | Ir5 | Ag1 | 83.24(8) |
| Ir4 | Ag1 | 2.859(3) | Ir2 | Ir1 | Ir4 | 61.28(5) |
| Ir5 | Ag1 | 2.766(3) | | | | |
| Ir5 | Ag2 | 2.781(3) | | | | |
| Ir8 | Ag2 | 2.941(3) | | | | |
| Ir4 | C14 | 2.11(3) | | | | |
| Ag1 | C14 | 2.56(3) | | | | |
| Ag2 | C16 | 2.74(9) | | | | |
| Ag2 | C17 | 2.42(4) | | | | |
| Ag2 | C18 | 2.71(3), | | | | |
| Ag2 | C24 | 2.27(3) | | | | |
| Ir8 | C24 | 2.13(3) | | | | |

[a] Estimated Standard deviations in the least significant figure are given in parentheses.

Table 6.6 Selected intramolecular angles and bond distances for compound **6.5**.[a]

| **Distances** | | | **Angles** | | | |
|---|---|---|---|---|---|---|
| Atom | Atom | Distance (Å) | Atom | Atom | Atom | Angle(deg) |
| Ir1 | Ir2 | 2.7264(8) | C14 | Ir2 | Ir1 | 94.9(4) |
| Ir1 | Ir3 | 2.7217(7) | Ag1 | Ir2 | Ir3 | 59.87(2) |
| Ir1 | Ir4 | 2.7209(9) | N1 | Ag1 | Ir2 | 144.0(4) |
| Ir2 | Ir3 | 2.8141(7) | Ir2 | Ir1 | Ir4 | 62.190(16) |
| Ir2 | Ir4 | 2.8133(6) | | | | |
| Ir3 | Ir4 | 2.7802(8) | | | | |
| Ir1 | Ag1 | 2.8711(13) | | | | |
| Ir3 | Ag1 | 2.8374(10) | | | | |
| Ir4 | Ag1 | 2.8724(14) | | | | |
| Ir2 | C14 | 2.102(16) | | | | |
| Ag1 | C14 | 2.171(9) | | | | |
| Ag1 | N1 | 2.190(12) | | | | |
| C1 | N1 | 1.102(18) | | | | |
| C1 | C2 | 1.42(2) | | | | |

[a] Estimated Standard deviations in the least significant figure are given in parentheses.

Table 6.7 Selected intramolecular angles and bond distances for compound **6.6**.[a]

| **Distances** | | | **Angles** | | | |
|---|---|---|---|---|---|---|
| Atom | Atom | Distance (Å) | Atom | Atom | Atom | Angle(deg) |
| Ir1 | Ir2 | 2.7282(6) | C4 | Ir3 | Ir1 | 167.1(3) |
| Ir1 | Ir3 | 2.7566(6) | Ag1 | Ir2 | Ir3 | 61.30(2) |
| Ir1 | Ir4 | 2.7309(6) | P1 | Ag1 | Ir2 | 130.49(7) |
| Ir2 | Ir3 | 2.8017(6) | Ir2 | Ir1 | Ir4 | 61.080(15) |
| Ir2 | Ir4 | 2.7740(6) | | | | |
| Ir3 | Ir4 | 2.7941(6) | | | | |
| Ir2 | Ag1 | 2.9263(9) | | | | |
| Ir3 | Ag1 | 2.9219(9) | | | | |
| Ir4 | Ag1 | 2.9382(9) | | | | |
| Ir3 | C4 | 2.144(11) | | | | |
| Ag1 | C4 | 2.506(10) | | | | |
| Ag1 | P1 | 2.417(3) | | | | |

[a] Estimated Standard deviations in the least significant figure are given in parentheses.

## References


1) (a) Van Koten, G. *J. Organomet. Chem.* **1990**, *400*, 283 – 301. (b) Meyer, E. M.; Gambarotta, S.; Floriani, C.; Chiesi-Villa, A.; Guastini, C. *Organometallics*, **1989**, *8*, 1067 – 1079.

2) (a) Bradford, C. W.; Nyholm, R. S.; Gainsford, G. J.; Guss, J. M.; Ireland, P. R.; Mason, R. *J. Chem. Soc. Chem. Commun.* **1972**, 87 - 89. (b) Arce, A. J.; Arrojo, P.; Deeming, A. J.; De Sanctis, Y. *J. Chem. Soc., Chem. Commun.* **1991**, 1491 – 1492. (c) Adams, R. D.; Captain, B. and Zhu, L. *Inorg. Chem.*, **2007**, *46*, 4605 – 4611. (d) Deng, M. and Leong, W. K. *J. Chem. Soc., Dalton Trans.* **2002**, 1020 - 1023. (e) Adams, R. D. and Pearl, W. C., Jr., *J. Organomet. Chem.*, **2011**, *696*, 1198 - 1210. (f) Garcia, M. E.; Ramos, A.; Ruiz, M. A.; Lanfranchi, M. and Marchio, L. *Organometallics*, **2007**, *26*, 6197 - 6212. (g) Briard, P.; Cabeza, J. A.; Llamazares, A.; Ouahab, L. and Riera, V. *Organometallics*, **1993**, *12*, 1006 - 1008. (h) Cabeza, J. A.; Franco, R. J.; Llamazares, A. and Riera, V. *Organometallics*, **1994**, *13*, 55-59.

3) (a) Moret, M.-E.; Chen, P. *Organometallics* **2008**, *27*, 4903–4916. (b) Moret, M.-E.; Chen, P. *J. Am. Chem. Soc.* **2009,** *131*, 5675 – 5690. (c) Fernandez, E. J.; Laguna, A.; Lopez-de-Luzuriaga, J. M.; Monge, M.; Montiel, M.; Elena Olmos, M.; Rodriguez-Castillo, M. *Organometallics* **2006,** *25*, 3639-3646.

4) (a) Cotton, F. A. *Prog. Inorg. Chem.* **1976**, *21*, 1 - 28. (b) Colton, R.; McCormick, M. G. *Coord. Chem. Rev.* **1980**, *31*, 1-52.

5) (a) Adams, R. D.; Kan, Y.; Zhang, Q. *Organometallics* **2011**, *30*, 328 – 333. (b) Farrugia, L. J.; Miles, A. D.; Stone, F. G. A. *J. Chem. Soc., Dalton Trans.* **1984**, 2415 - 2422. (c) Hoferkamp, L. A.; Rheinwald, G.; Stoeckli-Evans, H.; Suss-Fink, G. *Organometallics* **1996**, *15*, 704 - 712. (d) Shima, T.; Suzuki, H. *Organometallics* **2005**, *24*, 1703 - 1708. (e) Akita, M.; Hua, R.; Oku, T.; Tanaka, M.; Moro-oka, Y. *Organometallics* **1996**, *15*, 4162 - 4177. (f) Alvarez, M. A.; Garcia, M. E.; Martinez, M.E.; Ramos, A.; Ruiz, M.A. *Organometallics* **2009**, *28*, 6293 - 6307.

6) Al-Mandhary Muna, R. A.; Lewis, J.; Raithby, P. R. *J. Organometal. Chem.* **1997**, *530*, 247 – 250.

7) Adams, R. D.; Chen, M. *Organometallics*, **2011**, *30*, 5867 - 5872.

8) Adams, R. D.; Chen, M. *Organometallics*, **2012**, *31*, 445 - 450.

9) Adams, R. D.; Chen, M.; Yang, X. *Organometallics*, **2012**, *31*, 3588 – 3598.

10) Adams, R. D.; Chen, M. *Organometallics*, **2012**, *31*, 6457 − 6465.

11) (a) Crabtree, R. H. *Topics Organomet. Chem.* **2011**, *34*, 1-10. (b) Montserrat, D.; Oscar, P.; Claver, C. *Topics Organomet. Chem.* **2011**, *34*, 11-29. (c) Woodmansee,

D. H.; Pfaltz, A. *Topics Organomet. Chem.* **2011**, *34*, 31-76. (d) Choi, J.; Goldman, A. S. *Topics Organomet. Chem.* **2011**, *34*, 139-167. (e) Hartwig, J. F.; Pouy, M. J. *Topics Organomet. Chem.* **2011**, *34*, 169-208. (f) Choi, J.; MacArthur, A. H. R.; Brookhart, M.; Goldman, A. S. *Chem. Rev.* **2011**, *111*, 1761 – 1779.

12) (a) Lu, J.; Pedro Serna, P.; Aydin, C.; Browning, N. D.; Gates, B. C. *J. Am. Chem. Soc.* **2011**, *133*, 16186 – 16195**.** (b) Gates, B. C., *Chem. Rev.* **1995**, *95*, 511 – 522. (c) Bayram, E.; Zahmakiran, M.; Ozkar S.; Finke, R. G. *Langmuir*, **2010**, *26*, 12455 – 12464. (d) Uzun, A.; Dixon, D. A.; Gates, B. C. *ChemCatChem* **2011**, *3*, 95 – 107. (e) Kulkarni, A.; Lobo-Lapidus, R.; Gates, B. *Chem. Commun.*, **2010**, 46, 5997 - 6015. (f) Fonseca, G. S.; Umpierre, A.P.; Fichtner, P. F. P.; Teixeira, S. R.; Dupont, J. *Chem. Eur. J.* **2003**, *9*, 3263 – 3269. (g) Gates, B. C. in *Catalysis by Di- and Polynuclear Metal Complexes*, Adams, R. D. and Cotton, F. A. Eds., Wiley-VCH Publishers, New York, 1998, Ch. 14.

13) (a) Oliver-Meseguer, J.; Cabrero-Antonino, J. R.; Dominquez, I.; Leyva-Perea, A.; Corma, A. *Science*, **2012**, *338*, 1452 – 1455. (b) Haruta, M. *Gold Bull.* **2004**, *37*, 27 - 36 (c) Haruta, M. *Catal. Today* **1997**, *36*, 153 – 166. (d) Haruta, M.; Date, M. *Appl. Catal. A: Gen.* **2001**, *222*, 427 – 437. (e) Hashmi, A. S. K.; Hutchings, G. J. *Angew. Chem. int. Ed.* **2006**, *45*, 7896 – 7936. (f) Della Pina, C.; Falletta, E.; Prati, L.; Rossi, M. *Chem. Soc. Rev.* **2008**, *37*, 2077 – 2095. (g) Lee, S.; Molina, L. M.; Lopez, M. J.; Alonso, J. A.; Hammer, B.; Lee, B.; Seifert, S.; Winans, R. E.; Elam, J. W.; Pellin, M. J.; Vajda, S. *Angew. Chem. int. Ed.* **2009**, *48*, 1467 – 1471. (h) Bravo-Suarez, J. J.; Lu, J.; Fujitani, T.; Oyama, S. T. *J. Catal.* **2008**, *255*, 114 – 126. (i) Herzing, A. A.; Kiely, C. J.; Carley, A. F.; Landon, P.; Hutchings, G. J. *Science* **2008**, *321*, 1331 – 1335. (j) Miedziak, P.; Sankar, M.; Dimitratos, M.; Lopez-Sanchez, J. A.; Carley, A. F.; Knight, D. W.; Taylor, S. H.; Kiely, C. J.; Hutchings, G. J. *Catal. Today* **2011**, *164*, 315–319.

14) (a) Zhang, Y.; Cui, X.; Shi, F.; Deng, Y. *Chem. Rev.* **2012**, *112*, 2467–2505. (b) Hutchings, G. J. *Chem. Commun.* **2008**, 1148 – 1164. (c) Lopez-Sanchez, J. A.; Dimitratos, N.; Glanvilla, N,; Kesavan, L.; Hammond, C.; Edwards, J. K.; Carley, A. F.; Kiely, C. J.; Hutchings, G. J. *Applied Catalysis A: General* **2011**, *391*, *400 – 406.* (d) Enache, D. I.; Edwards, J. K.; Landon, P.; Solsona-Espriu, B.; Carley, A. F.; Herzing, A. A.; Watanabe, M.; Kiely, C. J.; Knight, D. W.; Hutchings, G. J. *Science* **2006**, *311*, 362 – 365. (e) Ortiz-Soto, L. B.; Alexeev, O. S.; Amiridis, M. D. *Langmuir* **2006,** *22,* 3112-3117. (f) Evans, J.; Gao, J. *J. Chem. Soc., Chem. Commun.* **1985**, 39 - 40. (g) Li, Y.; Pan, W.-X.; Wong, W.-T. *J. Cluster Sci*. **2002**, *13*, 223 – 233.

15) Sabater, S.; Mata, J. A.; Peris, E. *Chem. Eur. J.* **2012**, *18*, 6380 – 6385.

16) (a) Sculfort, S.; Braunstein, P. *Chem. Soc. Rev.* **2011**, *40*, 2741–2760. (b) Salter, I. D. *Adv. Organomet. Chem.***1989**, *29*, 249 – 343. (c) Salter, I. D. in *Comprehensive Organometallic Chemistry II,* Abel, E. W.; Stone, F. G. A.; Wilkinson, G., Oxford, UK, **1995**, Vol. 10, Ch. 5, pp 255 – 322.

17) (a) Mamontov, G.V.; Magaev, O.V.; Knyazev, A.S.; Vodyankina, O.V. *Catal, Today* **2013**, *203*, 122– 126. (b) Yamamoto, R.; Sawayama, Y.; Shibahara, H.; Ichihashi, Y.; Nishiyama, S.; Tsuruya, S. *J. Catal.* **2005**, *234*, 308-317.

18) SAINT+, version 6.2a, Bruker Analytical X-ray Systems, Inc., Madison, WI, 2001.

19) G. M. Sheldrick, SHELXTL, version 6.1, Bruker Analytical X-ray Systems, Inc., Madison, WI, 1997.

20) Gaussian 09, Revision C.01, suite of programs for ab initio calculation; Frisch, M. J.; Trucks, G. W.; Schlegel, H. B.; Scuseria, G. E.; Robb, M. A.; Cheeseman, J. R.; Scalmani, G.; Barone, V.; Mennucci, B.; Petersson, G. A.; Nakatsuji, H.; Caricato, M.; Li, X.; Hratchian, H. P.; Izmaylov, A. F.; Bloino, J.; Zheng, G.; Sonnenberg, J. L.; Hada, M.; Ehara, M.; Toyota, K.; Fukuda, R.; Hasegawa, J.; Ishida, M.; Nakajima, T.; Honda, Y.; Kitao, O.; Nakai, H.; Vreven, T.; Montgomery, Jr., J. A.; Peralta, J. E.; Ogliaro, F.; Bearpark, M.; Heyd, J. J.; Brothers, E.; Kudin, K. N.; Staroverov, V. N.; Kobayashi, R.; Normand, J.; Raghavachari, K.; Rendell, A.; Burant, J. C.; Iyengar, S. S.; Tomasi, J.; Cossi, M.; Rega, N.; Millam, N. J.; Klene, M.; Knox, J. E.; Cross, J. B.; Bakken, V.; Adamo, C.; Jaramillo, J.; Gomperts, R.; Stratmann, R. E.; Yazyev, O.; Austin, A. J.; Cammi, R.; Pomelli, C.; Ochterski, J. W.; Martin, R. L.; Morokuma, K.; Zakrzewski, V. G.; Voth, G. A.; Salvador, P.; Dannenberg, J. J.; Dapprich, S.; Daniels, A. D.; Farkas, Ö.; Foresman, J. B.; Ortiz, J. V.; Cioslowski, J.; Fox, D. J. Gaussian, Inc., Wallingford CT, 2010.

21) Chai, J. -D.; Head-Gordon, M. *Phys. Chem. Chem. Phys.* **2008**, *10*, 6615 - 6620.

22) (a) Figgen, D.; Rauhut, G.; Dolg, M.; Stoll, H. *Chem. Phys.* **2005**, *311*, 227 - 244. (b) Peterson, K. A.; Puzzarini, C.; *Theor. Chem. Acc.* **2005**, *114*, 283 - 296.

23) Figgen, D.; Peterson, K.A.; Dolg, M.; Stoll, H. *J. Chem. Phys.* **2009**, *130*, 164108-1 – 164108-13.

24) Dunning Jr., T. H. *J. Chem. Phys.* **1989**, *90*, 1007 - 1023.

25) (a) Jensen, F. *Chem. Theory Comput.* **2010**, *6*, 2726 - 2735. (b) Thanthiriwatte, K. S.; Hohenstein, E. G.; Burns, L. A.; Sherrill, C. D. *J. Chem. Theory Comput.* **2011**, *7*, 88 - 96.

26) ADF2012; SCM Theoretical Chemistry, Vrije Universiteit, Amsterdam, The Netherlands, http://www.scm.com.

27) (a) Tao, J.; Perdew, J.P.; Staroverov, V.N. and Scuseria, G.E., *Physical Review Letters*, **2003**, 91, 146401-146404. (b)Staroverov, V.N.; Scuseria, G.E.; Tao, J. and Perdew, J.P., *J. Chem. Phys.*, **2003**, 119, 12129.

28) (a) Bader, R. F. W. *Atoms in Molecules: A Quantum Theory*, Oxford, Clarendon, 1990. (b) Cortés-Guzmán, F.; Bader, R. F. W. *Coord. Chem. Rev.* **2005**, *249*, 643.

29) AIMAll, Version 12.11.09, Keith, T. A. TK Gristmill Software, Overland Park KS, USA, 2012 (aim.tkgristmill.com).

30) Wiberg, K. B. *Tetrahedron* **1968**, *24*, 1083 - 1096.

31) Glendening, E. D.; Badenhoop, J. K.; Reed, A. E.; Carpenter, J. E.; Bohmann, J. A.; Morales, C. M.; Weinhold, F. *NBO 5.0*. Theoretical Chemistry Institute, University of Wisconsin, Madison, 2001.

32) Mayer, I. *J. Comput. Chem.* **2007**, *28*, 204 - 221.

33) Olmstead, M. M.; Power, P. P. *J. Am. Chem. Soc.* **1990,** *112*, 8008 - 8014.

34) Gambarotta, S.; Strobgo, S.; Floriani, C.; Chiesi-Villa, A.; Guastini, C. *Organometallics* **1984**, *3*, 1444 - 1445.

35) Della Pergola, R.; Garlaschelli, L.; Demartin, F.; Manassero, M.; Masciocchi, N. *J. Organomet. Chem.* **1992**, *436*, 241 – 253.

36) Fajardo, M.; Gomez-Sal, M. P.; Holden, H. D.; Johnson, B. F. G.; Lewis, J.; McQueen, R. C. S.; Raithby, P. R. *J. Organomet. Chem.*, **1984**, *267*, C25-C28.

37) Heaton, B. T.; Strona, L.; Martinengo, S.; Strumolo, D.; Albano, V. G.; Braga, D. *J. Chem. Soc., Dalton Trans.* **1983,** 2175 – 2182.

# BIBLIOGRAPHY

"A Biographical Memoir of Vladimir Haesnsel" written by Stanley Gembiki, published by the National Academy of Sciences in **2006**.

Adams, R. D. in *Comprehensive Organometallic Chemistry*, Abel, E. W.; Stone, F. G. A.; Wilkinson, G.; Pergamon, **1995**, Vol. 10, Ch. 1, pp 1 – 22.

Adams, R. D. in *The Chemistry of Metal Cluster Complexes*, Shriver, D. F.; Kaesz, H. D.; Adams, R. D., VCH Publishers, **1990**, Ch. 3, pp 121 – 170.

Adams, R. D.; Blom, D. A.; Captain, B.; Raja, R.; Thomas, J. M.; Trufan, E., *Langmuir*, **2008**, 24, 9223-9226.

Adams, R. D.; Boswell, E. M.; Captain, B.; Hungria, A. B.; Midgley, P. A.; Raja, R.; Thomas, J. M., *Angew. Chem.. int. Ed.*, **2007**, 46, 8182-8185.

Adams, R. D.; Captain, B. and Zhu, L. *Inorg. Chem.*, **2007**, 46, 4605 – 4611.

Adams, R. D.; Captain, B.; Smith, Jr., J. L. *Inorg. Chem.* **2005**, 44, 1413 – 1420.

Adams, R. D.; Chen, M. *Organometallics*, **2011**, 30(21), 5867-5872.

Adams, R. D.; Chen, M. *Organometallics*, **2012**, 31(1), 445-450.

Adams, R. D.; Chen, M. *Organometallics*, **2012**, 31, 6457-6465.

Adams, R. D.; Chen, M.; Trufan, E.; Zhang, Q. *Organometallics* **2011**, 30, 661-664.

Adams, R. D.; Chen, M.; Yang, X. *Organometallics*, **2012**, 31, 3588 – 3598.

Adams, R. D.; Kan, Y.; Zhang, Q. *Organometallics* **2011**, 30, 328 – 333.

Adams, R. D.; Rassolov, V.; Zhang, Q. *Organometallics* **2012**, 31, 2961 - 2964.

Adams, R. D.; Trufan, E. *Organometallics* **2010**, 29, 4346-4353.

Adams, R. D.; Trufan, E., *Phil. Trans Royal. Soc.* **2010**, 368, 1473-1493.

Adams, R. D.; Yang, L. W. *J. Am. Chem. Soc.* **1983**, 105, 235 – 240.

Adams, R.D.; Captain, B.; Hall, M.B.; Smith, J. L.; Webster, C.E. *J. Am. Chem. Soc.* **2005**, 127, 1007-1014.

Adams, R.D.; Captain, B.; Smith, J. L. *Inorg. Chem.* **2005**, 44, 1413-1420.

Adams, R.D.; Chen, M.; Trufan, E. *J. Organomet. Chem.* **2011**, 2894-2898.

Adams, R.D.; Fang, F.; Zhang, Q.; Hall, M.B.; Trufan, E. *Organometallics* **2012**, 31, 2621-2630.

Adams, R.D.; Trufan, E. *Organometallics* **2010**, 29, 4346-4353.

ADF2012; SCM Theoretical Chemistry, Vrije Universiteit, Amsterdam, The Netherlands, http://www.scm.com.

AIMAll, Version 12.11.09, Keith, T. A. TK Gristmill Software, Overland Park KS, USA, **2012** (aim.tkgristmill.com).

Akita, M.; Hua, R.; Oku, T.; Tanaka, M.; Moro-oka, Y. *Organometallics* **1996**, 15, 4162 - 4177.

Albano, V. G.; Braga, D.; Ros, R.; Scrivanti, A. J. Chem. Soc., *Chem. Commun.*, **1985**, 866 - 868.

Al-Mandhary Muna, R. A.; Lewis, J.; Raithby, P. R. *J. Organometal. Chem.* **1997**, 530, 247 – 250.

Al-Mandhary, M. R. A.; Lewis, J.; Raithby, P. R. *J. Organomet. Chem.* **1997**, 536-537, 549 – 551.

Alvarez, M. A.; Garcia, M. E.; Martinez, M.E.; Ramos, A.; Ruiz, M.A. *Organometallics* **2009**, 28, 6293 - 6307.

Amoroso, A. J.; Johnson, B. F. G.; Lewis, J.; Raithby, P. R.; Wong, W.-T. *J. Chem. Soc., Chem. Commun.* **1991**, 814 – 815.

Angoletta, M.; Malatesta, L.; Caglio, G. *J. Organomet. Chem.* **1975**, 94, 99 – 106.

Araujo, M.H.; Avent, A.G.; Hitchcock, P.B.; Nixon, J.F.; Vargas, M.D. *Organometallics*, **1998**, 17, 5460-5466.

Arce, A. J.; Arrojo, P.; Deeming, A. J.; De Sanctis, Y. *J. Chem. Soc., Chem. Commun.* **1991**, 1491 – 1492.

Arena, C. G.; Drommi, D.; Faraone, F.; Lanfranchi, M.; Nicolo, F.; Tiripicchio, A. *Organometallics*, **1996**, 15, 3180-3175.

Argo, A. M.; Odzak, J. F.; Gates, B. C. *J. Am. Chem. Soc.* **2003**, 125, 7107-7115.

Argo, A. M.; Odzak, J. F.; Goellner, J. F.; Lai, F. S.; Xiao, F.-S.; Gates, B. C. *J. Phys. Chem. B* **2006**, 110, 1775-1786.

Argo, A.M.; Odzak, J. F.; Gates, B.C. *J. Am. Chem. Soc.* **2003**, 125, 7107-7115.

Aydin, C.; Lu. J.; Browning, N.D.; Gates, B.C. *Angew. Chem. Int. Ed.* **2012**, 51, 5929-5934.

Bader, R. F. W. *Atoms in Molecules: A Quantum Theory*, Oxford, Clarendon, **1990**.

Bailey, P. J.; Conole, G.; Johnson, B. F. G.; Lewis, J.; McPartlin, M.; Moule, A.; Powell, H. R.; Wilkinson, D. A. *J. Chem. Soc., Dalton Trans.*, **1995**, 741 - 751.

Bau, R.; Chiang, M. Y.; Wei, C.-Y.; Garlaschelli, L.; Martinengo, S.; Koetzle, T. F. *Inorg. Chem.* **1984**, 23, 4758 – 4762.

Bau, R.; Drabnis, M. H. *Inorg. Chim. Acta* **1997**, 259, 27-50.

Bayram, E.; Zahmakiran, M.; Ozkar S.; Finke, R. G. *Langmuir*, **2010**, 26, 12455 – 12464.

Bellon, P.; Manassero, M.; Sansoni, M. *J. Chem. Soc., Dalton Trans.* **1973**, 2423 – 2427.

Benvenutti, M.H.; Hitchcock, P.B.; Nixon, J.F.; Vargas, M.D. *Chem. Commun.* **1996**, 441-443.

Bojan, R. V.; López-de-Luzuriaga, J. M.; Monge, M.; Olmos, M. E. . *J. Organomet. Chem.* **2010**, 696, 2385 – 2393.

Bradford, C. W.; Nyholm, R. S.; Gainsford, G. J.; Guss, J. M.; Ireland, P. R.; Mason, R. *J. Chem. Soc. Chem. Commun.* **1972**, 87 - 89.

Braga, D.; Grepioni, F.; Livotto, F. S.; Vargas, M. D. *J. Organomet. Chem.* **1990**, 391, C28 – C32.

Braga, D.; Grepioni, F.; Righi, S.; Johnson, B. F. G.; Frediani, P.; Bianchi, M.; Piacenti, F.; Lewis, J. *Organometallics*, **1992**, 11, 706 - 711.

Braunstein, P.; Rose, J. in *Catalysis by Di- and Polynuclear Metal Cluster Complexes*; Adams, R.D., Cotton, F.A.; Eds.; Wiley-VCH: New York, **1998**; Chapter 13.

Bravo-Suarez, J. J.; Lu, J.; Fujitani, T.; Oyama, S. T. *J. Catal.* **2008**, 255, 114 – 126.

Briard, P.; Cabeza, J. A.; Llamazares, A.; Ouahab, L. and Riera, V. *Organometallics*, **1993**, 12, 1006 - 1008.

Brivio, E.; Alessandro Cerrioti, A.; Della Pergola, R.; Garlaschelli, L.; Demartin, F.; Manassero, M.; Sansoni, M.; Zanello, P.; Laschi, F.; Heaton, B. T. *J. Chem. Soc., Dalton Trans.*, **1994**, 3237 - 3242.

Brune, H.A.; Schmidtberg, G.; Weisemann, C. *J. Organomet. Chem.* **1989**, 371, 121-127.

Burch, R. *J. Catal.* **1981**, 71, 348-359.

Burch, R.; Garla, L.C. *J. Catal.* **1981**, 71, 360-372.

Cabeza, J. A.; Franco, R. J.; Llamazares, A. and Riera, V. *Organometallics*, **1994**, 13, 55-59.

Castiglioni, M.; Giordano, R.; Sappa, E. *J. Organomet. Chem.* **1987**, 319, 167-181.

Ceriotti, A.; Della Pergola, R.; Garlaschelli, L.; Manassero, M.; Masciocchi, N. *Organometallics* **1995**, 14, 186 – 193.

César, V.; Bellemin-Laponnaz, S.; Gade, L. H. *Chem. Soc. Rev.* **2004**, 33, 619 – 636.

Chai, J. -D.; Head-Gordon, M. *Phys. Chem. Chem. Phys.* **2008**, 10, 6615 - 6620.

Chihara, T.; Komoto, R.; Kobayashi, K.; Yamazaki, H.; Matsuura, and Y. *Inorg. Chem.*, **1989**, 28, 964 - 967.

Chihara, T.; Sato M.; Konomoto, H.; Kamiguchi, S.; Ogawa, H.; Wakatsuki, Y. *J. Chem. Soc., Dalton Trans.* **2000**, 2295 - 2299.

Chini, P. *J. Organomet. Chem.* **1980**, 200, 37-61.

Chini, P.; Ciani, G.; Garlaschelli, L.; Manassero, M.; Martinengo, S.; Sironi, A.; Canziani, F. *J. Organomet. Chem.*, **1978**, 152, C35-C38.

Choi, J.; Goldman, A. S. *Top. Organomet. Chem.* **2011**, 34, 139-168.

Choi, J.; MacArthur, A. H. R.; Brookhart, M.; Goldman, A. S. *Chem. Rev.* **2011**, 111, 1761 – 1779.

Church, T. L.; Andersson, P. G. *Coord. Chem. Rev.* **2008**, 252, 513 – 531.

Churchill, M. R.; Hutchinson, J. P. *Inorg. Chem.* **1987**, 17, 3528 – 3535.

Ciani, G.; Garlaschelli, L.; Manassero, M.; Martinengo, S.; Sironi, A.; Canziani, F., *J. Organomet. Chem.*, **1980**, 199, 271-279.

Colton, R.; McCormick, M. G. *Coord. Chem. Rev.* **1980**, 31, 1-52.

Comstock, M. C.; Prussak-Wieckowska, T.; Wilson, S. R.; Shapley, J. R. *Organometallics* **1997**, 16, 4033 – 4040.

Cortés-Guzmán, F.; Bader, R. F. W. *Coord. Chem. Rev.* **2005**, 249, 643.

Cotton, F. A. *Prog. Inorg. Chem.* **1976**, 21, 1 - 28.

Crabtree, R. H. *Topics Organomet. Chem.* **2011**, 34, 1-10.

Crabtree, R.H.; Mihelcic, J.M.; Quirk, J.M. *J. Am. Chem. Soc.* **1979**, 101, 7738-7740.

de Araujo M. H.; M. D.; Braga, D.; Grepioni, F. *Polyhedron* **1998**, 17, 2865-2875.

Della Pergola, R.; Ceriotti, A.; Garlaschelli, L.; Demartin, F.; Manassero, M.; Masciocchi, N.; Sansoni, M. *Inorg. Chem.* **1993**, 32, 3277-3281.

Della Pergola, R.; Demartin, F.; Garlaschelli, L.; Manassero, M.; Martinengo, S.; Masciocchi, N.; Zanello, P. *Inorg. Chem.* **1993**, 32, 3670 – 3674.

Della Pergola, R.; Demartin, F.; Garlaschelli, L.; Manassero, M.; Martinengo, S.; Masciocchi, N.; Sansoni, M. *Organometallics* **1991**, 10, 2239 – 2247.

Della Pergola, R.; Garlaschelli, L.; Demartin, F.; Manassero, M.; Masciocchi, N. *J. Organomet. Chem.* **1992**, 436, 241 – 253.

Della Pergola, R.; Garlaschelli, L.; Demartin, F.; Manassero, M.; Masciocchi, N.; Sansoni, M.; Fumagalli, A. *Dalton, Trans.* **1989**, 1109-1116.

Della Pergola, R.; Garlaschelli, L.; Manassero, M.; Sansoni, M. *J. Cluster Sci.* **1999**, 12, 109 – 119.

Della Pergola, R.; Garlaschelli, L.; Manassero, M.; Sansoni, M.; Strumolo, D. *J. Cluster Sci.* **2001**, 12, 23 – 34.

Della Pina, C.; Falletta, E.; Prati, L.; Rossi, M. *Chem. Soc. Rev.* **2008**, 37, 2077 – 2095.

Deng, M. and Leong, W. K. *J. Chem. Soc., Dalton Trans.* **2002**, 1020 - 1023.

Adams, R. D. and Pearl, W. C., Jr., *J. Organomet. Chem.*, **2011**, 696, 1198 - 1210.

Didillon, B.; Candy, J.P.; Lepepetier, F.; Ferretti, O.A.; Basset, J.M. *Studies Surf. Sci. Catal.* **1993**, 78, 147-154.

Dombek, B.D. *Organometallics*, **1985**, 4, 1707-1712.

Dunning Jr., T. H. *J. Chem. Phys.* **1989**, 90, 1007 - 1023.

Eaborn, C.; Kundu, K.; Pidcock, A. *J. Organomet. Chem.* **1979**, 170, C18-C20.

Eaborn, C.; Odell, K. J.; Pidcock, A. *J. Chem. Soc. Dalton Trans.* **1978**, 1288-1294.

Eaborn, C.; Odell, K. J.; Pidcock, A. *J. Chem. Soc. Dalton Trans.* **1978**, 357-368.

Eaborn, C.; Odell, K. J.; Pidcock, A. *J. Chem. Soc. Dalton Trans.* **1979**, 134-138.

Eaborn, C.; Odell, K. J.; Pidcock, A. *J. Chem. Soc. Dalton Trans.* **1979**, 758-760.

Eaborn, C.; Odell, K. J.; Pidcock, A. *J. Organomet. Chem.* **1975**, 96, C38-C40.

Eaborn, C.; Odell, K. J.; Pidcock, A. *J. Organomet. Chem.* **1978**, 146, 17-21.

Enache, D. I.; Edwards, J. K.; Landon, P.; Solsona-Espriu, B.; Carley, A. F.; Herzing, A. A.; Watanabe, M.; Kiely, C. J.; Knight, D. W.; Hutchings, G. J. *Science* **2006**, 311, 362 – 365.

Espinet, P.; Echavarren, A. M. *Angew. Chem. Int. Ed*. **2004**, 43, 4704 – 4734.

Evans, J.; Gao, J. *J. Chem. Soc., Chem. Commun.* **1985**, 39 - 40.

Fajardo, M.; Gomez-Sal, M. P.; Holden, H. D.; Johnson, B. F. G.; Lewis, J.; McQueen, R. C. S.; Raithby, P. R. *J. Organomet. Chem.*, **1984**, 267, C25-C28.

Farrugia, L. J.; Miles, A. D.; Stone, F. G. A. *J. Chem. Soc., Dalton Trans.* **1984**, 2415 - 2422.

Femoni C.; Iapalucci, M. C.; Longoni G.; Svensson, P. H. *Inorg. Chim. Acta* **2002**, 330, 111 - 117.

Fernandez, E. J.; Laguna, A.; Lopez-de-Luzuriaga, J. M.; Monge, M.; Montiel, M.; Elena Olmos, M.; Rodriguez-Castillo, M. *Organometallics* **2006**, 25, 3639-3646.

Figgen, D.; Peterson, K.A.; Dolg, M.; Stoll, H. *J. Chem. Phys.* **2009**, 130, 164108-1 – 164108-13.

Figgen, D.; Rauhut, G.; Dolg, M.; Stoll, H. *Chem. Phys.* **2005**, 311, 227 - 244.

Fonseca, G. S.; Umpierre, A.P.; Fichtner, P. F. P.; Teixeira, S. R.; Dupont, *J. Chem. Eur. J.* **2003**, 9, 3263 – 3269.

Fonseca, G.S.; Umpierre, A.P.; Fichtner, P.F.P.; Teixeira, S.R.; Dupont, *J. Chem. Eur. J.* **2003**, 9, 3263-3269.

Freeman, M. J.; Orpen, A. G.; Salter, I. D. *J. Chem. Soc., Dalton Trans.* **1987**, 379 – 390.

Fumagalli, A.; Della Pergola, R.; Bonacina, F.; Garlaschelli, L.; Moret, M.; Sironi, A. *J. Am. Chem. Soc.* **1989**, 111, 165-173.

Fumagalli, A.; Koetzle, T.F.; Takusagawa, F. *J. Organomet. Chem.* **1981**, 213, 365-377.

Fung, A.S.; McDevitt, M.R.; Tooley, P.A.; Kelley, M.J.; Koningsberger, D.C.; Gates, B.C. *J.Catal.* **1993**, 140, 190-208.

G. M. Sheldrick, SHELXTL, version 6.1, Bruker Analytical X-ray Systems, Inc., Madison, WI, **1997**

Gabbai, F. P.; Schier, A.; Reide, J., Schmidbaur, H. *Chem. Ber./Recueil* **1997**, 130, 111-113.

Gambarotta, S.; Strobgo, S.; Floriani, C.; Chiesi-Villa, A.; Guastini, C. *Organometallics* **1984**, 3, 1444 - 1445.

Garcia, M. E.; Ramos, A.; Ruiz, M. A.; Lanfranchi, M. and Marchio, L. *Organometallics*, **2007**, 26, 6197 - 6212.

Garlaschelli, L.; Martinengo, S.; Chini, P.; Canziani, F.; Bau, R. *J. Organomet. Chem.* **1981**, 213, 379-388.

Gates, B. C. *Chem. Rev.* **1995**, 95, 511-522.

Gates, B. C. in *Catalysis by Di- and Polynuclear Metal Complexes*, Adams, R. D. and Cotton, F. A. Eds., Wiley-VCH Publishers, New York, **1998**, Ch. 14.

Gates, B. C., *Chem. Rev.* **1995**, 95, 511 – 522.

Gaussian 09, Revision B.01, suite of programs for ab initio calculation; Frisch, M. J.; Trucks, G. W.; Schlegel, H. B.; Scuseria, G. E.; Robb, M. A.; Cheeseman, J. R.; Scalmani, G.; Barone, V.; Mennucci, B.; Petersson, G. A.; Nakatsuji, H.; Caricato, M.; Li, X.; Hratchian, H. P.; Izmaylov, A. F.; Bloino, J.; Zheng, G.; Sonnenberg, J. L.; Hada, M.; Ehara, M.; Toyota, K.; Fukuda, R.; Hasegawa, J.; Ishida, M.; Nakajima, T.; Honda, Y.; Kitao, O.; Nakai, H.; Vreven, T.; Montgomery, Jr., J. A.; Peralta, J. E.; Ogliaro, F.; Bearpark, M.; Heyd, J. J.; Brothers, E.; Kudin, K. N.; Staroverov, V. N.; Kobayashi, R.; Normand, J.; Raghavachari, K.; Rendell, A.; Burant, J. C.; Iyengar, S. S.; Tomasi, J.; Cossi, M.; Rega, N.; Millam, N. J.; Klene, M.; Knox, J. E.; Cross, J. B.; Bakken, V.; Adamo, C.; Jaramillo, J.; Gomperts, R.; Stratmann, R. E.; Yazyev, O.; Austin, A. J.; Cammi, R.; Pomelli, C.; Ochterski, J. W.; Martin, R. L.; Morokuma, K.; Zakrzewski, V. G.; Voth, G. A.; Salvador, P.; Dannenberg, J. J.; Dapprich, S.; Daniels, A. D.; Farkas, ?.; Foresman, J. B.; Ortiz, J. V.; Cioslowski, J.; Fox, D. J. Gaussian, Inc., Wallingford CT, 2010.

Glendening, E. D.; Badenhoop, J. K.; Reed, A. E.; Carpenter, J. E.; Bohmann, J. A.; Morales, C. M.; Weinhold, F. NBO 5.0. Theoretical Chemistry Institute, University of Wisconsin, Madison, **2001**.

Gupta, M.; Hagen, C.; Kaska, W. C.; Cramer, R. E.; Jensen C. M. *J. Am. Chem. Soc.* **1997**, 119, 840-841.

Haensel, V. "*Chemistry of Petroleum Hydrocarbons*", eds Brooks, B.T.; Boord, C.E.;Kurtz, S.S. and Schmerling, L., New York, Reinhold **1955**, 6, 189.

Harding, M. M.; Nicholls, B. S.; Smith, A. K., *J. Chem. Soc., Dalton Trans.* **1983**, 1479-1481.

Hartwig, J. F.; Pouy, M. *J. Topics Organomet. Chem.* **2011**, 34, 169-208.

Hartwig, J. F.; Stanley, L. M. *Acc. Chem Res.* **2010**, 43, 1461 – 1475.

Haruta, M. *Catal. Today* **1997**, 36, 153 – 166.

Haruta, M. *Gold Bull.* **2004**, 37, 27 - 36.

Haruta, M.; Date, M. *Appl. Catal. A: Gen.* **2001**, 222, 427 – 437.

Hashmi, A. S. K.; Hutchings, G. J. *Angew. Chem. int. Ed.* **2006**, 45, 7896 – 7936.

Hawkins, S.M.; Hitchcock, P.B.; Lappert, M.F.; Rai, A.K.; *Chem.Commun.* **1986**, 1689-1690.

Hay, C. M.; Johnson, B. F. G.; Lewis, J.; McQueen, R. C. S.; Raithby, P. R.; Sorrell, R. M.; Taylor, M. J. *Organometallics* **1985**, 4, 202 – 205.

Heaton, B. T.; Strona, L.; Martinengo, S.; Strumolo, D.; Albano, V. G.; Braga, D. *J. Chem. Soc., Dalton Trans.* **1983**, 2175 – 2182.

Heng, W. Y.; Hu, J.; Yip, J. H. *Organometallics*, **2007**, 26, 6760-6768.

Herzing, A. A.; Kiely, C. J.; Carley, A. F.; Landon, P.; Hutchings, G. J. *Science* **2008**, 321, 1331 – 1335.

Hirano, M.; Akita, M.; Tani, K.; Kumagai, K.; Kasuga, N.; Fukuoka, A.; Komiya, S. *Organometallics* **1997**, 16, 4206-4213.

Hoferkamp, L. A.; Rheinwald, G.; Stoeckli-Evans, H.; Suss-Fink, G. *Organometallics* **1996**, 15, 704 - 712.

Holt, M.S.; Wilson, W.L.; Nelson, J.H. *Chem. Rev.* **1989**, 89, 11-49.

Hungria, A. B.; Raja, R.; Adams, R. D.; Captain, B.; Thomas, J. M.; Midgley, P. A.; Golvenko, V., Johnson, B. F. G., *Angew. Chem. int. Ed.*, **2006**, 45, 4782-4785.

Hutchings, G. J. *Chem. Commun.* **2008**, 1148 – 1164.

Huttner, G.; Schneider, J.; Muller, H. D.; Mohr, G.; Seyerl, J. V.; Wohlfahrt, L. A*ngew. Chem. int. Ed.* **1979**, 18, 76 - 77.

Iwai, T.; Fujihara, T.; Terao, J.; Tsuji, Y. *J. Am. Chem. Soc.* **2012**, 134, 1268 – 1274.

Jackson, P. F.; Johnson, B. F. G.; Lewis, J.; Nelson, W. J. H.; McPartlin, M. *J. Chem. Soc., Dalton Trans.*, **1982**, 2099.

Jensen, C. M. *Chem. Commun.* **1999**, 2443 – 2449.

Jensen, F. *Chem. Theory Comput.* **2010**, 6, 2726 - 2735.

Jerdev, D. I.; Olivas, A.; Koel, B. E., *J. Catal.* **2002**, 205, 278-288.

Jones, J. H. *Platinum Metals Rev.* **2000**, 44, 94 – 105.

Kulkarni, A.; Lobo-Lapidus, R.; Gates, B. *Chem. Commun.*, **2010**, 46, 5997 - 6015.

L. Malatesta, L. Naldini, G. Simonetta and F. Cariati, *Coord. Chem. Rev.* **1966**, 1, 255-262.

Lafaye, G.; Micheaud-Especel, C.; Montassier, C.; Marecot, P. *Appl.Catal. A: Gen.* **2004**, 257, 107-117.

Lafaye, G.; Micheaud-Especel,, G.; Montassier, C.; Marecot, P. *Appl. Catal. A: Gen.* **2002**, 230, 19-30.

Lafaye, G.; Mihut, C.; Especel, C.; Marecot, P.; Amiridis, M.D. *Langmuir*, **2004**, 20, 10612-10616.

Lee, S.; Molina, L. M.; Lopez, M. J.; Alonso, J. A.; Hammer, B.; Lee, B.; Seifert, S.; Winans, R. E.; Elam, J. W.; Pellin, M. J.; Vajda, S. *Angew. Chem. int. Ed.* **2009**, 48, 1467 – 1471.

Li, F.; Gates, B. C. *J. Phys. Chem. C* **2007**, 111 262-267.

Li, Y.; Pan, W.-X.; Wong, W.-T. *J. Cluster Sci.* **2002**, 13, 223 – 233.

Li, Y.; Wong, W. T. *Eur. J. Inorg. Chem.* **2003**, 2651 - 2662.

Liu, F.; Goldman, A.S. *Chem. Commun.* **1999**, 655-656.

Liu, F.; Pak, E.B.; Singh, B.; Jensen, C.M.; Goldman, A.S. *J. Am. Chem. Soc.* **1999**, 125, 7770-7771.

Livotto, F. S.; Vargas, M. D.; Braga, D.; Grepioni, F.; *J. Chem. Soc. Dalton Trans.* **1992**, 577 – 584.

Lopez-Sanchez, J. A.; Dimitratos, N.; Glanvilla, N,; Kesavan, L.; Hammond, C.; Edwards, J. K.; Carley, A. F.; Kiely, C. J.; Hutchings, G. *J. Applied Catalysis A*: General **2011**, 391, 400 – 406.

Lu, J.; Aydin, C.; Browning, N.D.; Gates, B.C. *J. Am. Chem. Soc.* **2012**, 134, 5022-5025.

Lu, J.; Aydin, C.; Browning, N.D.; Wang, L.; Gates, B.C. *Catal. Lett.* **2012**, 142, 1445-1451.

Lu, J.; Pedro Serna, P.; Aydin, C.; Browning, N. D.; Gates, B. C. *J. Am. Chem. Soc.* **2011**, 133, 16186 – 16195.

Lu, J.; Serna, P.; Aydin, C.; Browning, N.D.; Gates, B.C. *J. Am. Chem. Soc.* **2011**, 133, 16186-16195.

Lu, S.-M.; Han, X.-W.; Zhou, Y.-G. *Adv. Synth. Catal.* **2004**, 346, 909 – 912.

M. T. Ahmet, A. Houlton, C. S. Frampton, J.R. Miller, R. M. Roberts, J. Silver and B.Yavari, *J. Chem. Soc. Dalton Trans.*, **1993**, 1, 3085-3092.

Macleod, N.; Fryer, J.R.; Stirling , D.; Webb, G. *Catal. Today* **1998**, 46, 37-54.

Mamontov, G.V.; Magaev, O.V.; Knyazev, A.S.; Vodyankina, O.V. *Catal, Today* **2013**, 203, 122– 126.

Margalef-Catala, R.; Claver, C.; Salagre, P.; Fernandez, E. *Tetrahedron: Asymmetry* **2000**, 11, 1469.

Matthias, W.; Haenel, M. W.; Oevers, S.; Angermund, K.; Kaska, W. C.; Fan, H.-J.; Hall, M. B. *Angew. Chem. int. Ed.* **2001**, 40, 3596 – 3600.

Mayer, I. *J. Comput. Chem.* **2007**, 28, 204 - 221.

McVicker, G.B.; Daage, M.; Touvelle, M.S.; Hudson, C.W.; Klein, D.P.; Baird, W.C.; Cook, B.R.; Chen, J.G.; Hantzer, S.; Vaughan, D.E.W.; Ellis, E.S.; Feeley, O.C. *J. Catal.* **2002**, 210, 137-148.

Meyer, E. M.; Gambarotta, S.; Floriani, C.; Chiesi-Villa, A.; Guastini, C. *Organometallics*, **1989**, 8, 1067 – 1079.

Meyer, N.; Lehmann, C. W.; Lee, T. K. M.; Rust, J.; Yam, V. W. W.; Mohr, F. *Organometallics* **2009**, 28, 2931-2934.

Meyer, N.; Sivanathan, S.; Mohr, F. *J. Organomet. Chem.* **2011**, 696, 1244-1247.

Miedziak, P.; Sankar, M.; Dimitratos, M.; Lopez-Sanchez, J. A.; Carley, A. F.; Knight, D. W.; Taylor, S. H.; Kiely, C. J.; Hutchings, G. *J. Catal. Today* **2011**, 164, 315–319.

Mingos, D. M. P. *Acc. Chem. Res.* **1984**, 17, 311 – 319.

Molter, A.; Mohr, F. Z. *Anorg, Allg. Chem.* **2009**, 635, 134-138.

Montserrat, D.; Oscar, P.; Claver, C. *Topics Organomet. Chem.* **2011**, 34, 11-29.

Moret, M.-E.; Chen, P. *J. Am. Chem. Soc*. **2009**, 131, 5675 – 5690.

Moret, M.-E.; Chen, P. *Organometallics* **2008**, 27, 4903–4916.

Moura, F. C. C.; dos Santos, E. N.; Lago, R. M.; Vargas, M. D.; Araujo, M. H. *J. Molec. Catal. A: Chem.* **2005**, 226, 243 – 251.

Muetterties, E. L. *Bull. Soc. Chim. Belg.* **1975**, 84, 959-986.

Muetterties, E. L. *Bull. Soc. Chim. Belg.* **1976**, 85, 451-470.

Muetterties, E.L.; Rhodin, T.N.; Band, E.; Brucker, C.F.; Retzer, W.R. *Chem. Rev.* **1979**, 79, 91-136.

Neale, N.R.; Tilley T.D., *J. Am. Chem. Soc.* **2005**, 127, 14745-14755.

Nicholls, J. N.; Raithby, P. R.; Vargas, M. D. *J. Chem. Soc., Chem. Commun.* **1986**, 1617 – 1619.

Oliver-Meseguer, J.; Cabrero-Antonino, J. R.; Dominquez, I.; Leyva-Perea, A.; Corma, A. *Science*, **2012**, 338, 1452 – 1455.

Olmstead, M. M.; Power, P. P. *J. Am. Chem. Soc.* **1990**, 112, 8008 - 8014.

Orpen, A. G.; Salter, I. D. *Organometallics* **1991**, 10, 111 – 117.

Ortiz-Soto, L. B.; Alexeev, O. S.; Amiridis, M. D. *Langmuir* **2006**, 22, 3112-3117.

Park, Y. K.; Ribeiro, F.H.; Somorjai, G.A. *J. Catal.* **1998**, 178, 66-75.

Partyka, D. V.; Zeller, M.; Hunter, A. D.; Gray, T. G. *Angew. Chemie*, **2006**, 45(48), 8188-8191.

Pereira, R.M.S.; Fujiwara, F.Y.; Vargas, M. D. *Organometallics* **1997**, 16, 4833-4838.

Perry, M. C.; Cui, X. H.; Powell, M. T.; Hou, D. R.; Reibenspies, J. H.; Burgess, K. *J. Am. Chem. Soc.* **2003**, 125, 113 – 123.

Peterson, K. A.; Figgen, D.; Dolg, M.; Stoll, H. *J. Chem. Phys.* **2007**, 126, 124101.

Peterson, K. A.; Puzzarini, C.; *Theor. Chem. Acc.* **2005**, 114, 283 - 296.

Piccolo, L.; Nassreddine, S.; Aouine, M.; Geantet, C. *J. Catal.* **2012**, 292, 173-180.

Psaro, R.; Dossi, C.; Della Pergola, R.; Garlaschelli, L.; Calmotti, S.; Marngo, S.; Bellatreccia, M.; Zanoni, R., *Appl. Catal. A: Gen.* **1995**, 121, L19-L23.

Rice, R.W.; Lu, K. *J.Catal.* **1982**, 77, 104-117.

Ros, R. and Scrivanti, A. *J. Chem. Soc., Dalton Trans.* **1986**, 11 2411-2421.

Ros, R.; Canziani, F.; Roulet, R. *J. Organomet. Chem.*, **1984**, 267, C9 – C12.

Ros, R.; Scrivanti, A. *J. Chem. Soc. Dalton Trans.* 1986, 11 2411-2421.

Ros, R.; Scrivanti, A.; Albani, V.G.; Braga, D.; Garlaschelli, L., *J. Chem. Soc., Dalton Trans.*, **1986**, 2411-2421.

Ros, R.; Scrivanti, A.; Roulet, R. *J. Organomet. Chem.*, **1986**, 303, 273 – 282.

Ros, R.; Tassan, A.; Rosario Scopelliti, R.; Roulet, R. *Inorg. Chim. Acta* **2005**, 358, 2327 – 2331.

Sabater, S.; Mata, J. A.; Peris, E. *Chem. Eur. J.* **2012**, 18, 6380 – 6385.

Sablong, R.; Osborn, J.A. *Tetrahedron: Asymmetry* **1996**, 7, 3059.

SAINT+, version 6.2a, Bruker Analytical X-ray Systems, Inc., Madison, WI, **2001**.

Salter, I. D. *Adv. Organomet. Chem.***1989**, 29, 249 – 343.

Salter, I. D. in *Comprehensive Organometallic Chemistry II*, Abel, E. W.; Stone, F. G. A.; Wilkinson, G., Oxford, UK, **1995**, Vol. 10, Ch. 5, pp 255 – 322.

Salter, I. D. in *Metal Clusters in Chemistry, Braunstein*, P.; Oro, L. A.; Raithby, P. R., Eds., Wiley-VCH, Weinheim, Ch. 1.27, pp 509 – 534.

Sayers, D.E.; Lytle, F.W.; and Stern, E. *Phys. Rev. Lett.* **1971**, 27, 1204-1207.

Sculfort, S.; Braunstein, P. *Chem. Soc. Rev.* **2011**, 40, 2741–2760.

Senn, D. R.; Gladysz, J. A.; Emerson, K.; Larsen, R. D. *Inorg. Chem.* **1987**, 17, 2737-2739.

Shi, L. L .; Zhao, S. S .; Zhao, S. S .; Li, H .; Su, Z. *Theor. Chem. Acc.* **2009**, 124, 29-36.

Shima, T.; Suzuki, H. *Organometallics* **2005**, 24, 1703 - 1708.

Sinfelt J. H. *Bimetallic Catalysts: Discoveries, Concepts, and Applications*; John Wiley & Sons, New York, **1983**.

Sinfelt, J.H. and Via, G.H. *J.Catal.* **1979**, 56, 1-11.

Sinfelt, J.H. *Chem. Eng. News.* **1972**, 50, 18-19.

Sinfelt, J.H. *J. Catal.* **1973**, 29, 308-315.

Sinfelt, J.H.; Carter, J.L.; and Yates, D.J.C. *J. Catal.* **1972**，24, 283-296.

Sinfelt, J.H.; Lam, Y.L.; Cusumano, J.A.; and Barnett, A. E. *J. Catal.* **1976**, 42, 227-237.

Sinfelt, J.H.; Via, G.H. ; and Lytle, F.W. *J. Chem. Phys.* **1982**, 76, 2779-2789.

Srinivasan, R.; Davis, B.H. *Platinum Met. Rev.* **1992**, 36, 151.

Staroverov, V.N.; Scuseria, G.E.; Tao, J. and Perdew, J.P., *J. Chem. Phys.*, **2003**, 119, 12129.

Stuntz, G. F.; Shapley, J. R.; Pierpont, C. G. *Inorg. Chem.* **1978**, 17, 2596 – 2603.

Suggs, J. W.; Lee, K. S. *J. Organomet. Chem.* **1986**, 299, 297-309.

Tanaka, R.; Yamashita, M.; Nozaki, K. *J. Am. Chem. Soc.* **2009**, 131, 14168 - 14169.

Tao, J.; Perdew, J.P.; Staroverov, V.N. and Scuseria, G.E., *Physical Review Letters*, **2003**, 91, 146401-146404.

Teller, R.G.; Bau, R. *Struct. Bonding* **1981**, 41, 1-82.

Thanthiriwatte, K. S.; Hohenstein, E. G.; Burns, L. A.; Sherrill, C. D. *J. Chem. Theory Comput.* **2011**, 7, 88 - 96.

Thomas, J. M.; Adams, R. D.; Boswell, E. M.; Captain, B.; Gr?nbeck, H.; Raja, R., *Faraday Disc.* **2008**, 138, 301-315.

Thomas, J.M.; Johnson, B.F.G.; Raja, R.; Sankar, G.; Midgley, P.A. *Acc. Chem. Res.* **2003**, 36, 20-30.

Uzun, A.; Dixon, D. A.; Gates, B. C. *ChemCatChem* **2011**, 3, 95 – 107.

Van Koten, G. *J. Organomet. Chem.* **1990**, 400, 283 – 301.

Vaska L. *Accounts. Chem. Res.* **1968**, 1, 335-344.

Wade, K. in *Transition Metal Clusters*, Johnson, B. F. G., Ed.; Wiley, New York, **1980**, Ch. 3.

Watson, A.J.A.; Williams, J.M.J. *Science* **2010**, 329, 635-636.

Weisemann, C.; Schmidtberg, G.; Brune, H.A. *J. Organomet. Chem.* **1989**, 362, 63-76.

Weisemann, C.; Schmidtberg, G.; Brune, H.A. *J. Organomet. Chem.* **1989**, 365, 403-412.

Wiberg, K. B. *Tetrahedron* **1968**, 24, 1083 - 1096.

Woodmansee, D. H.; Pfaltz, A. *Top. Organomet. Chem.* **2011**, 34, 31-76.

Xu, W.; Rosini, G. P.; Gupta M.; Jensen C.M.; Kaska, W.C.; Krogh-Jespersen, K.; Goldman, A.S. *Chem. Commun.* **1997**, 2273-3374.

Xu, Z.; Xiao, F.-S.; Purnell, S. K.; Alexeev, O.; Kawi, S.; Deutsch, S.; Gates, B. C. *Nature* **1994**, 372, 346-348.

Yabe,Y.; Maegawa, T.; Monguchi, Y.; Sajiki, H. Tetrahedron **2010**, 66, 8654 – 8660.

Yamamoto, R.; Sawayama, Y.; Shibahara, H.; Ichihashi, Y.; Nishiyama, S.; Tsuruya, S. *J. Catal.* **2005**, 234, 308-317.

Yang, X. *ACS Catal.* **2011**, 8, 849 - 854.

Zhang, Y.; Cui, X.; Shi, F.; Deng, Y. *Chem. Rev.* **2012**, 112, 2467–2505.